THE UNIVERSITY *of* EDINBURGH

Insights into Inhibition of Heme-Dependent Dioxygenases

Georgios Pantouris

Thesis presented for the degree of Doctor of Philosophy

The University of Edinburgh

2012

To my wife, Dignora, the fundamental brick of this trial

Declaration

The work presented in this thesis is the original work of the author, except where specific reference is made to other sources. It has not been submitted in part, or in whole, for any other degree.

Georgios Pantouris

Acknowledgements

My warmest thank should go to my supervisor Dr. Chris G. Mowat, who has been a great mentor and friend over the past three years. The knowledge and skills I gained, because of him, will always accompany me for the rest of my research journey. Thank you Chris! Particular thanks should also go to Prof. Steve Chapman and Dr. Simon Daff for their guidance, support and advises. I would also like to thank Dr. Sarah J. Thackray for her help throughout the PhD and Martin, Laura and Ben for the unforgettable moments we had in the lab. My warmest thanks should go to my family and particularly to mum and dad. I owe you my life and everything I have succeeded so far.

Thank you all, my Scottish adventure was a pleasure!

Georgios Pantouris

Abstract

Tryptophan 2,3-dioxygenase (TDO), along with indoleamine 2,3-dioxygenase (IDO) and indoleamine 2,3-dioxygenase-2 (IDO2) are the three enzymes that catalyse oxidation of L-tryptophan (L-Trp) in the first step of the kynurenine pathway. Despite the fact that all three catalyse the same reaction, they were detected and characterized in different chronological periods; TDO, IDO and IDO2 were discovered in 1936, 1967 and 2007 respectively. Years of studies showed that abnormal regulation of L-Trp, in the first step of kynurenine pathway, is related with several disorders, including cancer. Regardless of their distinct dissimilarities, TDO, IDO and IDO2 were all detected in various cancers, supporting tumour escape and survival. The early identification of IDO immunomodulatory action (1990s) led to intense research for the development of IDO inhibitors, but not TDO. Despite this effort, the most pharmacologically suitable IDO inhibitor, 1-methyltryptophan (1-MT), appears to be ineffective as monotherapeutic drug. Discovery of IDO2 showed that 1-MT action is not fully understood, raising questions about the biological significance of IDO2.

The ultimate goal of the current study was to address the problems outlined above. Because TDO and IDO are two druggable molecular targets, the discovery of a new class of effective inhibitors was pursued. Plate screening of ~2800 potential inhibitor compounds obtained from National Cancer Institute (NCI), USA, indicated seven promising compounds that inhibit both TDO and IDO in either nanomolar or low micromolar range. Interestingly, of these seven inhibitors, six have been identified to have cytotoxic action against several types of tumour cell lines (NCI data). *NSC 26326*, known as β-lapachone, is a natural occurring quinone and the strongest inhibitor of all seven. This NCI compound inhibits both TDO and IDO with inhibition constants of ~30-70 nM and 97 ± 14 nM respectively. Like *NSC 26326*, *NSC 36398* is another natural occurring product and the only compound that showed selectivity against TDO with inhibition constant of 16.3 ± 3.8 μM. Among the seven compounds that displayed promise as inhibitors of TDO and IDO was mitomycin C. Mitomycin C, which is an approved oncology drug and a known inhibitor of IDO

(K_i = 24.2 ± 1.2 μM), is also inhibitor of TDO with inhibition constant of 2.86 ± 0.03 μM. Another major goal of the current work was the discovery of isatin derivatives as inhibitors of TDO and IDO. Using the tryptophan-like structure of isatin as starting point, a number of structural modifications were carried out (structure-activity relationship (SAR)) succeeding the optimization of their inhibition activity. This new family of TDO and IDO inhibitors demonstrated inhibition potencies in the low micromolar range with 5,7-dicholoisatin to reach the nanomolar range (in the case of TDO). Halogenation of isatin and its derivatives was found to increase noticeably the inhibition potencies of these molecules by 12fold and 6fold for TDO and IDO respectively while breakdown of isatin's pyrrolidine ring had a disastrous result on the inhibition of both enzymes. Combinations of 1-MT with either the newly-identified NCI inhibitors or the isatin derivatives were also examined. The *in vitro* combinations of 1-MT with either the NCI inhibitors or the isatin derivatives revealed an additive effect without though excluding the possibility of synergistic effect *in vivo*.

The specificity of TDO, IDO and IDO2 against the two stereoisomers of 1-MT was also investigated, with interesting results. While IDO is inhibited only by the L-isoform of 1-MT (K_i = 18.0 ± 3.4 μM), IDO2 is inhibited by both 1-Me-L-Trp and 1-Me-D-Trp with inhibition constants of 306 ± 17 μM and 3419 ± 259 μM respectively. Biochemical characterization of human IDO2 was another goal of the current thesis, which completed successfully. Kinetic, redox and inhibition study of human IDO2 indicated significant differences in comparison with human IDO something which suggests the potential implication of IDO2 in an identified biological pathway (other than tryptophan catabolism function).The findings presented herein help to solve the mystery of 1-MT action, at least *in vitro*, give answers in regards to IDO2 function, and provide a number of new, promising inhibitors for TDO and IDO.

Contents

Chapter 1 - Introduction

Chapter 2 - Materials and Methods

Chapter 3 - Identification and characterisation of inhibitors of TDO and IDO

Chapter 4 - Isatins as inhibitors for TDO and IDO

Chapter 5 - Biochemical Characterization of Human Indoleamine 2,3-Dioxygenase-2

Chapter 6 - Conclusions

Abbreviations

Abs	Absorbance
BSA	Bovine serum albumin
Da	Daltons
DMAB	Dimethylaminobenzaldehyde
CN^-	Cyanide
CO	Carbon monoxide
CV	Column volume
DMSO	Dimethyl sulfoxide
D-Trp	D-tryptophan
E^o	Standard reduction potential
E_m	Midpoint potential
FAD	Flavin adenine dinucleotide
FDA	Food and Drug Administration
FMN	Flavin Mononucleotide
Fe^{+2}	Ferrous iron
Fe^{+3}	Ferric iron
IDO	Indoleamine 2,3-dioxygenase
IDO2	Indoleamine 2,3-dioxygenase-2
IPTG	Isopropyl-β-D-thiogalactopyranoside
HCl	Hydrochloric acid
hIDO	*Homo sapiens* indoleamine 2,3-dioxygenase
hIDO2	*Homo sapiens* indoleamine 2,3-dioxygenase-2
HOs	Heme oxygenases
Hsp90	Heat shock protein 90
HPLC	High-performance liquid chromatography
hTDO	*Homo sapiens* tryptophan 2,3-dioxygenase
H_2O	Water
H_2O_2	Hydrogen peroxide
H55A	Histidine 55 to alanine mutant

H55S	Histidine 55 to serine mutant
IDO	Indoleamine 2,3-dioxygenase
k_{cat}	Rate constant at substrate saturation
K_d	Dissociation constant
K_i	Inhibition constant
K_{si}	Self-inhibition constant
K_m	Michaelis constant
KMO	Kynurenine-3-monoxygenase
KP_i	Potassium Phosphate: K_2HPO_4/KH_2PO_4
L-Trp	L-tryptophan
LB	Luria Bertani
MeCN	Acetonitrile
MTH-Trp	Methylthiohydantoin-DL-tryptophan
MWCO	Molecular weight cut off
NAD^+	Nicotinamide adenine dinucleotide
NCI	National cancer institute
NO	Nitric oxide
OTTLE	Optically transparent thin layer electrochemistry
O_2	Molecular oxygen
PAGE	Polyacrylamide gel electrophoresis
PEG	Polyethyleneglycol
pfTDO	*Pseudomonas fluorescens* tryptophan 2,3-dioxygenase
PI	Phenylimidazole
PMSF	Phenylmethylsulfonyl fluoride
ROS	Reactive oxygen species
rpm	Revolutions per minute
rmTDO	*Ralstonia metallidurans* tryptophan 2,3-dioxygenase
SAR	Structure-activity relationship
SDS	Sodium dodecyl sulphate
SHE	Standard hydrogen electrode
sIDO	*Shewanella oneidensis* indoleamine 2,3-dioxygenase
TCEP	*tris*(2-carboxyethyl)phosphine

TDO	Tryptophan 2,3-dioxygenase
TRIS	Tris[hydroxymethyl]aminoethane
UV	Ultraviolet
Vis	Visible
v/v	Volume per volume
w/v	Weight per volume
xcTDO	*Xanthomonas campestris* tryptophan 2,3-dioxygenase
1-Me-L-Trp	1-methyl-L-tryptophan
1-Me-D-Trp	1-methyl-D-tryptophan
1-MT	1-methyltryptophan
4-PI	4-phenylimidazole
5-F-Trp	5-fluorotryptophan
5-HO-L-Trp	5-hydroxy-L-Tryptophan
5-Me-Trp	5-methyltryptophan
5-MeO-Trp	5-methoxytryptophan
6-F-Trp	6-fluorotryptophan
6-Me-Trp	6-methyltryptophan

Standard Symbols

m	metre	**M**	molar
g	gram	**^{o}C**	degree Celsius
l	litre	**V**	volt
s	second	**Å**	Angstrom

Amino Acids

A	Ala	Alanine	**M**	Met	Methionine
C	Cys	Cysteine	**N**	Asn	Asparagine
D	Asp	Aspartic acid	**P**	Pro	Proline
E	Glu	Glutamic acid	**Q**	Gln	Glutamine
F	Phe	Phenylalanine	**R**	Arg	Arginine
G	Gly	Glycine	**S**	Ser	Serine
H	His	Histidine	**T**	Thr	Threonine
I	Ile	Isoleucine	**V**	Val	Valine
K	Lys	Lysine	**W**	Trp	Tryptophan
L	Leu	Leucine	**Y**	Tyr	Tyrosine

Chapter 1

Introduction

1.1 Heme-dependent proteins

Heme-dependent proteins are a family of metalloproteins that contain one or more heme groups, which may or may not be covalently bound to the polypeptide chain. The study of this family is estimated to have started in the 19th century, when hemoglobin from several animals was recognised and crystallised for the first time [(1)]. Heme proteins are responsible for a number of functions including electron transfer (e.g. cytochrome c), catalysis (e.g. catalase), oxygen transport and storage (e.g. hemoglobin and myoglobin) and signal transduction (e.g. nitric oxide synthase). Regardless of the functional specificity of each one, heme-dependent proteins share the same chromophore; a porphyrin moiety with an iron atom at the centre. The porphyrin moiety may be derivatised in various ways, and thus hemes are classified into several categories, of which heme a, heme b, heme c and heme d are the most common [(2)]. The structural characteristics of each type are illustrated in figure 1.1.

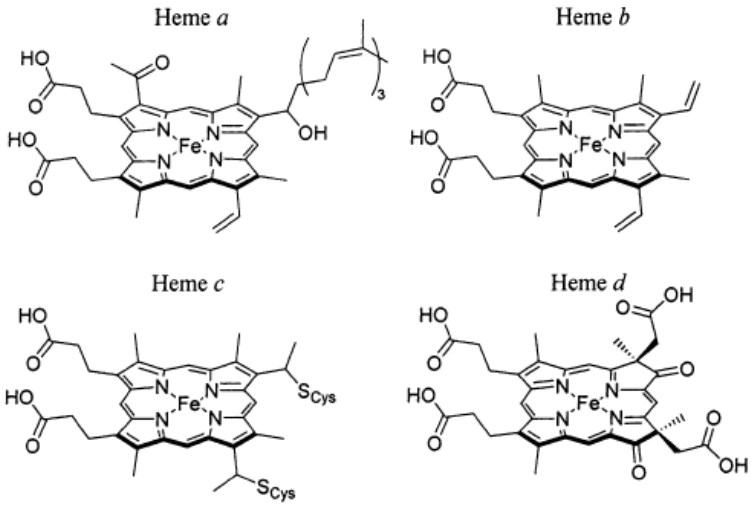

Figure 1.1: Chemical structures of the most common types of heme (*taken from ref. 2*)

Between the four, iron (II) protoporphyrin IX (heme b) is the most common one. It serves as the template from which the other three types (a, c and d) are biosynthetically derived [(2)]. Incorporation of the iron atom into any type of porphyrins occurs *in vivo* via an enzyme called ferrochelatase [(3)]. During that process, four of the six coordination positions of iron are utilized for binding with the 4 nitrogen atoms of porphyrin while the other two remain free for interactions with the active site of the given protein and a ligand such as oxygen (O_2), nitric oxide (NO) and carbon monoxide (CO). During the several functions of heme proteins, the iron atom can generally adopt two stable oxidation forms, the ferric (Fe^{+3}) and the ferrous (Fe^{+2}) form. In addition to these two oxidation stages, heme can also adopt the ferryl (Fe^{+4}) form, transiently, as part of the enzyme's catalytic circle. In cytochrome P450 (CYP 450) monooxygenases, heme iron-bound dioxygen is believed to form compound-I species ($Fe^{4+}=O^{2-}$ with a π-cation radical on the porphyrin ring) while in dioxygenases (indoleamine 2,3-dioxygenase), it was shown that catalysis occurs via a compound-II species ($Fe^{4+}=O^{2-}$ without a π-cation radical on the porphyrin ring) [(4), (5)].

1.2 Oxygenases

At the beginning of the 1930s the scientific world believed that incorporation of molecular oxygen into a substrate was completely forbidden. According to Heinrich Wieland, a German Nobel Laureate in chemistry and the father of "dehydrogenation theory", dioxygen could serve only as acceptor of electrons *via* several carriers [(6)]. Oxygen atoms that were incorporated into a substrate were considered to be derived from the oxygen atoms of water molecules.

In 1955 Osamu Hayaishi from Japan and Howard S. Mason from the US, working independently, demonstrated for the first time that dioxygen has the ability to react directly with a target molecule. While Hayaishi demonstrated the incorporation of molecular oxygen into catechol to produce cis,cis-muconic acid [(7)] (fig. 1.2), Mason showed the oxidation of 3,4-dimethylphenol to 4,5–dimethylcatechol using an oxygen atom from molecular oxygen [(8)]. Both of these reactions were catalysed by a new enzyme family, which we call today oxygenases.

Oxygenases are defined as the enzymes that catalyse the incorporation of one or both atoms of dioxygen into the substrate. According to the number of oxygen atoms that are incorporated into the substrate, oxygenases are divided into monooxygenases and dioxygenases.

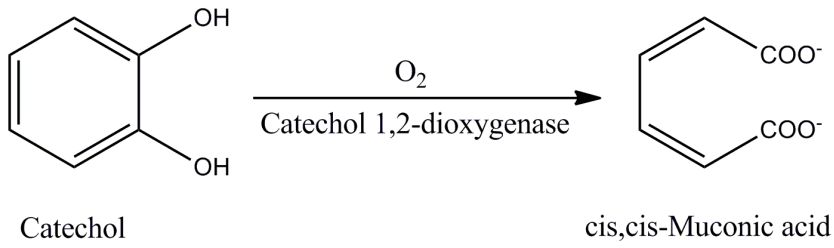

Catechol cis,cis-Muconic acid

Figure 1.2: The reaction catalysed by catechol 1,2-dioxygenase; the first dioxygenase was discovered by Hayaishi and his co-workers in 1955 [(7)].

1.2.1 Monooxygenases

Monooxygenases are responsible for the enzymatic integration of an oxygen atom of dioxygen into the substrate, with the second oxygen being reduced to water. Further classification of monooxygenases reveals two subcategories [(9)]; the internal monooxygenases where all the electrons required for the reaction come from the substrate (e.g. Arginine 2-monooxygenase EC 1.13.12.1, *see reaction I*) and the external monooxygenases where the electrons are obtained from coenzymes such as NADPH and FAD (e.g. Flavin-containing monooxygenase EC 1.14.13.8, *see reaction II*). Heme oxygenases (HOs), flavin-containing monooxygenase (FMO) protein family, and cytochromes P450 are the most well-known monooxygenases.

L-Arginine + O_2 → *4-guanidinobutanamide* + CO_2 + H_2O *(I)*

N,N-dimethylaniline + *NADPH* + O_2 → *N,N-dimethylaniline N-oxide* + $NADP^+$ + H_2O *(II)*

1.2.2 Dioxygenases

Dioxygenases catalyse reactions in which both atoms of molecular oxygen are inserted into the substrate(s). Dioxygenases can be categorized into three groups [9]. When both oxygen atoms from the molecular oxygen are fused into the same substrate then this class of dioxygenases is known as intramolecular dioxygenases (e.g. tryptophan 2,3-dioxygenase EC 1.13.11.11, indoleamine 2,3-dioxygenase EC 1.13.11.52). However, when the oxygen atoms go to different substrates then these enzymes are called intermolecular dioxygenases (e.g. proline 3-hydroxylase EC 1.14.11.28). The third class of dioxygenases (miscellaneous dioxygenases) includes several types of enzymes which are not well characterized but are essential for numerous metabolic reactions (e.g. tryptophan 2'-dioxygenase EC 1.13.99.3, *see reaction below*). More information about mono- and dioxygenases can be obtained from http://enzyme.expasy.org/.

L-tryptophan + O_2 → *(indol-3-yl) glycolaldehyde* + CO_2 + NH_3

1.3 Tryptophan metabolism

L-Tryptophan is one of the nine essential amino acids that humans receive *via* their diet. Processing of L-tryptophan leads to three possible products; nicotinamide adenine dinucleotide (NAD^+), serotonin, or protein synthesis (fig. 1.3).

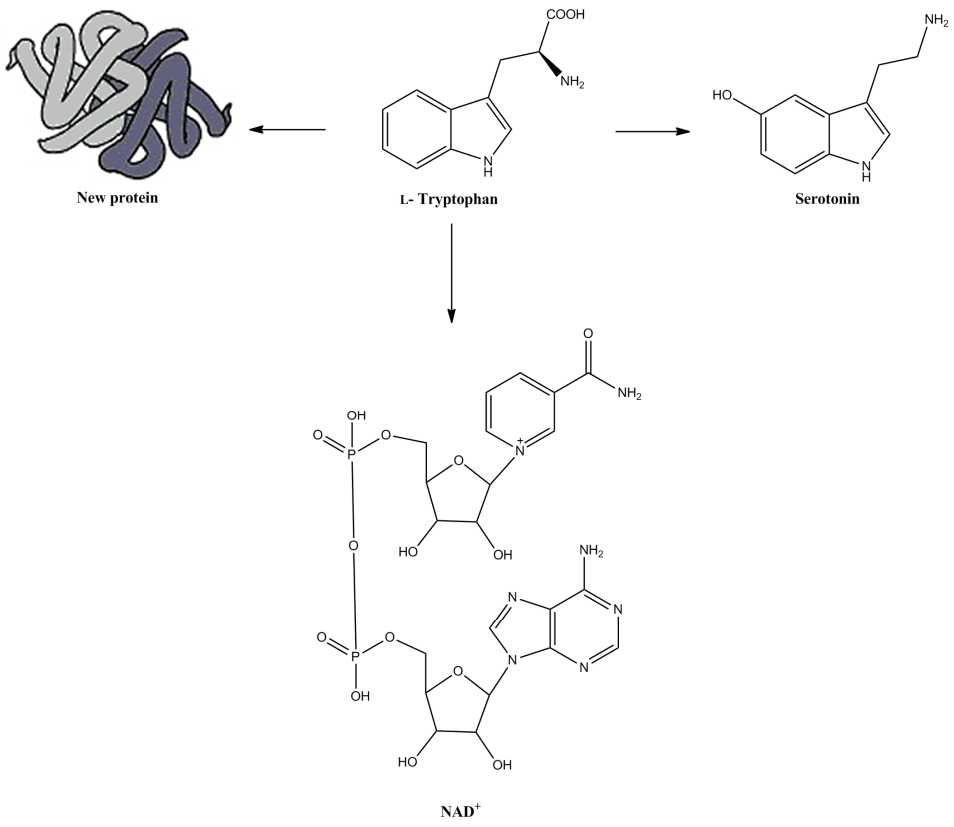

Figure 1.3: Tryptophan metabolism leads to three possible products; nicotinamide adenine dinucleotide (NAD^+), serotonin or the biosynthesis of a new protein.

According to its needs, human body uses a small proportion of L-Trp (~ 5%) for the production of neurotransmitter molecules (serotonin and melatonin) and the biosynthesis of new proteins while the rest ≥ 95% follows the kynurenine pathways for biosynthesis of NAD^+ **(10)**.

1.3.1 The serotonin pathway

Via a pathway known as the serotonin pathway, L-Trp undergoes a number of structural modifications leading to serotonin and subsequently to melatonin (fig. 1.4). This minor pathway of L-Trp degradation has a major functional significance influencing a broad range of physiological systems including the central nervous system, cardiovascular regulation, respiration, sexual behaviour and pain sensitivity [11].

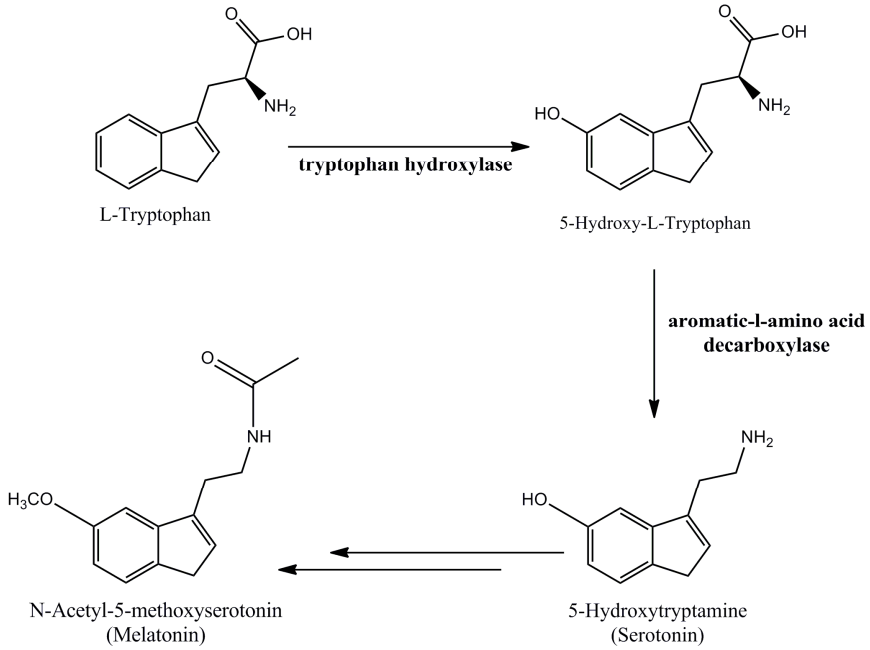

Figure 1.4: Chemical modifications of L-Trp in the serotonin pathway that lead to biosynthesis of serotonin and melatonin.

In the initial step of the serotonin pathway, L-Trp undergoes hydroxylation at the 5' position of the indole ring giving 5-hydroxy-L-tryptophan (5-OH-L-Trp). This reaction is catalysed by tryptophan hydroxylase, an iron-dependent enzyme that uses 5,6,7,8-tetrahydrobiopterin (BH_4) as co-factor. Following this, in a reaction catalysed by aromatic-l-amino acid decarboxylase, 5-OH-L-Trp undergoes decarboxylation producing 5-hydroxytryptamine or serotonin. Biosynthesis of serotonin triggers

melatonin production *via* a two-step process [12]. During that process, serotonin undergoes *N*-acetylation of the amino group followed by *o*-methylation of the 5'-hydroxyl group. These two reactions are catalysed by the enzymes *N*-acetyltransferase and hydroxyindole-*o*-methyltransferase respectively.

1.3.2 The kynurenine pathway

The kynurenine pathway is the main route for L-Trp catabolism, leading to the production of nicotinamide adenine dinucleotide (NAD^+). Nicotinamide adenine dinucleotide (NAD^+) is an essential coenzyme for all living cells, and it is involved in a number of redox reactions (calcium homeostasis, energy metabolism, mitochondrial functions, gene expression, cell death and ageing) [13], [14]. In addition to NAD^+, the kynurenine pathway produces a number of active metabolites which are essential for homeostasis and will be described below.

The pathway is initiated by incorporation of molecular oxygen into L-Trp for production of N-formylkynurenine (fig. 1.5). This reaction is catalysed by one of three enzymes known as tryptophan 2,3-dioxygenase (TDO), indoleamine 2,3-dioxygenase (IDO) and indoleamine 2,3-dioxygenase-2 (IDO2). Despite the fact that these enzymes catalyse the same reaction, their expression patterns and signalling pathways differ [10], [15]. N-formylkynurenine is an unstable metabolite (*in vitro*) that is quickly transformed into L-kynurenine, the first stable product of the pathway. Kynurenine can subsequently be metabolized by three different enzymes for biosynthesis of kynurenic acid, anthranilic acid or 3-hydroxykynurenine. These enzymes are kynurenine aminotransferase, kynureninase and kynurenine hydroxylase respectively. Under normal conditions kynurenine hydroxylase has the highest affinity for kynurenine and therefore kynurenine is transformed into 3-hydroxykynurenine [16].

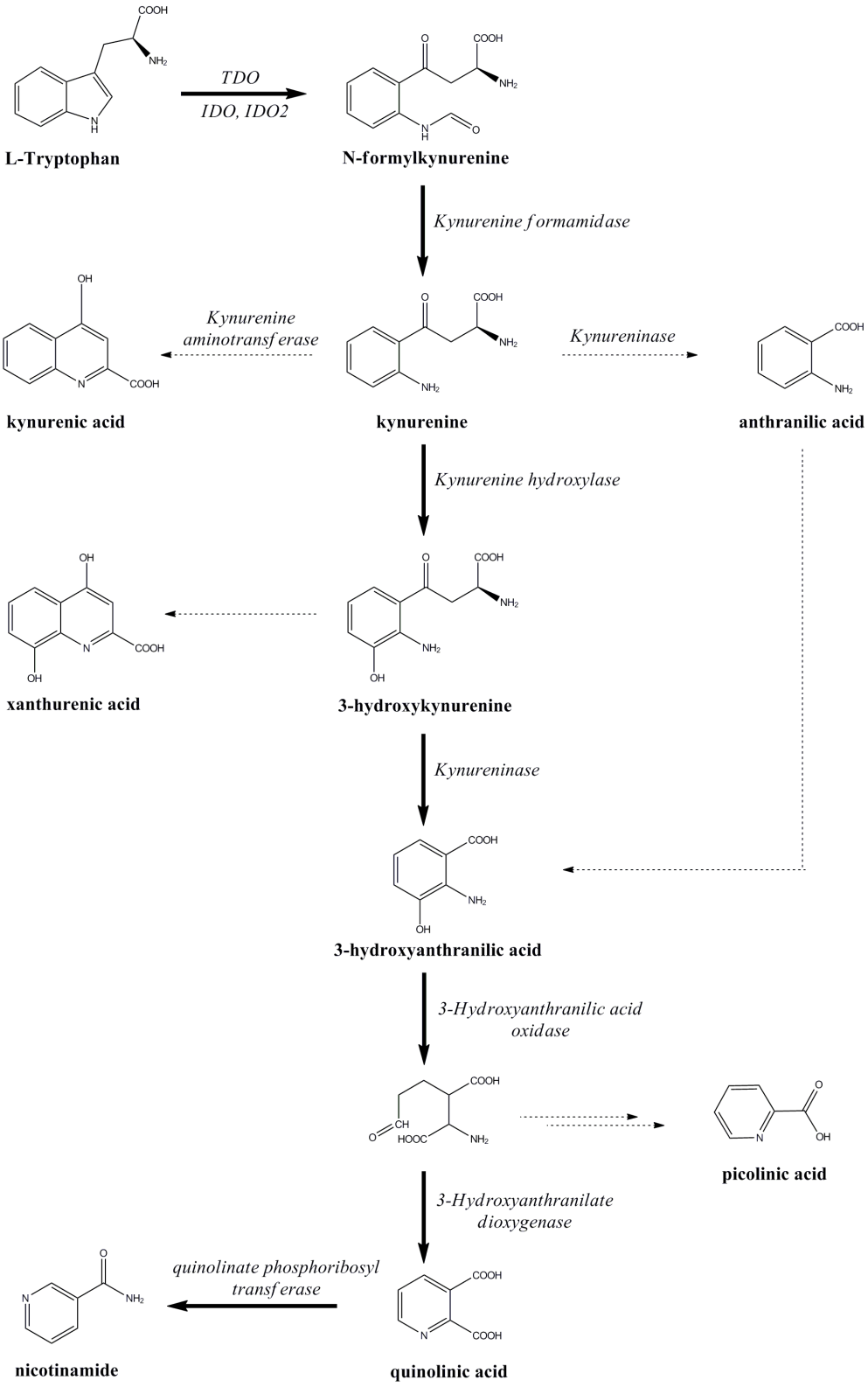

Figure 1.5: The enzymes and intermediates of the kynurenine pathway.

Kynurenic acid, under physiological conditions, is considered as an endogenous "neuroprotectant" which is found in the brain of mammals at nanomolar concentrations [17]. As an antagonist to quinolinic acid, kynurenic acid acts on several receptors (N-methyl-D-aspartate receptor, α-amino-3-hydroxy-5-methyl-4-isoxazolepropionic acid receptor and G protein-coupled receptor 35) inhibiting activation of intracellular enzymes, which are related with production of reactive oxygen species (ROS) [15]. In contrast with kynurenic acid, 3-hydroxykynurenine and 3-hydroxyanthranilic acid are toxic metabolites of the kynurenine pathway with established roles in DNA damage [18]. Through a series of reactions these two intermediates can undergo auto-oxidation with the accompanying generation of superoxide anions followed by the synthesis of hydrogen peroxide (fig. 1.6).

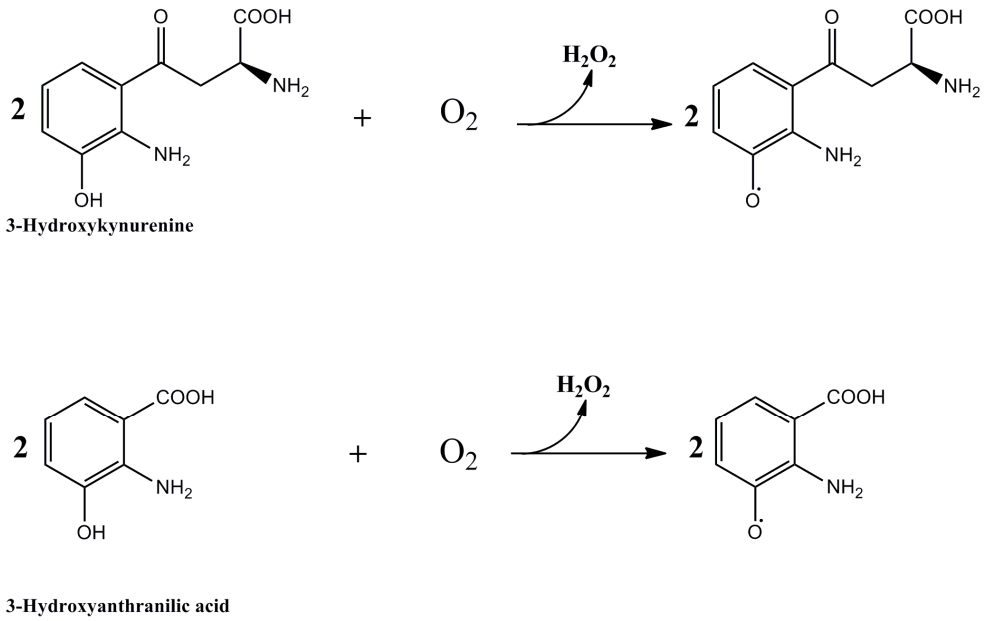

Figure 1.6: Oxidation of 3-hydroxykynurenine and 3-hydroxyanthranilic acid is accompanied with production of reactive oxygen species.

Production of 3-hydroxyanthranilic acid can be achieved either via the enzyme kynureninase (for which 3-hydroxykynurenine is a substrate) or the non-specific hydroxylation of anthranilic acid, a side product of the kynurenine pathway. At that point, 3-hydroxyanthranilic acid oxidase breaks the aromatic ring of 3-

hydroxyanthranilic acid producing the intermediate 2-amino-3-carboxymuconic semialdehyde. This intermediate can follow two routes for biosynthesis of either picolinic acid or quinolinic acid. The side branch which is responsible for production of picolinic acid is a two step pathway. More specifically, the enzyme amino-ß-carboxymuconate-semialdehydedecarboxylase converts the intermediate mentioned above to 2-aminomuconic semialdehyde with subsequent non enzymatic conversion to picolinic acid [19]. In the main route, a non enzymatic rearrangement of 2-amino-3-carboxymuconic semialdehyde allows the synthesis of quinolinic acid. While picolinic acid production is considered as beneficial, biosynthesis of quinolinic acid is thought to be detrimental. Studies on picolinic acid showed that it has neuroprotectant, antiviral and antimicrobial properties [19]. On the other hand, quinolinic acid is related with activation of NMDA receptors (mentioned above), mitochondrial dysfunction and free radical generation [10].

1.4 The kynurenine pathway in disease states

As has become apparent from many years of studies, dioxygenation of L-Trp in the first step of the kynurenine pathway is the crucial point and rate-limiting step that influences the whole pathway. Whereas the implication of TDO/IDO/IDO2 in cancer will be discussed in the sections 1.5, 1.7 and 1.8, this section is focused on diseases, which are related with upregulation of these enzymes and accumulation of the kynurenine pathway metabolites. Examination of patients or animal subjects with inflammatory neurological diseases showed that accumulation of quinolinic acid is implicated in HIV infection [20], cerebral malaria [21] and ischemic brain injury [22]. Moreover, direct intracerebral injection of quinolinic acid into rats causes neural death [23], [24]. Some other kynurenine pathway metabolites, such as 3-hydroxyanthranilic acid and 3-hydroxykynurenine, are normally present in the lens of the eye. These two molecules act as UV filters protecting the retina from UV light. However, accumulation of 3-hydroxyanthranilic acid and 3-hydroxykynurenine in the eye is related to the formation of free radicals that contribute to lens damage [25].

1.5 Tryptophan 2,3-dioxygenase (TDO)

Tryptophan 2,3-dioxygenase (TDO), a cytosolic protein, is one of the three enzymes (along with indoleamine 2,3-dioxygenase (IDO) and indoleamine 2,3-dioxygenase-2 (IDO2)) that catalyse L-tryptophan dioxygenation. Molecular oxygen is incorporated into L-tryptophan giving N-formylkynurenine as the product, in the first step of the kynurenine pathway (fig. 1.7).

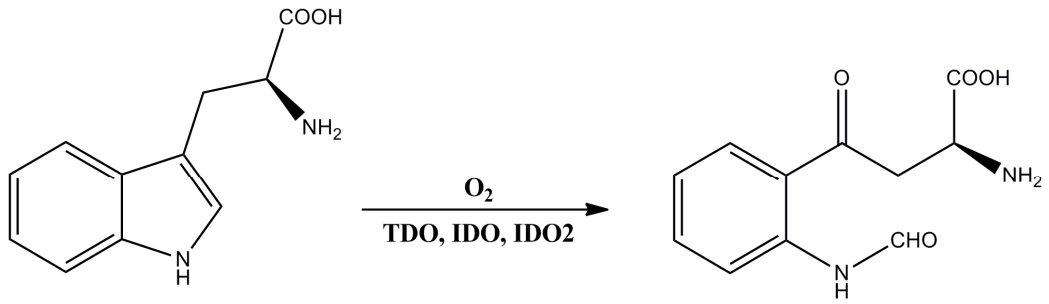

L-Tryptophan **N-formylkynurenine**

Figure 1.7: Dioxygenation of L-Trp, a reaction catalysed by TDO, IDO and IDO2.

Tryptophan 2,3-dioxygenase was initially isolated in 1936 by Kotake *et al.*, who were working on the metabolic pathway of tryptophan in mammals [(26)]. Because of the enzyme's ability to cleave the pyrrole ring of tryptophan, it was initially named tryptophan pyrrolase, to be renamed later as tryptophan 2,3-dioxygenase. The gene responsible for the expression of human TDO protein is located on the long arm of chromosome 4 (4q31-q32) and it contains 12 exons (information about the TDO gene that has been used in the current thesis is given in section 2.3). The messenger RNA comprises 1693 nucleotides which in turn are translated into a functional protein of 406 amino acid residues [(27)]. Although TDO is mainly expressed in the liver, it has been also found in the pituitary gland, embryonic tissue, mammary gland, bladder, muscle, eye, colon, lung, connective tissue, blood, brain, heart, testis, pancreas and skin after stimuli [(27)]. TDO has been found in eukaryotes such as human [(28)], rat [(29)], rabbit [(30)] and prokaryotes like *Ralstonia metallidurans (rmTDO)* [(31)], *Xanthomonas campestris (xcTDO)* [(32)] and *Pseudomonas fluorescens (pfTDO)* [(33)].

While eukaryotic TDOs contain around 400 amino acids, prokaryotic TDOs are composed of ~300 amino acids. Among the prokaryotic TDOs that have been studied is xcTDO, the only solved TDO crystal structure with L-Trp bound [32]. Its sequence identity with hTDO is 34% and the amino acid sequences of both xcTDO and hTDO are given in figure 1.8. Whilst the identities between prokaryotic and eukaryotic TDO sequences vary between 20-40 %, the sequence homology of human TDO with other members of that family, such as IDO, is not higher than 10 %. Despite the fact that the crystal structure of human TDO is not available as yet, the basic structural characteristics of the enzyme can be inferred through the knowledge gained from other TDOs (crystal structures of *rm*TDO [31] and *xc*TDO [32]). TDO is a homotetrameric protein that contains four b-type hemes, one in the active site of each monomer. More details about the available crystal structures and their characteristics are given in section 1.9.

```
Xc_TDO ------------------MPVDKNLRD-LEPGIHTDLEGRLTYGGYLRLDQLLSAQQPLSE 42
Hs_TDO MSGCPFLGNNFGYTFKKLPVEGSEEDKSQTGVNRASKGGLIYGNYLHLEKVLNAQELQSE 60

Xc_TDO P---AHHDEMLFIIQHQTSELWLKLLAHELRAAIVHLQRDEVWQCR------KVLARSKQ 93
Hs_TDO TKGNKIHDEHLFIITHQAYELWFKQILWELDSVREIFQNGHVRDERNMLKVVSRMHRVSV 120

Xc_TDO VLRQLTEQWSVLETLTPSEYMGFRDVLGPSSGFQSLQYRYIEFLLGNKN----PQMLQVF 149
Hs_TDO ILKLLVQQFSILETMTALDFNDFREYLSPASGFQSLQFRLLENKIGVLQNMRVPYNRRHY 180

Xc_TDO AYDPAGQAR--LREVLEAPSLYEEFLRYLARFGHAIPQQY-------------------- 187
Hs_TDO RDNFKGEENELLLKSEQEKTLLELVEAWLERTPGLEPHGFNFWGKLEKNITRGLEEEFIR 240

Xc_TDO ---------QARDWTAAHVADDTLRPVFER--------------------------IYEN 212
Hs_TDO IQAKEESEEKEEQVAEFQKQKEVLLSLFDEKRHEHLLSKGERRLSYRALQGALMIYFYRE 300

Xc_TDO TDRYWREYSLCEDLVDVETQFQLWRFRHMRTVMRVIGFKRGTGGSSGVGFLQQALA--LT 270
Hs_TDO EPRFQVPFQLLTSLMDIDSLMTKWRYNHVCMVHRMLGSKAGTGGSSGYHYLRSTVSDRYK 360

Xc_TDO FFPELFDVRTSVGVDNRPPQGSADAGKR------------------ 298
Hs_TDO VFVDLFNLSTYLIPRHWIPKMNPTIHKFLYTAEYCDSSYFSSDESD 406
```

Figure 1.8: Amino acid sequences of xcTDO (top) and human TDO (bottom), with the identical and similar amino acids highlighted in red and blue respectively. These two enzymes share 34 % homology.

In terms of substrate selectivity, TDO can be considered as a highly selective enzyme that catalyses oxidation of L-Trp and a few other tryptophan derivatives like 5-fluorotryptophan [34]. In contrast with IDO, where its expression is induced by IFN-γ, TDO expression is trigged by glucocorticoid hormones and regulated by the availability of L-Trp [35].

Because of the neurotoxic properties of particular kynurenines, TDO was though to be implicated only in neurological disorders. However, a recent study has provided evidence for the implication of TDO in cancer biology, something which refreshes the interest in this specific enzyme [36]. According to these findings, examination of glioma cancer cells revealed an increased level of kynurenine, purely synthesized by TDO. These kynurenine molecules serve as endogenous ligands for human aryl hydrocarbon receptor (AHR) which in turn promotes tumour-cell survival and motility. Moreover, an independent study of 104 human tumour lines, coming from Pilotte *et al.*, showed the expression of TDO in 20 of them and the co-expression of TDO and IDO in another 16 [37]. All these findings clearly point out the important role of TDO in cancer biology and the need of developing new inhibitors for the enzyme.

1.6 Indoleamine 2,3-dioxygenase (IDO)

Indoleamine 2,3-dioxygenase (IDO) was first isolated from rabbit intestine and characterized in 1978 by Hayaishi *et al.* [38]. In contrast with TDO, IDO can be found only in eukaryotes, and more specifically in mammals. It is a monomeric protein (M.W. = 45 kDa) composed of 403 amino acids and catalyses oxidation of L-Trp, D-Trp, 1-Me-L-Trp and various tryptophan-like molecules. IDO is expressed in several tissues (but not the liver) and it is induced by IFN-γ. All the basic characteristics of IDO are presented in table 1.1 and compared with those of TDO [35]. Despite the numerous differences, both IDO and TDO have crucial involvement in L-tryptophan regulation.

	IDO	TDO
reaction	Oxidation of L-tryptophan to N-formylkynurenine	
gene localization	chromosome 8p12-p11	chromosome 4q31-q32
subunits /size	monomer (45 kDa)	tetramer (191 kDa)
found in	eukaryotes	prokaryotes and eukaryotes
expression induced by	IFN-γ	glucocorticoid hormones
distribution in the human body	all tissues except liver	mainly expressed in the liver
substrate inhibition	> 50 μM	no inhibition
substrate specificity	L-Trp, D-Trp, 1-Me-L-Trp, 5-F-Trp, 6-F-Trp, serotonin, tryptamine, 5-OH-Trp	L-Trp, 5-F-Trp, 6-F-Trp

Table 1.1: Comparison between IDO and TDO basic characteristics.

1.7 The immunomodulatory role of IDO and TDO

After the discovery of IDO, it was believed that the enzyme had mainly antimicrobial action because of its ability to control the availability of an essential amino acid in the inflammatory environment [(39), (40)]. However, a groundbreaking discovery in 1998 came to change ideas about the enzyme and its functions. That year, Munn and co-workers reported that IDO action in pregnant mice prevented rejection of allogeneic foetuses, something which demonstrates an immunomodulatory role for the enzyme [(41)]. This publication was the first among numerous others that relate IDO function with the immune system. In the years following, a number of new pieces of evidence came to show that IDO plays a key role in regulating immune evasion by tumours [(42)]. The findings clearly showed that a variety of human tumours use IDO as a shield against the immune system. More specifically, it is found that IDO activation in patients with particular cancers is related to disease progression, low survival rates

and poor response against various chemotherapeutic and immunotherapeutic agents [42]. Despite the fact that TDO was likely to be involved in cancer biology, the finding could not prove it. Thanks to the discovery of Opitz *et al.* [36] both IDO and TDO have been formally associated with cancer. The immunosuppressive role of TDO and IDO is based on two theories [43]; the tryptophan starvation theory and the tryptophan metabolite theory. According to the first theory, it has been proposed that the enzymes could have similar effects on T cells as they have on bacteria. In this way depletion of tryptophan increases the sensitivity of T lymphocytes driving them to apoptosis [43]. After this hypothesis Frumento *et al.* examined *in vitro* models of T cell activation in the presence and absence of L-Trp. Interestingly, they observed that lack of L-Trp did not affect T cell proliferation [44]. This finding, in combination with the fact that reduced levels of L-Trp can rapidly be replenished by diffusion from surrounding tissues, makes tryptophan starvation less likely to occur *in vivo*. In contrast with the first theory, the tryptophan metabolite theory implicates tryptophan catabolic metabolites such as kynurenine, 3-hydroxykynurenine, 3-hydroxyanthranilic acid and quinolinic acid in apoptosis of T cells. In section 1.5, it was shown that kynurenine serves as endogenous ligand for human aryl hydrocarbon receptor (AHR), which in turns promotes tumour survival. This serves to reinforce the second scenario. While the precise mechanism of TDO and IDO action remains to be determined, both theories can plausibly explain T-cell survival and action.

1.8 Indoleamine 2,3-dioxygenase-2 (IDO2)

Indoleamine 2,3-dioxygenase-2 (IDO2) is a third enzyme that catalyses oxidation of L-tryptophan in the first step of the kynurenine pathway. IDO2 is encoded by a gene which is located on chromosome 8 (8p11.21) and presents a tail-to-head arrangement with IDO. Because of its position and transcriptional function, LOC169355 (as it was known before 2007) was renamed to IDO2 [45]. The full length protein product (human IDO2) comprises 420 amino acids and it shares 72% identities with mouse IDO2, 45% identities with mouse IDO and 44% identities with human IDO [46]. Regarding its expression pattern, it has been found that human IDO2 is expressed in

a subset of tissues that express IDO. While IDO mRNA is found in various tissues, IDO2 mRNA is detected only in liver, small intestine, spleen, placenta, thymus, lung, brain, kidney, and colon [45]. As reported in section 1.6, IDO expression is strongly induced by IFN-γ, something which has not been confirmed for IDO2. A study on mice demonstrated that during malaria infection IDO and IDO2 are induced in different tissues (endothelium and kidney respectively) and in contrast with IDO, the expression levels of IDO2 are not influenced by the presence of IFN-γ [46]. IDO2 localization on chromosome 8, in combination with its reduced catalytic efficiency could suggest that the enzyme is the product of gene duplication. Nevertheless, the distinct characteristics of hIDO2 reinforce the possibility of it having a new immunomodulatory role. Studies on mice showed that both IDO and IDO2 are expressed in particular tissues (e.g. epididymis), supporting the idea of IDO2 implication in an unidentified signalling pathway [47].

Like IDO and TDO, IDO2 has an active role in cancer biology. In 2009, Löb *et al.* first implicated IDO2 in cancer, showing expression of the enzyme in gastric, colon and renal tumours [48]. After these findings, an independent study from Sørensen *et al.* came to verify the importance of IDO2 in tumour escape and survival [49]. According to their work, in peripheral blood samples obtained from both healthy donors and cancer patients, there was noticed a spontaneous cytotoxic T-cell reactivity against IDO2. These T cells were shown to be cytotoxic effector cells that recognize and kill tumour cells [49]. Although IDO2 is a relatively newly discovered enzyme, findings suggest that it is an important enzyme in cancer biology.

1.9 The crystal structures of TDO and IDO proteins

Crystal structures of two TDOs and one IDO have been reported so far. While the two TDO structures come from bacterial species, *Ralstonia metallidurans* TDO (rmTDO) [31] and *Xanthomonas campestris* TDO (xcTDO) [32], the IDO structure is from *Homo sapiens* (hIDO) [50]. Details regarding these crystal structures are presented in table 1.2.

Enzyme	Active site ligand	Resolution (Å)	PDB code	UNIPROT
xcTDO [32]	None, L-Trp, 6-F-Trp	2.7, 1.6 and 1.8	2NW7, 2NW8, 2NW	Q8PDA8
rmTDO [31]	None	2.4	2N0X	Q1LK00
hIDO [50]	4-Phenylimidazole, CN^-	2.3 and 3.4	2D0T, 2D0U	P14902

Table 1.2: Crystallographic data for the TDO and IDO crystal structures.

1.9.1 TDO crystal structure

X. campestris TDO (xcTDO) and *R. metallidurans* TDO (rmTDO) share 47% sequence identity [51]. Despite the fact that both of these are bacterial enzymes and share less than 40 % identity with the human TDO, the xcTDO structure in particular provides great insight into the structure-function relationship. In contrast with rmTDO, xcTDO has been crystallised in the ferrous active form with the substrate bound, something crucial for better understanding of the enzyme and its function. In addition to this, the xcTDO structure is at a higher resolution. For those reasons, xcTDO will be the only TDO structure discussed below. Each TDO monomer is composed of twelve α-helices (αA-αL) and no β-strands [32] (fig. 1.9). Helices αB and αC are highly hydrophobic and are located in the interface between two of the monomers.

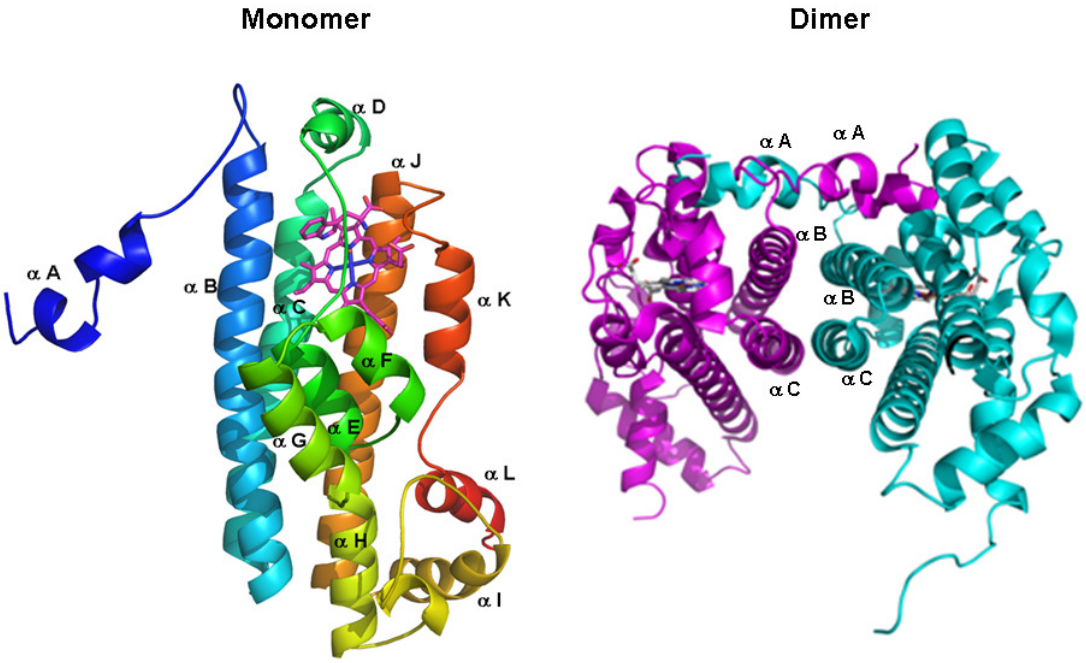

Figure 1.9: Illustration of the xcTDO monomer and dimer. The monomer is composed of twelve α-helices, and part of helix αA of one monomer contributes to formation of the substrate binding site in the adjacent monomer, leading to a 'dimer of dimers' arrangement for the tetramer (*taken from ref. 51 and 52*).

In addition to those regions forming the tetramer interface it is interesting to observe that adjacent monomers are intimately associated *via* a segment of 20 residues from their N-termini, including helix αA (fig 1.9) [(32)]. A number of these residues have essential involvement in active site functionality. With this in mind the TDO tetramer is perhaps best described as a dimer of dimers. Similar to helix αA, the helices αB and αD and loops αD-αE and αJ-αK play an important role in substrate binding and stability. More specifically, the carboxyl group of L-Trp displays an ion-pair interaction with arginine 117, and is hydrogen bonded to tyrosine 113 and threonine 254 (fig. 1.10). The substrate ammonium group is recognized by the 7-propionate group of the heme, while also forming hydrogen bonds with threonine 254 and a

water molecule that is present in the active site of the binary complex. The nitrogen atom of the indole ring is hydrogen-bonded to histidine 55, a conserved amino acid in all TDOs. Finally, the indole ring is held in place and stabilized by van der Waals interactions with a number of hydrophobic amino acids. Some of those, such as tyrosines 24 and 27, and leucine 28, come from the N- terminal segment of the adjacent monomer.

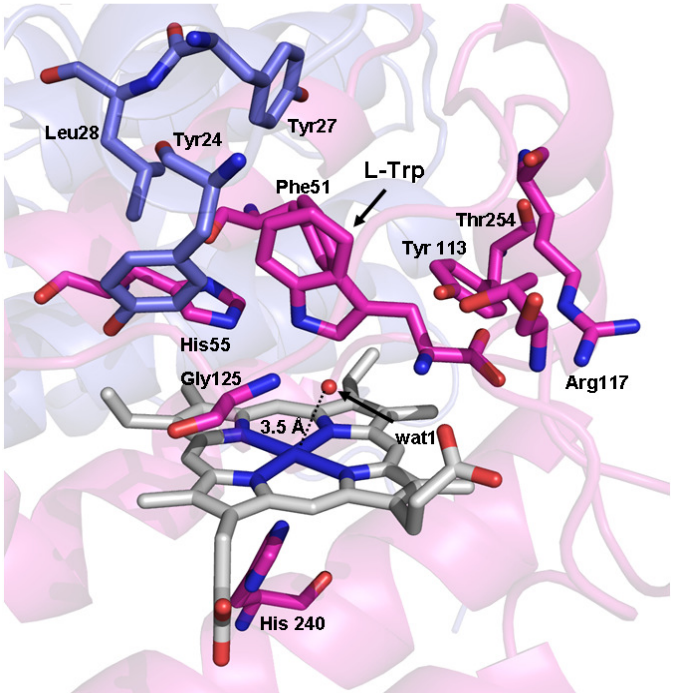

Figure 1.10: XcTDO active site and the interaction with L-Trp (*taken from ref. 52*)
The crystal structure of reduced TDO revealed eight L-Trp binding sites per tetramer [32].

Four of these are located in the active site of each monomer, while the other four are in the area of the tetramer interface (fig. 1.11). Binding of L-Trp in the interface area of the tetramer could suggest a potential allosteric role. Nevertheless the enzyme's kinetic findings showed no allosteric effect [32], and as such any allosteric behaviour in xcTDO is yet to be proved.

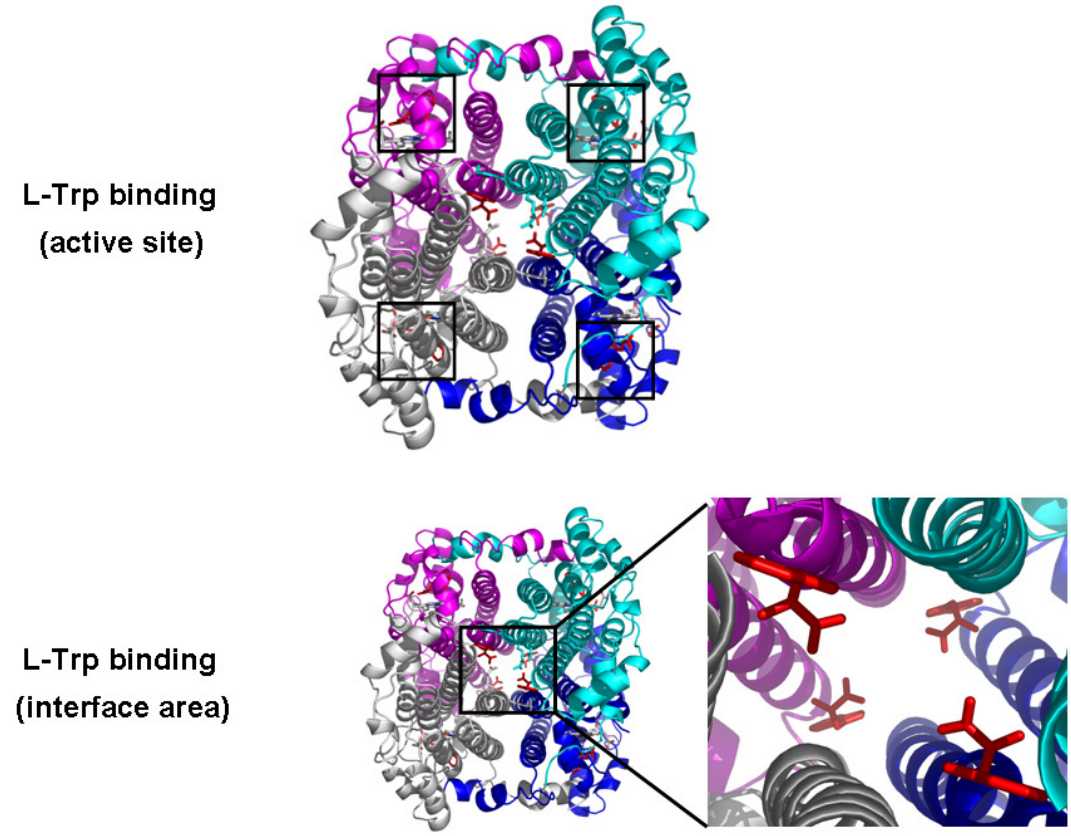

Figure 1.11: The xcTDO tetramer and the eight L-Trp binding sites. Four L-Trp molecules bind in the active sites of the four monomers while the other four can be seen in the interface area of the tetramer (*taken from ref. 51*).

1.9.2 IDO crystal structure

The crystal structure of human IDO was published in 2006 by Sugimoto *et al*., and it is the only eukaryotic IDO structure available [50]. Despite this important discovery, the structure yields little information about the substrate's interactions at the active site. Both of the ligands present in the structures of IDO, 4-phenylimidazole (4-PI) and cyanide (CN^-), are inhibitors of the enzyme, binding to the heme iron. The crystal structures of IDO in complex with 4-phenylimidazole and cyanide were solved at 2.3 and 3.4 Å respectively and for this reason only the 4-PI-bound structure will be discussed below.

The human IDO monomer can be considered as two domains; the large (C-terminal) and the small (N-terminal) domains (fig. 1.12). The large domain is shown in green, the small one in blue. In a cavity between them lies the heme moiety (yellow) with 4-PI directly coordinated to the heme iron.

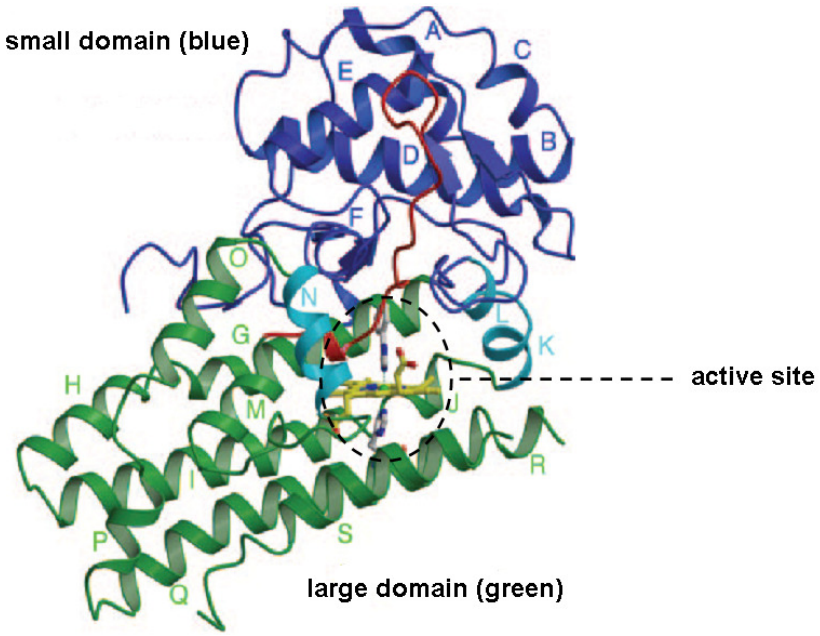

Figure 1.12: IDO crystal structure with 4-PI bound (*taken from ref. 50*)

The large domain of hIDO is composed of 13 α-helices and two 3_{10} helices while the small domain consists of six α-helices, three 3_{10} helices and two β-sheets. The domains interact *via* helices K, L and N, which are shown in cyan, and are joined together *via* a loop region (shown in red) which lies above the sixth coordination site of the heme.

In the active site of the 4-PI-bound structure the ligand is surrounded by a number of polar and non polar amino acids (fig. 1.13). One of the helices of the large domain, helix Q, interacts directly with the heme iron providing an imidazole group (the side chain of His 346) as endogenous ligand. In order to probe the roles of some of these residues, site-directed mutagenesis of Ser167, Cys129 and Phe163 to alanine (S167A, C129A and F163A) showed no significant effect on enzyme activity and thus providing information regarding the function of these amino acids in the catalytic mechanism [(50)]. In contrast, substitution of Phe226 and Arg231 by alanine (F226A and R231A) caused a dramatic drop in the enzymatic activity, suggesting the involvement of these amino acids in L-Trp recognition. More specifically, mutation of Phe226 and Arg231 had as consequence the drop of the activity ($kcat/K_m$) by a factor of 97-fold and 55-fold respectively [(50)].

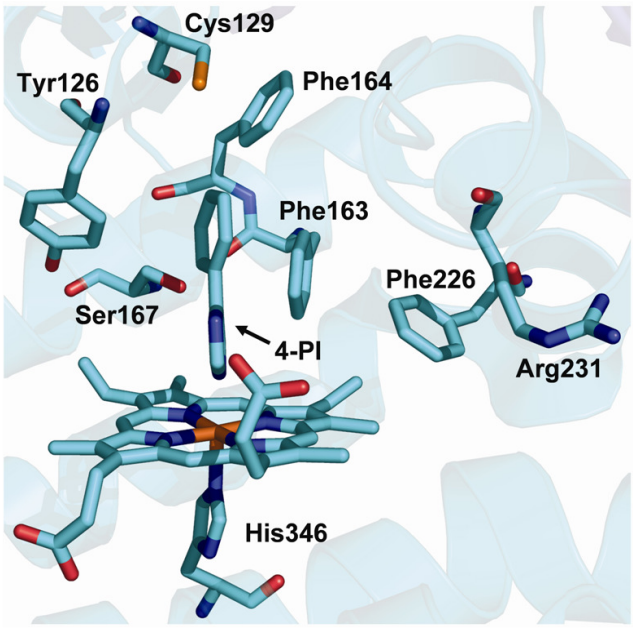

Figure 1.13: The IDO active site in the presence of a heme-specific inhibitor 4-Phenylimidazole (*taken from ref. 52*)

1.10 Binary and Ternary complexes in TDO and IDO

Formation of the catalytically-active TDO ternary complex (Trp-Fe^{2+}-O_2) has been proposed to be an ordered process with L-Trp binding first, then O_2 [32]. Electrochemical studies have shown that ferrous TDO does not form a stable complex with dioxygen [34], while the ferric form does not bind dioxygen. In addition, when the heme iron is in the inactive, ferric form, substrate binding is disfavoured with respect to the ferrous form [32]. Reduction of TDO/IDO has been studied both *in vitro* and *in vivo*. *In vitro* reduction of TDO/IDO can be achieved *via* ascorbic acid and methylene blue [53]. *In vivo*, cytochrome b_5 has been proposed to fulfil this role [54]. In comparison with TDO, IDO appears to react with specific oxygen species in both ferrous and ferric forms. In contrast with TDO, IDO can bind either L-Trp or dioxygen first to form two distinct stable binary complexes [51]. Subsequent binding of dioxygen or L-Trp respectively will lead to the formation of the ternary complex. This is not the only difference between TDO and IDO. At the end of each catalytic cycle, IDO undergoes auto-oxidation, something that does not happen with TDO [55]. Therefore the continual re-reduction of IDO is a precondition for activity. Formation of the binary and ternary complexes is explained further in the following diagram (fig. 1.14).

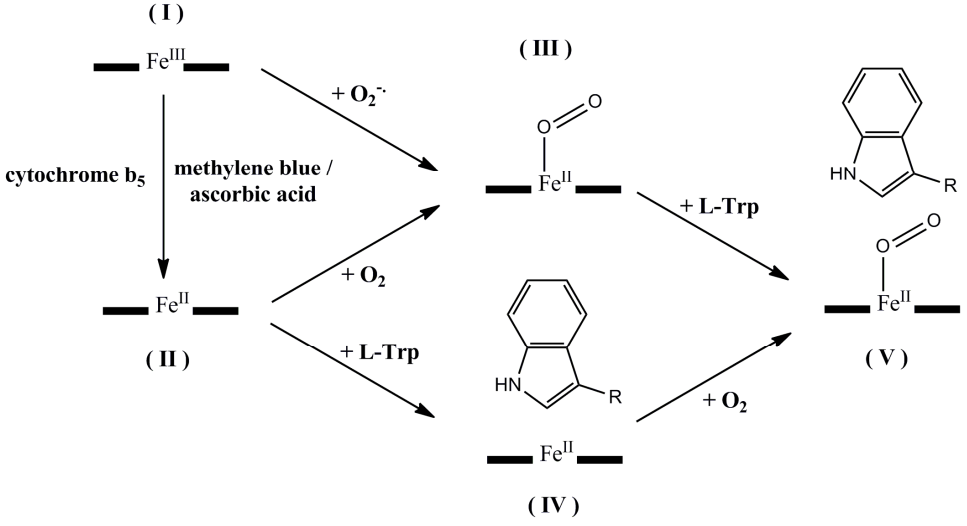

Figure 1.14: Formation of the binary and ternary complexes in TDO (I→II→IV→V) and IDO (both routes).

1.11 Catalytic Mechanism

The catalytic mechanism of N-formylkynurenine formation has been the subject of research for many years. Despite the fact that study of heme dioxygenases has continued for more than 70 years, since the discovery of TDO [26], the reaction mechanism of both TDO and IDO is still not clarified. As figure 1.15 illustrates, the first step of TDO and IDO dioxygenation can proceed *via* either an ionic or a radical mechanism. According to the first proposed mechanism (fig. 1.15A) [55], dioxygenation of tryptophan involves the action of an active site base. This active site base could be either an active site residue like histidine, or a water molecule, and serves as a nucleophile, abstracting a proton from the indole nitrogen. The base-catalysed deprotonation of the indole nitrogen can proceed *via* an ionic mechanism and demands the base to be in an appropriate position. The publication of the xcTDO crystal structure in 2007 revealed that the base-catalysed mechanism using a water molecule is unlikely because there is none present in the active site when L-Trp is bound [32]. From the currently available crystal structure of IDO, the occupancy of solvent in the active site upon substrate binding is unclear [50]. Despite this, the crystal structure of xcTDO has a histidine residue (His55) in an appropriate position that could serve the role of a base. The hIDO structure, on the other hand, contains a serine residue (Ser167) at the corresponding position, raising further questions [50]. Single point mutations of both Ser167 in IDO, and His55 in TDO, showed that neither of these are essential for catalytic activity, thus making a base-catalysed mechanism involving a protein-derived active site base unlikely [56, 57].

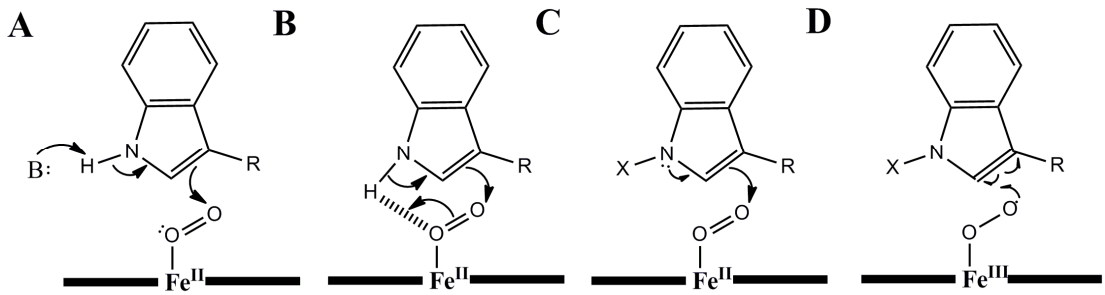

Figure 1.15: Oxygen activation proceeds via one of the four potential routes; **(A)** Base-catalysed, **(B)** concerted oxygen-ene, **(C)** direct electrophilic addition, **(D)** radical addition at (i) C2 or (ii) C3 (*taken from ref. 60*)

After the abandonment of the first scenario, it was proposed that dioxygen could play the role of the active site base in an "oxygen-ene"-type reaction (fig. 1.15B) [50]. This reaction mechanism was initially suggested because 1-methyltryptophan (1-MT) was found to be an inhibitor of IDO. In this way the methylation of the indole nitrogen is expected to prevent the initial deprotonation step and, therefore, turnover. However, it has been shown that while N-methylation affects the enzyme's catalytic activity, 1-MT can also serve as a substrate. These findings show that deprotonation of the indole nitrogen is not essential for activity and therefore reveals the weakness of the "oxygen-ene" type reaction [58].

Consequently, direct electrophilic addition of dioxygen is one of the two most likely mechanisms. Instead of deprotonation, the lone pair electrons of nitrogen can initiate the reaction as figure 1.15C illustrates. Addition of oxygen to either the C2 or C3 position of the electron-rich indole ring seems to be favourable. Regarding the last potential route (a radical mechanism), catalysis can proceed via direct addition of O_2 either to the C3 position or the C2 position of L-Trp (fig. 1.15D). Although both electrophilic and radical addition are the most likely to occur, neither is well-established.

Instead of incorporation of both oxygen atoms simultaneously, the most recent findings support the idea that dioxygen inserts into tryptophan in steps [59, 60]. Both of the last two oxygen activation processes (electrophilic and radical) are consistent with the mechanism proposed in figure 1.16. According to this mechanism, either electrophilic or radical routes lead to the formation of a ferryl heme species with concomitant formation of an epoxide intermediate species. The formation of a ferryl heme intermediate was first detected by Yeh and co-workers using resonance Raman methodology [61]. The epoxide intermediate was detected indirectly using mass spectrometry experiments [59]. During this study, Raven and co-workers identified a cyclic aminoacetal structure (m/z = 221) which was proposed to be a byproduct of the reaction that originates from collapse of the initially formed (and unstable) 2,3-epoxide by monooxygenation of L-Trp. In the proposed mechanism in fig 1.16, ring-opening of the epoxide intermediate is followed by the insertion into the indole ring of the second oxygen atom, and then ring cleavage for N-formylkynurenine formation.

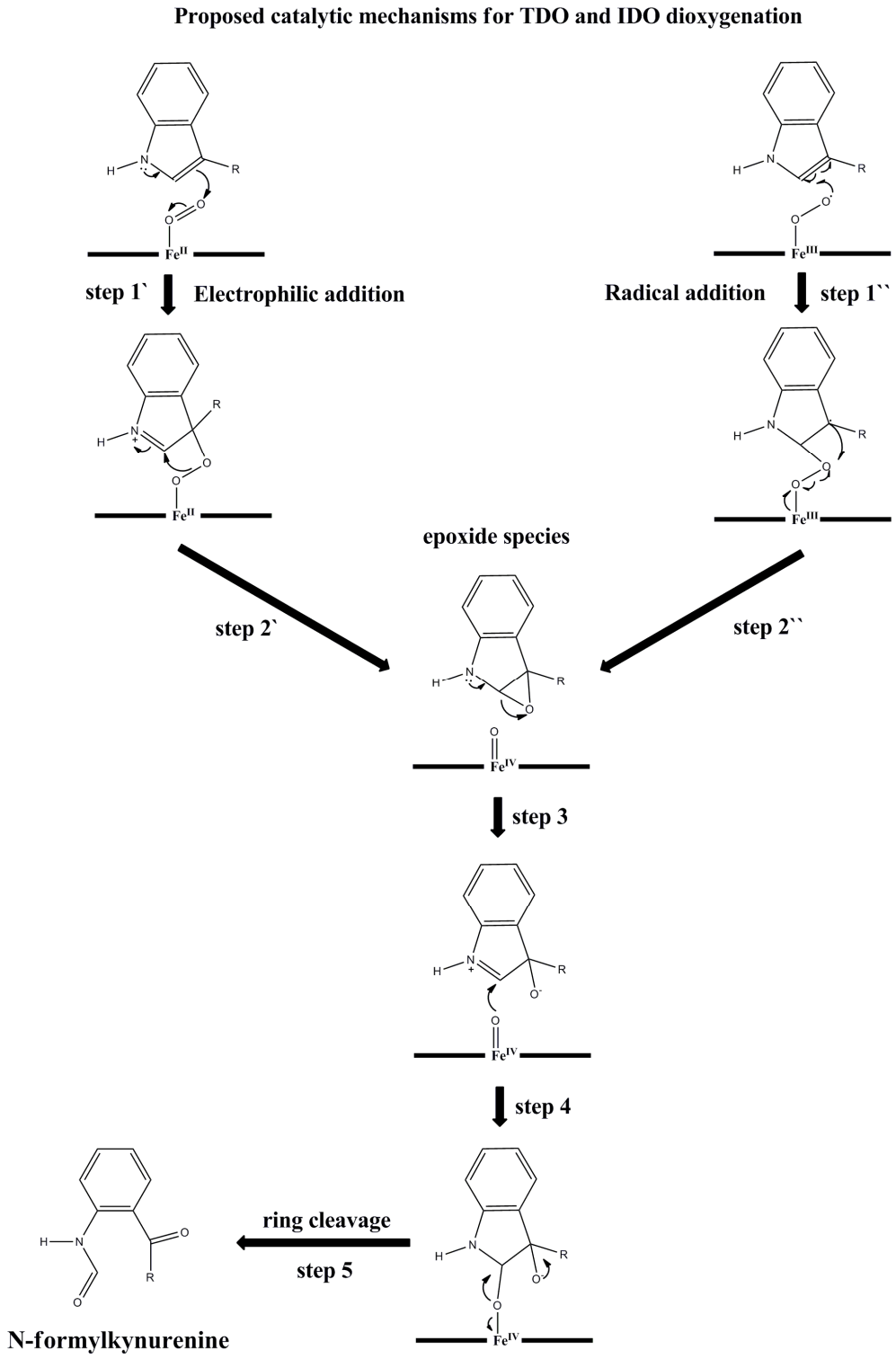

Figure 1.16: The proposed mechanism for N-formylkynurenine formation [59-61]

1.12 Inhibition studies

Inhibition of tryptophan dioxygenation in the first step of kynurenine pathway is of great interest to the pharmaceutical and medical communities, not only because of the rate-limiting nature of the reaction over the whole kynurenine pathway, but also because it manages the amount of L-Trp used for biosynthesis of neurotransmitter molecules (serotonin, melatonin). With the implication of roles for TDO [36], IDO [42] and IDO2 [48, 49] in cancer, the potential need for development of drugs to target these enzymes has arisen. While IDO2 is a newly-discovered enzyme with an unexplained catalytic behaviour (the turnover rate with L-Trp as substrate is unlikely to represent biologically-relevant activity) [62], only inhibitors of the well-studied TDO and IDO will be discussed. In the case of TDO, at this point it can be said that the list of identified inhibitors is not so impressive. This is likely due to the fact that TDO's immunomodulatory action was ambiguous until 2011 [36]. Nevertheless, the most potent TDO inhibitors published so far belong to the family of 3-(2-pyridylethenyl)-indoles, with inhibition constants between 30-100 nM (fig. 1.17) [63], [64]. Among the 3-(2-pyridylethenyl)-indoles that are shown below, 3-pyridyl and 4-pyridyl revealed the highest inhibition potency with inhibition constants of 40 nM and 30 nM respectively [63]. Most of the substitutions that had been introduced to these structures had a detrimental effect on TDO inhibition activity, especially substitutions at the indole-nitrogen. However, fluorine substitution in the 5 or 6 position of the indole ring was found to be well tolerated, conserving the inhibition constants between 30 nM and 50 nM [63].

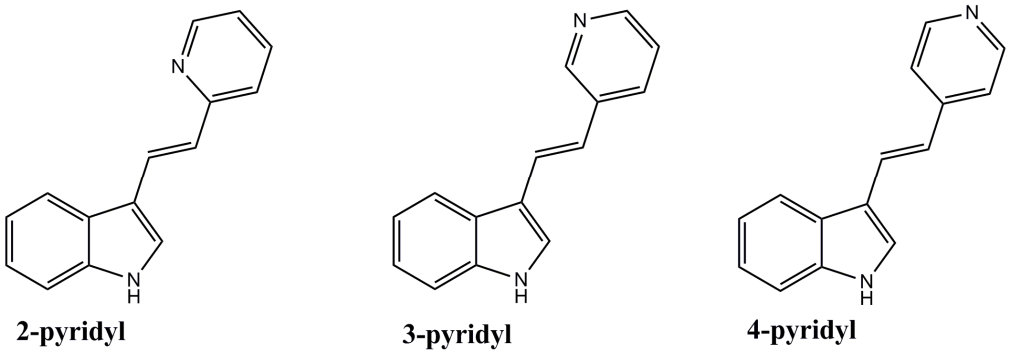

Figure 1.17: 3-(2-pyridylethenyl)-indoles as specific TDO inhibitors.

In contrast with TDO, the list of IDO inhibitors is longer and has greater chemical diversity (fig. 1.18).

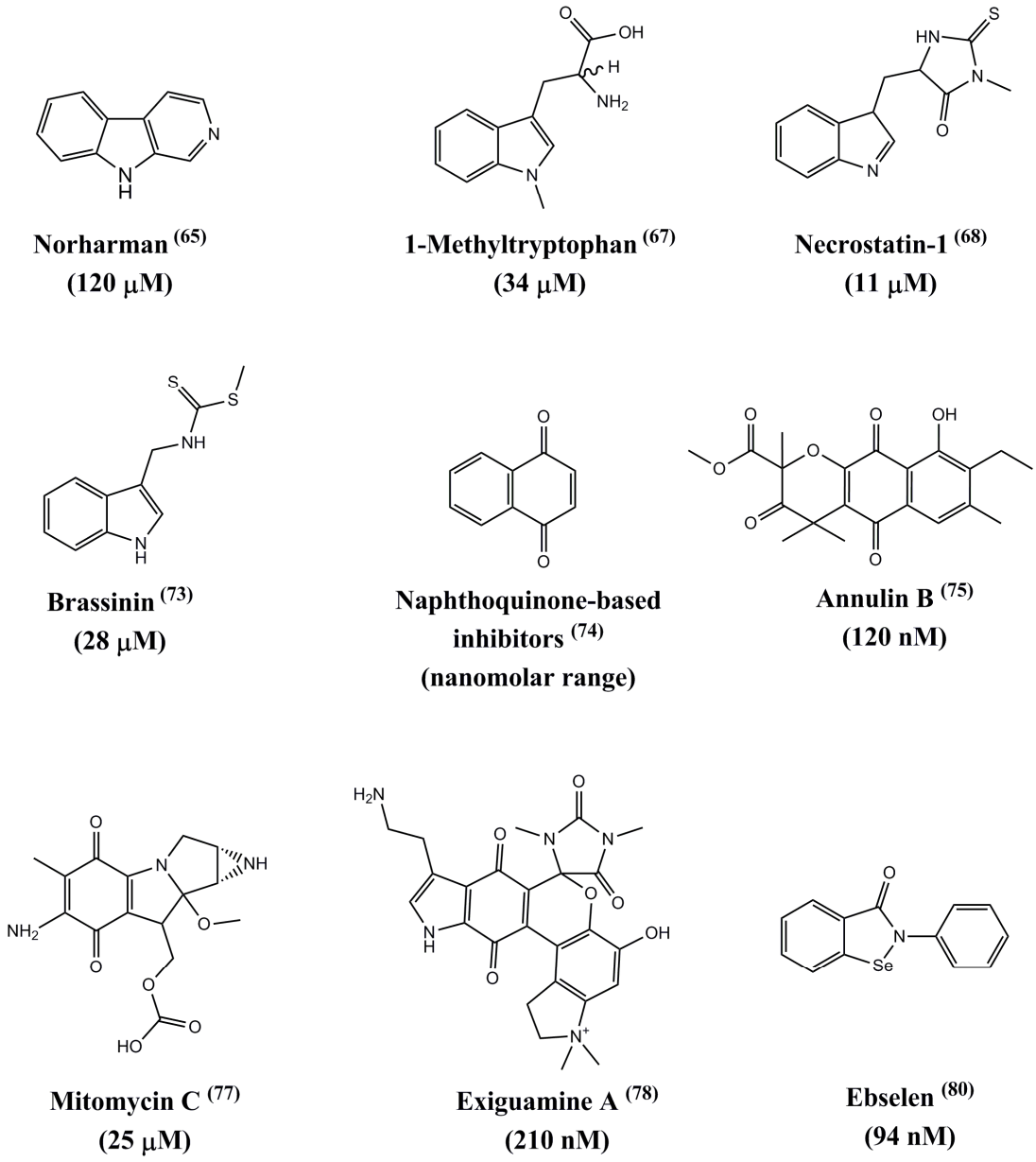

Figure 1.18: The most potent IDO inhibitors published so far.

Norharman (or β-carboline) is among the first published IDO inhibitors [65], with kinetic studies using rabbit intestinal IDO yielding an inhibition constant of 120 μM. Five years after the discovery of norharman, it was shown that the molecule is a competitive inhibitor of IDO, binding to the heme iron [66] (fig. 1.19). Despite the fact that the author of the original study reported norharman as a non-competitive inhibitor of IDO, its competition with O_2 for binding to the heme iron demonstrates a clear competitive character.

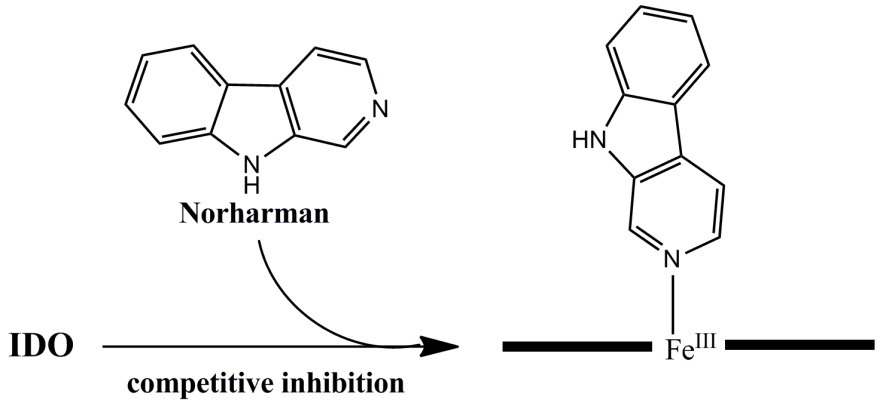

Figure 1.19: Inhibition of IDO by Norharman [66]

Two years after the identification of norharman as a non-specific heme binding inhibitor of IDO, Sono and co-workers published the discovery of a new IDO inhibitor, 1-methyltryptophan (1-MT) [67]. 1-MT is a tryptophan analogue with a methyl group on the nitrogen of the indole ring (fig. 1.18). Because of its structure, 1-MT is a competitive inhibitor of L-Trp with an inhibition constant of 34 μM [68]. It exists in two stereoisomeric forms, 1-methyl-L-tryptophan (1-Me-L-Trp) and 1-methyl-D-tryptophan (1-Me-D-Trp), each of which has unique inhibition behaviour against IDO. Among the IDO inhibitors that have been reported up to date, 1-MT is the most famous and well-studied. This is related with the favourable pharmacokinetic characteristics of the molecule, such as oral availability, low toxicity, low clearance and low protein binding [69]. In addition to those characteristics, 1-MT is a selective IDO inhibitor with no inhibitory activity against TDO. As the model in figure 1.20 illustrates, the active site of xcTDO contains a histidine residue (His55), which in the presence of L-Trp forms hydrogen bonds with

the nitrogen of the indole ring. Methylation of the indole nitrogen may disrupt this hydrogen bonding causing a clash of the histidine residue with the methyl group of 1-MT. This phenomenon does not occur in IDO because the equivalent amino acid is serine (Ser167). Despite the favourable pharmacokinetic characteristics of 1-MT, *in vivo* studies showed that it can retard tumour growth but not prevent progression [43]. These findings raised concerns about its usefulness as monotherapeutic drug. Combination of 1-MT with other chemotherapeutic drugs showed that the molecule can act synergistically for inhibition of IDO [70], but as yet only 1-Me-Trp (1MT) has been used in clinical trials. Conflicting results show that the function of 1-Me-Trp *in vivo* is not fully understood [70]. While 1-Me-Trp exists as two stereoisomers (D-, L-), it is unclear what the effect of each isomer is in the human body.

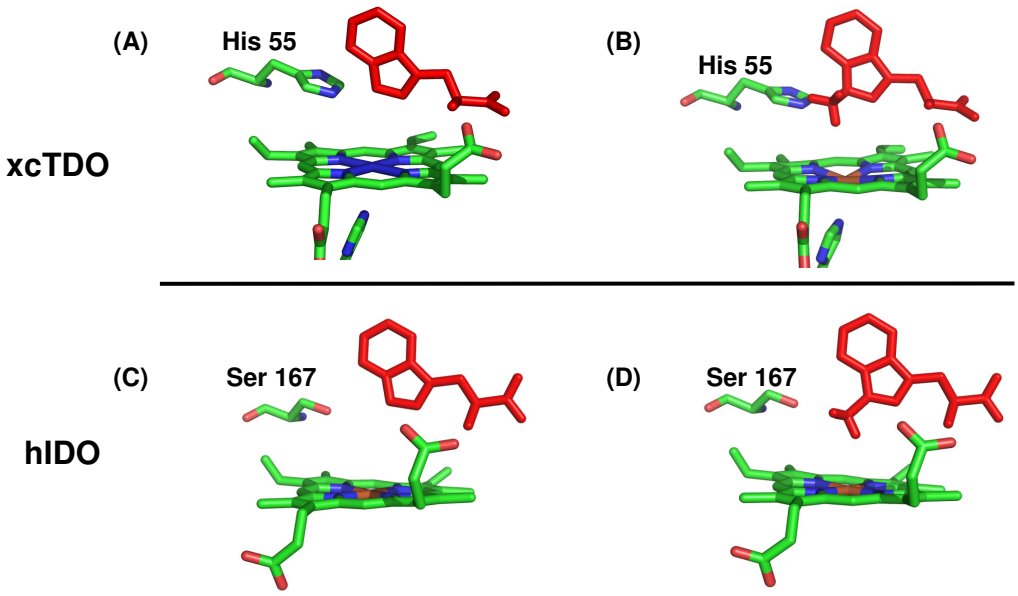

Figure 1.20: (A) The crystal structure of xcTDO with L-Trp bound [32]. (B) A model that is based on the published crystal structure (A) and explains the potential orientation of 1-MT in the active site of xcTDO. The methyl group of 1-MT clashes with the active site residue His55 causing steric effect. The models (C) and (D) propose the potential binding of L-Trp (C) and 1-MT (D) in the active site of hIDO. The presence of Ser167 (hIDO active site) allows 1-MT to interact with the IDO active site, something which cannot occur in TDO due to the presence of His55 (*The models B, C and D were kindly provided by Dr. Sarah J. Thackray*).

In vitro examination of the two stereoisomers revealed that the L-enantiomer is a significantly better inhibitor of hIDO than the D-enantiomer. 1-Methyl-L-tryptophan is found to inhibit IDO with K_i = 19 μM while 1-methyl-D-tryptophan has no effect at concentrations up to 100 μM [(71)]. However, *in vivo* studies showed a significantly higher efficiency of the D-isomer in reversing the suppression of T cells. Studies on mice demonstrated that 1-Me-D-Trp is more effective as an anticancer agent in chemo-immunotherapy regimens using particular chemotherapeutic agents [(71)]. These findings clearly show the implication of the D-enantiomer in cancer biology. The antitumour property of 1-Me-D-Trp could not be explained until the discovery of IDO2, leading to the suggestion that the inhibitory action of 1-Me-D-Trp could be related with IDO2. The presence of hIDO2 mRNA in particular cancers, in combination with its distinct characteristics indicates a potential immunomodulatory role which is unrelated to that of IDO. Inhibition findings show that 1-Me-D-Trp inhibits IDO2 but it is ineffective against recombinant IDO [(72)].

Attempts to identify other inhibitors of IDO, with higher potency than 1-MT, led to interest in methylthiohydantoin-DL-tryptophan (MTH-Trp) or necrostatin-1. MTH-Trp is a competitive inhibitor of IDO with an inhibition constant of 11 μM [(68)]. Cell-based assays showed that the molecule is 20-fold more potent than 1MT, more soluble in aqueous solution and more rapidly cleared from serum. In terms of the oral bioavailability of MTH-Trp, it has been found that is equally as available as 1-MT [(68)].

Another class of IDO inhibitors is related to the plant extract brassinin [(73)]. Brassinin is natural occurring product with anticancer properties. Brassinin and its 5-bromo substituted derivative behave as competitive inhibitors of IDO with inhibition constants of 28 μM and 25 μM respectively [(73)]. Cell-based assays showed that both brassinin and 5-bromo-brassinin are bioavailable inhibitors of IDO with EC_{50} (half maximal effective concentration) values of 38 μM and 24 μM respectively.

Another large set of IDO inhibitors are naphthoquinone-based. The idea of developing naphthoquinone-based inhibitors was taken from the natural product menadione (fig. 1.21), which was found to be active in mouse tumour models, inhibiting IDO [(74)].

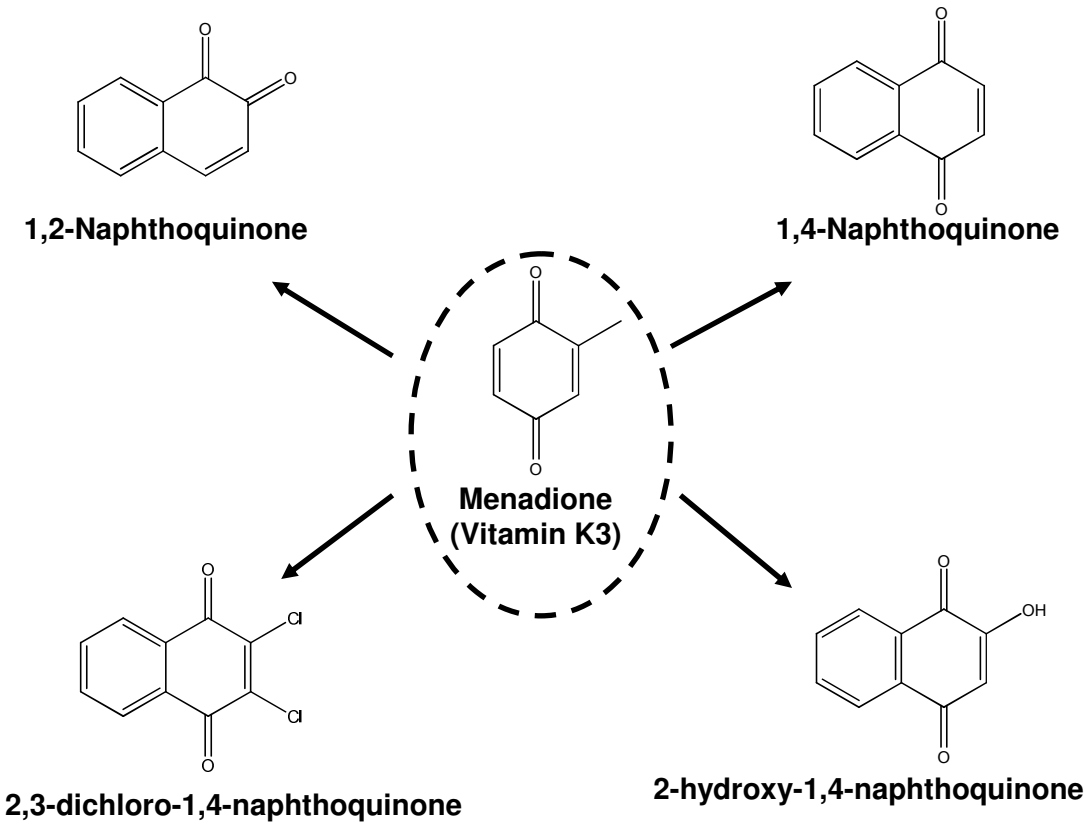

Figure 1.21: Representative naphthoquinone-based inhibitors that were used by Kumar *et al.* as inhibitors of IDO [(74)].

Screening of these molecules demonstrated that motifs such as 1,2-naphthoquinone or 1,4-naphthoquinone are essential for IDO inhibition (fig. 1.21). Substitutions on either benzene or quinone rings do not eliminate the inhibition potency of the molecule. In contrast, the benzoquinone derivatives were inactive, highlighting the necessity of a benzene-quinone structure for activity as an IDO inhibitor. The results of this study showed that these molecules behave as non-competitive inhibitors with inhibition constants significantly lower than those reported for 1-MT, MTH-Trp and brassinin (the most potent inhibitors revealed values for K_i = 61-70 nM) [(74)].

Within the list of IDO inhibitors there are a series of natural products coming from the marine hydroid *Garveia annulata*. Among those molecules that have been identified as IDO inhibitors are annulin A, B and C (K_i = 690 nM, 120 nM and 140 nM respectively), 2-hydroxygarveatin E (K_i =1.4 μM) and garveatin A, C and E (K_i =3.2 μM, 1.2 μM and 3.1 μM respectively) (fig. 1.22) [75].

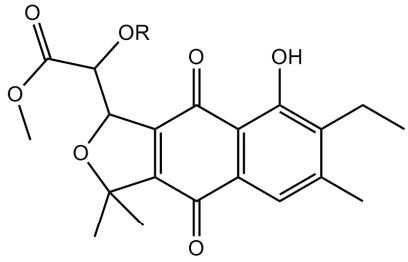

R = H Annulin A (690 nM)
R = Me Annulin C (140 nM)

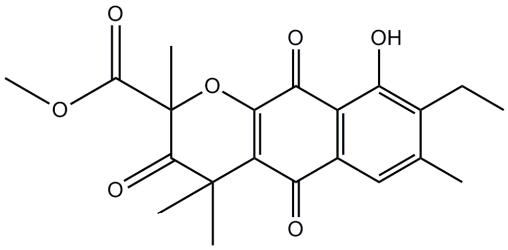

Annulin B (120 nM)

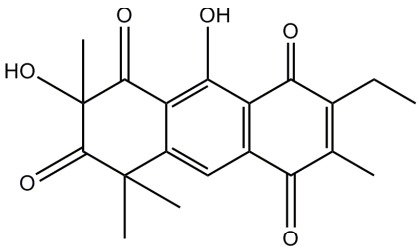

2-Hydroxygarveatin E (1.4 μM)

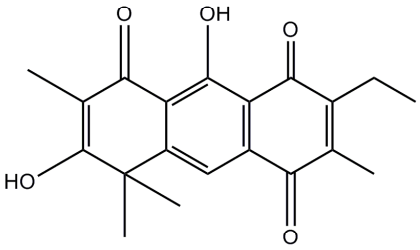

Garveatin E (3.1 μM)

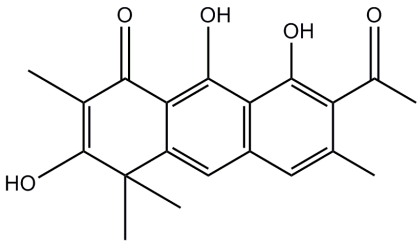

Garveatin A (3.2 μM)

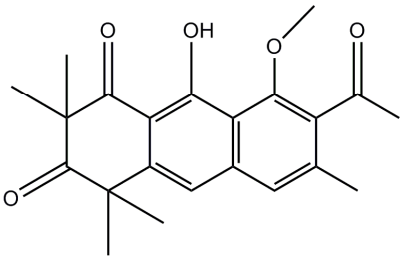

Garveatin C (1.2 μM)

Figure 1.22: Natural product extracts with good inhibition potencies against IDO [75].

Like annulins, mitomycin C also contains the benzoquinone moiety (fig. 1.18). Mitomycin C is another natural occurring product, isolated from *Streptomyces*, with well-studied chemotherapeutic properties. It is believed that its antitumour potency is related to the ability of mitomycin C to form interactions with DNA. These interactions could be either interstrand (between two adjacent DNA strands) or intrastrand (between two points of the same DNA strand) [(76)]. The consequence of this cross-linking is the inhibition of DNA synthesis. Because of this property, mitomycin C is approved, by FDA, to be used alone or with other drugs for treatment of gastric (stomach) and pancreatic adenocarcinoma. More details about the molecule can be found at http://www.cancer.gov/cancertopics/druginfo/mitomycinc. In addition to this, mitomycin C (fig. 1.18) is also a reported IDO inhibitor. Findings show that the molecule inhibits IDO in an uncompetitive fashion with an inhibition constant of 25 μM [(77)]. *In vitro* screening for identification of new IDO inhibitors revealed another natural product with high inhibition potency. Exiguamine A, a methanol extract of the sponge *Neopetrosia exigua*, was found to inhibit IDO with K_i = 210 nM [(78)]. Based on the fact that exiguamine A combines some of the structural characteristics of tryptamine and annulin C (fig. 1.23), a number of new IDO inhibitors were synthesized with structures more simple than exiguamine A. Consequently, the newly-synthesized IDO inhibitors revealed inhibition potencies between 190 nM and 10.9 μM [(79)].

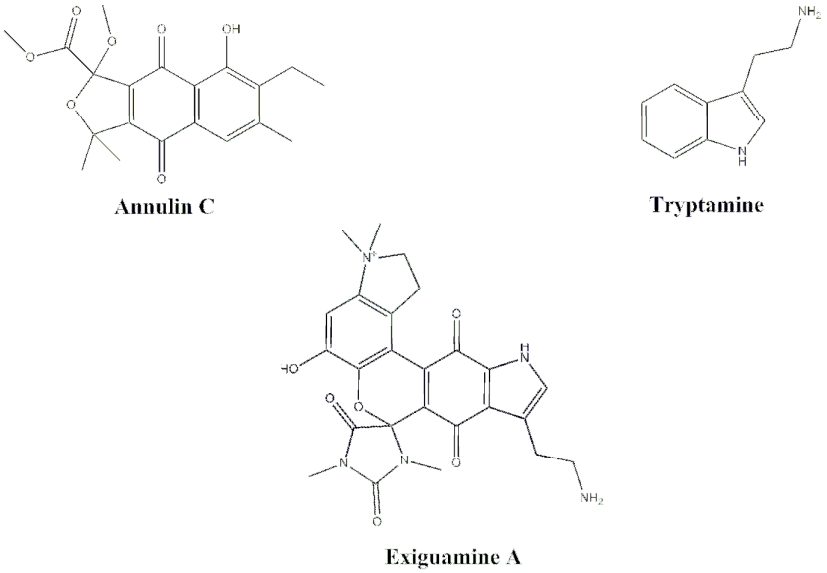

Figure 1.23: Exiguamine A combines structural features of tryptamine and annulin C.

In the same list of IDO inhibitors, ebselen should be included. Ebselen, which is also known as 2-phenyl-1,2-benzisoselenazol-3(2H)-one, is found to inhibit IDO with an inhibition constant of 94 nM [(80)]. Experimental results showed that the molecule reacts with multiple cysteine residues of IDO, something which inactivates the enzyme (fig. 1.24). However, removal of ebselen can reverse the inhibition effect, restoring IDO enzymatic activity. These findings suggest that some cysteine residues (eight in total) play a crucial role in the enzyme's stability.

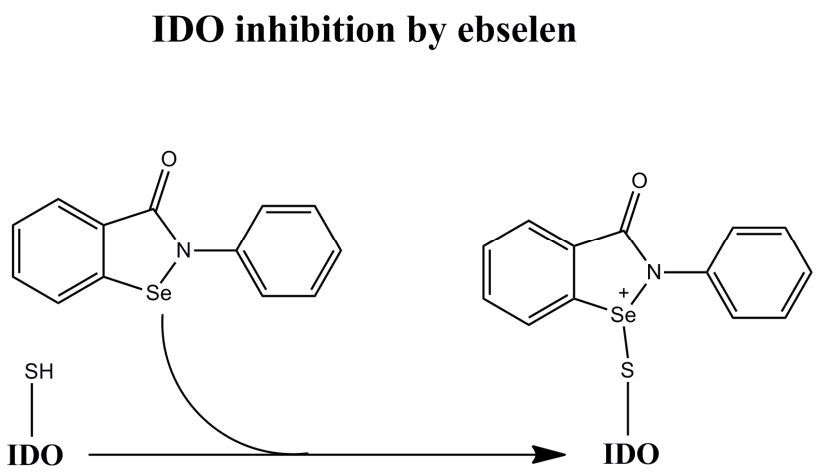

Figure 1.24: Illustration of IDO inactivation by ebselen [(80)].

1.13 Objectives

The implication of TDO and IDO in severe disorders, including tumour growth, is well documented. In the last few years attention has begun to focus on the development of compounds that could inhibit the action of these enzymes. Numerous inhibitors have been reported so far but only one has been used in clinical trials. Despite its favourable pharmacokinetic characteristics and the specificity against IDO, 1-MT is not the ideal inhibitor. Whereas 1-MT is found in two stereoisoforms, it is unclear how each stereoisomer behaves against IDO and IDO2. The actual inhibition potency of 1-Me-L-Trp and 1-Me-D-Trp *in vivo* is yet to be evaluated. The early identification of IDO as an immunomodulatory enzyme focused interest in the development of IDO inhibitors, while TDO was considered to be of much lower priority. This is particularly obvious if we consider that the best TDO inhibitors published were published in the 1990s, with little recent literature forthcoming.

The aim of this thesis is to identify novel inhibitors for both IDO and TDO that can be used as template for the development of a new class of therapeutic agents. As a starting point, published hTDO and hIDO were evaluated. Using the knowledge gained from previous studies, and the recently available structural knowledge of TDO and IDO, a series of potential inhibitors was screened and characterised. Central to this approach was the kind provision of access to the chemical repository collection of synthetic molecules and pure natural products held by the National Cancer Institute (USA).

In addition to this, characterisation of the selectivity of 1-MT inhibition is another major subject of the thesis. The recent discovery of IDO2 and its reported expression in particular cancers has raised a lot of questions about its biological role. Despite that, the fundamental biochemical characteristics of the enzyme are still to be assessed. Through the *in vitro* biochemical characterization of IDO2, the potential biological role of the enzyme in terms of substrate specificity and 1-MT inhibition selectivity will be evaluated. The findings will be compared with the corresponding results for IDO and potential unique characteristics of either IDO or IDO2 will be clarified.

1.14 References

(1) Edsall J.T., *Blood and hemoglobin: the evolution of knowledge of functional adaption in a biochemical system*, ***J History Biol***, 1972, 5, 205–257

(**2**) Charles J.R. and Brian R. G., *Heme Protein Assemblies*, ***Chem. Rev.,*** 2004, 104, 617-649

(3) Wu C.K., Dailey H. A., Rose J. P., Burden A., Sellers V. M. and Wang B.C., *The 2.0 Å structure of human ferrochelatase, the terminal enzyme of heme biosynthesis*, ***Nature Structural Biology***, 2001, 8,156-160

(4) Sono M., Roach M.P., Coulter E.D., and Dawson J.H., *Heme-Containing Oxygenases*, ***Chem. Rev.***, 1996, 96, 2841–2887

(5) Millett E.S., Efimov I., Basran J., Handa S., Mowat C.G. and Raven E.L., *Heme-containing dioxygenases involved in tryptophan oxidation*, ***Curr. Opin. Chem. Biol.***, 2012, 16, 60-6

(6) Hayaishi O., *An odyssey with oxygen*, ***Biochemical and Biophysical research communication***, 2005, 338, 2-6

(7) Hayaishi O., Katagiri M. and Rothberg S., *Mechanism of the pyrocatechase reaction*, ***J. Am. Chem. Soc.***,1955, 77, 5450-5451

(8) Mason H. S., Fowlks W. L., and Peterson E., *Oxygen transfer and electron transport by the phenolase complex*, ***J. Am. Chem. Soc.***,1955,77, 2914-2915

(9) Boyer P.D., *The enzymes; Oxidation – Reduction*, 1975, 3rd edition, Vol. XII, Academic Press, New York

(10) Stone T.W. and Darlington L.G., *Endogenous kynurenines as targets for drug discovery and development*, ***Nature rev. drug discovery***, 2002, 1, 609-620

(**11**) Lucki I., *The Spectrum of Behaviors Influenced by Serotonin*, ***Biol. Psychiatry***, 1988, 44, 151-162

(12) Badawy A.A.-B., *Tryptophan metabolism in alcoholism*, ***Nutrition Research* Reviews**, 2002, 15, 123–152

(**13**) Belenky P., Bogan K.L. and Brenner C., *NAD+ metabolism in health and disease*, ***Trends Biochem. Sci.***, 2007, 32, 12-19

(14) Lin S.J and Guarente L., *Nicotinamide adenine dinucleotide, a metabolic regulator of transcription, longevity and disease*, ***Current Opinion in Cell Biology***, 2003, 15, 241–246

(**15**) Chen Y. and Guillemin G.J., *Kynurenine Pathway Metabolites in Humans: Disease and Healthy States*, ***International Journal of Tryptophan Research***, 2009, 2, 1-19

(**16**) Erhardt S., Olsson S.K. and Engberg G., *Pharmacological Manipulation of Kynurenic Acid*, ***CNS drugs***, 2009, 23, 91-101

(17) Moroni F., Russi P., Lombardi G., Beni M. and Carlh V.**,** *Presence of Kynurenic Acid in the Mammalian Brain*, ***Journal of Neurochemistry***, 1988, 51, 177-180

(18) Hiraku Y., Inoue S., Oikawa S., Yamamoto K., Tada S., Nishino K., Kawanishi S., *Metal-mediated oxi-dative damage to cellular and isolated DNA by certain tryptophan metabolites*, ***Carcinogenesis***, 1995, 16, 349 – 356

(19) Grant R.S., Coggan S.E. and Smythe G.A., *The Physiological Action of Picolinic Acid in the Human Brain*, ***International Journal of Tryptophan Research***, 2009, 2, 71–79

(20) Heyes M.P., Brew B.J., Martin A., Price R.W., Salazar A.M., Sidtis J.J., Yergey J.A., Mouradian M.M., Sadler A.E., Keilp J., Rubinow D. and Markey S.P., *Quinolinic acid in cerebrospinal fluid and serum in HIV-1 infection: relationship to clinical and neurologic status*, ***Ann. Neurol.***, 1991, 29, 202–209

(21) Sanni L.A., Thomas S.R., Tattam B.N., Moore D.E., Chaudhri G., Stocker R. and Hunt N.H., *Dramatic changes in oxidative tryptophan metabolism along the kynurenine pathway in experimental cerebral and noncerebral malaria*, ***Am. J. Pathol.***, 1998 52, 611–619

(22) Saito K., Nowak T.S., Markey S.P., and Heyes M.P., *Mechanism of delayed increases in kynurenine pathway metabolism in damaged brain regions following transient cerebral ischemia*, ***J. Neurochem.***, 1993, 60, 180–192

(23) Schwarch R., Whetsell Jr W.O. and Mangano R.M., *Quinolinic acid: an endogenous metabolite that produces axion-sparing lesions in rat brain*, ***Science***, 1983, 219, 316-18

(24) Kim J.P., *Quinolinate neurotoxicity in cortical cell culture*, ***Neuroscience***, 1987, 23, 423-432

(25) Takikawa O., *Clinical aspects of indoleamine 2,3-dioxygenase (IDO)-initiated tryptophan metabolism: IDO is a target of drug discovery for various diseases*, ***International Congress Series***, 2007, 1304, 290–297

(26) Kotake Y. and Masayama, I., *The intermediary metabolism of tryptophan. XVIII. The mechanism of formation of kynurenine from tryptophan*, ***Z. Physiol. Chem.***, 1936, 243, 237–244

(27) Murray M.F., *The Human Indoleamine 2,3-Dioxygenase Gene and Related Human Genes*, ***Current Drug Metabolism***, 2007, 8, 197-200

(28) Comings D.E., Muhleman D., Dietz G., Sherman M. and Forest G.L., *Sequence of human tryptophan 2,3-dioxygenase (TDO2): presence of a glucocorticoid response-like element composed of a GTT repeat and an intronic CCCCT repeat*, ***Genomics***, 1995, 29, 390-396

(29) Maezono K., Tashiro K. and Nakamura T., *Deduced primary structure of rat tryptophan-2, 3-dioxygenase*, ***Biochem Biophys Res Commun.*** , 1990, 170, 176-81

(30) Bertazzo A., Ragazzi E., Biasiolo M., Costa C.V.L. and Allegri G., *Enzyme activities involved in tryptophan metabolism along the kynurenine pathway in rabbits*, ***Biochemica et Biophysica Acta***, 2001, 1527, 167-175

(31) Zhang Y., Kang S.A., Mukherjee T., Bale S., Crane B.R., Begley T.P. and Ealick S.E., *Crystal structure and mechanism of tryptophan 2,3-dioxygenase, a heme enzyme involved in tryptophan catabolism and in quinolinate biosynthesis*, ***Biochemistry***, 2007, 46, 145-155

(32) Forouhar F., Anderson J.L., Mowat C.G., Vorobiev S.M., Hussain A., Abashidze M., Bruckmann C., Thackray S.J., Seetharaman J., Tucker T., Xiao R., Ma L.C., Zhao L., Acton T.B., Montelione G.T., Chapman S.K., Tong L., *Molecular insights into substrate recognition and catalysis by tryptophan 2,3-dioxygenase*, ***Proc. Natl. Acad. Sci.***, 2007, 104, 473-478

(33) Ishimura, Y., *L-Tryptophan 2,3-dioxygenase (tryptophan pyrrolase) (Pseudomonas fluorescens)*, ***Methods in Enzymology***, 1970, 17, 429-434

(34) Basran J., Rafice S.A., Chauhan N., Efimov I., Cheesman M.R., Ghamsari L., and Raven E.L., *A Kinetic, Spectroscopic, and Redox Study of Human Tryptophan 2,3-Dioxygenase*, ***Biochemistry***, 2008**,** 47, 4752–4760

(35) Batabyal D. and Yeh S.R., *Human Tryptophan Dioxygenase: A comparison with Indoleamine 2,3-Dioxygenase*, ***J. Am. Chem. Soc.***, 2007, 129,15690-15701

(36) Opitz C.A., Litzenburger U.M., Sahm F., Ott M., Tritschler I., Trump S., Schumacher T., Jestaedt L., Schrenk D., Weller M., Jugold M., Guillemin G.J., Miller C.L., Lutz C., Radlwimmer B., Lehmann I., Deimling A.V., Wick W. and Platten M., *An endogenous tumour-promoting ligand of the human aryl hydrocarbon receptor*, ***Nature***, 2011, 478, 197-203

(37) Pilotte L., Larrieu P., Stroobant V., Colau D., Dolušic E., Frédérick R., De Plaen E., Uyttenhove C., Wouters J., Masereel B. and Van den Eynde B.J., *Reversal of tumoral immune resistance by inhibition of tryptophan 2,3-dioxygenase*, ***PNAS***, 2012, 109, 2497–2502

(38) Yamamoto S. and Hayaishi O., *Tryptophan pyrrolase of rabbit intestine. D- and L-tryptophan-cleaving enzyme or enzymes*, ***J Biol Chem.***, 1967, 242, 5260-6

(39) Pfeffekorn E. R., *Interferon gamma blocks the growth of Toxoplasma gondii in human fibroblasts by inducing the host cells to degrade tryptophan*, ***Proc. Natl. Acad. Sci.***, 1984, 81, 908-912

(40) Yoshida R. and Hayaishi O, *Induction of pulmonary Indoleamine 2,3-dioxygenase by intraperitoneal injection of bacterial lipopolysaccharide*, ***Proc. Natl. Acad. Sci.***, 1978 75, 3998-4000

(41) Munn D.H., Zhou M., Attwood J.T., Bondarev I., Conway S.J., Marshall B., Brown C., Mellor A.L., *Prevention of allogeneic fetal rejection by tryptophan catabolism*, ***Science***, 1998, 281, 1191–1193

(42) Liu X., Newton R.C., Friedman S.M. and Scherle P.A., *Indoleamine 2,3 - Dioxygenase, an Emerging Target for Anti-Cancer Therapy*, ***Current Cancer Drug Targets***, 2009, 9, 938-952

(43) Löb S., Königsrainer A., Rammensee H.G., Opelz G. and Terness P., *Inhibitors of indoleamine-2,3-dioxygenase for cancer therapy: can we see the wood for the trees?*, ***Nature Reviews Cancer***, 2009, 9, 445-452

(44) Frumento G., Rotondo R., Tonetti M., Damonte G., Benatti U. And Ferrara G.B., *Tryptophan-derived Catabolites Are Responsible for Inhibition of T and Natural Killer Cell Proliferation Induced by Indoleamine 2,3-Dioxygenase*, ***J. Exp. Med***, 2002, 196, 459-468

(45) Metz R., DuHadaway J. B., Kamasani U., Laury-Kleintop L., Muller A.J. and Prendergast G., *Novel Tryptophan Catabolic Enzyme IDO2 Is the Preferred Biochemical Target of the Antitumor Indoleamine 2,3-Dioxygenase Inhibitory Compound D-1-Methyl-Tryptophan*, ***Cancer Res***, 2007, 67, 15

(46) Chang M.Y., Metz R., Muller A.J., Prendergast G.C.,
IDO2 (indoleamine 2,3-dioxygenase 2) (2009)Atlas Genet Cytogenet Oncol Haematol
URL: http://AtlasGeneticsOncology.org/Genes/IDO2ID44387ch8p11.html

(47) Ball H.J., Yuasa H.J., Austin C.J.D., Weiser S. and Hunt N.H., *Indoleamine 2,3-dioxygenase-2; a new enzyme in the kynurenine pathway*, ***The International Journal of Biochemistry & Cell Biology***, (2009), 41, 467–471

(48) Löb S., Königsrainer A, Zieker D., Brücher B. L. D. M., Rammensee H.G., Opelz G. and Terness P., *IDO1 and IDO2 are expressed in human tumors: levo- but not dextro-1-methyl tryptophan inhibits tryptophan catabolism*, ***Cancer Immunol Immunother***, 2009, 58, 153–157

(49) Sørensen R.B., Køllgaard T., Andersen R.S., Huibert van den Berg J., Svane I.M., Straten P., and Andersen M.H., *Spontaneous Cytotoxic T-Cell Reactivity against Indoleamine 2,3-Dioxygenase-2*, ***Cancer Res****,* 2011, 71, 2038-2044

(50) Sugimoto H., Oda S.I, Otsuki T., Hino T., Yoshida T., and Shiro Y., *Crystal structure of human indoleamine 2,3-dioxygenase: Catalytic mechanism of O2 incorporation by a heme-containing dioxygenase*, ***Proc. Natl. Acad. Sci.***, 2006,103, 2611-2616

(51) Thackray S.J., *Enzymatic and Mechanistic Studies into Tryptophan 2,3-Dioxygenase*, Thesis presented for the degree of Doctor of Philosophy**,** 2008**,** University of Edinburgh

(52) Bruckmann C., *Structural studies on heme containing proteins*, Thesis presented for the degree of Doctor of Philosophy**,** 2008**,** University of Edinburgh

(53) Sono M., *The roles of superoxide anion and methylene blue in the reductive activation of indoleamine 2,3-dioxygenase by ascorbic acid or by xanthine oxidase-hypoxanthine*, ***J. Biol. Chem.***,1989, 264, 1616-1622

(54) Maghzal G.J., Thomas S.R., Hunt N.H. and Stocker R., *Cytochrome b5, Not Superoxide Anion Radical, Is a Major Reductant of Indoleamine 2,3-Dioxygenase in Human Cells*, ***J. Biol. Chem.***,2008, 18, 12014–12025

(55) Sono M., Roach M.P., Coulter E.D., and Dawson J.H., *Heme-Containing Oxygenases*, ***Chem. Rev.***, 1996, 96, 2841-2887

(56) Chauhan N., Basran J., Efimov I., Svistunenko D.A., Seward H.E., Moody P.C.E. and Raven E.L., *The Role of Serine 167 in Human Indoleamine 2,3-Dioxygenase: A Comparison with Tryptophan 2,3-Dioxygenase*, ***Biochemistry***, 2008, 47, 4761–4769

(57) Thackray S.J., Bruckmann C., Anderson J.L.R., Campbell L.P., Xiao R., Zhao L., Mowat C.G., Forouhar F., Tong L. and Chapman S.K., *Histidine 55 of Tryptophan 2,3-Dioxygenase Is Not an Active Site Base but Regulates Catalysis by Controlling Substrate Binding*, ***Biochemistry***, 2008, 47, 10677–10684

(58) Chauhan N., Thackray S.J., Rafice S.A., Eaton G., Lee M., Efimov I., Basran J., Jenkins P.R., Mowat C.G., Chapman S.K., and Raven E.L., *Reassessment of the Reaction Mechanism in the Heme Dioxygenases*, ***J. Am. Chem. Soc.***, 2009, 131, 4186 – 4187

(59) Basran J., Efimov I., Chauhan N., Thackray S.J., Krupa J.L., Eaton G.,Griffith G.A., Mowat C.G., Handa S., and Raven E.L., *The Mechanism of Formation of N-Formylkynurenine by Heme Dioxygenases*, ***J. Am. Chem. Soc.***,2011, 133, 16251–16257

(60) Efimov I., Basran J., Thackray S.J., Handa S., Mowat C.G., and Raven E,L., *Structure and Reaction Mechanism in the Heme Dioxygenases*, ***Biochemistry***, 2011, 50, 2717–2724

(61) Lewis-Ballester A., Batabyal D., Egawa T., Lu C., Lin Y., Marti M. A., Capece L., Estrin D. A., and Yeh S. R., *Evidence for a ferryl intermediate in a heme-based dioxygenase*, ***PNAS***, 2009, 106, 17371–1737

(62) Yuasa H.J., Ball H.J., Ho Y.F., Austin C.J.D., Whittington C.M., Belov K., Maghzal G.J, Jermiin L.S., and Hunt N.H., *Characterization and evolution of vertebrate indoleamine 2, 3-dioxygenases IDOs from monotremes and marsupials*, ***Comparative Biochemistry and Physiology,*** Part B, 2009, 153, 137–144

(63) Madge D.J., Hazelwood R., Iyer R., Jones H.T. and Salter M., *Novel Tryptophan Dioxygenase Inhibitors and combined Tryptophan Dioxygenase/5-HT Reuptake Inhibitors*, ***Bioorganic & Medicinal Chemistry Letters***, 1996, 6, 857-860

(64) Salter M., Hazelwood R., Pogson C. I., Iyer R. and Madge D. J., *The effects of a novel and selective inhibitor of Tryptophan 2,3-Dioxygenase on tryptophan and serotonin metabolism in the rat*, ***Biochemical Pharmacology***, 1995, 49, 1435-1442

(65) Eguchi N., Watanabe Y., Kawanishi K., Hashimoto Y. and Hayaishi O., *Inhibition of indoleamine 2,3-dioxygenase and tryptophan 2.3-dioxygenase by β-carboline and indole derivatives*, ***Archives of Biochemistry and Biophysics***, 1984, 232, 602–609

(66) Sono M. and Cady S.G., *Enzyme kinetic and spectroscopic studies of inhibitor and effector interactions with indoleamine 2,3-dioxygenase. 1. Norharman and 4-phenylimidazole binding to the enzyme as inhibitors and heme ligands*, ***Biochemistry***, 1989, 28, 5392-9

(67) Cady S.G. and Sono M., *1-Methyl-DL-tryptophan, β-(3-benzofuranyl)-DL-alanine (the oxygen analog of tryptophan), and β-[3-benzo(b)thienyl]-DL-alanine (the sulfur analog of tryptophan) are competitive inhibitors for indoleamine 2,3-dioxygenase*, ***Archives of Biochemistry and Biophysics***, 1991, 291, 326-33

(68) Muller A.J., DuHadaway J.B., Donover P.S., Sutanto-Ward E. and Prendergast G.C., *Inhibition of indoleamine 2,3-dioxygenase, an immunoregulatory target of the cancer suppression gene Bin1, potentiates cancer chemotherapy*, ***Nature Medicine***, 2005, 3, 312-19

(69) Muller A.J. and Scherle P.A., Targeting the mechanisms of tumoral immune tolerance with small-molecule inhibitors, ***Nature Reviews. Cancer***, 2006, 6, 613-25

(70) Pucchio T.D., Danese S., Cristofaro R.D., and Rutella S., *Inhibition of indoleamine 2,3-dioxygenase: a review of novel patented lead compounds*, ***Expert Opin. Ther. Patents***, 2010, 20, 229-250

(71) Hou D.Y., Muller A.J., Sharma M.D., DuHadaway J., Banerjee T., Johnson M., Mellor A.L., Prendergast G.C., and Munn D.H., *Inhibition of Indoleamine 2,3-Dioxygenase in Dendritic Cells by Stereoisomers of 1-Methyl-Tryptophan Correlates with Antitumor Responses*, ***Cancer Res.***, 2007, 67, 792-801

(72) Metz R., DuHadaway J.B., Kamasani U., Laury-Kleintop L., Muller A.J. and Prendergast G.C.*, Novel tryptophan catabolic enzyme IDO2 is the preferred biochemical target of the antitumor indoleamine 2,3-dioxygenase inhibitory compound d-1-methyl-tryptophan*, ***Cancer Res.***, 2007, 67,7082–7087

(73) Banerjee T., DuHadaway J.B., Gaspari P., Sutanto-Ward E., Munn D.H., Mellor A.L., Malachowski W.P., Prendergast G.C., and Muller A.J., *A key in vivo antitumor mechanism of action of natural product-based brassinins is inhibition of indoleamine 2,3-dioxygenase*, ***Oncogene***, 2008, 27, 2851–2857

(74) Kumar S., Malachowski W.P., DuHadaway J.B., LaLonde J.M., Carroll P.J., Jaller D., Metz R., Prendergast G.C., and Muller A.J., *Indoleamine 2,3-Dioxygenase Is the Anticancer Target for a Novel Series of Potent Naphthoquinone-Based Inhibitors*, ***J. Med. Chem.***, 2008, *51,* 1706–1718

(75) Pereira A., Vottero E., Roberge M., Grant Mauk A., and Andersen R.J., *Indoleamine 2,3-Dioxygenase Inhibitors from the Northeastern Pacific Marine Hydroid Garveia annulata,* ***J. Nat. Prod.,*** 2006, 69, 1496-1499

(76) Bizanek R., McGuinness B.F., Nakanishi K., and Tomasz M., *Isolation and Structure of an Intrastrand Cross-Link Adduct of Mitomycin C and DNA*, ***Biochemistry***, 1992, *31,* 3084-3091

(77) Lu C., Lin Y., and Yeh S.R., *Inhibitory Substrate Binding Site of Human Indoleamine 2,3-Dioxygenase*, ***J. Am. Chem. Soc.***, 2009, 131, 12866–12867

(78) Brastianos H.C., Vottero E., Patrick B.O., Soest R. V., Matainaho T., Mauk A.G., and Andersen R.J., *Exiguamine A, an Indoleamine-2,3-dioxygenase (IDO) Inhibitor Isolated from the Marine Sponge Neopetrosia exigua*, ***J. Am. Chem. Soc.***, 2006, 128, 16046-16047

(79) Carr G., Chung M. K. W., Mauk A.G., and Andersen R.J., *Synthesis of Indoleamine 2,3-Dioxygenase Inhibitory Analogues of the Sponge Alkaloid Exiguamine A*, ***J. Med. Chem.***, 2008, *51,* 2634–2637

(80) Terentis A.C., Freewan M., Plaza T.S.S., Raftery M.J., Stocker R., and Thomas S.R., *The Selenazal Drug Ebselen Potently Inhibits Indoleamine 2,3- Dioxygenase by Targeting Enzyme Cysteine Residues*, ***Biochemistry***, 2010, 49, 591–600

Chapter 2

Materials and Methods

2.1 Materials

Most of the chemicals used (L-Trp, D-Trp, L-ascorbate, bovine liver catalase, methylene blue, inhibitors and tryptophan analogues) including those for buffers (Sigma-Aldrich) were of the highest analytical grade (≥97% purity) and were used without further purification. 1-Me-L-Trp and 1-Me-D-Trp (95% purity, Sigma-Aldrich) were purified further as described below. Inhibitors obtained from the National Cancer Institute, USA, were used as received. Details about the purity of particular compounds can be found at the following URL (http://dtp.nci.nih.gov/repositories.html).

2.2 High-performance liquid chromatography (HPLC)

Further purification of 1-Me-L-Trp and 1-Me-D-Trp (95% purity as purchased from Sigma-Aldrich) demanded usage of high-performance liquid chromatography (HPLC). The whole procedure was based on a previous published protocol [(1)]. Before the initiation of the purification process, 1-Me-L-Trp and 1-Me-D-Trp were dissolved in 90 % H_2O -10% MeCN, at final concentrations between 1-2 mM, and the resulting solution filtered using Millipore syringe filters (0.22 μm pore size). Two litres of the running buffer, 90 % H_2O -10% MeCN, were also filtered and sonicated for removal of contaminants and air bubbles. Prior to loading the sample, the reverse phase C18 column (250 × 4.6 mm) was preincubated with at least 1 CV of the running buffer (90 % H_2O -10% MeCN). The UV detectors and temperature were set at 280 nm and 25 ^{o}C correspondingly. The sample's injection volume and flow rate were adjusted to 1ml and 1ml/min respectively and the pure 1-Me-L-Trp/ 1-Me-D-

Trp peak was eluted after ~17 min (fig. 2.1). The purified 1-Me-L-Trp/ 1-Me-D-Trp sample was confirmed *via* mass spectrometry analysis which was carried out at University of Edinburgh, School of Chemistry by the MS service. Important to be reported is that the retention time of 1-Me-L-Trp/ 1-Me-D-Trp peak could easily be affected by slight changes of the sample concentrations, loading volumes and H_2O-MeCN ratio.

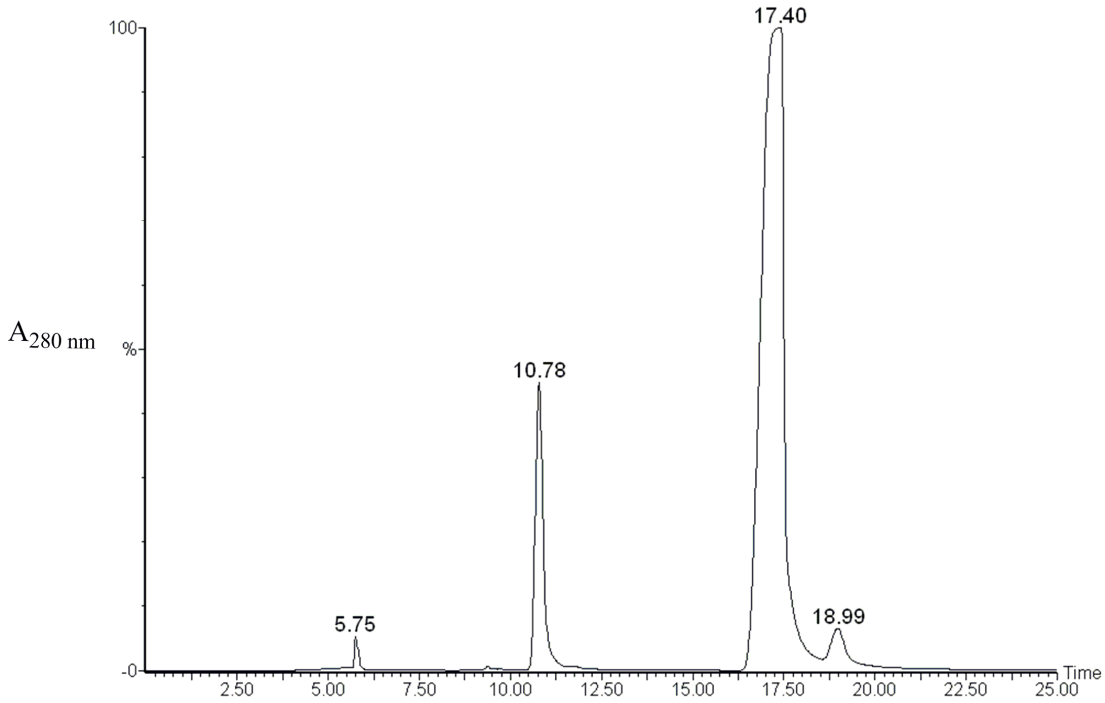

Figure 2.1: Elution of pure 1-Me-D-Trp (17.40 min) using (90 % H_2O -10% MeCN) RP-HPLC.

2.3 Plasmids, expression strains, and storage

The full-length human IDO (hIDO) construct fused into a ToPO plasmid (Invitrogen) was expressed using BL21 (DE3) *E. coli* cells, with a 6-His tag at the N-terminus. The coding region of human TDO (hTDO), ligated into a pET28a plasmid, was expressed using Rosetta (DE3) plysS cells, having a 6-His tag in the C-terminus. The plasmids for expression of hTDO and hIDO were kindly provided by Prof. Emma L. Raven, University of Leicester, UK [(2)]. The full-length *human* IDO2 (hIDO2) construct was fused into a pDEST plasmid (Invitrogen) and expressed using BL21 (DE3) *E. coli* cells, with an N-terminal 6-His tag. The plasmid for expression of hIDO2 was kindly provided by Dr. Helen J. Ball, University of Sydney, Australia [(3)]. For long term storage of each expression strain 930µl of *E. coli* culture media were mixed with 70 µl dimethyl sulfoxide (DMSO) and stored at -80 ^{o}C. All the information regarding the plasmids and cell lines used in this study is given in table 2.1.

Enzyme	Plasmid	*E. coli* cell line	Antibiotic resistance	6-His tag
hTDO	pET28a	Rosetta (DE3) plysS	kanamycin, chloramphenicol	C-terminus
hIDO	ToPO	BL21 (DE3)	amplicillin	N-terminus
hIDO2	pDEST	BL21 (DE3)	amplicillin	N-terminus

Table 2.1: Information regarding the plasmids and *E. coli* cell lines used in this work.

2.4 Growth and expression

Bacterial strains containing the hTDO, hIDO or hIDO2 encoding plasmids were cultured in Luria Bertani broth (10 g tryptone, 5 g yeast and 10g NaCl dissolved in 1L H_2O), also known as LB, previously sterilised by autoclaving at 121 ºC for 20 minutes. Starter cultures for large scale growth were prepared by inoculating 20 ml of sterile LB media (supplemented with 100 µl of the appropriate antibiotic) with some of the DMSO cell stock *via* a sterile pipette tip. For hIDO and hIDO2, the antibiotic used was 100 µl of 25 mg/ml amplicillin while for hTDO, 100 µl of 25 mg/ml kanamycin. The mixture of sterile media, antibiotic and *E. coli* expression strain was then incubated for 24 hours at 37 ºC with shaking at 225 rpm. For large scale growth, flasks containing 600 ml LB broth were inoculated with 1 ml of starter culture and either 500 µl of 25 mg/ml amplicillin (hIDO and hIDO2) or 500 µl of 25 mg/ml kanamycin (hTDO). Flasks were incubated with shaking at 37 ºC and 200 rpm until the OD_{600} reached 0.6. Protein production was then induced by addition of isopropyl-β-D-1-thiogalactopyranoside (IPTG) to a final concentration of 250 mgl^{-1}. The culture medium was supplemented with 0.5 ml of 5 mM hemin solution per flask to maximize heme incorporation. The temperature was also decreased to 22 ºC and left for a further 12 hours with shaking at 135 rpm until the cells were harvested by centrifugation (10 minutes at 8000 rpm) using a Sorvall RC-5B refrigerated centrifuge at 4 ºC. The resulting cell pellets were either lysed and the protein purified immediately or stored at -20 ºC until required.

2.5 Enzyme extraction and purification

2.5.1 Buffers used during the extraction and purification processes

Buffer A (lysis buffer): **i)** 20 mM TrisHCl buffer pH 8.0,
ii) 300 mM in NaCl,
iii) 10 mM in imidazole,
iv) 1mM in tris(2-carboxyethyl)phosphine (TCEP)

Buffer B (washing buffer): **i)** 20 mM TrisHCl buffer pH 8.0,
ii) 300 mM in NaCl,
iii) 20 mM in imidazole,
iv) 1mM in tris(2-carboxyethyl)phosphine (TCEP)

Buffer C (elution buffer): **i)** 20 mM TrisHCl buffer pH 8.0,
ii) 300 mM in NaCl,
iii) 250 mM in imidazole,
iv) 1mM in tris(2-carboxyethyl)phosphine (TCEP)

Buffer D (storage buffer): **i)** 20 mM TrisHCl buffer pH 8.0,
ii) 1mM in tris(2-carboxyethyl)phosphine (TCEP)

2.5.2 Cell lysis

The harvested cells were resuspended in buffer A, and cell lysis was initiated by incubating 200ml of cell suspension for 30 minutes with hen egg white lysozyme (1 mg per ml of suspension), phenylmethylsulfonyl fluoride (PMSF) (2 mg per ml of suspension) and 1 complete protease inhibition tablet (Sigma). Lysis was completed by ultrasonication of the suspension on ice. Cell debris was then removed *via* centrifugation for 1 hour at 20000 rpm and 4 ºC, and the supernatant collected.

2.5.3 Chromatographic purification

For purification of hIDO or hIDO2, the supernatant (~200-250 ml) from the previous step was loaded onto a Ni-agarose column previously equilibrated with buffer A. In contrast, the hTDO-containing supernatant was loaded onto a Ni-agarose column in batches of 100 ml. Reduction of the loading volume was necessary in order to avoid protein aggregation onto the column. hIDO and hIDO2 proteins were washed with 5 column volumes (CV) of buffer B and eluted using the same buffer but containing a higher concentration of imidazole (buffer C- elution buffer). hTDO protein was washed using 30-50 ml of buffer B and eluted in the same way. Size exclusion chromatography (either Superdex 75 for hIDO and hIDO2 or Superdex 200 for hTDO) was also used in order to remove imidazole (information about the elution times of hTDO and hIDO2 are given in Appendix F). The column was pre-equilibrated with buffer D for at least 1 CV and the proteins collected were judged to be pure and homogeneous. The imidazole-free proteins were then concentrated by centrifugation using Amicon Centricon filter devices of either 30 kDa molecular weight cut off (MWCO) for hIDO and hIDO2 or 100 kDa MWCO for hTDO. The diluted proteins were centrifuged at 2500 rpm until they reached concentrations between 150 and 400 μM; hTDO and hIDO2 up to 150 μM, hIDO up to 400 μM (for calculation of proteins concentration see section 2.6.3). Aliquots of 200-400 μl hTDO, hIDO and hIDO2 proteins were flash frozen in cryovials using liquid nitrogen and stored at -80 ºC until required.

2.6 Purity determination

2.6.1 SDS-PAGE analysis

Sample preparation requires denaturation of the proteins. To accomplish this an Eppendorf tube containing 25 µl SDS sample buffer (TrisHCl, SDS, glycerol, β-mercaptoethanol and bromophenol blue), 75µl water and 1 µl protein sample was boiled for about 3 minutes. Following this a small volume of the mixture (~10-20 µl) was loaded onto a pre-poured 4–12 % Bis-Tris gel (Invitrogen). The gel tank was filled with running buffer and the voltage was set at 150 V for approximately one hour. At the end of this process, the gel was removed from the tank and stained for total protein content.

2.6.2 Coomassie staining

Post-electrophoresis gels were soaked in Coomassie Brilliant Blue G-250 for about 15 minutes to stain the sample blue (through the interaction of Coomassie blue with arginine and histidine residues and the aromatic amino acids of the protein). The gel was then washed with water and destained with a mixture comprised of 10% glacial acetic acid, 40% MeOH and 50% water. The gel was kept in the destaining solution for 3-4 hours or until bands were visible. An example of hTDO staining can be observed in figure 2.2. The first lane is occupied by molecular weight markers, while the other four lanes (lanes 2, 3, 4 and 5) contain protein samples at different concentrations.

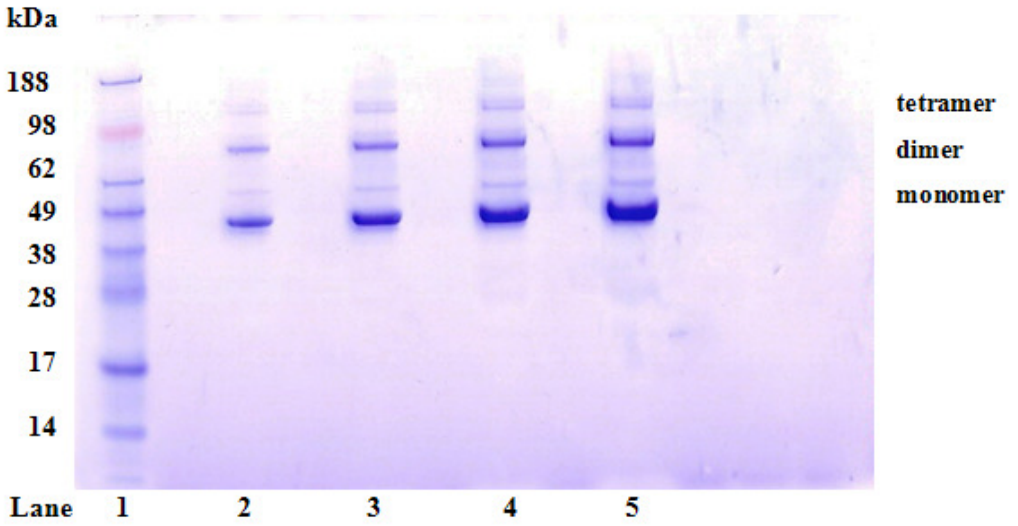

Figure 2.2: A representative example of SDS-PAGE analysis using hTDO. The first lane contains molecular markers, lanes 2, 3, 4 and 5 contain hTDO.

2.6.3 UV/Vis spectrophotometric analysis

Spectrophotometric examination of a protein provides information about its purity and concentration. The peaks in the UV/visible spectra indicate the presence of different chromophores in the sample. While the peak at ~280 nm reflects the absorption of aromatic residues of the protein, peaks above 400 nm are due to absorption by the heme. The absorbance of the heme can be influenced by the status of the iron atom (ferric/ferrous), the presence of ligands (L-Trp, L-Trp + O_2, O_2, CO, CN^-) and the source of the protein (human, rat). Using a Shimadzu UV-2101, PC spectrophotometer and quartz cuvette with a 1 cm path length, the purity of hIDO (black), hIDO2 (red) and hTDO (blue) have been monitored (fig. 2.3). The maximum absorbance of the Soret peak (405-409 nm), in combination with the Beer-Lambert law [$A=cl\varepsilon$ where A = absorbance, c = enzyme concentration ($molL^{-1}$), l = the path length of the sample (cm) and ε = extinction coefficient of the sample ($Lmol^{-1}cm^{-1}$)] may be used to calculate the concentration of the sample. Bradford and pyridyl

assays, which are described in sections 2.6.4 and 2.6.5, are used to work out % heme incorporation, and/or to work out the extinction coefficient for each protein. Once the coefficient is known UV/Vis spectrophotometric analysis is the best way to measure protein concentration. The extinction coefficients of hTDO, hIDO and hIDO2 are 197,000 $M^{-1}cm^{-1}$, 172,000 $M^{-1}cm^{-1}$ and 126,000 $M^{-1}cm^{-1}$ correspondingly.

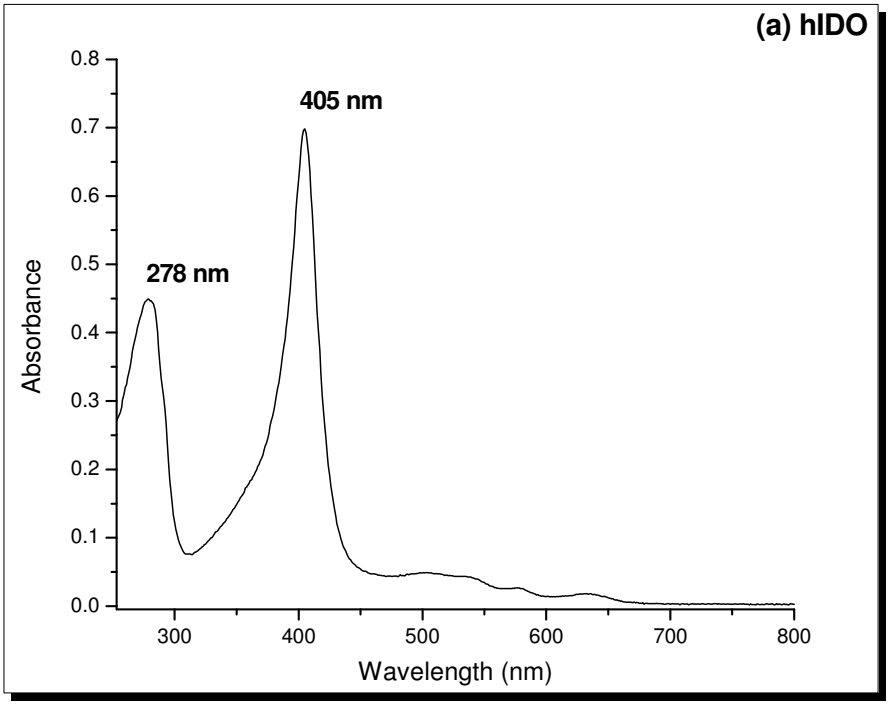

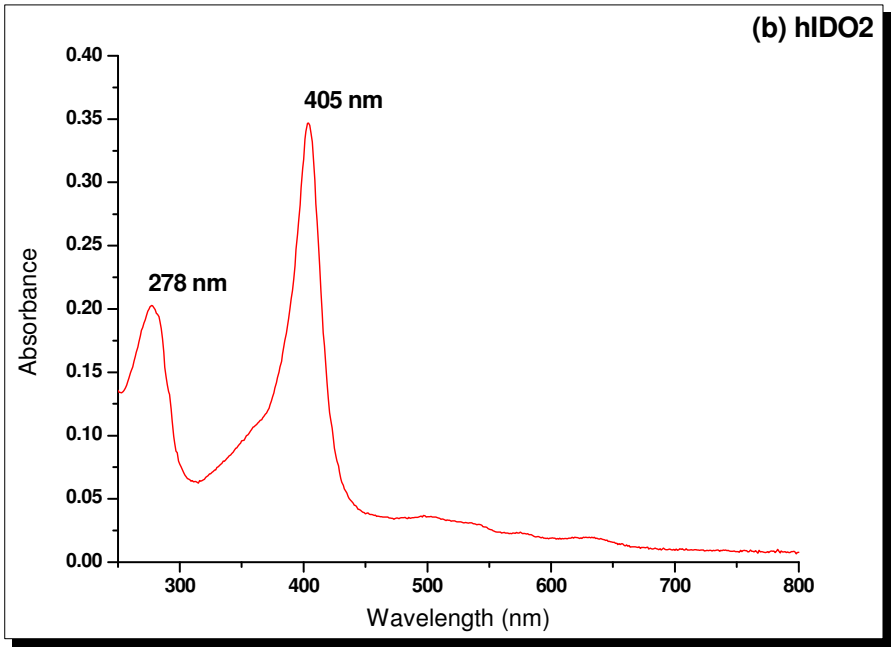

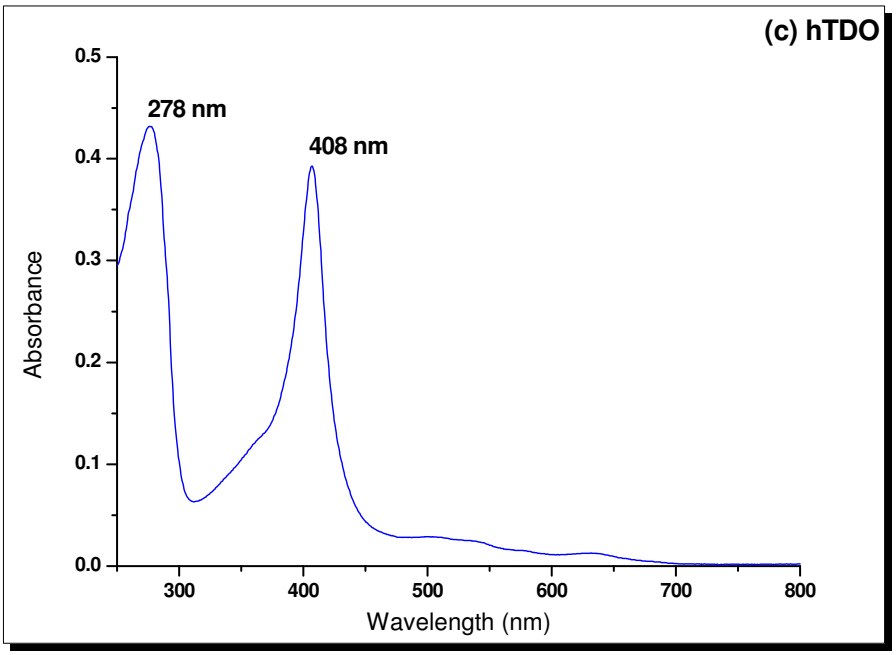

Figure 2.3: The absorption spectra of (a) hIDO (black), (b) hIDO2 (red) and (c) hTDO (blue) after purified. The peak at ~280 nm reflects the total protein content, while the peak at ~405 nm (for hIDO and hIDO2) and ~408 nm (for hTDO) are the heme Soret peaks. Using the extinction coefficient of the Soret heme peak, the concentration of the functional protein (protein + heme) can be determined.

2.6.4 Bradford assay

The concentrations of hTDO, hIDO and hIDO2 were determined using the Bradford assay [4]. Coomassie Brilliant Blue G-250, the dye used, has an absorbance maximum at 465 nm. In the presence of a protein this maximum absorbance shifts to 595 nm due to interaction between the protein and the dye (fig. 2.4).

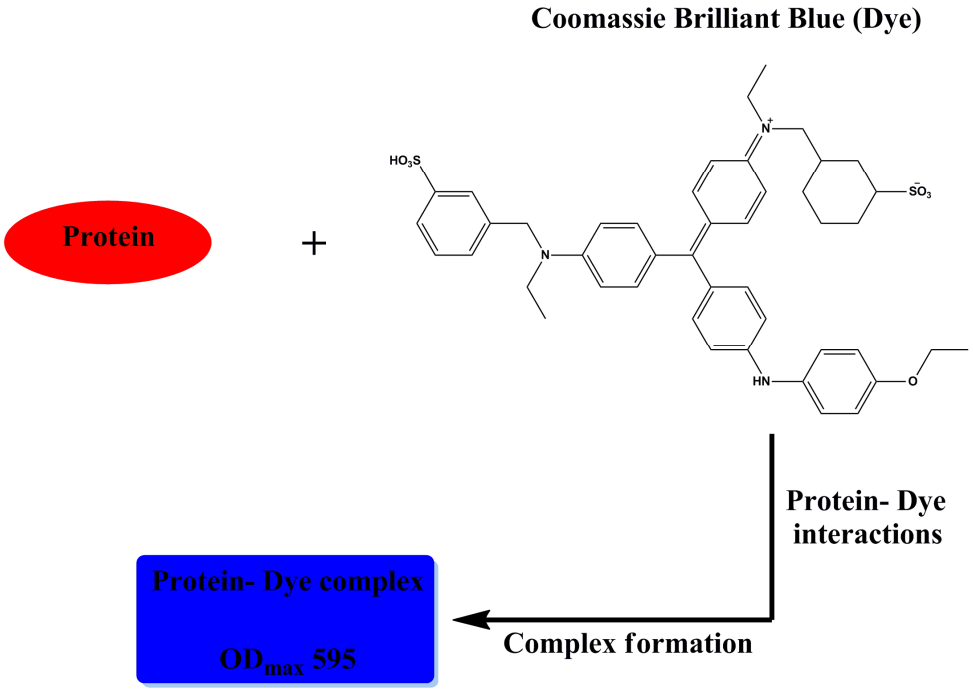

Figure 2.4: Principle of the Bradford assay [4]

Bovine serum albumin (BSA) solutions were used as protein standards. BSA solutions of known concentration were prepared, with absorbance values at 595 nm lying between 0 and 1.0 absorbance units. A standard curve was constructed by plotting A_{595} *vs* BSA concentration. The absorbance values of unknown concentrations of the proteins of interest were then compared with the standard curve, and the accurate protein concentrations were found using Microcal Origin software (fig. 2.5). Results were obtained in triplicate and at least two different protein concentrations were used in order to ensure the accuracy of the result.

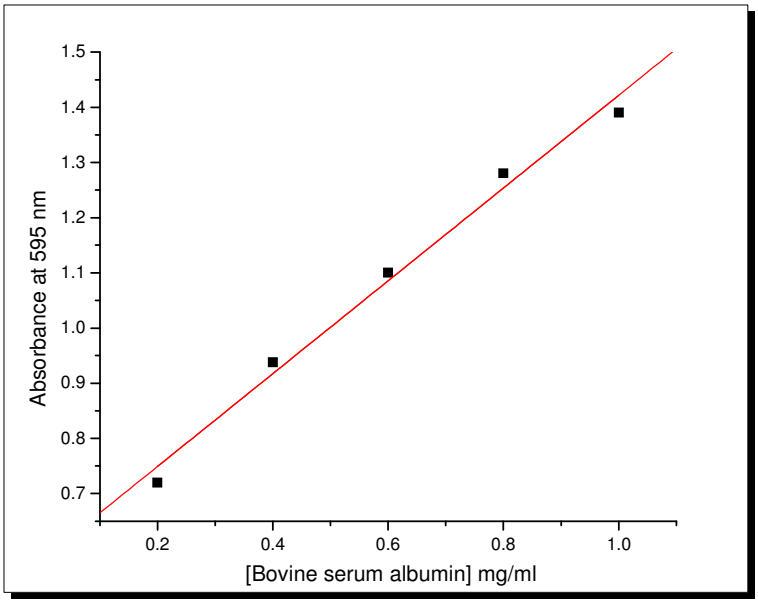

Figure 2.5: Standard graph of bovine plasma albumin absorbance against concentration. The unknown sample of a given protein must have an absorbance within the monitored range and the accurate concentration is calculated using the x-axis values.

2.6.5 Pyridine hemochrome assay

Heme is an essential cofactor for TDOs and IDOs, and knowledge of the level of heme occupancy is important for activity measurements and in crystallographic studies. The level of incorporation of heme into enzymes used in this work was calculated *via* the pyridine hemochrome assay [5]. In a quartz cuvette with a 1 cm path length, 20 µl of 5 µM protein was mixed with an equal volume of reagent A (Stock comprising 200 µl of 5 M NaOH, 2.5 ml pyridine, 2.3 ml H_2O). A solution of $Na_2S_2O_4$ (10 µl of 5 mg ml^{-1}) was immediately added and the UV/vis spectrum was recorded from 250-800 nm (Shimadzu UV-2101PC). The difference extinction coefficient $\Delta\varepsilon_{556\text{-}540}$ (22.1 $mM^{-1}cm^{-1}$) was used for heme concentration determination. Results were obtained in triplicate.

2.7 Enzyme kinetics

Kinetic analyses of hTDO, hIDO and hIDO2 were carried out by monitoring formation of N-formylkynurenine or N-formyl-kynurenine analogue over time. The formation of product was calculated using the change in absorbance at 321 nm, the wavelength where the molecule has the maximum absorbance. Each experiment was carried out either in 50 mM TrisHCl pH 8.0 (hTDO) or 100 mM KP_i pH 6.5 (hIDO) or 100 mM KP_i pH 7.5 (hIDO2). All the assay components were dissolved in the appropriate buffer at final concentrations of 20 mM ascorbate, 10 μM methylene blue and 10 μg/ml catalase. Substrate (L-Trp and its analogues) and enzyme concentrations were varied depending on the combination of enzyme/substrate used. The experiments were carried out under aerobic conditions at 25 ^{o}C using a thermostatically controlled water bath. Data obtained were fitted to the Michaelis-Menten equation and analyzed using Microcal Origin software.

2.8 Determination of the pH dependence of IDO2 activity

Determination of the optimum pH for enzymatic activity of hIDO2 was carried out by monitoring the formation of N-formyl-L-kynurenine over time in 100 mM potassium phosphate (KP_i) buffer with the pH varied within the range 5.8 to 8.0 at increments of 0.2 pH units. The experiment was based on the protocol described in section 2.7. Data obtained were analyzed using Microcal Origin software.

2.9 Microplate inhibition assay

The hTDO, hIDO and hIDO2 inhibition assays were carried out according to the method of Takikawa *et al.*[6] with minor modifications. The assays were carried out in a 96-well microplate with the components dissolved in either 100 mM KP_i pH 6.5(hTDO, hIDO) or 100 mM KP_i pH 7.5 (hIDO2). Each well contained 200 µl of assay mixture. The reaction mixture was comprised of 20 µl of 0.4 M ascorbic acid, 4 µl of 1 mM methylene blue, 4 µl of 10 mg/ml catalase, 20 µl L-tryptophan at final assay concentrations between 0- 800µM (hTDO), 0-45 µM (hIDO) and 0-8 mM (hIDO2), 2 µl of the inhibitor and 50 µl of the enzyme at final concentrations of 20 nM (hTDO), 10 nM (hIDO) and 900 nM (hIDO2) and 100µl of KPi buffer. The reaction mixture was incubated at room temperature for either 15 min (hIDO), 20 min (hTDO) or 30 min (hIDO2) and the reaction was terminated by adding 40 µl of trichloroacetic acid (30% w/v) into each well. Subsequently the microplate was transferred into an oven and incubated at 50 ºC for 30 min. The microplate was then centrifuged for 15 min at 4000 rpm and 125 µl of the supernatant transferred to a new microplate and mixed with equal volume of 4-dimethylaminobenzaldehyde (DMAB) in acetic acid (2% w/v). Finally, the absorbance was measured at 490 nm (fig 2.6), where the kynurenine-DMAB complex has a maximum ($\varepsilon_{490\ nm}$= 1500 $M^{-1}cm^{-1}$). The data was analyzed using Microcal Origin software. Calculation of the kynurenine-dimethylaminobenzaldehyde (DMAB) extinction coefficient was achieved using the above described method with minor modifications. The standard assay mixture (200 µl per well) contained 20 µl of 0.4 M ascorbic acid, 4 µl of 1 mM methylene blue, 4 µl of 10 mg/ml catalase, 20 µl L-kynurenine at final assay concentrations between 0-250 µM and 152 µl of the appropriate KP_i buffer. The data obtained were processed and analyzed using Microcal Origin software.

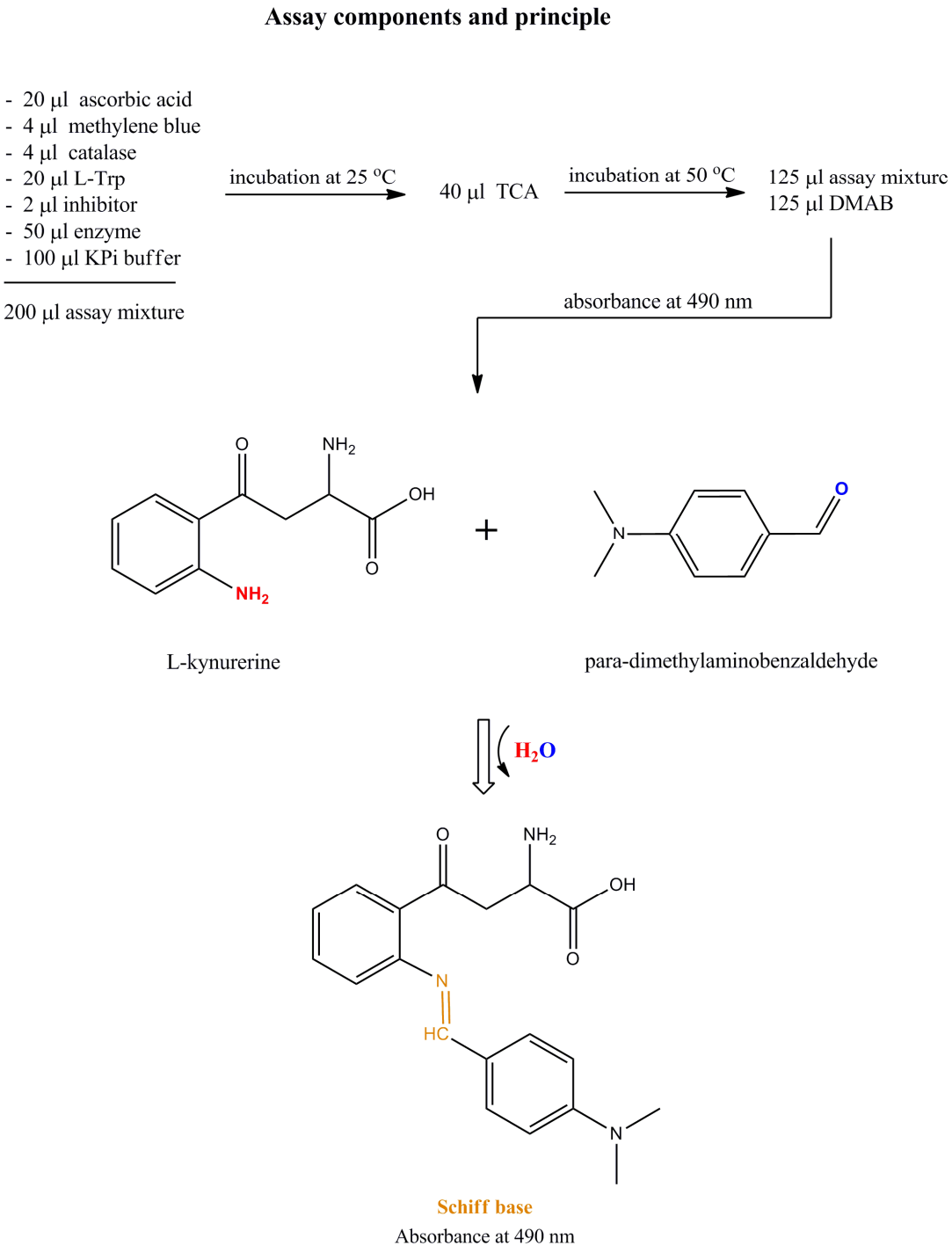

Figure 2.6: The components of microplate inhibition assay and its principle. Kynurenine reacts with DMAB producing a schiff base, which absorbs at 490 nm.

2.10 Enzyme inhibition assay - cuvette method

A cuvette-based inhibition assay was used as a control and as a means of confirming the accuracy of the microplate inhibition assay for TDO. To reduce further the chance of mistakes, two TDO inhibition results, obtained from the microplate assay, were compared with the corresponding cuvette outcomes. In the case of IDO, microplate results were compared with the corresponding published ones. The cuvette inhibition assay was carried out by monitoring formation of N-formylkynurenine over time. All the reaction components, including substrate, were dissolved in 50 mM TrisHCl pH 8.0. The final concentrations of the assays reagents were 20 mM ascorbate, 10 μM methylene blue, 10 μg/ml catalase and 400 nM hTDO. Substrate and inhibitor concentrations were varied between 0-250 μM and 0-8 μM respectively. The experiments were carried out under aerobic conditions at 25 ^{o}C using a thermostatically controlled water bath. Data obtained were analyzed using Microcal Origin software.

2.11 IDO double inhibitor assay

The purpose of this IDO double inhibition assay is to assess the combined effect of the most potent NCI compounds with 1MT in IDO inhibition. The assay was carried out as described in section 2.9 (microplate inhibition assay) with minor modifications. 34 nM hIDO was incubated with 50, 100, 200 and 400 μM 1-MT for five minutes, in order to allow equilibration and binding of the inhibitor with the enzyme. Following this the IDO/1-MT mixture was added into a 96-well microplate and combined with 100 μM of NCI inhibitor (identified by microplate screening as described in section 2.9), dissolved in DMSO (1% DMSO final concentration). After addition of both 1-MT and NCI inhibitor to IDO, the reaction was initiated by adding 100 μM mixture of L-Trp, ascorbate, methylene blue and catalase at concentrations mentioned in section 2.9. The reaction was allowed to proceed for 20 min and then terminated by adding 40 μl of trichloroacetic acid (30% w/v) into each well.

Subsequently the microplate was transferred into an oven and incubated at 50 ºC for 30 min. The microplate was then centrifuged for 15 min at 4000 rpm and 125 µl of the supernatant transferred to a new microplate and mixed with equal volume of 4-dimethylaminobenzaldehyde (DMAB) in acetic acid (2% w/v).

2.12 Redox potentiometry

Optically transparent thin layer electrochemical (OTTLE) analysis is an electrochemical technique useful for the study of heme environment, of heme-contained proteins, in the presence and absence of a particular substrate or inhibitor. The experiment was carried out under anaerobic conditions at 25 °C using a modified quartz EPR cell [7]. Samples of hTDO, hIDO and hIDO2 were prepared in 0.1 M TrisHCl buffer, pH 7.5, 500 mM in KCl, 10 % glycerol (v/v) giving final enzyme concentrations from 40-60 µM. A number of mediators (2-hydroxy-1,4-naphthoquinone (-145 mV vs. SHE), 5-hydroxy-1,4-naphthoquinone (-3 mV vs. SHE), phenazine ethosulfate (+55 mV vs. SHE), phenazine methosulfate (+82 mV vs. SHE), and 1,2-naphthoquinone (+135 mV vs. SHE) were also added in order to secure efficient reduction and re-oxidation of the enzyme (Table 2.2). Electrochemical titration of the enzymes was performed in the presence and absence of L-Trp and its analogues. All ligands were in excess, according to their solubility. All potentials measured were corrected relative to the SHE (standard hydrogen electrode) and data (wavelengths of Fe^{3+} and Fe^{2+} versus potentials) were fitted to Nernst equation (Microcal Origin) (fig. 2.7).

Mediators	Midpoint potential (mV)
2-hydroxy-1,4-naphthoquinone	-145
5-hydroxy-1,4-naphthoquinone	-3
phenazine ethosulfate	+ 55
phenazine methosulfate	+ 82
1,2-naphthoquinone	+ 135

Table 2.2: The mediators used in this study and their midpoint potentials.

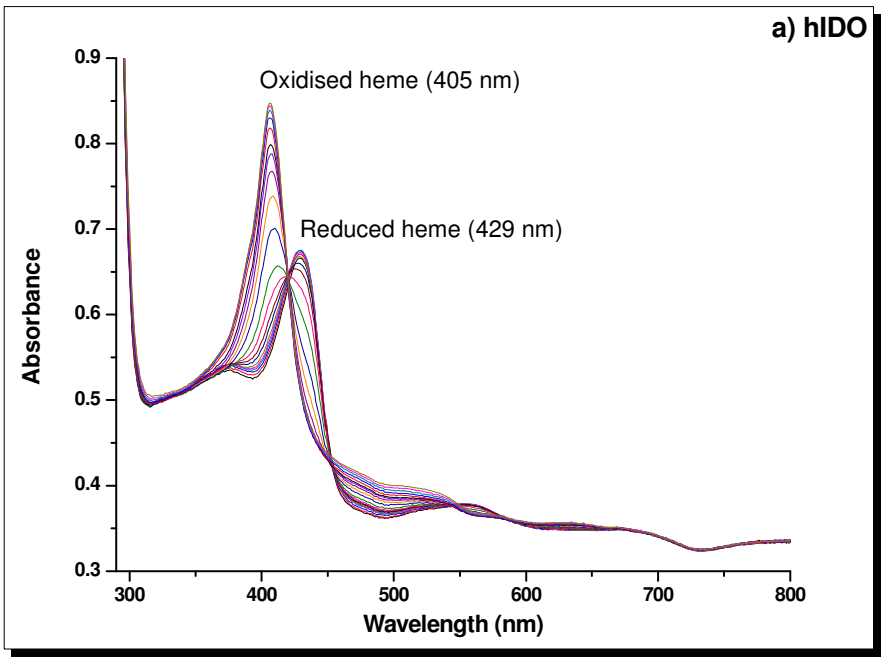

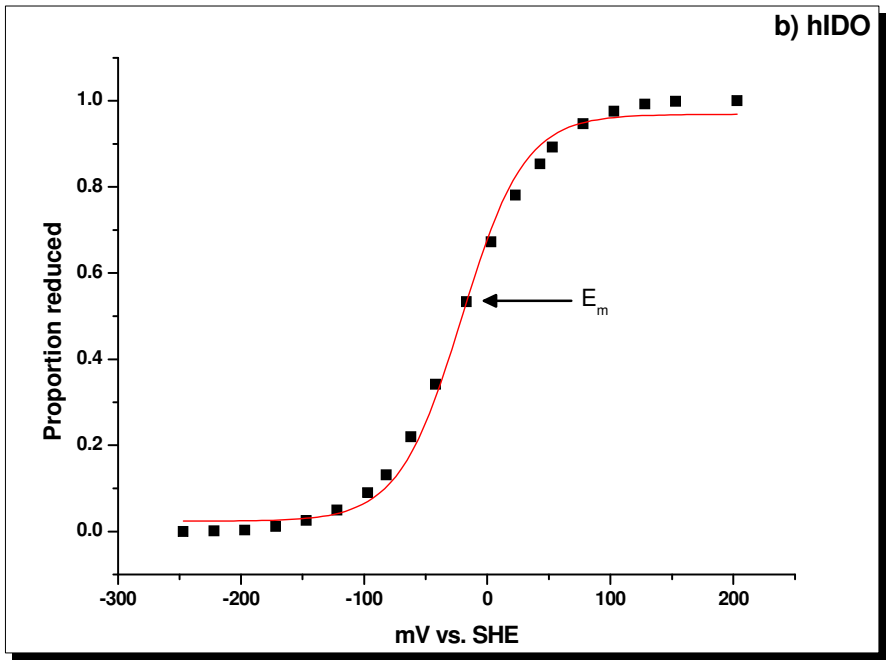

Figure 2.7: a) Absorbance changes of hIDO in correlation with changes of the potential. **b)** Calculation of the protein's mid point potential

2.13 References

(1) Chauhan N., Thackray S.J., Rafice S.A., Eaton G., Lee M., Efimov I., Basran J., Jenkins P.R., Mowat C.G., Chapman S.K., and Raven E.L., *Reassessment of the Reaction Mechanism in the Heme Dioxygenases***, *J. Am. Chem. Soc.***, 2009, 131, 4186 – 4187

(2) Rafice S.A., *The oxidation of L-Tryptophan in Biology by Human Heme Dioxygenases*, Thesis presented for the degree of Doctor of Philosophy**,** 2009**,** University of Leicester

(3) Ball H.J., Sanchez-Perez A., Weiser S., Austin C.J.D., Astelbauer F., Miu J., McQuillan J.A., Stocker R., Jermiin L.S. and Hunt N.H., *Characterization of an indoleamine 2,3-dioxygenase-like protein found in humans and mice*, ***Gene***, 2007, 396, 203–213

(4) Bradford M.M., *A rapid and sensitive method for the quantitation of microgram quantities of protein utilizing the principle of protein-dye binding*, ***Analytical Biochemistry***, 1976, 72, 248-54

(5) Berry, E. A. and Trumpower B. L., *Simultaneous determination of hemes a, b, and c from pyridine hemochrome spectra*, ***Analytical Biochemistry***, 1987, 161, 1-15

(6) Takikawa O., Kuroiwa T., Yamazaki F., and Kido R., *Mechanism of interferon-gamma action. Characterization of indoleamine 2,3-dioxygenase in cultured human cells induced by interferon-gamma and evaluation of the enzyme-mediated tryptophan degradation in its anticellular activity*, ***J. Biol. Chem.***,1988, 263, 2041-8

(7) Ost T. W. B., Clark J. P., Mowat C.G., Miles C.S., Walkinshaw M.D., Reid G.A., Chapman S.K. and Daff S., *Oxygen Activation and Electron Transfer in Flavocytochrome P450 BM3*, ***J. Am. Chem. Soc.,*** 2003, 125, 15010-15020

Chapter 3

Identification and characterisation of inhibitors of TDO and IDO

3.1 Introduction

This chapter describes efforts towards the development of TDO and IDO inhibitors. This involved screening of ~3000 potential TDO/IDO inhibitors and characterisation of the 67 most promising compounds. Among the molecules that have been tested there is a number of previously published inhibitors of either TDO or IDO, compounds that form part of the libraries of the National Cancer Institute, USA, isatin derivatives, a series of natural products, DNA bases, kynurenine-3-monoxygenase (KMO) inhibitors, tryptophan derivatives and kynurenine/serotonin metabolites (fig. 3.1).

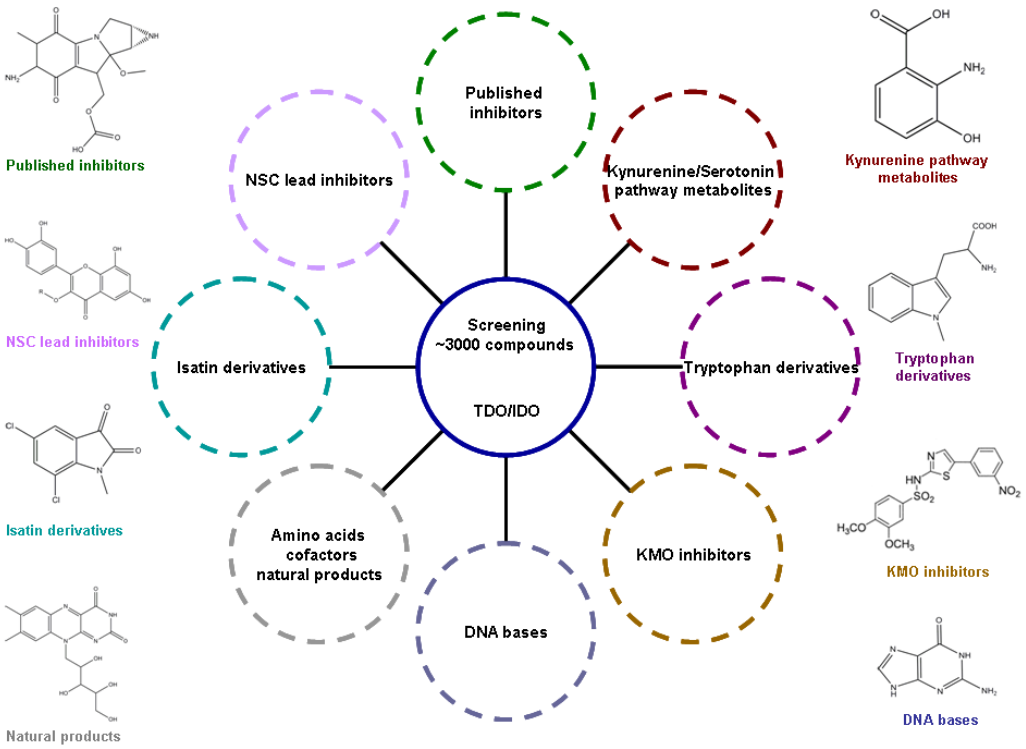

Figure 3.1: A brief summary of the ~3000 lead molecules that have been tested as inhibitors of TDO and IDO enzymes

Of the compounds tested as inhibitors of TDO/IDO, these can be divided into two main categories; i) The molecules that were obtained from the National Cancer Institute USA (~2800) (http://dtp.nci.nih.gov/repositories.html), and ii) the molecules that were ordered individually from several pharmaceutical and other companies (~210). A list of the individually ordered compounds can be found in Appendix A. In the case of the compounds obtained from the NCI, these have been further categorised into; i) approved oncology drug sets I and II, ii) natural product sets I and II, iii) mechanistic set and iv) diversity set II. Compounds in all sets were provided in 96-well microplates, as 20 μl of a 10mM solution in 100% DMSO. The plates that contained these molecules were shipped frozen in dry ice. The approved oncology drug sets contain most current FDA-approved anticancer drugs. Further information about the purity of particular sets/compounds is given at the URL provided in section 2.1. The natural product sets, composed of naturally occurring molecules, were selected according to their origin, purity (>90%), structural diversity and availability. The mechanistic diversity set, on the other hand, contains molecules that revealed inhibition potency against various human tumour cell lines. Last but not least is the diversity set, where the choice of the molecules was based on their structural diversity (hydrogen bond acceptor, hydrogen bond donor, positive charge, aromatic, hydrophobic, acid and base). Regarding the individually chosen molecules, selection was based on their structural similarities with either L-Trp, previously published inhibitors of IDO/TDO, or other molecules that were identified during this study as potent inhibitors of TDO/IDO. A number of natural occurring products such as vitamins are also included in the same list. Excluding isatin derivatives, which are discussed separately in Chapter 4, all the other groups of inhibitors (fig. 3.1) will be discussed in this chapter.

3.2 Microplate versus cuvette inhibition assay

Prior to the characterization of the various TDO and IDO inhibitors, it was necessary to verify the accuracy of the microplate inhibition assay. For this reason TDO microplate results with mitomycin C and r493171 as inhibitors, and IDO microplate results with mitomycin C and 1-Me-L-Trp as inhibitors, were compared with the corresponding cuvette (fig. 3.2) and published results respectively (Table 3.1). The structures of the three inhibitors, used in this trial, are illustrated in figure 3.3.

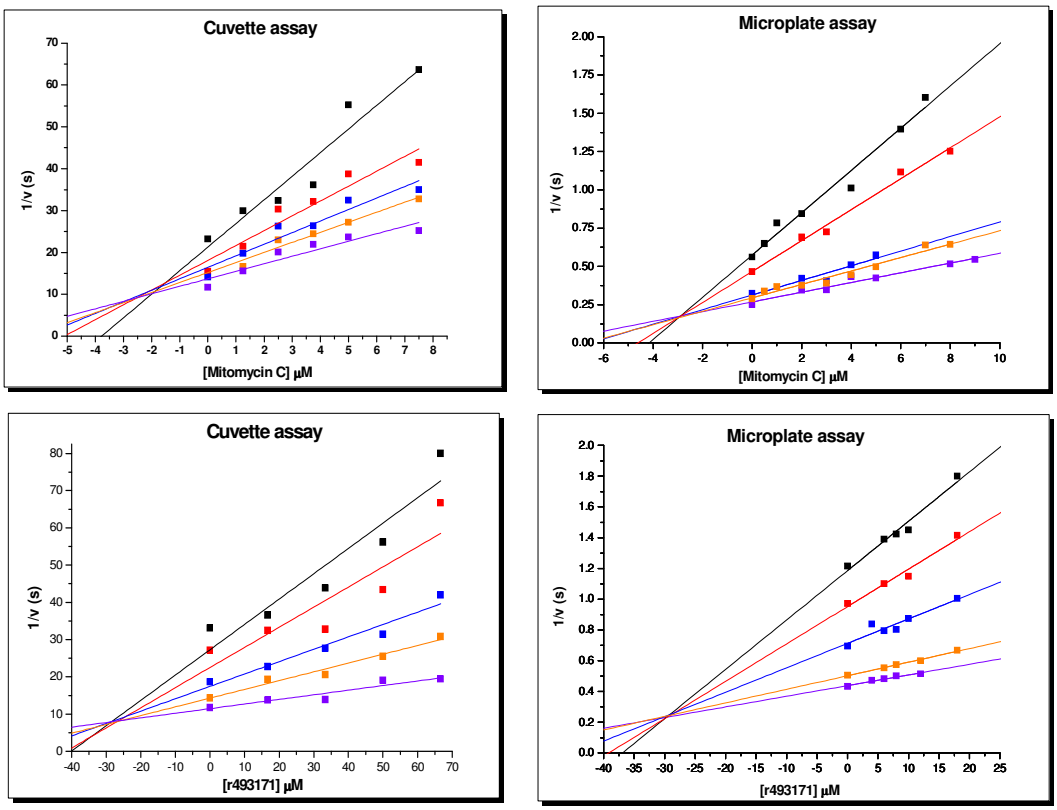

Figure 3.2: Dixon plots of hTDO using mitomycin C (top) and r493171 (bottom) as inhibitors. For the cuvette assays, the concentrations of L-Trp used (all in µM) were: 80 and 40 (black), 125 and 60 (red), 150 and 80 (blue), 200 and 125 (orange), 250 and 150 (violet) for mitomycin and r493171 respectively. For the microplate assays, the concentrations of L-Trp used (all in µM) were: 300 and 300 (black), 350 and 350 (red), 600 and 500 (blue), 700 and 700 (orange), 800 and 800 (violet) for mitomycin and r493171 respectively.

As figure 3.2 shows, the cuvette inhibition assay findings were consistent with the corresponding microplate ones. While the cuvette assay for hTDO revealed inhibition constants of 2.52 ± 0.4 μM and 28.7 ± 2.3 μM for mitomycin C and r493171 respectively, the microplate assay provided inhibition constants of 2.86 ± 0.03μM and 29.8 ± 2.4 μM. Similarly, IDO microplate inhibition assay results for mitomycin C and 1-Me-L-Trp, were confirmed by the equivalent published ones (Table 3.1).

Inhibitor	hTDO inhibition constant		hIDO Inhibition constant	
	microplate (μM)	cuvette (μM)	microplate (μM)	published (μM)
Mitomycin C	2.86 ± 0.03	2.52 ± 0.4	24.2 ± 1.2	25 [(1)]
1-Me-L-Trp	-	-	18.0 ± 3.4	19 [(2)]
r493171	29.8 ± 2.4	28.7 ± 2.3	-	-

Table 3.1: Inhibition of TDO and IDO by mitomycin C, 1-Me-L-Trp and r493171. Accuracy of the microplate inhibition assay is verified by the cuvette assay and previous published results, ref. (1) and (2).

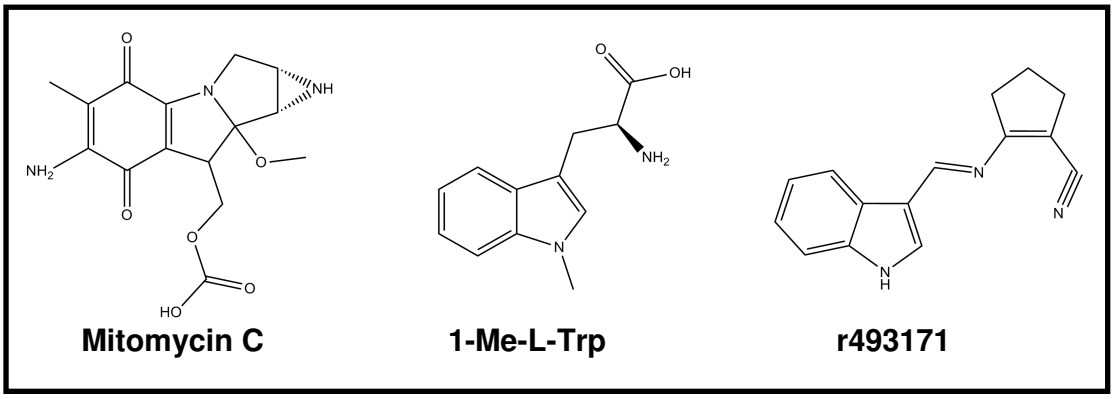

Figure 3.3: The TDO and IDO inhibitors used for verification of the microplate assay accuracy.

3.3 Published TDO/IDO inhibitors

The starting point in this work was to determine the specificity of published TDO/IDO inhibitors for either enzymes, this being a key step toward the development of specificity TDO/IDO inhibitors. Whereas this work examines the *in vitro* behaviour of hTDO and hIDO only, the term specificity refers to the selective inhibition of either hTDO or hIDO. Previous studies have thus far demonstrated that pyridyl compounds and 1-MT are the only specific inhibitors for TDO and IDO respectively [(3), (4)]. While molecules such as naphthoquinones, ebselen and mitomycin C are published IDO inhibitors, their specificity against TDO has never been stated. Phenylimidazole and norharman, on the other hand, are known to inhibit both enzymes, and this is related with the ability of the two molecules to interact with the heme iron of TDO and IDO. For this reason, phenylimidazole and norharman will not be discussed further [(5)]. The findings in regards to the most important TDO/IDO published inhibitors are summarised in table 3.2, and the aim of this section is to study these inhibitors and confirm or refute, where necessary, the published results.

IDO inhibitors	TDO inhibitors	IDO and TDO
1-Me-Tryptophan	Pyridyls	Phenylimidazole
Naphthoquinones		Norharman
Ebselen		
Mitomycin C		

Table 3.2: Specificity of TDO and IDO inhibitors as categorised according to previous findings.

3.3.1 1-Methyltryptophan

In order to confirm the specificity of 1-MT against IDO and understand further the way that the molecule inhibits the enzyme, the kinetic, inhibition and redox responses of IDO and TDO against L-Trp, D-Trp and the two stereoisomers of 1-MT (1-Me-L-Trp and 1-Me-D-Trp) were examined.

3.3.1.1 Turnover kinetics of D- and L-Trp and their 1-methylated derivatives

Kinetic characterisation of IDO and TDO was carried out as described in section 2.7 and the kinetic parameters for IDO and TDO with L-Trp, D-Trp, 1-Me-L-Trp and 1-Me-D-Trp as substrate are presented in table 3.3. It was found that the physiologically-relevant substrate for these enzymes, L-Trp, is oxidised more efficiently by IDO (k_{cat}/K_m = 0.14 $\mu M^{-1}s^{-1}$) than TDO (k_{cat}/K_m = 0.018 $\mu M^{-1}s^{-1}$). In terms of substrate affinity, L-Trp has a 5-fold lower value of K_m for IDO (20. 9 ± 4 µM) than for TDO (K_m = 112 ± 24 µM) while in terms of turnover rate, IDO has a k_{cat} value around 1.5 times greater than TDO.

	hIDO			hTDO		
Substrate	**k_{cat} / K_m ($\mu M^{-1}s^{-1}$)**	**k_{cat} (s^{-1})**	**K_m (µM)**	**k_{cat} / K_m ($\mu M^{-1}s^{-1}$)**	**k_{cat} (s^{-1})**	**K_m (µM)**
L-Trp	**0.142**	**3.0 ± 0. 2** **3.1 ± 0.2 (1)**	**20. 9 ± 4** **15 ± 2 (1)**	**0.018**	**2. 02 ± 0.04** **1.4 ± 0.019 (6)**	**112 ± 24** **222 ± 15 (6)**
D-Trp	**0.009**	**2. 7 ± 0. 3** **5.9 ± 0.3 (1)**	**296 ± 19** **(2.6 ± 0.2) × 10^3 (1)**	**0.0002**	**0. 47 ± 0. 04** **Not available**	**2200 ± 324** **Not available**
1- Me-L-Trp	**0.0009**	**0.062 ± 0.001** **0.064 ± 0.003 (1)**	**70 ± 1** **62 ± 9 (1)**	**-**	**dnb**	**dnb**
1-Me-D-Trp	**0.0001**	**0. 095 ±0. 007** **Not available**	**660 ± 43** **Not available**	**-**	**dnb**	**dnb**

Table 3.3: Kinetic characteristics of hIDO and hTDO for L-Trp, D-Trp and their 1-methylated derivatives, dnb = does not bind. For comparison, the published kinetic data for hIDO and hTDO, obtained from independent studies, are also presented. The data marked in blue were taken from ref. (1), while the data shown in green from ref. (6).

In the case of D-Trp turnover by TDO and IDO, some differences were apparent. In terms of k_{cat} values, IDO retained its turnover ability at the same level as with L-Trp (3.0 ± 0.2 s^{-1} and 2.7 ± 0.3 s^{-1} for L-Trp and D-Trp respectively), while TDO turns over D-Trp approximately 4-fold more slowly (k_{cat} = 2.02 ± 0.04 s^{-1} for L-Trp and 0.47 ± 0.04 s^{-1} for D-Trp). As expected, the affinities of both IDO and TDO for D-Trp were lower, in contrast with L-Trp, demonstrating the enzymes' selectivity for the L-isomer of tryptophan. The 8-fold difference in the catalytic efficiency of the two enzymes observed for L-Trp increased further for D-Trp, showing the distinct dissimilarities of the two enzymes in terms of substrate specificity. More specifically, D-Trp, is turned over more efficiently (45-fold) by IDO (k_{cat}/K_m = 0.009 $\mu M^{-1}s^{-1}$) than TDO (k_{cat}/K_m = 0.0002 $\mu M^{-1}s^{-1}$). The experimental results of TDO and IDO for L-Trp and D-Trp are presented in figure 3.4.

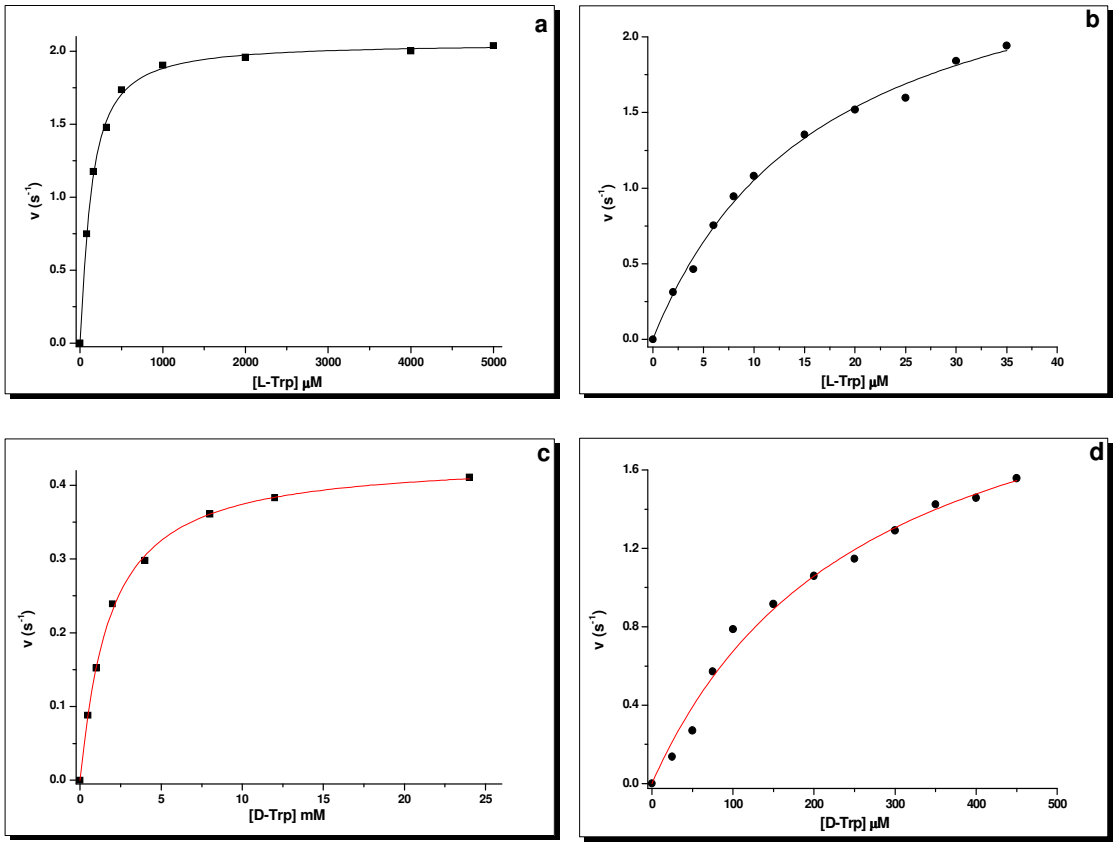

Figure 3.4: TDO (a, c) and IDO (b, d) turnover assays for L-Trp (black curves) and D-Trp (red curves).

Examination of turnover with the methylated derivatives of D- and L-Trp revealed no catalytic activity for TDO, something which is in agreement with the model and experiment results of Chauhan *et al.* [7]. According to their proposition, a steric clash which occurs between a histidine residue in TDO (His55 for xcTDO or His76 for hTDO) and the methyl group of 1-MT prevents the binding of the molecule in the active site of the enzyme. In contrast, IDO oxidized both 1-Me-L-Trp and 1-Me-D-Trp. The L-isomer of 1-MT binds to the enzyme fairly strongly (K_m = 70 ± 1 μM), acting as a slow substrate. On the other hand, binding of 1-Me-D-Trp is less favourable (K_m = 660 ± 43 μM). Similar to the findings for L-Trp and D-Trp, the k_{cat} values for the 1-methyl derivatives of D- and L-Trp are comparable (0.062 ± 0.001 s^{-1} and 0.095 ± 0.007 s^{-1} for 1-Me-L-Trp and 1-Me-D-Trp respectively). The turnover graphs of IDO for 1-Me-L-Trp and 1-Me-D-Trp are illustrated below (fig. 3.5)

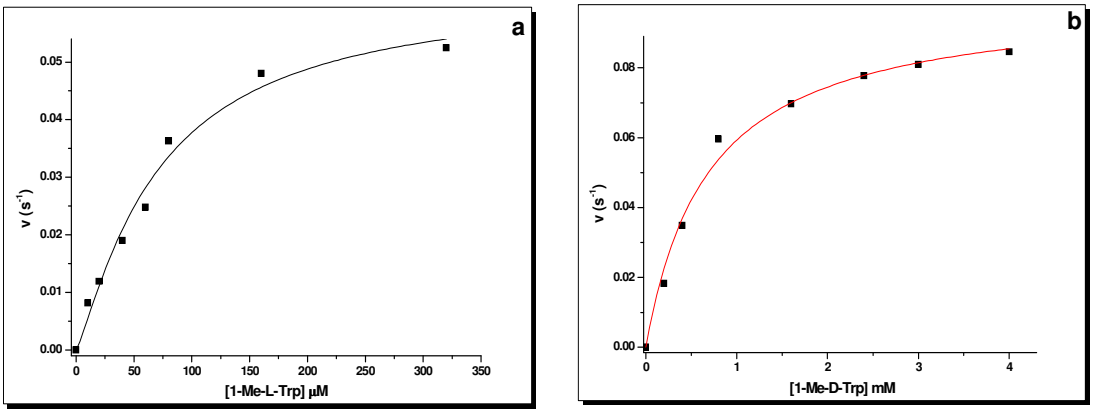

Figure 3.5: IDO turnover for 1-Me-L-Trp (a) and 1-Me-D-Trp (b)

3.3.1.2 Inhibition of hIDO and hTDO by L-Trp, D-Trp, 1-Me-L-Trp and 1-Me-D-Trp

Although IDO is a monomeric protein, the inhibition data indicated that substrate inhibition occurs at L-Trp concentrations ≥50 μM (Table 3.4). According to recent findings this phenomenon is not related with an allosteric effect (a secondary binding site for L-Trp) but it has to do with the order that L-Trp and O_2 bind at the active site of the enzyme [8]. At low substrate concentrations, O_2 binds first allowing the

formation of a ferric superoxide intermediate. However, at high substrate concentrations (≥50 µM) the order is reversed affecting the formation of ferric superoxide intermediate and therefore the catalytic ability of IDO. Despite the fact that TDO is a tetrameric protein with two L-Trp binding sites per monomer, inhibition of the enzyme by L-Trp was not observed. As figure 3.6 shows, D-Trp inhibits both enzymes but with different affinities.

	L-Trp	D-Trp	1-Me-L-Trp	1-Me-D-Trp
	K_{si} (µM)	K_i (µM)	K_i (µM)	K_i (µM)
hIDO	**50**	**543 ± 35**	**18.0 ± 3.4**	**ni**
hTDO	**ni**	**5030 ± 60**	**dnb**	**dnb**

Table 3.4: Inhibition of hIDO and hTDO in the presence of D-Trp, 1-Me-L-Trp and 1-Me-D-Trp. ni = no inhibition, dnb = does not bind.

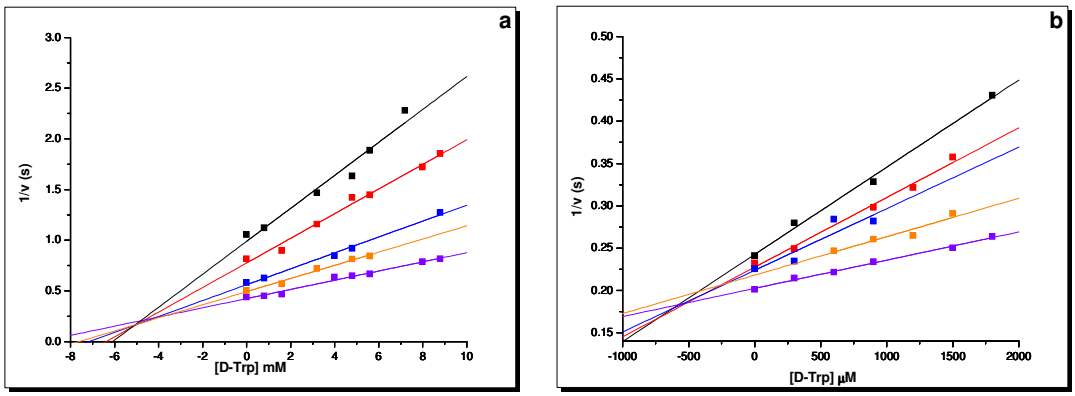

Figure 3.6: Dixon plots of TDO (a) and IDO (b) using D-Trp as inhibitor. The concentrations of L-Trp used (all in µM) were: 300 and 25 (black), 400 and 30 (red), 600 and 35 (blue), 700 and 40 (orange), 800 and 45 (violet) for TDO (a) and IDO (b) respectively.

While IDO displayed a K_i value of 543 ± 35 µM, TDO inhibition is significantly weaker, yielding a K_i value of 5030 ± 60 µM. These K_i values are broadly in line with the difference between the D-Trp K_m values given for each enzyme in table 3.3. Study of the N1-methylated derivatives of L-Trp and D-Trp revealed no inhibition of TDO. This observation is in line with their lack of binding to TDO as explained above. However, IDO enzymatic activity was found to be affected by the presence of 1-Me-L-Trp, which was found to inhibit the enzyme with a K_i value of 18.0 ± 3.4 µM. A Dixon plot for inhibition of IDO by 1-Me-L-Trp is given in figure 3.7. While 1-Me-L-Trp is a good inhibitor of IDO, 1-Me-D-Trp did not affect the activity of the enzyme, showing that only the L-isomer of 1-MT is a valid inhibitor of IDO.

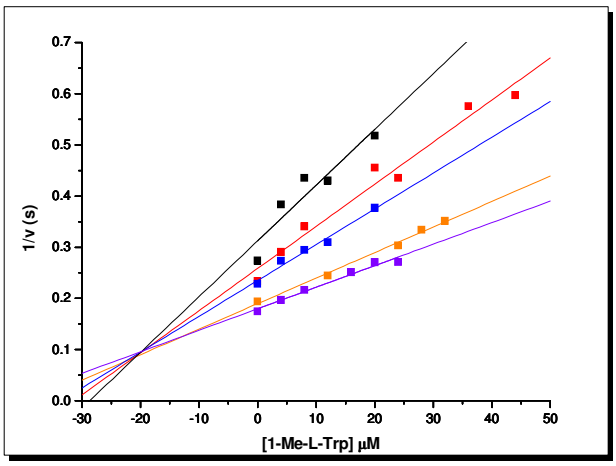

Figure 3.7: Dixon plot of IDO using 1-Me-L-Trp as inhibitor. The concentrations of L-Trp used (all in µM) were: 20 (black), 25 (red), 30 (blue), 40 (orange) and 45 (violet).

3.3.1.3 Electrochemical analysis of IDO and TDO

Electrochemical analysis of TDO and IDO was carried out as described in section 2.12. The electrochemical behaviour of IDO and TDO was examined in the absence and presence of L-Trp, D-Trp, 1-Me-L-Trp and 1-Me-D-Trp and the results are presented in table 3.5. For both IDO and TDO, the presence of L-Trp caused a shift in the heme midpoint potentials of +38 mV and +129 mV respectively (fig. 3.8),

which is presumed to be indicative of conformational changes occurring at the active sites of the two enzymes upon L-Trp binding. In the case of TDO this has been discussed as supporting the idea that TDO is an induced-fit enzyme [9]. In the presence of D-Trp, however, only TDO shows a potential shift (+77 mV relative to the substrate-free enzyme), while the 1-methylated derivatives cause no shift in potential in IDO, and do not bind to TDO at all. It is interesting to note that despite the fact that 1-Me-L-Trp is a relatively good inhibitor of IDO there is little effect upon the heme potential upon binding, raising questions about the nature of ligand and inhibitor binding in turnover and non-turnover situations.

Substrate	Em hIDO (mV vs. SHE)	Em hTDO (mV vs. SHE)
Free	**- 54 ± 8**	**-82 ± 1**
L-Trp	**-16 ± 6**	**47 ± 2**
D-Trp	**-57 ± 12**	**-5 ± 1**
1-Me-L-Trp	**-48 ± 8**	**-**
1-Me-D-Trp	**-55 ± 4**	**-**

Table 3.5: Reduction potentials of hIDO and hTDO as free enzyme or saturated with L-Trp, D-Trp, 1-Me-L-Trp and 1-Me-D-Trp.

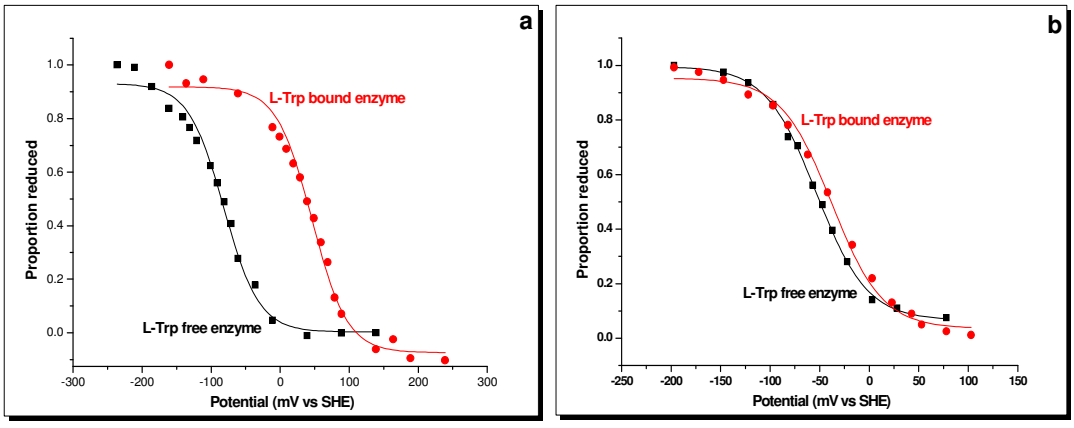

Figure 3.8: Reduction potentials of (a) hTDO and (b) hIDO as free enzymes (black curves) and in the presence of L-Trp (red curves).

3.3.2 Naphthoquinone-based inhibitors

The naphthoquinone-based inhibitors are a family of inhibitors with important impact in IDO inhibition [10]. Naphthoquinone-based drugs are well studied and used for treatment of various types of cancer. A recent FDA-approved drug with a naphthoquinone moiety is mitomycin C, which is also an inhibitor of IDO and will be discussed below. In addition to their proved pharmaceutical usefulness, naphthoquinone-like structures are also found in a number of natural occurring products such as vitamin K.

According to Kumar *et al.* [10], this class of molecules inhibits IDO activity with satisfactory inhibition potency, but without clarifying whether they are also inhibitors for TDO. The findings of Kumar and co-workers supported the notion that the essential moiety for IDO inhibition is either 1,2-naphthoquinone or 1,4-naphthoquinone, reporting at the same time that the equivalent benzoquinones are inactive (fig. 3.9).

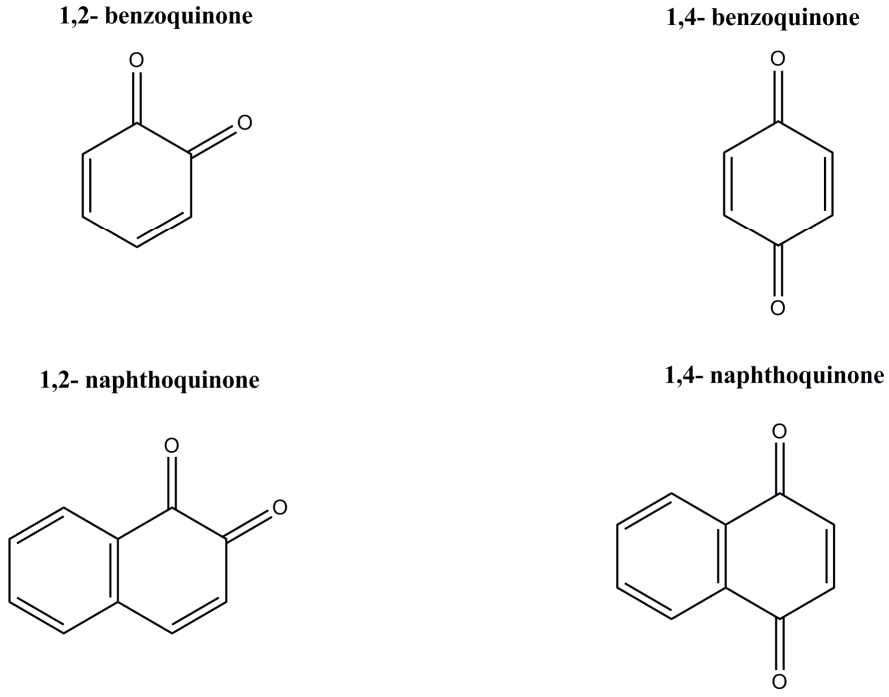

Figure 3.9: Benzoquinones and naphthoquinones. A previous study has suggested that naphthoquinone moiety is the smallest active IDO inhibitor [10]. However, it is demonstrated here that benzoquinones are also active TDO inhibitors.

From figure 3.10 it can be seen that both 1,4-benzoquinone (blue curve) and tetrachloro-1,2-benzoquinone (red curve) are inhibitors of TDO and IDO, thus showing that benzoquinone is the smallest active moiety that inhibits both enzymes (fig. 3.10). Testing various naphthoquinone-like molecules (14 in total), it was verified that this group of compounds are inhibitors of both TDO and IDO. Information about the structures of the naphthoquinone-based inhibitors that were used can be found in the inhibitors list (Appendix A, *numbers 72-84 and 86 in the list*). While reduction of 1,4-naphthoquinone to 1,4-dihydroxynaphthalene (the reduced form of 1,4-naphthoquinone contains hydroxyl groups at 1 and 4 positions of the aromatic ring) did not affect the inhibition potency of the molecule, insertion of an electron-withdrawing carboxylic acid group at the 2 position of the hydroquinone form caused the loss of inhibition activity in both TDO and IDO.

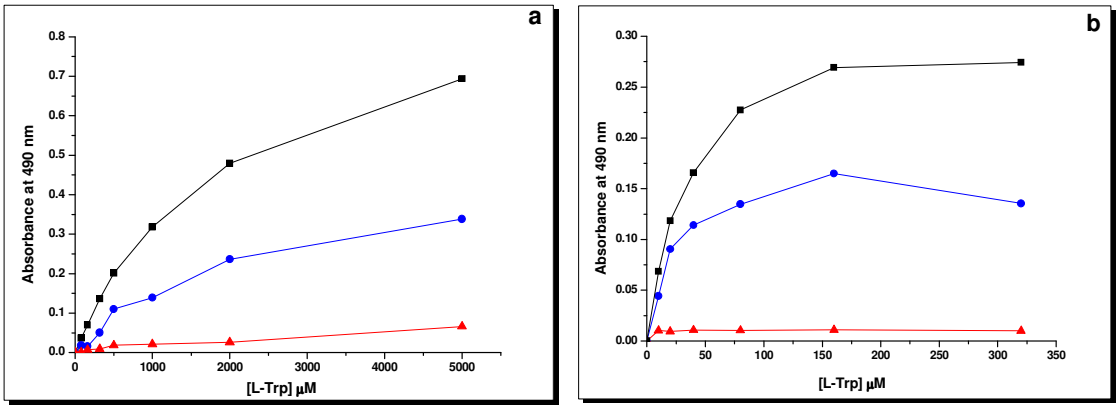

Figure 3.10: Inhibition of a) hTDO and b) hIDO by benzoquinones. The control curve (L-Trp) is shown in black while the reactions inhibited by 1,4-benzoquinone and tetrachloro-1,2-benzoquinone are shown in blue and red respectively. Both molecules were used at 400 µM final concentration.

3.3.3 Ebselen

Ebselen is another inhibitor of IDO, characterized as non-specific because of its ability to form Se-S bonds with the side chains of cysteine residues [11]. Due to this mode of action it is possible that ebselen could be also considered as an inhibitor of TDO (in contrast with IDO, which contains 8 cysteine residues, TDO has only 3). Indeed, as figure 3.11 shows, ebselen inhibits both TDO and IDO. However, the potency of this molecule against the two enzymes differs, being noticeably stronger as an inhibitor for IDO than it is for TDO.

While it might be said that ebselen's proposed mode of inhibition may render it completely non-specific, the conclusions revealed from ebselen's action are highly interesting. Terentis and co-workers showed that the action of this inhibitor implies structural modification of IDO, something which in turn affects the active site of the enzyme and its activity [11]. Herein it is shown that the effect of 400 μM ebselen, in inhibition of IDO and TDO, is significantly different. Mutation of TDO cysteine residues could provide important information about the cysteines' implication on enzyme's stability/activity.

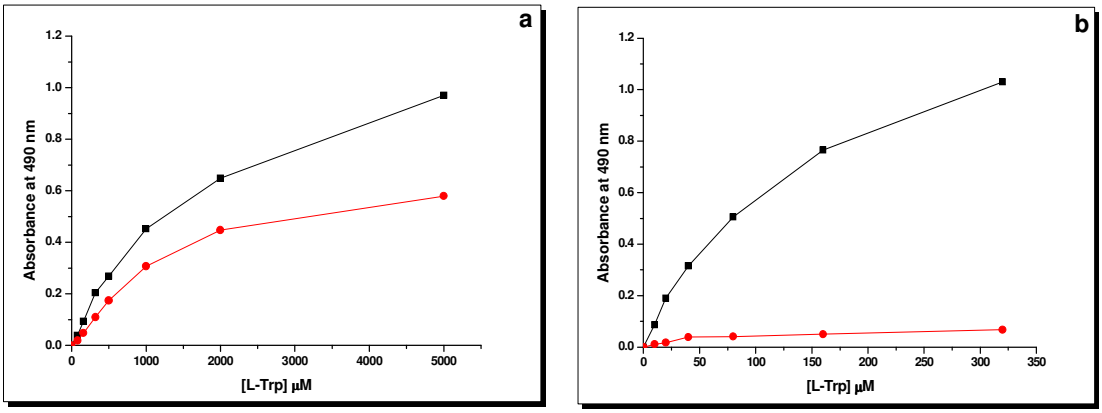

Figure 3.11: Inhibition of a) hTDO and b) hIDO by ebselen. The control curve (L-Trp) is shown in black while the ebselen-inhibited reaction is shown in red. The final concentration of ebselen was 400μM.

3.3.4 Mitomycin C

In 2009, Lou and co-workers published a paper in which mitomycin C was reported as inhibitor of IDO [(1)]. Table 3.1 demonstrates that mitomycin C inhibits TDO as well, with an inhibition constant of 2.86 ± 0.03μM. Comparison between the two enzymes showed that mitomycin C is more potent TDO inhibitor than IDO. Considering the fact that mitomycin C is an approved oncology drug, its inhibition action against IDO will be examined further in section 3.4.

3.3.5 3-(2-pyridylethenyl)indoles

Findings published in the 1990s characterised this family of molecules as inhibitors for TDO with inhibition constants in the nanomolar range [(12), (13)]. *In vitro* studies now reveal that the pyridyl molecules inhibit both TDO and IDO enzymes. The inhibition activity of 2-pyridyl against the two enzymes is shown in figure 3.12. In addition, the 3-pyridyl and 4-pyridyl compounds were also tested with similar outcomes (no specificity against TDO). The structures of these molecules can be found in chapter 1, section 1.17.

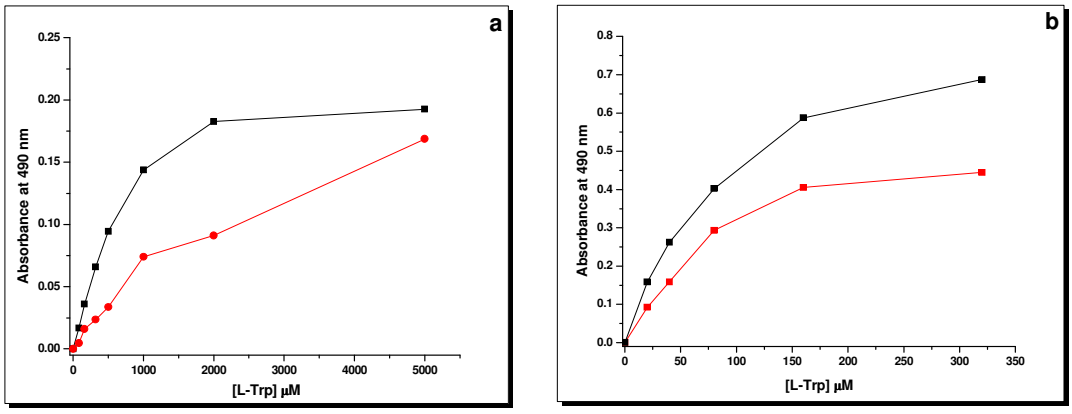

Figure 3.12: Inhibition of a) hTDO and b) hIDO by 2-pyridyl (400 μM). These findings clarify that pyridyl compounds show no specificity against TDO. The control curve (non-inhibited reaction) is shown in black while the reaction that is inhibited by 2-pyridyl is presented in red.

3.4 National Cancer Institute library compounds as TDO and IDO inhibitors

Plate screening of ~2800 potential inhibitor compounds obtained from the National Cancer Institute indicated that 7 of these compounds (fig. 3.13) displayed promise as inhibitors of both TDO and IDO, as evidenced by inhibition constants either in the nanomolar or low micromolar range (Table 3.6). The Dixon plots for each of these potent lead molecules are shown in figure 3.14. Interestingly, of these seven inhibitors, six have been identified to have cytotoxic action against several types of tumour cells (NCI data). NSC 26326, known as β-lapachone, is a natural occurring quinone that can be isolated from the lapacho tree (*Tabebuia avellanedae*). A series of studies [14-19] have shown that NSC 26326 affects the survival rate of cancer cells such as pancreatic, breast, colon, retinoblastoma, leukaemia and non-small-cell lung cancer. Of all the reported inhibitors herein, NSC 26326 is the strongest inhibitor of both IDO and TDO with inhibition constants of 97 ± 14 nM and 30-70 nM respectively. Like NSC 26326, NSC 36398 is another natural product that belongs to the class of flavonoids. Among the several flavonoids that have been examined (Appendix A), NSC 36398 is the most potent inhibitor of TDO with a K_i of 16.3 ± 3.8 μM. In contrast with TDO, IDO was not found to be inhibited by NSC 36398 at concentrations up to 100 μM. The low toxicity of flavonoids in combination with their previously reported anticancer function makes NSC 36398 an attractive lead in cancer therapy [20]. NSC 267461, or nanomycin A, is a naphthoquinone based inhibitor, inhibiting IDO and TDO with K_i values of 950 ± 270 nM and 360 ± 30 nM respectively. NSC 267461 is active in 59 tumour cell lines, killing several types of cancer cells [21].

NSC 111041 also inhibits TDO and IDO with inhibition constants of 1.1 ± 0.3 μM and 4.3 ± 0.9 μM respectively. Examination of this compound revealed activity against colon and breast tumour cell lines [21]. NSC 255109 (17-aminodemethoxygeldanamycin) is a good inhibitor for both TDO and IDO, with inhibition constants in the nanomolar range. For TDO, K_i was found to be 600 ± 70 nM and for IDO it was 1.4 ± 0.5 μM. Tests on tumour cell lines showed that NSC 255109 is active in 65 different cell lines and the types of cancer cells that this

compound is effective on are given in table 3.6 [21]. NSC 261726, or 3-deazaguanine, is an inhibitor with activity in the lower micromolar range (K_i values of 5.6 ± 0.4 μM and 21.4 ± 2.4 μM for TDO and IDO respectively). NSC 261726 was found to be active in colon and leukaemia tumour cell lines, something which increases the interest in this compound [21]. Despite the structural similarities between NSC 261726 and guanine, the latter showed no inhibitory activity on either TDO or IDO. Indeed, none of the heterocyclic nucleic acid bases indicated potential inhibition activity for IDO or TDO. Finally, among the compounds identified by screening is mitomycin C, an approved oncology drug with action in 74 tumour cell lines [21].

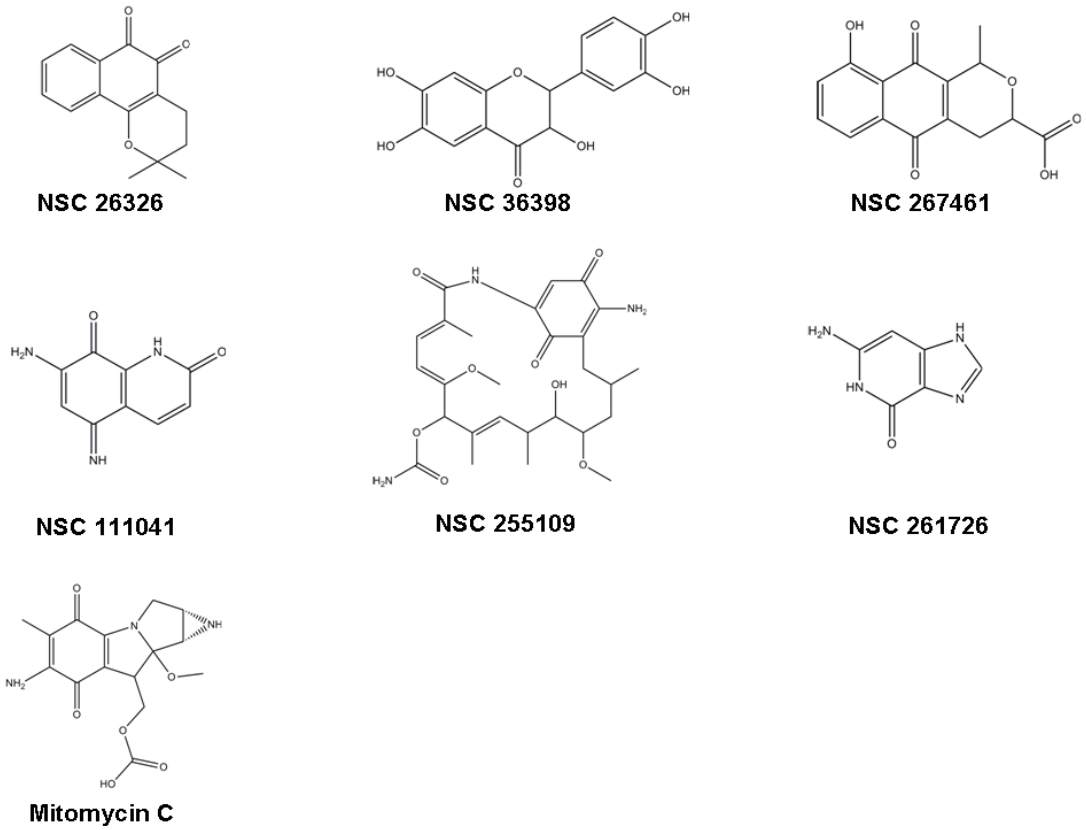

Figure 3.13: Structures of the seven NCI inhibitors that inhibit TDO and IDO with high affinity. Important to note is that these molecules are also active in various cancer cell lines (Table 3.6).

NSC	K_i (hTDO)	K_i (hIDO)	Active in tumour cell line
26326	**30-70 nM**	**97 ± 14 nM**	Pancreatic cancer, breast cancer, colon cancer, retinoblastoma, leukaemia and non-small-cell lung cancer
36398	**16.3 ± 3.8 µM**	**>100µM**	Ovarian cancer?
267461	**360 ± 30 nM**	**950 ± 270 nM**	Non-small cell lung cancer, melanoma cancer, prostate cancer, central nervous system cancer, small cell lung cancer, colon cancer, breast cancer, ovarian cancer, leukemia and renal cancer
111041	**1.1 ± 0.3 µM**	**4.3 ± 0.9 µM**	Colon cancer and breast cancer
255109	**600 ± 70 nM**	**1.4 ± 0.5 µM**	Non-small cell lung cancer, melanoma cancer, prostate cancer, central nervous system cancer, colon cancer, breast cancer, ovarian cancer, leukemia and renal cancer
261726	**5.6 ± 0.4 µM**	**21.4 ± 2.4 µM**	Colon cancer and leukemia
Mitomycin	**2.86 ± 0.03 µM**	**24.2 ± 1.2 µM**	Non-small cell lung cancer, melanoma cancer, prostate cancer, central nervous system cancer, small cell lung cancer, colon cancer, breast cancer, ovarian cancer, leukemia and renal cancer

Table 3.6: Inhibition constants of seven NCI inhibitors (measured in this work) against TDO and IDO. Information includes K_i values and which tumour cell lines are affected. More details about the tumour cell lines can be obtained from the NCI USA (http://dtp.nci.nih.gov/dtpstandard/ChemData/index.jsp)

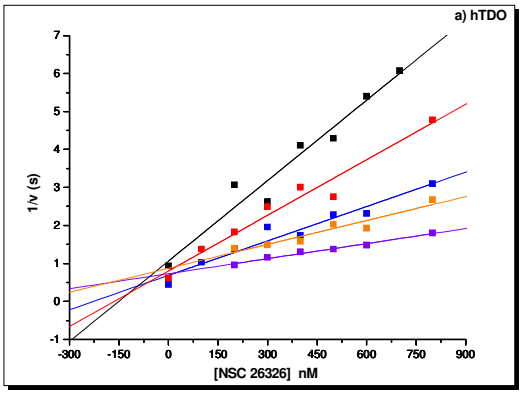
a) hTDO
1/v (s)
[NSC 26326] nM

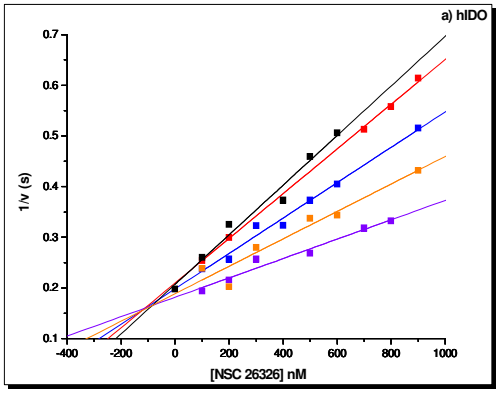
a) hIDO
1/v (s)
[NSC 26326] nM

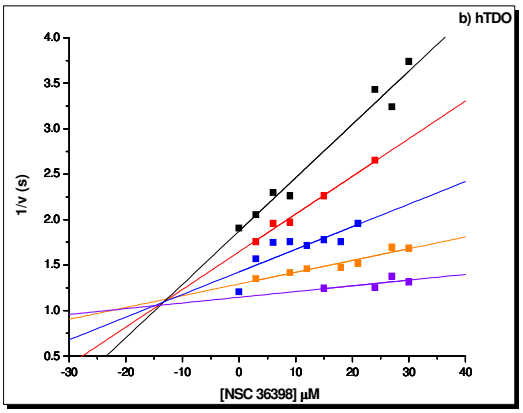
b) hTDO
1/v (s)
[NSC 36398] µM

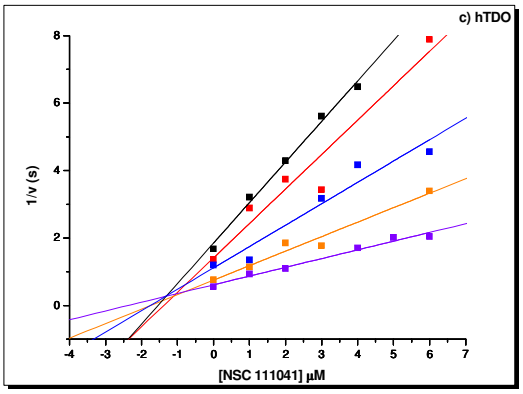
c) hTDO
1/v (s)
[NSC 111041] µM

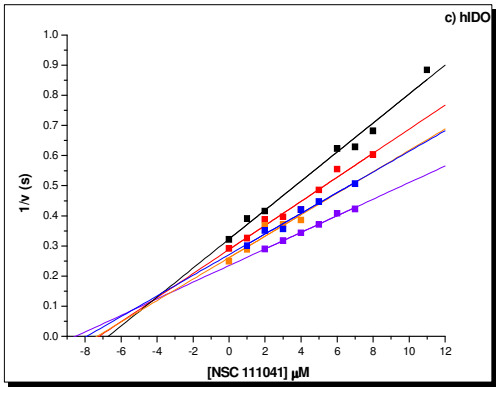
c) hIDO
1/v (s)
[NSC 111041] µM

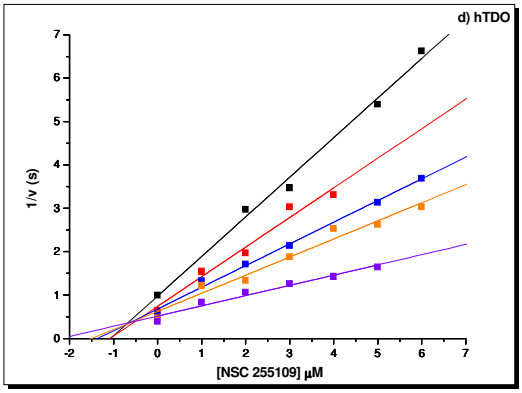
d) hTDO
1/v (s)
[NSC 255109] µM

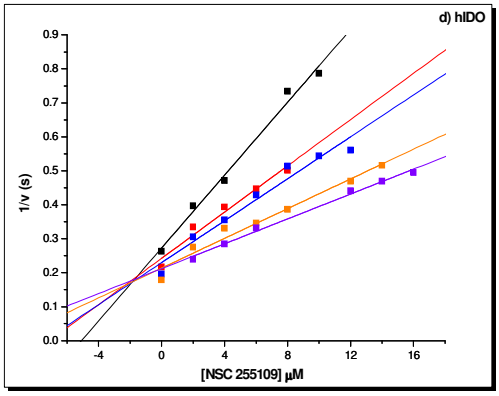
d) hIDO
1/v (s)
[NSC 255109] µM

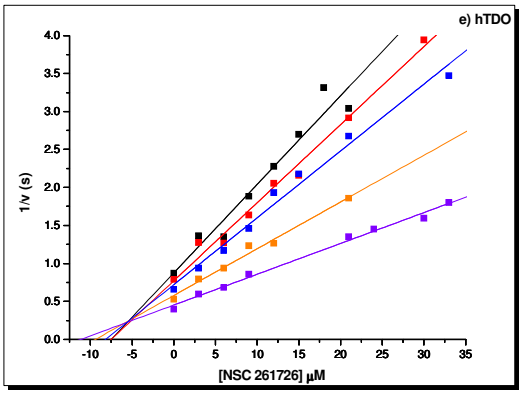
e) hTDO
1/v (s)
[NSC 261726] µM

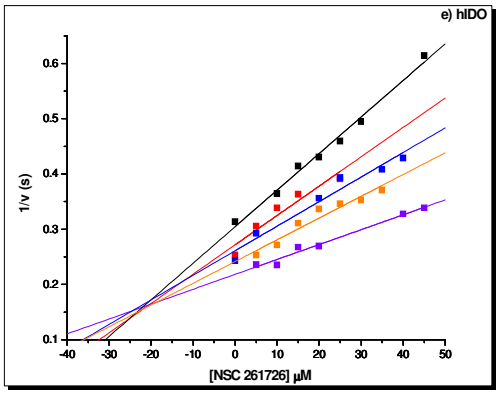
e) hIDO
1/v (s)
[NSC 261726] µM

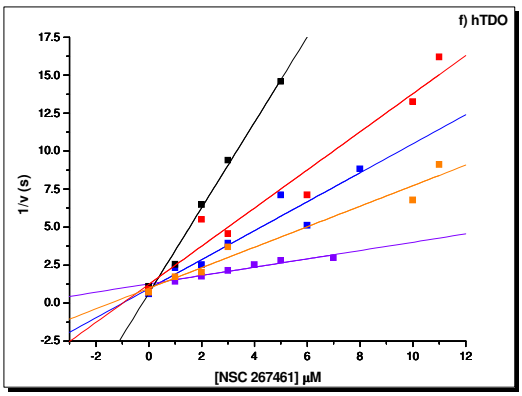
f) hTDO
1/v (s)
[NSC 267461] µM

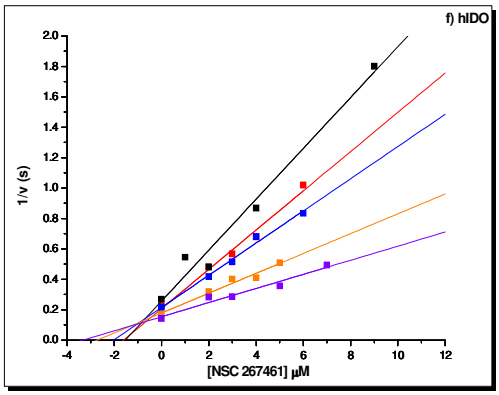
f) hIDO
1/v (s)
[NSC 267461] µM

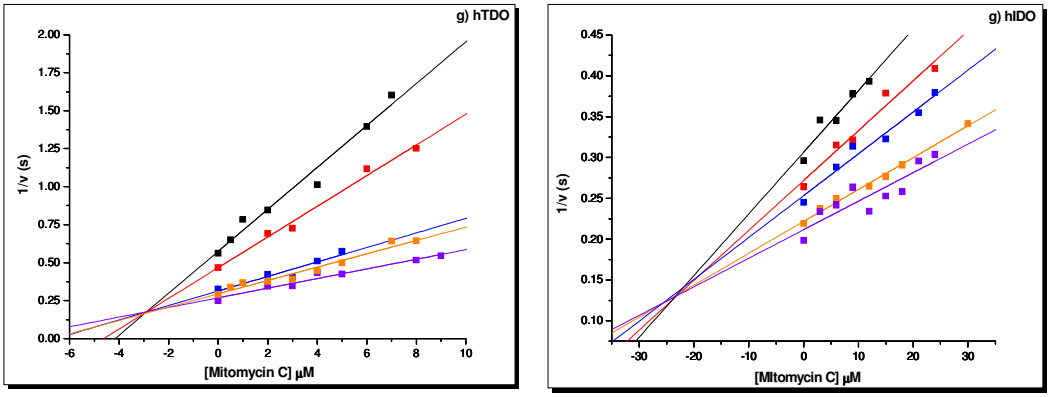

Figure 3.14: Dixon plots of hTDO (left column) and hIDO (right column) using a) NSC 26326, b) NSC 36398, c) NSC 111041, d) NSC 255109, e) NSC 261726, f) NSC 267461 and g) mitomycin C as inhibitors. (a) NSC 26326. Substrate concentrations used (all µM) were: TDO, 300 (black), 500 (red), 600 (blue), 700 (orange), 800 (violet); IDO, 15 (black), 25 (red), 30 (blue), 40 (orange), 45 (violet). (b) NSC 36398. Substrate concentrations (µM) were 300 (black), 350 (red), 400 (blue), 500 (orange), 600 (violet). (c) NSC 111041. Substrate concentrations used (all µM) were: TDO, 300 (black), 350 (red), 400 (blue), 600 (orange), 800 (violet); IDO, 15 (black), 20 (red), 25 (blue), 30 (orange), 45 (violet). (d) NSC 255109. Substrate concentrations used (all µM) were: TDO, 300 (black), 500 (red), 600 (blue), 700 (orange), 800 (violet); IDO, 15 (black), 30 (red), 35 (blue), 40 (orange), 45 (violet). (e) NSC 261726. Substrate concentrations used (all µM) were: TDO, 350 (black), 400 (red), 500 (blue), 600 (orange), 800 (violet); IDO, 15 (black), 25 (red), 30 (blue), 40 (orange), 45 (violet). (f) NSC 267461. Substrate concentrations used (all µM) were: TDO, 300 (black), 400 (red), 500 (blue), 600 (orange), 800 (violet); IDO, 15 (black), 20 (red), 25 (blue), 35 (orange), 45 (violet). (g) Mitomycin C. Substrate concentrations used (all µM) were: TDO, 300 (black), 350 (red), 600 (blue), 700 (orange), 800 (violet); IDO, 15 (black), 17.5 (red), 20 (blue), 22.5 (orange), 30 (violet).

3.4.1 Combination of 1-MT with the seven antitumour agents for hIDO inhibition

In this work we have combined 1-MT with the 7 NCI inhibitors that are mentioned above, in order to investigate the effect of combinations on inhibition of IDO. Having in mind the antitumour properties of 1-MT in combination with the assumption that the molecule has similar to L-Trp orientation in the active site of IDO (section 1.12), we combined 1-MT with the seven chemotherapeutic agents in order to achieve a more effective inhibition of IDO. The results obtained from this trial are shown in figure 3.15. From the figure it can be seen that consistent results are obtained in each of the seven individual assay plates in the presence of only 1-MT as an inhibitor. At 50 μM 1-MT around 88-97% of uninhibited activity is observed, dropping to ~55-60% of uninhibited activity at 400 μM 1-MT. In the presence of 100 μM NSC 26326 (IDO K_i = 97 ± 14 nM), it can be seen from figure 3.15 that there is almost complete inhibition of the enzyme, with only ~2 % of the inhibitor-free activity being observed. In this respect, the strength of inhibition of NSC 26326 means that further addition of increasing amounts of 1-MT has little appreciable effect on the overall inhibition observed. This type of response is also observed in the presence of NSC 267461 (IDO K_i = 950 ± 270 nM), with addition of 100 μM of the inhibitor leading to a loss of ~97% of the inhibitor-free activity, and the additional presence of 1-MT having little additional effect. Similar responses are also seen with NSC 111041 (IDO K_i = 4.3 ± 0.9 μM) and, to a lesser extent, NSC 255109 (IDO K_i = 1.4 ± 0.5 μM). In the case of NSC 111041, the presence of the inhibitor at 100 μM leads to loss of ~93% of IDO activity with 1-MT addition at 400 μM raising this level to ~96% inhibition. For NSC 255109 the effect is slightly less marked, with its presence at 100 μM resulting in around 90% inhibition of enzyme activity, while concomitant addition of increasing amounts of 1-MT causes a steady decrease in activity to a maximum of 96% inhibition at 400 μM 1-MT.

The remaining NCI compounds have less dramatic effects on IDO activity at 100 μM. The presence of 100 μM NSC 36398 (K_i > 100 μM) leads to retention of approximately 85% of uninhibited IDO activity. Combination of this inhibitor with

varying 1-MT concentrations revealed a consistent decrease in the enzyme's activity to around 80-85% of the activity in the presence of the same 1-MT concentration but in the absence of the NCI compound. With 100 µM NSC 261726 present (IDO K_i = 21.4 ± 2.4 µM) there is a decrease in enzyme activity to around 27% of the uninhibited value, while addition of 1-MT in tandem with NSC 261726 causes further inhibition by the same proportion as observed with increasing amounts of 1-MT but in the absence of the NCI compound (fig. 3.15). Finally, mitomycin C is known to inhibit IDO (section 1.12) with a K_i value of 24.2 ± 1.2 µM. Its presence in the assay at 100 µM causes activity to fall to ~36% of full activity, with additional inhibition by increasing concentrations of 1-MT following the same trend as observed for NSC 36398 and NSC 261726.

From these results it can be seen that the effect of using combinations of 1-MT with the newly-identified NCI compound inhibitors is simply additive, with the dominant effect being that of the better inhibitor (lower K_i value) in each pair.

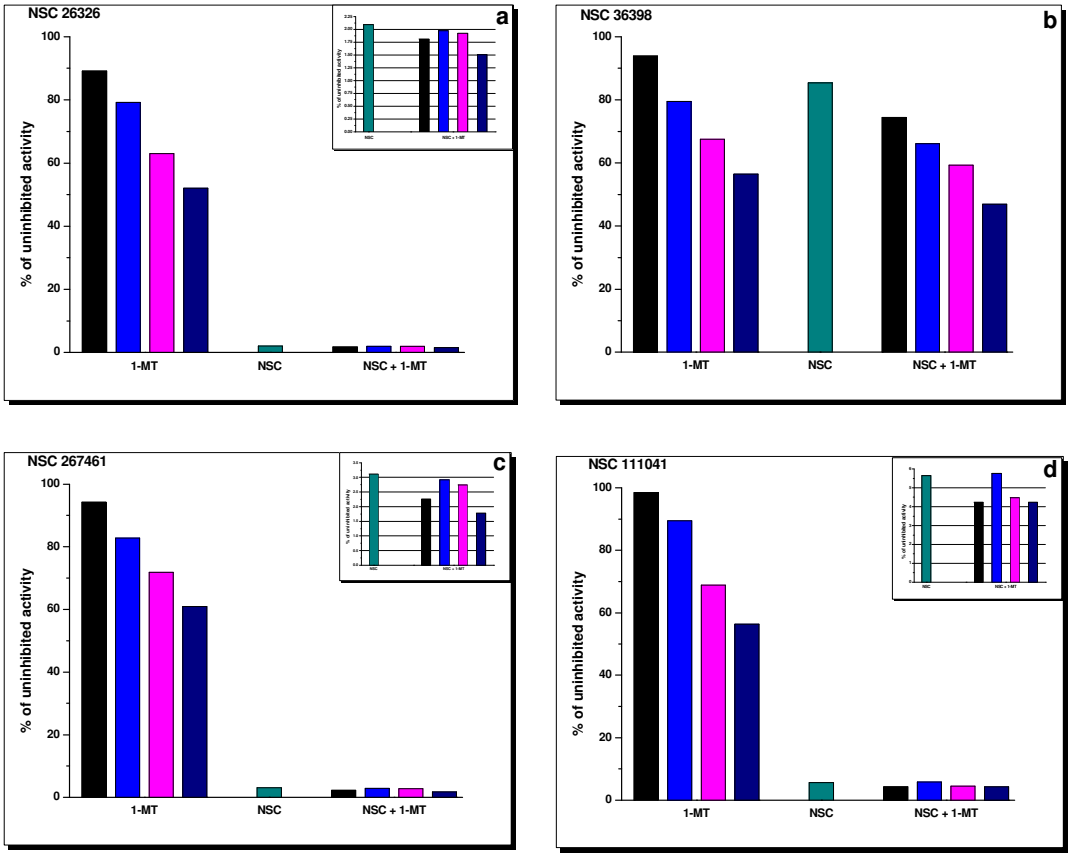

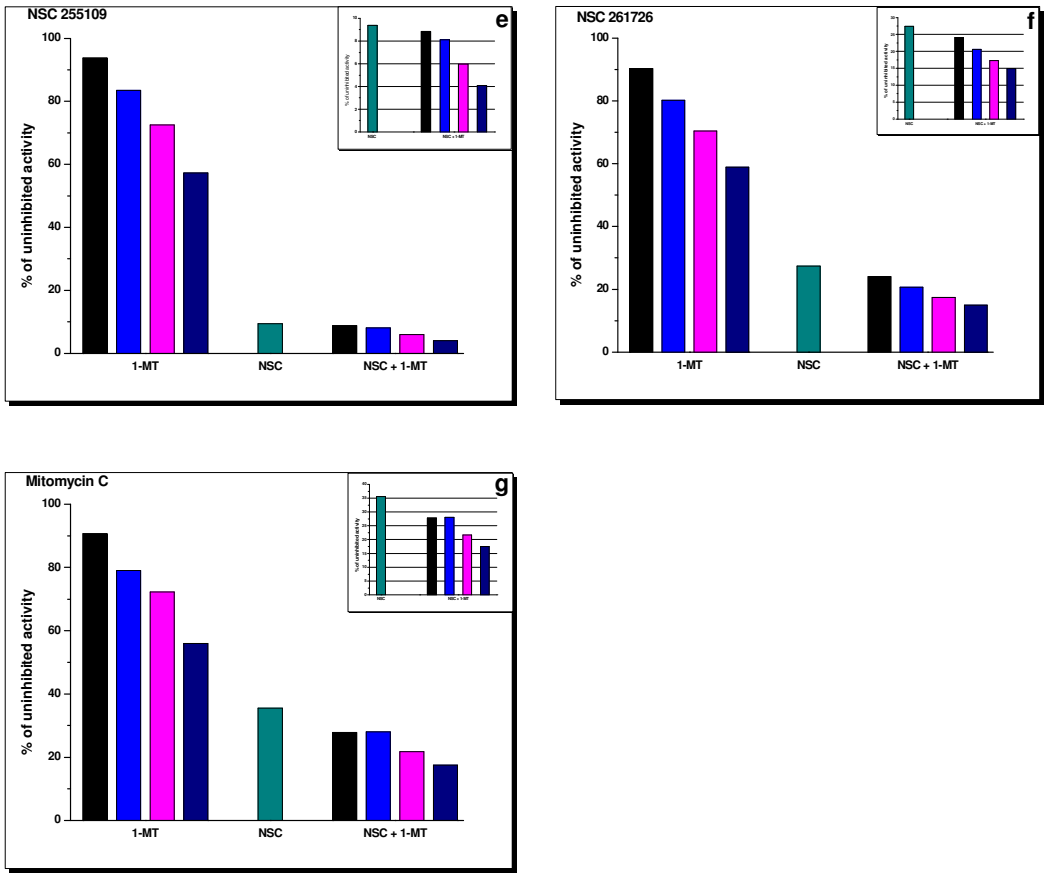

Figures 3.15: Combination of 1-MT with NCI inhibitors for inhibition of IDO. a) NSC 26326, b) NSC 36398, c) NSC 267461, d) NSC 111041, e) NSC 255109, f) NSC 261726 and g) mitomycin C. The black, blue, pink and navy blue columns represent 50 μM, 100 μM, 200 μM and 400 μM of 1-MT without and with 100 μM NCI inhibitors. In dark cyan is the NCI inhibitor at the same concentration as it is in the complex with 1-MT (100 μM)

3.5 Natural products

Whereas inhibition of IDO by natural products is well documented (see section 1.12), little is known about their action on TDO. This section examines the inhibition effect of various natural products on both TDO and IDO. Screening indicated several types of natural products (vitamin K1, flavones, NSC 100445 and riboflavin) with potential inhibition action against either TDO or IDO or both (fig. 3.16). The most potent flavone derivative inhibitor (NSC 36398) has already been discussed in section 3.4, so this section will focus on vitamin K1, NSC 100445 and riboflavin.

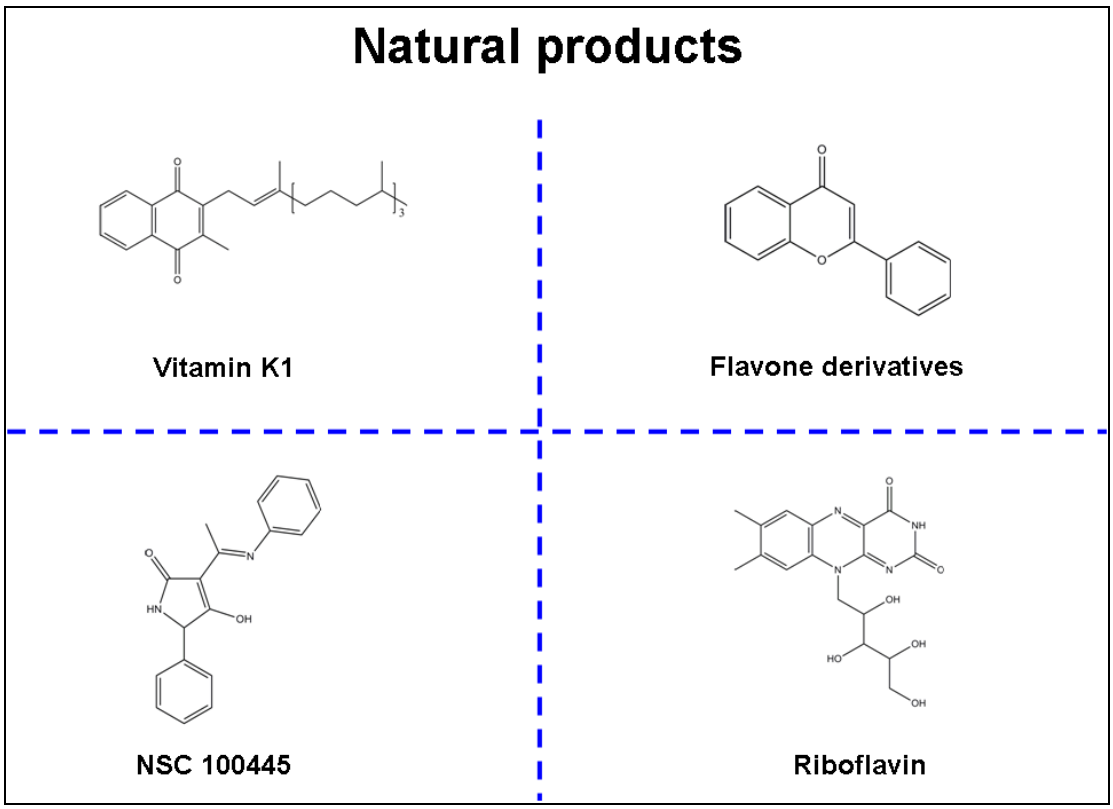

Figure 3.16: The structures of some natural products that have been identified herein as inhibitors of TDO and IDO.

3.5.1 Vitamin K1

Vitamin K1 is a naphthoquinone-based, fat-soluble natural product with inhibition activity against both enzymes (fig. 3.17). Because of its poor solubility in water, vitamin K1 is not a useful lead inhibitor for either TDO or IDO and therefore its study is terminated here.

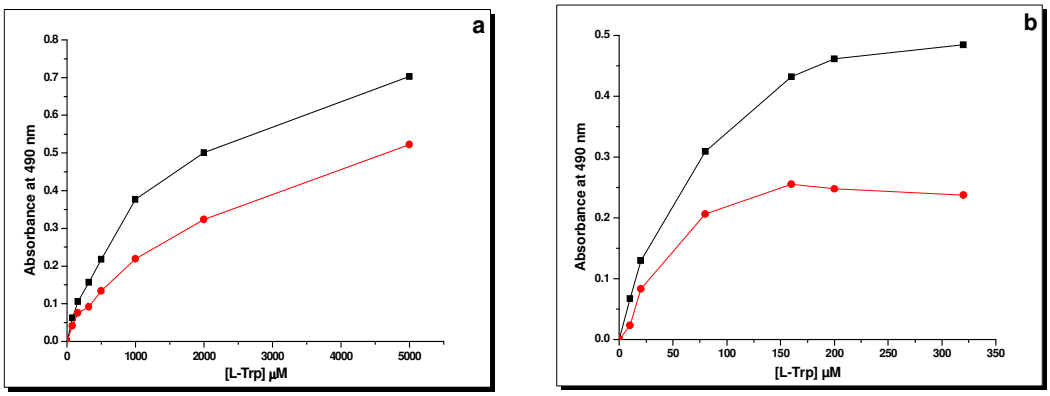

Figure 3.17: Demonstration of (a) TDO inhibition and (b) IDO inhibition by vitamin K1(400 µM final concentration). Control = black, vitamin K1= red.

3.5.2 NSC 100445

NSC 100445 is a weak inhibitor of TDO with negligible effect on IDO (fig. 3.18). Further understanding of its action demands development of NSC 100445 derivatives, something which is not within the aims of the current project.

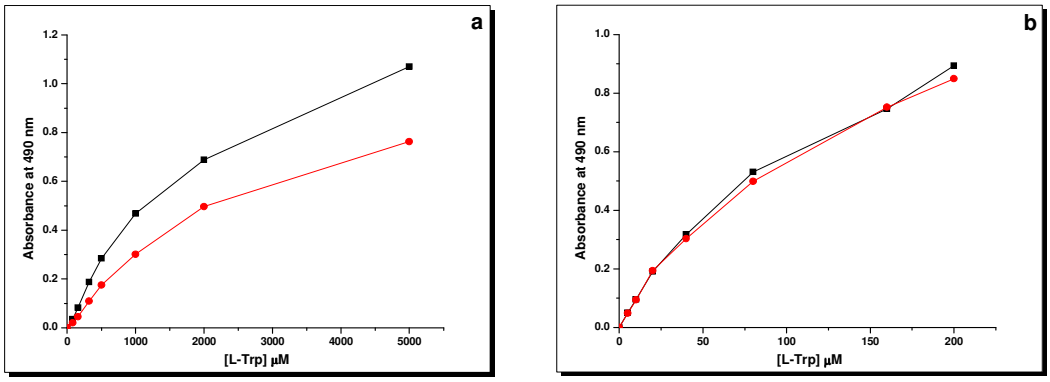

Figure 3.18: Inhibition of (a) TDO and (b) IDO by NSC 100445 (400 µM final concentration). Control = black, NSC 100445 = red.

3.5.3 Riboflavin

In contrast with vitamin K1, riboflavin which is also known as vitamin B2, is a water soluble natural product. Riboflavin was found to inhibit TDO and IDO enzymes with inhibition constants of 5.85 ± 0.47 μM and 10.3 ± 0.77 μM respectively (fig. 3.19).

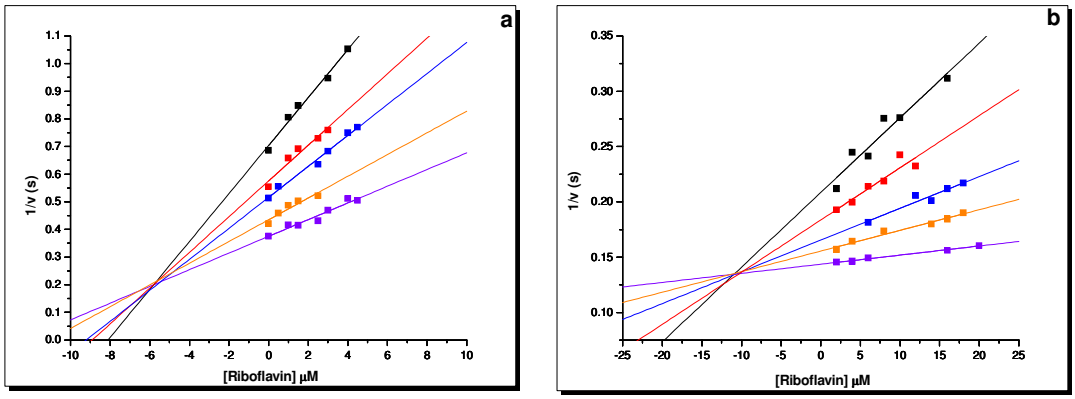

Figure 3.19: Dixon plots for inhibition of a) TDO and b) IDO by riboflavin. Substrate concentrations used (all μM) were: TDO, 300 (black), 350 (red), 400 (blue), 500 (orange), 600 (violet); IDO, 15 (black), 25 (red), 30 (blue), 40 (orange), 45 (violet).

Important to note is that riboflavin is the central component of flavin adenine dinucleotide (FAD) and flavin mononucleotide (FMN), the structures of which are presented in figure 3.20. FAD and FMN are co-factors of various proteins and implicated in a series of metabolic pathways. FAD is a co-factor of kynurenine-3-monoxygenase (KMO), an enzyme that participates in tryptophan metabolism, transforming kynurenine into 3-hydroxykynurenine.

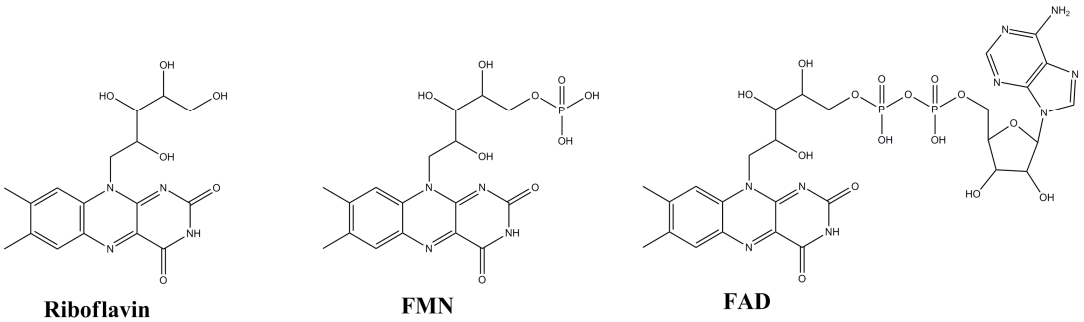

Figure 3.20: Structures of riboflavin, FMN and FAD

With this in mind, FMN and FAD were also tested as inhibitors of TDO and IDO and the results were compared with riboflavin findings (fig. 3.21). Interestingly, both FMN and FAD were found to inhibit TDO and IDO, but with lower potency than riboflavin.

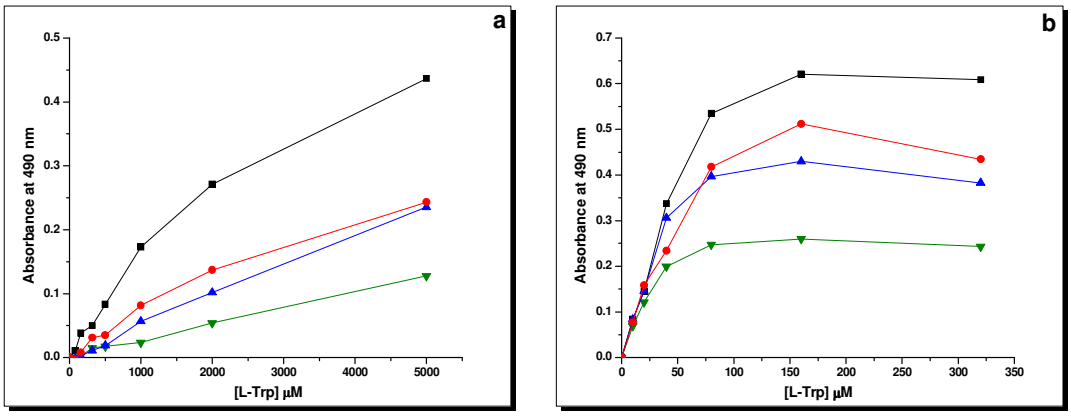

Figure 3.21: Inhibition of a) TDO and b) IDO by FAD (red), FMN (blue) and riboflavin (green). All three were used at 400 μM final concentration.

For a better understanding of the way that riboflavin inhibits the two enzymes, lumiflavin was also investigated as an inhibitor. Replacement of riboflavin's poly-hydroxyl tail by a methyl group gives lumiflavin. Lumiflavin is a less effective inhibitor than riboflavin (fig. 3.22), something which indicates implication of the poly-hydroxyl tail in the binding of the molecule.

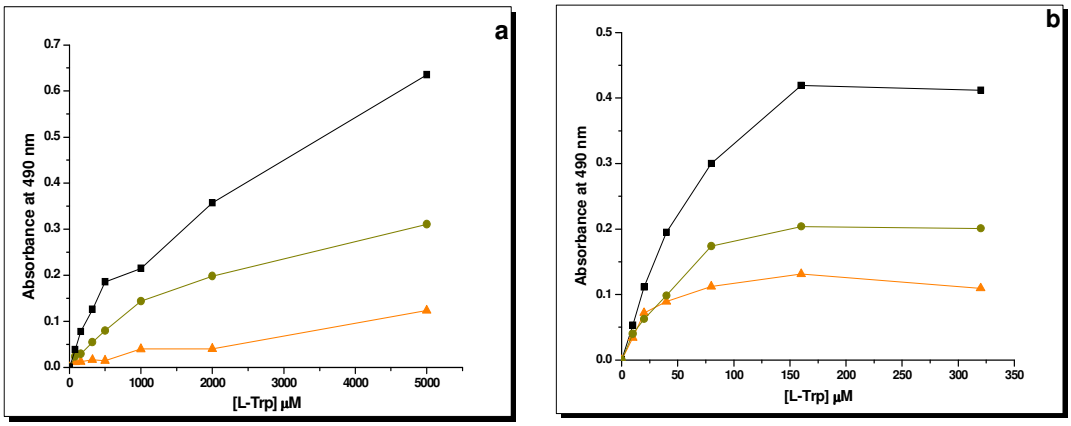

Figure 3.22: Inhibition of a) TDO and b) IDO by lumiflavin (dark yellow) and riboflavin (orange). Both molecules were used at 400 μM final concentration.

3.6 Kynurenine pathway metabolites

As potential inhibitors of TDO and IDO, it is logical to also investigate the kynurenine pathway metabolites. In total, six kynurenine pathway metabolites were tested (kynurenine, 3-hydroxykynurenine, kynurenic acid, 3-hydroxyanthranilic acid, anthranilic acid and NAD) but only one, 3-hydroxyanthranilic acid, revealed inhibition activity against both enzymes (fig. 3.23). The well-reported cytotoxic properties of 3-hydroxyanthranilic acid (section 1.3.2) discourage any trials of using this molecule for developing inhibitors for TDO and IDO.

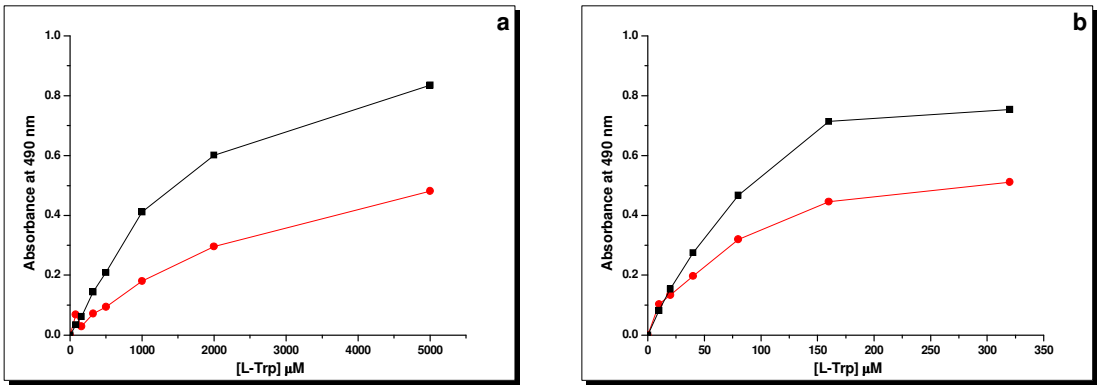

Figure 3.23: Inhibition of a) TDO and b) IDO by 3-hydroxyanthranilic acid (red). The inhibitor was used at 400 µM final concentration.

3.7 Other potential inhibitors

As the inhibitor list shows (Appendix A), the search for TDO/IDO inhibitors was not limited to the categories that are mentioned above. DNA/RNA bases, tryptophan and indole derivatives, and KMO inhibitors are among the molecules that have been also tested. However, none of these compounds indicated potential inhibition activity against either TDO or IDO.

3.8 Discussion

The starting point of this chapter was the study of the various published inhibitors. The conclusions from this trial are illustrated in table 3.7. 1-methyltryptophan is the only specific inhibitor for IDO while pyridyls showed no specificity against TDO. All the other inhibitors, naphthoquinones, ebselen, mitomycin C, phenylimidazole and norharman inhibit both enzymes.

"Before"

IDO inhibitors	TDO inhibitors	IDO and TDO
1-Me-Tryptophan Naphthoquinones Ebselen Mitomycin C	Pyridyls	Phenylimidazole Norharman

"After"

IDO inhibitors	TDO inhibitors	IDO and TDO
1-Me-Tryptophan		Phenylimidazole Norharman Naphthoquinones Ebselen Mitomycin C Pyridyls

Table 3.7: Allocation of the various TDO and IDO inhibitors as specific for either enzyme or not specific according to the published results ("before") and after this work ("after").

Inhibition, redox and turnover examination of hIDO and hTDO clearly points to 1-Me-L-Trp being the only inhibitor specific for hIDO. Neither 1-Me-L-Trp nor 1-Me-D-Trp inhibits hTDO. The specificity of hIDO for the L-isomer of 1-MT is illustrated by the turnover findings, which show that binding of 1-Me-D-Trp to IDO is unfavourable and therefore no inhibition is observed. The fairly high affinity of 1-Me-L-Trp, in combination with the poor turnover rate makes it (thus far) the only possible inhibitor for IDO, *in vitro*.

Despite this, phase I clinical trials for study of 1-Me-D-Trp as inhibitor of IDO are currently in progress (http://clinicaltrials.gov/ct2/show/NCT00617422). 1-Me-D-Trp is an ineffective *in vitro* inhibitor of IDO and the potential inhibition activity that this molecule may have in cancer cells could be related with inhibition of other than hIDO protein(s).

While many inhibitors of IDO have been identified and published, thus far none of them possess the properties of 1-MT. Because of its low toxicity and specificity for IDO, 1-MT has been studied extensively, but without any significant outcome, mainly because of its competitive type of inhibition. Nevertheless, combination of 1-MT with the seven chemotherapeutic agents, reported above, provides a new approach towards the potential use of 1-MT as an anticancer drug. β-Lapachone (NSC 26326), a promising anticancer agent, revealed synergistic action with 1-MT, causing further inhibition of hIDO. β-Lapachone is known for its selectivity in killing several types of cancer cells while leaving normal cells intact [(22), (23)]. Its action is highly depended on the expression of NAD(P)H: quinone oxidoreductase-1 (NQO1), an enzyme that catalyses reduction of quinones to hydroquinones. Various types of cancers, and in particular pancreatic cancer, overexpress NQO1 by more than 10-fold in comparison with normal cells [(24)]. Reduction of β-lapachone by NQO1 increases the amount of reactive oxygen species (ROS), causing apoptosis in cancer cells. Recent findings show that β-lapachone, under optimal conditions, causes neither toxicity nor haemolytic anemia to normal tissue [(24)]. In addition, it shows a synergistic effect with radiation, something which further increases the interest in this molecule [(25)]. In contrast with β-lapachone, the flavone-derivative NSC 36398, is not an ideal inhibitor for IDO. However, the molecule demonstrated a preference for TDO, inhibiting the enzyme in the low

micromolar range (K_i = 16.3 ± 3.8 μM). After testing numerous TDO and IDO inhibitors (~3000 compounds), NSC 36398 is the only compound that reveals selectivity for TDO. Considering flavones' low toxicity, NSC 36398 may well be a useful inhibitor for TDO. NSC 267461 or nanaomycin A is reported as an inhibitor of DNA (cytosine-5-)-methyltransferase 3 beta (DNMT3B), inducing DNA demethylation [(26)]. Although DNA methylation is essential during embryonic development, abnormal methylation of DNA silences many tumour suppressor genes, leading to cancer. The combined effect of nanaomycin A and 1-MT, allied to nanaomycin's ability to inhibit DNMT3B might increase the effectiveness of 1-MT *in vivo*, providing new insights in cancer treatment. NSC 255109 is a benzoquinone-based antibiotic and analogue of geldanamycin. Geldanamycin is a molecule with antitumour activity through its competitive binding to the ATP binding pocket of heat shock protein 90 (Hsp90) [(27)]. Because of geldanamycin's hepatotoxicity a number of analogues were developed by substitution at the 17-position of the maternal molecule. One of these is NSC 255109, a strong inhibitor of TDO and IDO. Phase I pharmacokinetic and pharmacodynamic studies of 17-allylamino-17-demethoxygeldanamycin (17-AAG), another geldanamycin analogue, showed that these derivatives can be safely administered in cancer patients, retaining their antitumour activity [(27), (28)]. These findings in combination with the strong inhibition activity of NSC 255109 for IDO and its synergistic action with 1-MT indicate the possibility of combination therapy with 1-MT.

NSC 261726 (3-deazaguanine) is a purine analog found to have antitumour activity on leukemia and colon cancer cells [(21)]**.** Because of its structural similarity with guanine, 3-deazaguanine is likely to suppress DNA synthesis. 3-deazaguanine can inhibit both TDO and IDO in the micromolar range and act synergistically with 1-MT for optimization of IDO inhibition. Binding of 3-deazaguanine is independent of L-Trp concentration and therefore combination of 3-deazaguanine with 1-MT can cause strong inhibition of IDO in the low micromolar range. Like 3-deazaguanine, mitomycin C can inhibit IDO in the presence of 1-MT. Bearing in mind that the list of TDO inhibitors is far from lengthy, these seven NCI inhibitors may provide a means of finding strong inhibitors for the enzyme. Their combination with 1-MT for inhibition of IDO, in combination with the good inhibition activity that these

inhibitors have on TDO, provides new insights into usage of these. Studying these inhibitors, it became apparent that their ability to kill cancer cells is related with influence on either two proteins (β-lapachone) or a protein and DNA (mitomycin C). Their action as inhibitors of TDO and IDO is a new development and in combination with the proven negative involvement of these proteins in cancer, it could be proposed that part of these molecules' anticancer ability is related with TDO and IDO.

3.9 References

(1) Lu C., Lin Y., and Yeh S.R., *Inhibitory Substrate Binding Site of Human Indoleamine 2,3-Dioxygenase*, ***J. Am. Chem. Soc.***, 2009, 131, 12866–12867

(2) Hou D.Y., Muller A.J., Sharma M.D., DuHadaway J., Banerjee T., Johnson M., Mellor A.L., Prendergast G.C., and Munn D.H., *Inhibition of Indoleamine 2,3-Dioxygenase in Dendritic Cells by Stereoisomers of 1-Methyl-Tryptophan Correlates with Antitumor Responses*, ***Cancer Res.***, 2007, 67, 792-801

(3) Salter M., Hazelwood R., Pogson C. I., Iyer R. and Madge D. J., *The effects of a novel and selective inhibitor of Tryptophan 2,3-Dioxygenase on tryptophan and serotonin metabolism in the rat*, ***Biochemical Pharmacology***, 1995, 49, 1435-1442

(4) Löb S., Königsrainer A., Rammensee H.G., Opelz G. and Terness P., *Inhibitors of indoleamine-2,3-dioxygenase for cancer therapy: can we see the wood for the trees?*, ***Nature Reviews Cancer***, 2009, 9, 445-452

(5) Sono M. and Cady S.G., *Enzyme kinetic and spectroscopic studies of inhibitor and effector interactions with indoleamine 2,3-dioxygenase. 1. Norharman and 4-phenylimidazole binding to the enzyme as inhibitors and heme ligands*, ***Biochemistry***, 1989, 28, 5392-9

(6) Basran J., Rafice S.A., Chauhan N., Efimov I., Cheesman M.R., Ghamsari L. and Raven E.L., *A Kinetic, Spectroscopic, and Redox Study of Human Tryptophan 2,3-Dioxygenase*, ***Biochemistry***, 2008, 47, 4752–4760

(7) Chauhan N., Thackray S.J., Rafice S.A., Eaton G., Lee M., Efimov I., Basran J., Jenkins P.R., Mowat C.G., Chapman S.K., and Raven E.L., *Reassessment of the Reaction Mechanism in the Heme Dioxygenases,* ***J. Am. Chem. Soc.***, 2009, 131, 4186 – 4187

(8) Efimov I., Basran J., Sun X., Chauhan N., Chapman S.K., Mowat C.G. and Raven E.L., *The Mechanism of Substrate Inhibition in Human Indoleamine 2,3-Dioxygenase*, ***J. Am. Chem. Soc.***, 2012, 134, 3034-3041

(9) Forouhar F., Anderson J.L., Mowat C.G., Vorobiev S.M., Hussain A., Abashidze M., Bruckmann C., Thackray S.J., Seetharaman J., Tucker T., Xiao R., Ma L.C., Zhao L., Acton T.B., Montelione G.T., Chapman S.K. and Tong L., *Molecular insights into substrate recognition and catalysis by tryptophan 2,3-dioxygenase*, ***Proc. Natl. Acad. Sci.***, 2007, 104, 473-478

(10) Kumar S., Malachowski W.P., DuHadaway J.B., LaLonde J.M., Carroll P.J., Jaller D., Metz R., Prendergast G.C., and Muller A.J., *Indoleamine 2,3-Dioxygenase Is the Anticancer Target for a Novel Series of Potent Naphthoquinone-Based Inhibitors*, ***J. Med. Chem.***, 2008, *51,* 1706–1718

(11) Terentis A.C., Freewan M., Plaza T.S.S., Raftery M.J., Stocker R., and Thomas S.R., *The Selenazal Drug Ebselen Potently Inhibits Indoleamine 2,3- Dioxygenase byTargeting Enzyme Cysteine Residues*, ***Biochemistry***, 2010, 49, 591–600

(12) Madge D.J., Hazelwood R., Iyer R., Jones H.T. and Salter M., *Novel Tryptophan Dioxygenase Inhibitors and combined Tryptophan Dioxygenase/5-HT Reuptake Inhibitors*, ***Bioorganic & Medicinal Chemistry Letters***, 1996, 6, 857-860

(13) Salter M., Hazelwood R., Pogson C. I., Iyer R. and Madge D. J., *The effects of a novel and selective inhibitor of Tryptophan 2,3-Dioxygenase on tryptophan and serotonin metabolism in the rat*, ***Biochemical Pharmacology***, 1995, 49, 1435-1442

(14) Bentle M. S., Reinicke K. E., Dong Y., Bey E. A., and Boothman D. A., *Nonhomologous End Joining Is Essential for Cellular Resistance to the Novel Antitumor Agent, B-Lapachone*, ***Cancer Res***, 2007, 67, 6936-6945

(15) Wuerzberger S. M., Pink J. J., Planchan S. M., Byers K.L., Bornmann W.G., and Boothman D.A., *Induction of Apoptosis in MCF-7:WS8 Breast Cancer Cells by b-Lapachone*, ***Cancer Res*** ,1998, 58, 1876-1885

(16) Huang L. and Pardee A.B., *β-Lapachone Induces Cell Cycle Arrest and Apoptosis in Human Colon Cancer Cells*, ***Molecular Medicine***, 1999, 5, 711–720

(17) Shah H.R., Conway R.M., Quill K.R.V., Madigan M.C., Howard S.A, Qi J., Weinberg V. and O'Brien J.M., *Beta-lapachone inhibits proliferation and induces apoptosis in retinoblastoma cell lines*,***Eye***, 2008, 22, 454–460

(18) Planchon S.M., Wuerzberger S., Frydman B., Witiak D.T., Hutson P., Church D.R., Wilding G., and Boothman D.A., *b-Lapachone-mediated Apoptosis in Human Promyelocytic Leukemia (HL-60) and Human Prostate Cancer Cells: A p53-independent Response*, ***Cancer Res***, 1995, 55, 3706-3711

(19) Bey E.A., Bentle M.S., Reinicke K.E., Dong Y., Yang C.R., Girard L., Minna J.D., Bornmann W.G., Gao J., and Boothman D.A., *An NQO1- and PARP-1-mediated cell death pathway induced in non-small-cell lung cancer cells by b-lapachone*, ***PNAS***, 2007, 104 , 11832–11837

(20) Luo H., Jiang B.H., King S.M., and Chen Y.C., *Inhibition of Cell Growth and VEGF expression in Ovarian Cancer Cells by Flavonoids*, ***Nutrition and Cancer***, 2008, 60, 800-809

(21) NCI data: http://dtp.nci.nih.gov/dtpstandard/ChemData/index.jsp

(22) Bey E. A., Bentle M. S., Reinicke K. E., Dong Y., Yang C.-R., Girard L., Minna J. D., Bornmann W. G., Gao J., and Boothman D. A, *An NQO1- and PARP-1-mediated cell death pathway induced in non-small-cell lung cancer cells by β-lapachone*, ***PNAS***, 2003, 104, 11832-37

(23) Li Y., Sun X., Mont J.T.L., Pardee A.B. and Li C.J., *Selective killing of cancer cells by β-lapachone: Direct checkpoint activation as a strategy against cancer*, ***PNAS***, 2003, 100, 2674-78

(24) Li L.S., Bey E.A., Dong Y., Meng J., Patra B., Yan J., Xie X.J., Brekken R.A., Barnett C.C., Bornmann W.G., Gao J. and Boothman D.A., *Modulating Endogenous NQO1 Levels Identifies Key Regulatory Mechanisms of Action of b-Lapachone for Pancreatic Cancer Therapy*, ***Clin Cancer Res***, 2011,17, 275-285

(25) Dong Y., Bey E.A., Li L.S., Kabbani W., Yan J., Xie X.J., Hsieh J.T., Gao J., and Boothman D.A., *Prostate Cancer Radiosensitization through Poly(ADP-Ribose) Polymerase-1 Hyperactivation*, ***Cancer Res***, 2010, 70, 8088-8096

(26) Kuck D., Caulfield T., Lyko F. and Medina-Franco J.L., *Nanaomycin A selectively inhibits DNMT3B and reactivates silenced tumor suppressor genes in human cancer cells*, ***Mol Cancer Ther.***, 2010, 9, 3015-23

(27) Bagatell R., Gore L., Egorin M.J., Ho R., Heller G., Boucher N., Zuhowski E.G., Whitlock J.A., Hunger S.P., Narendran A., Katzenstein H.M., Arceci R.J., Boklan J., Herzog C.E., Whitese L., Ivy S.P. and Trippett T.M., *Phase I Pharmacokinetic and Pharmacodynamic Study of 17-NAllylamino-17-Demethoxygeldanamycinin Pediatric Patientswith Recurrent or Refractory SolidTumors: A Pediatric Oncology Experimental Therapeutics Investigators ConsortiumStudy*, ***Clin Cancer Res***, 2007,13,1783-1788

(28) Hubbard J., Erlichman C., Toft D.O., Qin R., Stensgard B.A., Felten S., Eyck C.T., Batzel G., Ivy S.P. and Haluska P, *Phase I study of 17-allylamino-17 demethoxygeldanamycin, gemcitabine and/or cisplatin in patients with refractory solid tumors*, ***Invest New Drugs***,2011, 29, 473–480

Chapter 4

Isatins as inhibitors for TDO and IDO

4.1 Introduction

In the light of recent findings implicating TDO in cancer survival and migration [(1)], interest in inhibition of the tryptophan catabolic enzymes TDO and IDO is reinforced. In the search for new TDO/IDO inhibitors isatin was an attractive target, not only because of the tryptophan-like structure but also because of the established biological and pharmacological role of isatin derivatives as oncology drugs (http://www.fda.gov/NewsEvents/Newsroom/PressAnnouncements/2006/ucm108583.htm). In addition to their anticancer activity, isatin derivatives have several other applications as, for example, anticonvulsants, antimicrobials and antidepressants drugs [(2)].

Isatin or 1*H*-indole-2,3-dione is an orange-red crystalline compound, which was discovered in the 19th century as a result of indigo oxidation (fig. 4.1) and it is found in plants, fruits, animals and humans [(3)]. In humans, it is proposed that isatin is an endogenous product of tryptophan oxidation, occurring in the liver after the consumption of tryptophan-rich food [(4)].

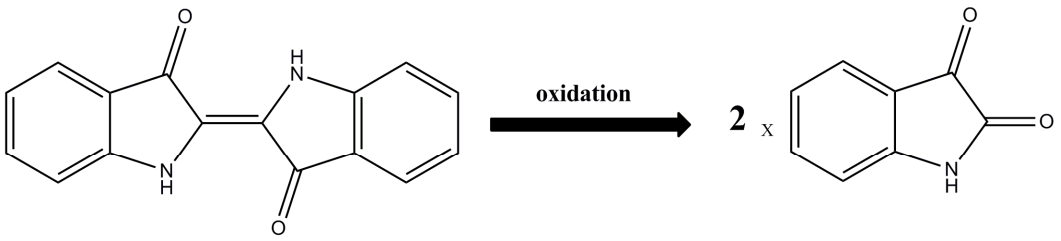

Indigo **Isatin**

Figure 4.1: Production of isatin from indigo oxidation. Oxidation of indigo causes breakdown of C=C bond producing two isatin molecules.

This chapter describes the inhibitory effects of isatin and a number of modified isatins on both TDO and IDO. The structural modifications were chosen carefully in order to obtain information about the functional groups of isatin, such as the two carbonyl groups, the nitrogen atom of the pyrrolidine ring, and the benzene and pyrrolidine rings (fig. 4.2).

In addition to this, the effect of combination of 1-MT and isatins on IDO inhibition was investigated (method described in section 2.11). The findings reveal these compounds to be a new class of TDO and IDO inhibitors with inhibition constants in the lower micromolar range.

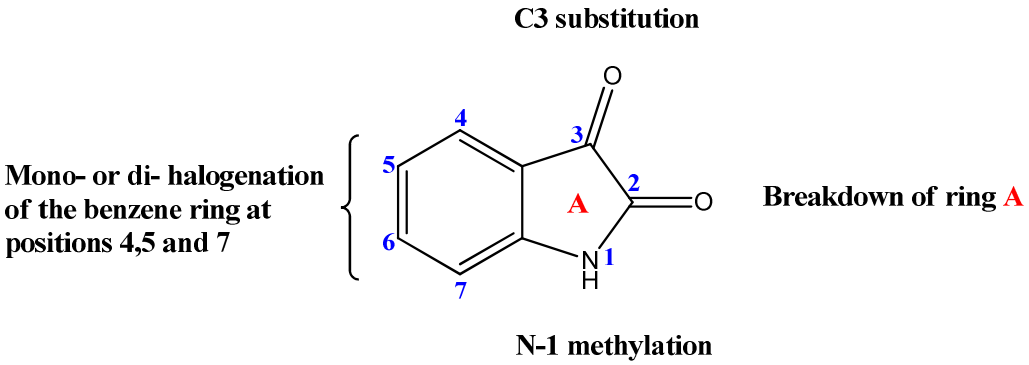

Figure 4.2: Illustration of positions for possible isatin modifications.

4.2 N-1 methylation of isatin

Isatin is a weak inhibitor of TDO/IDO enzymes with inhibition constants of 132 ± 4 μM and 89 ± 6 μM for TDO and IDO respectively (Table 4.1). Bearing in mind the specificity of 1-methyltryptophan (1-MT) as an IDO inhibitor only, the effect of the N1-methylation of isatin was investigated. The structure of 1-methylisatin is shown in figure 4.3. Interestingly, methylation of isatin caused a modest decrease in affinity towards both enzymes, shifting the inhibition constant from 132 ± 4 μM to 170 ± 13 μM for TDO and from 89 ± 6 μM to 111 ± 23 μM for IDO (Table 4.1).

4.3 Halogenation of isatin

Given the electron-withdrawing properties of halogens attached to aromatic rings, the inhibition potential of monochlorinated and dichlorinated isatins was investigated (fig. 4.3). Dixon plots for isatin and its chlorinated derivatives are illustrated in figure 4.4 while their inhibition constants are shown in table 4.1. Chlorination of isatin at the 5-position is found to increase isatin's inhibition effectiveness by 12-fold and 6-fold for TDO and IDO, with K_i values of 10.5 ± 0.4 μM and 15.2 ± 1 μM respectively. Movement of the chlorine atom from the 5-position to the 7-position of the benzene ring had a negligible effect on both enzymes, resulting in inhibition constants of 10.2 ± 0.7 μM (IDO) and 9.3 ± 0.4 μM (TDO).

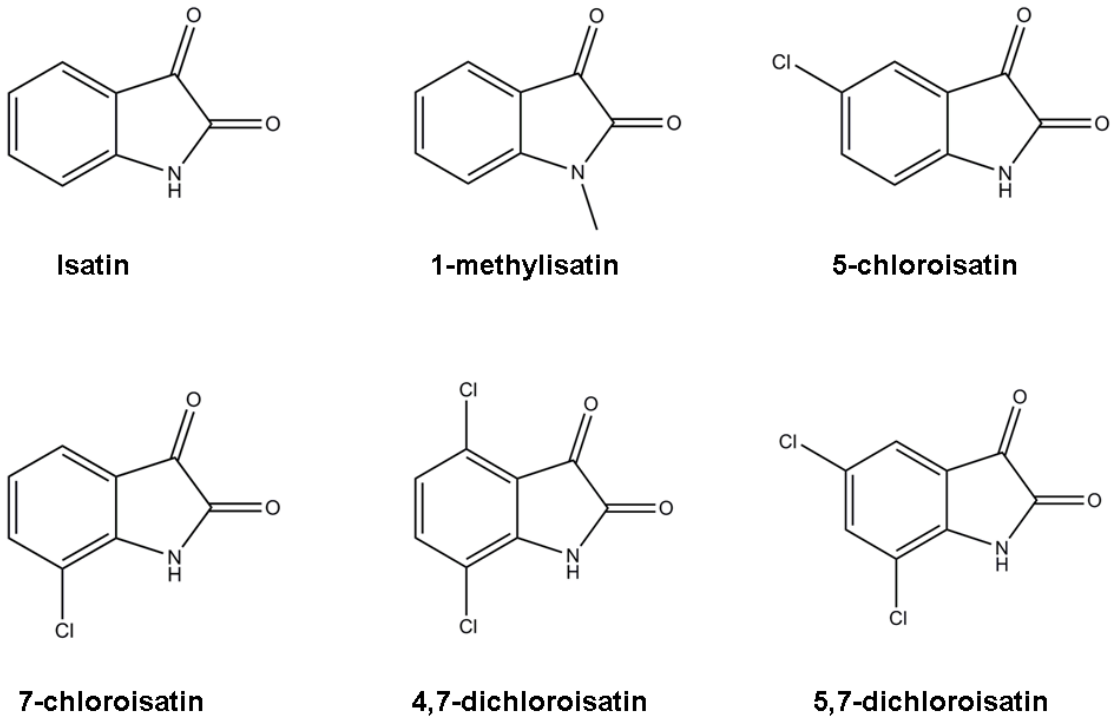

Figure 4.3: Chemical structures of isatin, 1-methylisatin and isatin's mono- and dichlorinated derivatives.

Dichlorination on the other hand, had a noticeable impact on TDO inhibition while leaving IDO fairly unaffected. In the presence of 4,7-dichloroisatin TDO inhibition was barely affected in comparison with the monochlorinated isatins, but the K_i was around 10-fold lower for 5,7-dichloroisatin in comparison with either of the monochlorinated isatins (0.8 ± 0.2 μM, Table 4.1). In the case of IDO, both 4,7-dichloroisatin and 5,7-dichloroisatin had similar impact on inhibition, offering minor optimization of the inhibition constant in contrast with the monochlorinated isatins. The position of chlorine atoms in the benzene ring of isatin proved to be important for the effectiveness of the potential inhibitor particular for TDO, something that cannot be said for IDO.

Inhibitor	TDO inhibition	IDO inhibition
isatin	132 ± 4 μM	89 ± 6 μM
1-methylisatin	170 ± 13 μM	111 ± 23 μM
5-chloroisatin	10.5 ± 0.4 μM	15.2 ± 1 μM
7-chloroisatin	9.3 ± 0.4 μM	10.2 ± 0.7 μM
4,7-dichloroisatin	3.8 ± 0.04 μM	6.0 ± 0.7 μM
5,7-dichloroisatin	0.8 ± 0.2 μM	5.9 ± 0.4 μM

Table 4.1: Inhibition of hTDO and hIDO by isatin, 1-methylisatin and chlorinated derivatives of isatin. The K_i values of isatin and its derivatives were measured as described in section 2.9

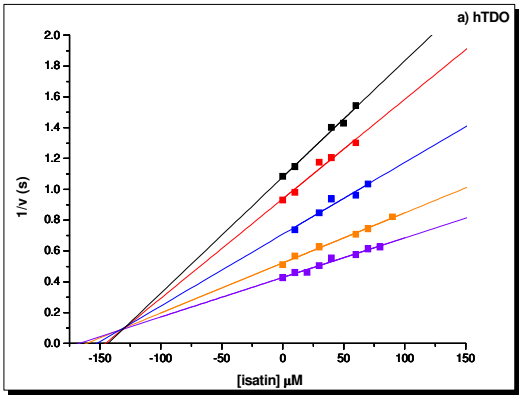
a) hTDO
1/v (s)
[isatin] µM

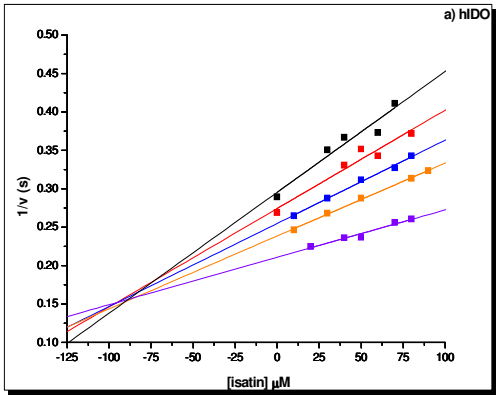
a) hIDO
1/v (s)
[isatin] µM

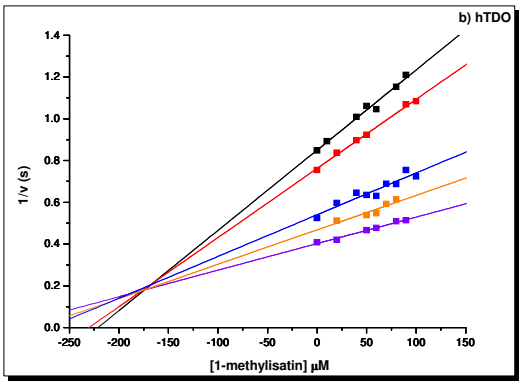
b) hTDO
1/v (s)
[1-methylisatin] µM

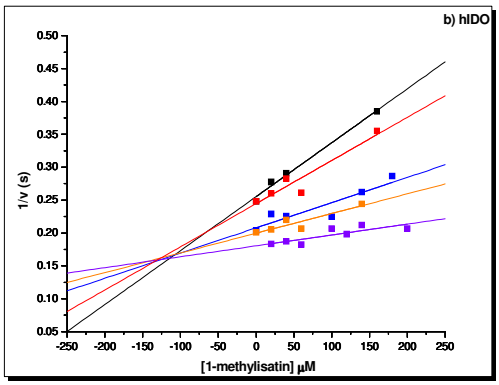
b) hIDO
1/v (s)
[1-methylisatin] µM

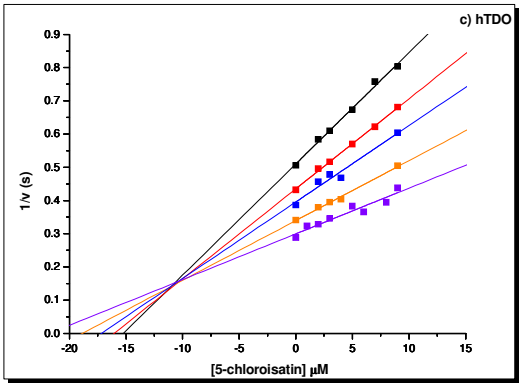
c) hTDO
1/v (s)
[5-chloroisatin] µM

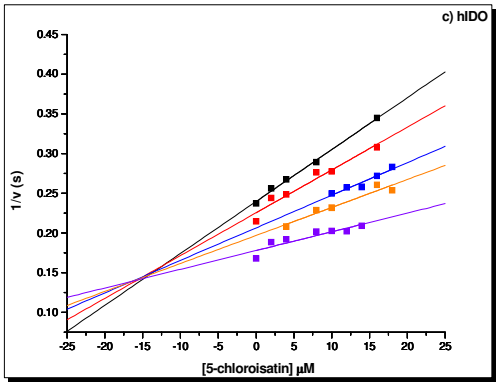
c) hIDO
1/v (s)
[5-chloroisatin] µM

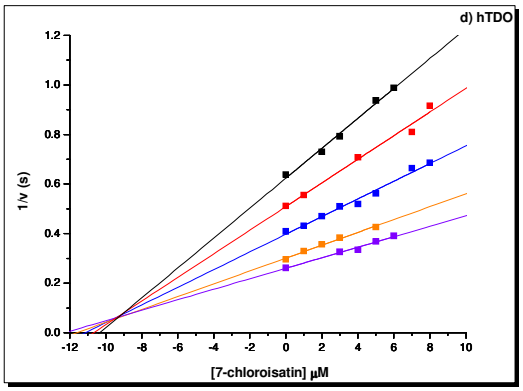
d) hTDO
1/v (s)
[7-chloroisatin] µM

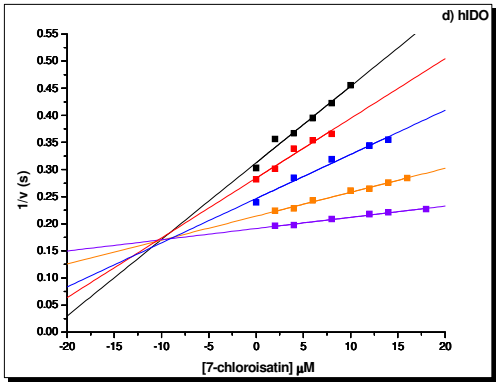
d) hIDO
1/v (s)
[7-chloroisatin] µM

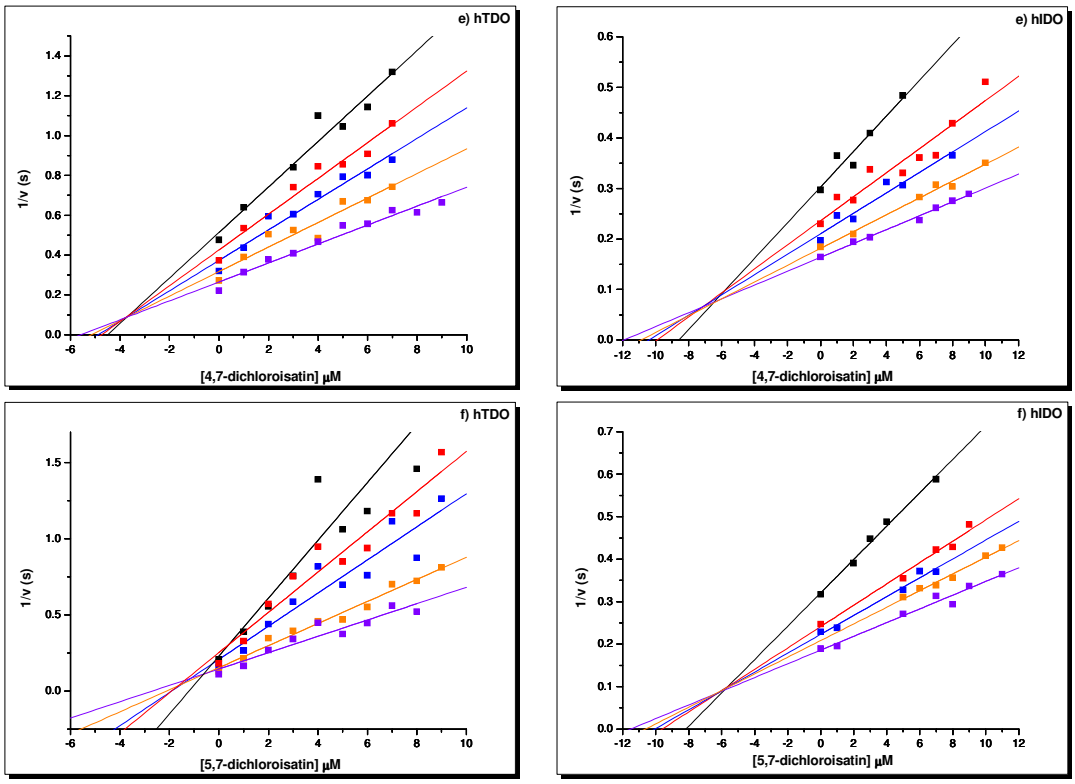

Figure 4.4: Dixon plots of hTDO (left column) and hIDO (right column) using a) isatin, b) 1-methylisatin, c) 5-chloroisatin, d) 7-chloroisatin, e) 4,7-dichloroisatin and f) 5,7-dichloroisatin as inhibitors. a) isatin. Substrate concentrations used (all µM) were: TDO, 300 (black), 350 (red), 500 (blue), 700 (orange), 800 (violet); IDO, 20 (black), 25 (red), 35 (blue), 40 (orange), 45 (violet). b) 1-methylisatin. Substrate concentrations (µM) were: TDO, 300 (black), 350 (red), 400 (blue), 600 (orange), 700 (violet); IDO, 20 (black), 25 (red), 35 (blue), 40 (orange), 45 (violet). c) 5-chloroisatin. Substrate concentrations used (all µM) were: TDO, 300 (black), 350 (red), 400 (blue), 500 (orange), 600 (violet); IDO, 25 (black), 30 (red), 35 (blue), 40 (orange), 45 (violet). d) 7-chloroisatin. Substrate concentrations used (all µM) were: TDO, 300 (black), 350 (red), 500 (blue), 700 (orange), 800 (violet); IDO, 15 (black), 20 (red), 25 (blue), 40 (orange), 45 (violet). e) 4,7-dichloroisatin. Substrate concentrations used (all µM) were: TDO, 300 (black), 400 (red), 500 (blue), 600 (orange), 800 (violet); IDO, 15 (black), 25 (red), 35 (blue), 40 (orange), 45 (violet). f) 5,7-dichloroisatin. Substrate concentrations used (all µM) were: TDO, 250 (black), 300 (red), 400 (blue), 600 (orange), 800 (violet); IDO, 15 (black), 25 (red), 30 (blue), 40 (orange), 45 (violet).

The effect of other halogens (F, Br and I) on isatin inhibition of TDO and IDO was also examined. Replacement of chlorine by fluorine, bromine or iodine atoms at either the 5- or 7-position of the indole ring revealed inhibition similar to the chloro-substituted molecule (fig. 4.5). Carefully examination of both 5- and 7- halogenated isatins revealed an increase of inhibition effectiveness based on the size of the halogen atom.

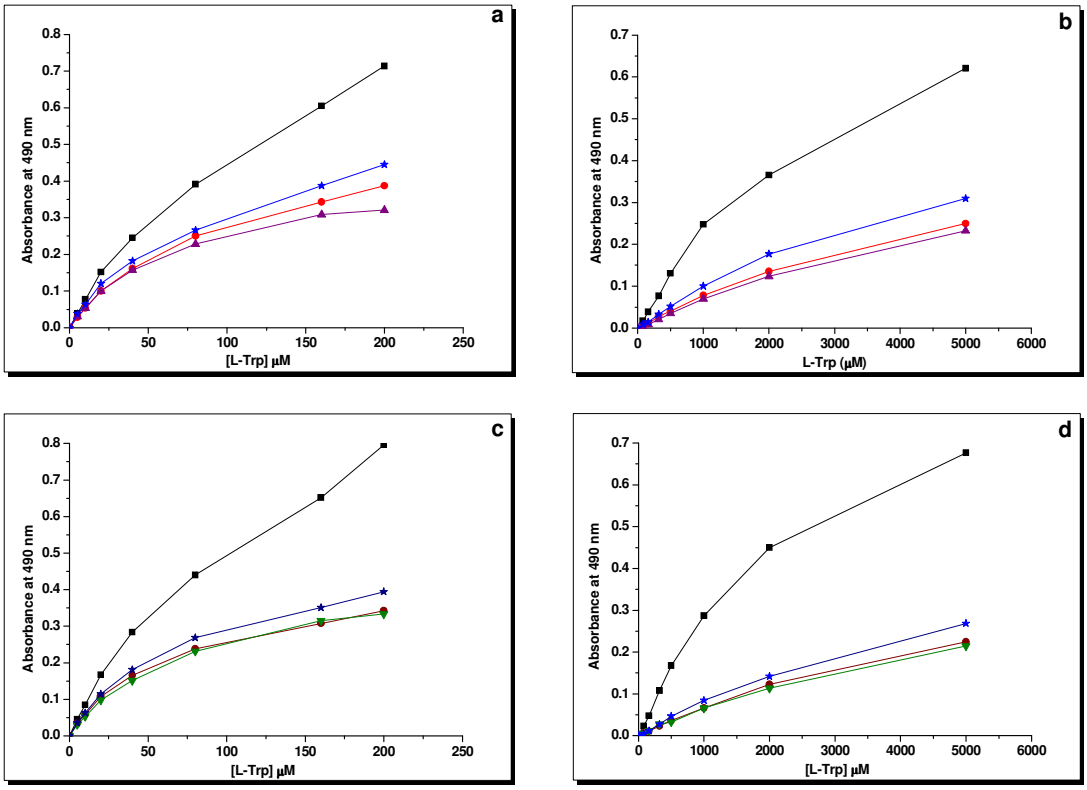

Figure 4.5: Tryptophan catabolic activity of IDO (left column) and TDO (right column) in the absence and presence of 5' halogenated (**a**, **b**) and 7' halogenated isatins (**c**, **d**). Figures **1a**, **1b** (*5' halogenated isatins - 400 µM*): Control- black (■), 5-fluoroisatin -blue (*), 5-chloroisatin - red (●), 5-Iodoisatin – purple (▲). Figures **1c**, **1d** (*7' halogenated isatins - 400 µM*): Control- black (■), 7-fluoroisatin – navy blue (*), 7-chloroisatin - wine (●), 7-bromoisatin – olive (▼).

4.4 Breakdown of isatin

After identifying isatin as a promising framework molecule for the potential development of TDO/IDO inhibitors, it was decided to attempt to characterise which part(s) of the molecule are most important in this respect. In particular, the aim was to examine the importance of the C2 and C3 carbonyl groups, the nitrogen atom and the pyrrolidine ring in the molecule's effectiveness as an inhibitor (fig. 4.6).

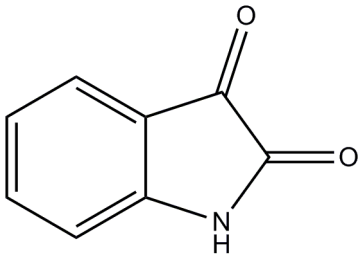

Isatin

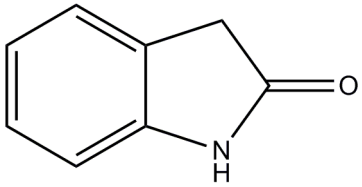

2-oxindole

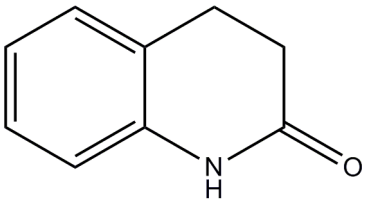

3,4-Dihydro-2(1H)-quinolinone

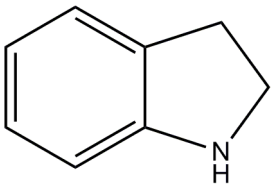

Indoline

Figure 4.6: Chemical structures of isatin, 2-oxindole, 3,4-dihydro-2(1H)-quinolinone and indoline.

The removal of the C3 carbonyl group of isatin produced 2-oxindole, a molecule with decreased inhibition activity compared to isatin itself (fig. 4.7). Comparing 2-oxindole with 3,4-dihydro-2(1H)-quinolinone (the 6-membered ring analogue) it can be seen that the pyrrolidine ring of 2-oxindole is marginally more effective than the piperidine ring of 3,4-dihydro-2(1H)-quinolinone showing that the inhibition ability of these molecules is affected by the orientation of C2 carbonyl group and the ring size. The removal of the C2 carbonyl group was also investigated by examining the effect of indoline. From figure 4.7 it can be seen that indoline, of the four molecules studied, is the weakest inhibitor, especially in the case of TDO.

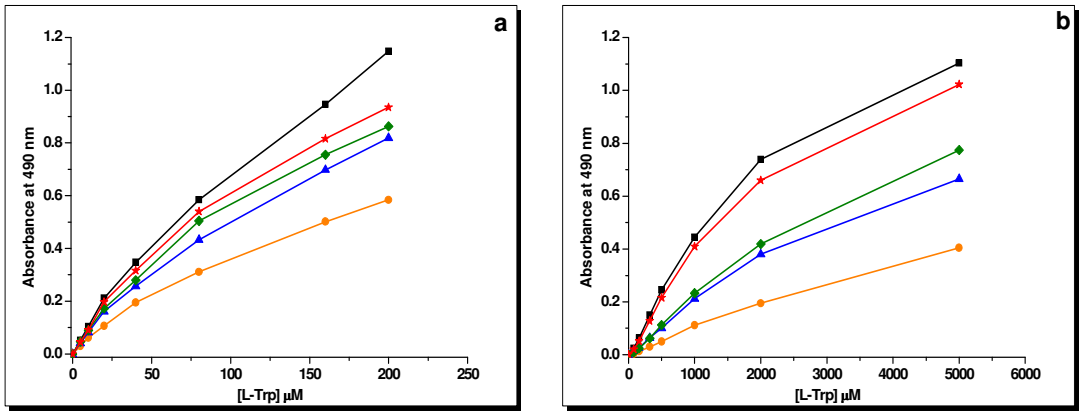

Figure 4.7: Inhibition of hIDO (**a**) and hTDO (**b**) by isatin and isatin-related molecules. Control (no inhibitor) - black (■), indoline - red (*), 3,4-dihydro-2(1H)-quinolinone-olive(♦), 2-oxindole – blue (▲), isatin - orange(●). The final concentration of inhibitors was 400 µM.

Given that the addition of chlorine to isatin was shown above to improve its inhibitory properties, the effect of chlorination of 2-oxindole and indoline was investigated. The ability of 5-chloro-2-oxindole and 5-chloroindoline to inhibit TDO and IDO is shown in figure 4.8, along with 5-chloroisatin. As may be expected, 5-chloro-2-oxindole is a stronger inhibitor than 5-chloroindoline, something which comes in agreement with the findings for the non-chlorinated molecules. However, both molecules revealed a significantly decreased inhibition strength in comparison with 5-chloroisatin.

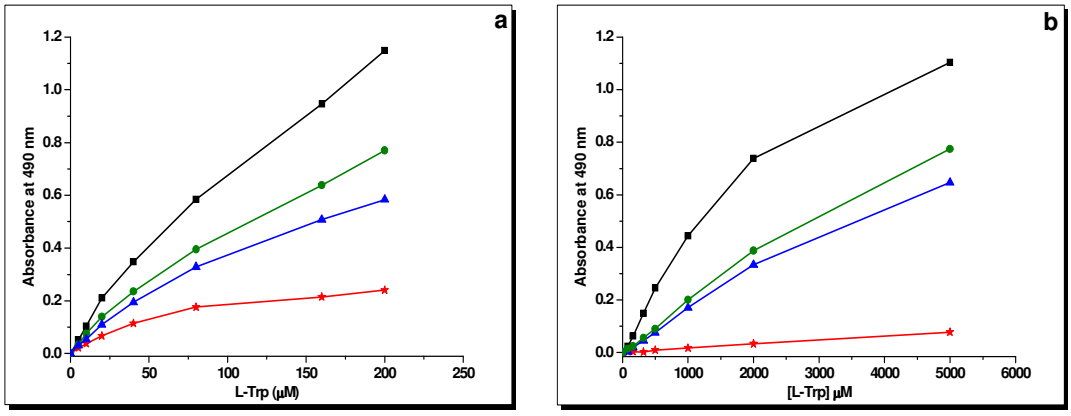

Figure 4.8: Inhibition of hIDO (**a**) and hTDO (**b**) using 5-chloro-2-oxindole, 5-chloroindoline and 5-chloroisatin as inhibitors. Control-black (■), 5-chloroindoline-olive(●), 5-chloro-2-oxindole–blue(▲), 5-chloroisatin - red (*).The final concentration of inhibitors was 400 μM.

Having investigated the effect of altering the structure of isatin by removing the carbonyl groups, methylating the nitrogen atom, and changing the pyrrolidine ring to a piperidine ring, the next step was to investigate the effect of breaking the 5-membered ring of isatin. In order to do this the following species were tested as inhibitors: N-(2,4-dichlorophenyl)acetamide**,** 2,5-dichloroformanilide, 2,4-dichloro-N-methylaniline and 2,4-dichloroaniline, the structures of which are shown in figure 4.9. As mentioned earlier, 5,7-dichloroisatin is a strong inhibitor of both TDO and IDO with inhibition constants of 800 nM and 6 μM respectively. Disrupting the 5-membered ring of 5,7-dichloroisatin has the consequence of causing the molecule to lose its inhibition ability in both enzymes. None of the molecules shown in figure 4.9 inhibited IDO and TDO at concentrations of up to 400 μM.

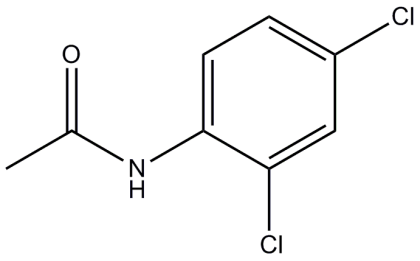

N-(2,4-Dichlorophenyl)acetamide

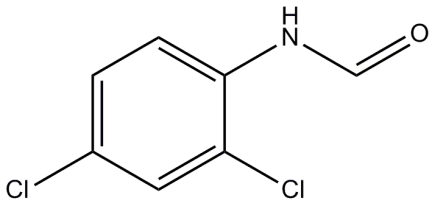

2,5-Dichloroformanilide

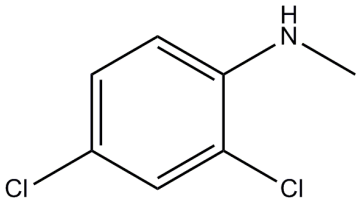

2,4-Dichloro-N-methylaniline

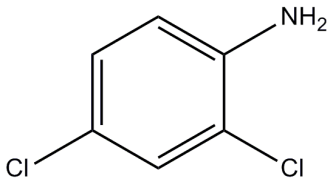

2,4-Dichloroaniline

Figure 4.9: Chemical structures of N-(2,4-dichlorophenyl)acetamide, 2,5-dichloroformanilide, 2,4-dichloro-N-methylaniline and 2,4-dichloroaniline.

4.5 Substitution at the C3 position of isatin

After showing the important role of the C3 carbonyl group for isatin's inhibition activity, a number of C3-substituted derivatives of 5,7-dichloroisatin were tested as inhibitors of the two enzymes. These molecules were provided by the National Cancer Institute (USA). The structures of the molecules that were used are shown in figure 4.10 and their inhibition graphs in figure 4.11. All the inhibitors yielded inhibition constants in the low micromolar range for both TDO and IDO (Table 4.2). An overall observation of table 4.2 reveals that these compounds inhibit TDO more effectively than IDO. Among the seven NCI inhibitors shown in figure 4.10, NSC 635312 and NSC 635297 demonstrated the lowest inhibition constants. Not surprisingly, replacement of a chlorine atom by a methyl group at 7' position of the indole ring reduces the ability of NSC 635435 to inhibit TDO and IDO, something

that confirms the previous findings (*see halogenation section*). Removal of aniline group from NSC 635411 and replacement by naphthalene ring (NSC 635328) had no significant effect on TDO inhibition. Although, on IDO that change reduced the inhibition potency of the molecule. Comparing the structures of NSC 635297 with NSC 635306 it concluded that the two hydroxyl groups of NSC 635297 are likely to be involved in hydrogen bonding. Taking away the hydroxyl group of benzene ring and transforming the other one to ethylene oxide had a negative influence on both enzymes. In the case of NSC 625910, changes on the benzene group of the C3 site chain had not a spectacular effect on enzymes inhibition, inhibiting TDO and IDO at 6.1 ± 0.5 μM and 10.7 ± 0.9 μM respectively. All inhibitors, presented in this section, have values from 1-12 μM for TDO, and 4-32 μM for IDO. Modifications at C3 do not appear to dramatically affect the inhibition strength of this family of molecules. However, modification at C3 seems to be important for inhibition activity because all of these are better inhibitors than isatin/methylisatin.

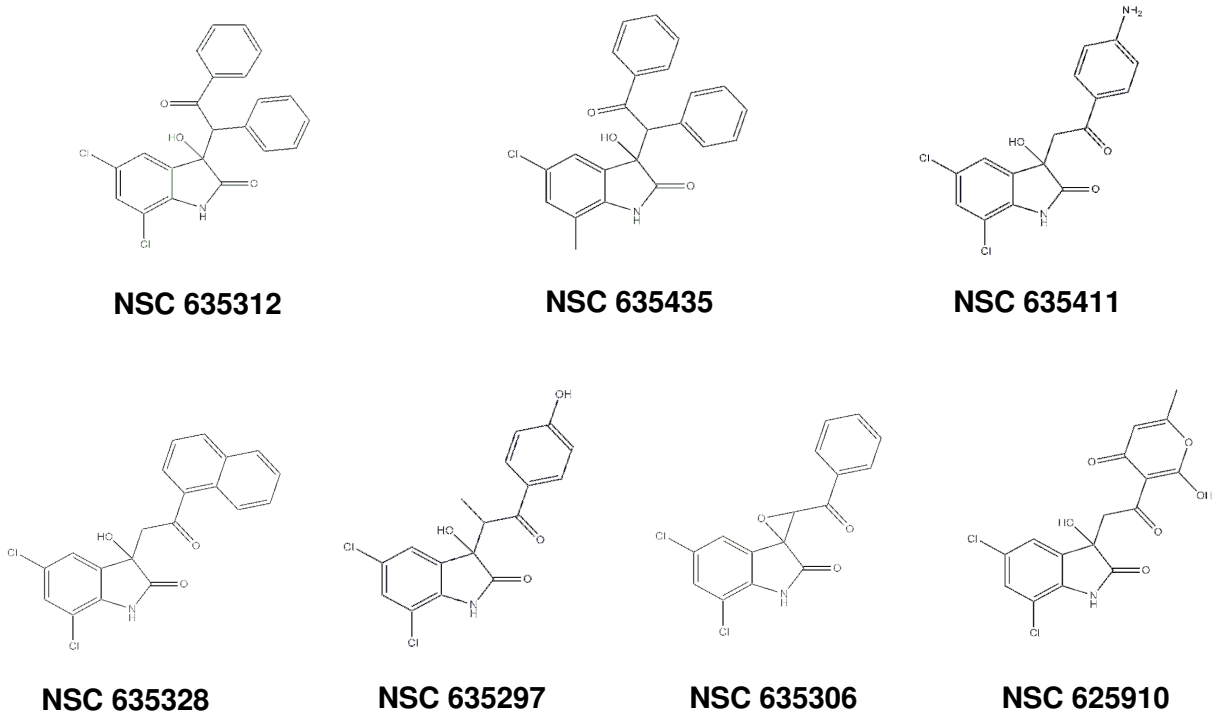

Figure 4.10: Chemical structures of NCI inhibitors that were used in this study.

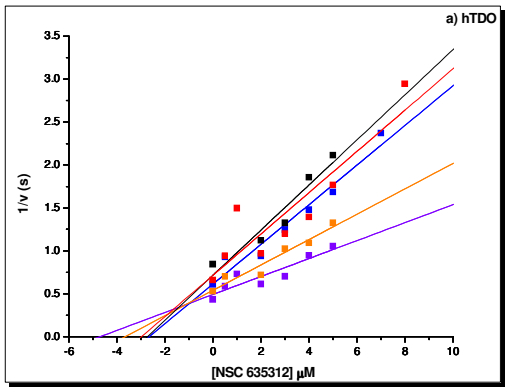
a) hTDO
1/v (s)
[NSC 635312] µM

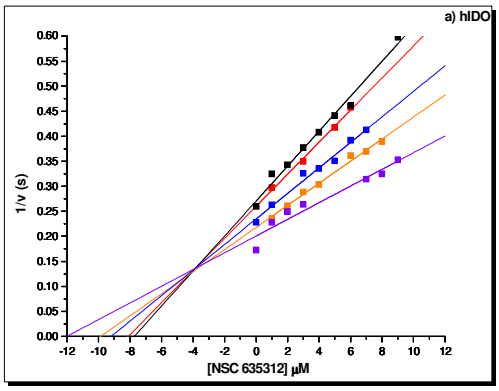
a) hIDO
1/v (s)
[NSC 635312] µM

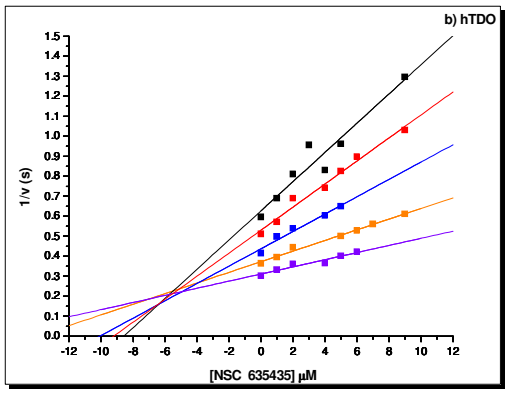
b) hTDO
1/v (s)
[NSC 635435] µM

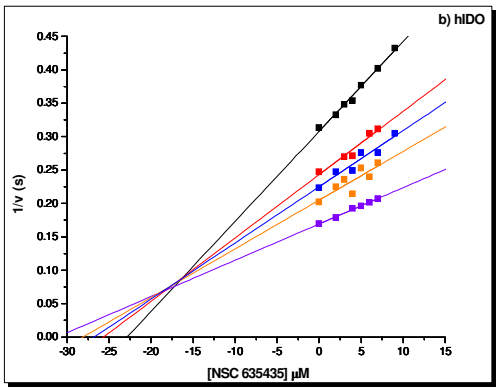
b) hIDO
1/v (s)
[NSC 635435] µM

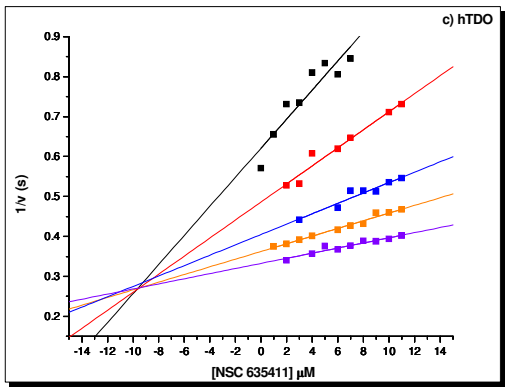
c) hTDO
1/v (s)
[NSC 635411] µM

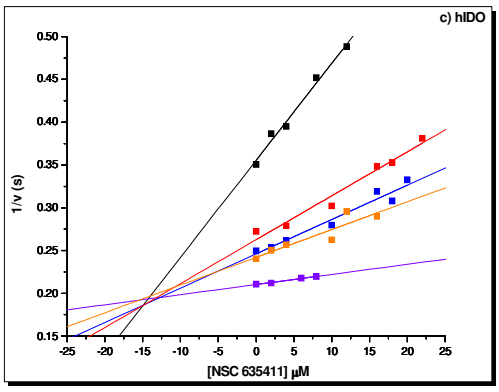
c) hIDO
1/v (s)
[NSC 635411] µM

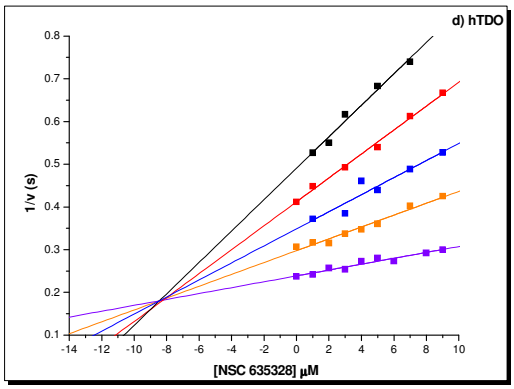
d) hTDO
1/v (s)
[NSC 635328] µM

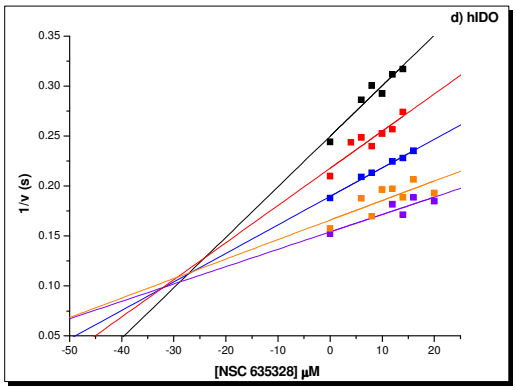
d) hIDO
1/v (s)
[NSC 635328] µM

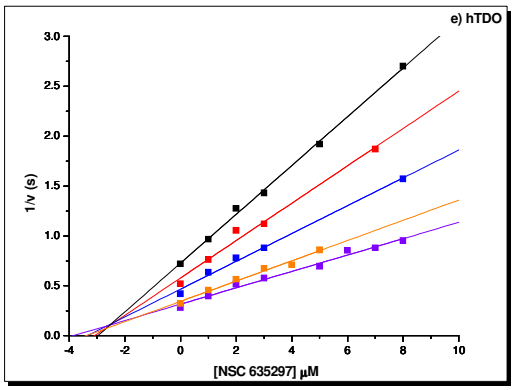
e) hTDO
1/v (s)
[NSC 635297] µM

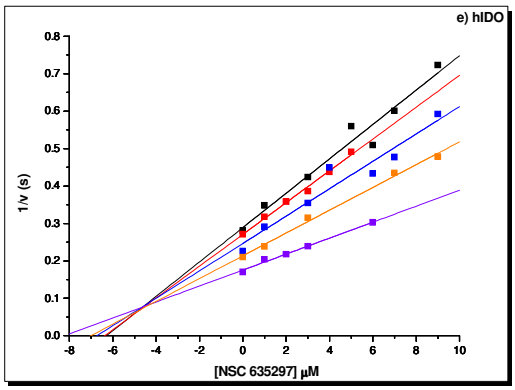
e) hIDO
1/v (s)
[NSC 635297] µM

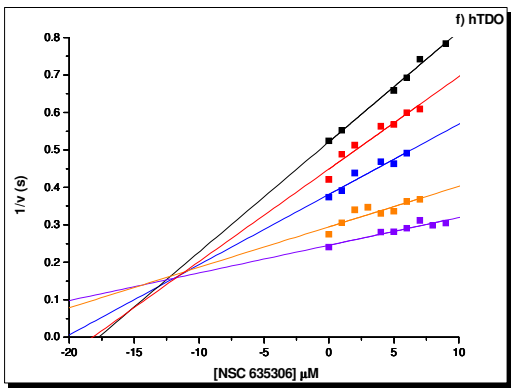
f) hTDO
1/v (s)
[NSC 635306] µM

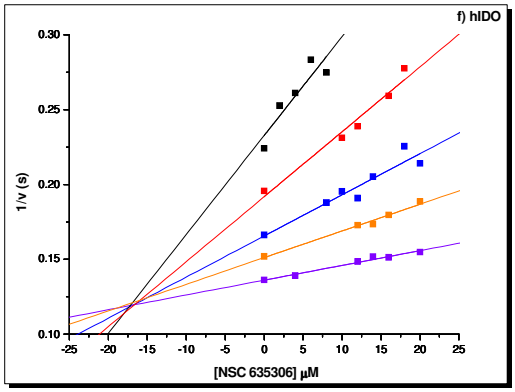
f) hIDO
1/v (s)
[NSC 635306] µM

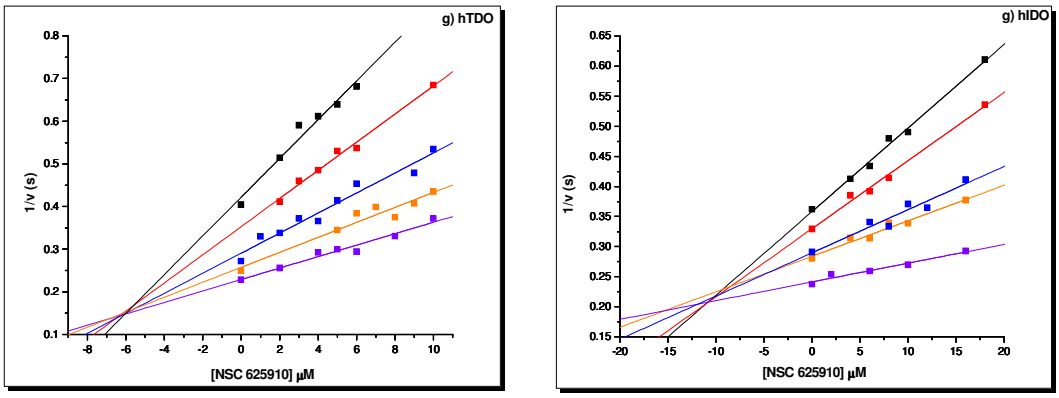

Figure 4.11: Dixon plots of hTDO (left column) and hIDO (right column) using a) NSC 635312, b) NSC 635435, c) NSC 635411, d) NSC 635328, e) NSC 635297, f) NSC 635306 and g) NSC 625910. a) NSC 635312. Substrate concentrations used (all µM) were: TDO, 300 (black), 350 (red), 400 (blue), 500 (orange), 600 (violet); IDO, 15 (black), 20 (red), 25 (blue), 30 (orange), 35 (violet). b) NSC 635435. Substrate concentrations (µM) were: TDO, 300 (black), 350 (red), 400 (blue), 700 (orange), 800 (violet); IDO, 15 (black), 25 (red), 30 (blue), 35 (orange), 45 (violet). c) NSC 635411. Substrate concentrations used (all µM) were: TDO, 300 (black), 400 (red), 500 (blue), 600 (orange), 700 (violet); IDO, 15 (black), 25 (red), 35 (blue), 40 (orange), 45 (violet). d) NSC 635328. Substrate concentrations used (all µM) were: TDO, 300 (black), 400 (red), 500 (blue), 600 (orange), 800 (violet); IDO, 15 (black), 20 (red), 25 (blue), 35 (orange), 40 (violet). e) NSC 635297. Substrate concentrations used (all µM) were: TDO, 300 (black), 400 (red), 500 (blue), 700 (orange), 800 (violet); IDO, 17.5 (black), 20 (red), 25 (blue), 30 (orange), 32.5 (violet). f) NSC 635306. Substrate concentrations used (all µM) were: TDO, 300 (black), 500 (red), 600 (blue), 700 (orange), 800 (violet); IDO, 15 (black), 20 (red), 25 (blue), 35 (orange), 45 (violet). g) NSC 625910. Substrate concentrations used (all µM) were: TDO, 400 (black), 500 (red), 600 (blue), 700 (orange), 800 (violet); IDO, 25 (black), 30 (red), 35 (blue), 40 (orange), 45 (violet).

Inhibitor's name	TDO inhibition	IDO inhibition
NSC 635312	1.4 ± 0.4 μM	3.9 ± 0.3 μM
NSC 635435	5.5 ± 0.6 μM	17 ± 1.7 μM
NSC 635411	9.6 ± 0.8 μM	13.9 ± 1.2 μM
NSC 635328	8.4 ± 0.1 μM	31.6 ± 5.9 μM
NSC 635297	2.5 ± 0.6 μM	4.6 ± 0.2 μM
NSC 635306	12.5 ± 1.3 μM	17 ± 1.2 μM
NSC 625910	6.1 ± 0.5 μM	10.7 ± 0.9 μM

Table 4.2: Inhibition effectiveness of NCI inhibitors, shown in figure 4.10, against TDO and IDO

4.6 Combination of 1-MT with isatin derivatives

In this section the behaviour of hIDO in the presence of 1-MT in combination with isatin derivatives is assessed. Given the specificity of IDO for 1-MT and the micromolar inhibition constants for the dichlorinated derivatives of isatin, the potential exists for these being a useful and potent inhibitor mixture for hIDO. The experiment was carried out as described in section 2.11. The findings of this trial are illustrated in figure 4.12. As expected, an increase in 1-MT concentration is related with a step-like increase of enzyme's inhibition, which can reach 60% inhibition at 400 μM 1-MT (fig. 4.12a-i). In the presence of 100 μM NSC 635312, IDO activity is inhibited by a percentage of ~80 %. Addition of 50 μM 1-MT has little appreciable effect on the overall inhibition observed, increasing further enzyme's inhibition by a factor of 5%. Increase of 1-MT concentration from 50 μM to 400 μM has as result

the step-like reduction of IDO activity, pointing out the additive effect that 1-MT has in the presence of a stronger inhibitor (NSC 635312). Similar response was also observed in the cases of 5,7-dichloroisatin and 5-chloroisatin. In the presence of 100 μM 5,7-dichloroisatin and 5-chloroisatin the enzyme activity reduced to ~18% and ~38% respectively while addition of 1-MT revealed analogous to NSC 635312 step-like reduction. In the case of NSC 635411, 100 μM of the NCI inhibitor and 50 μM of 1-MT have the same impact on IDO activity, reducing the uninhibited activity to ~68 %. Combination of NSC 635411 with 1-MT (up to 100 μM) demonstrated little appreciable effect on the overall inhibition. Nevertheless, increase of 1-MT concentration from 100 μM to 200 μM improved noticeably the inhibition effectiveness of the mixture by 20 % extra inhibition. This effect remained constant up to 400 μM 1-MT. Mixing of NSC 635328 with 1-MT had a similar to NSC 635411 response while the mixtures of NSC 635297, NSC 625910 and 7-chloroisatin with 1-MT revealed a unique behaviour. Addition of 50 μM 1-MT increased the effect of NSC 635297, NSC 625910 and 7-chloroisatin by 5%, 25% and 15%. However, this effect did not change in the presence of higher concentrations of 1-MT (100 μM, 200 μM and 400 μM).

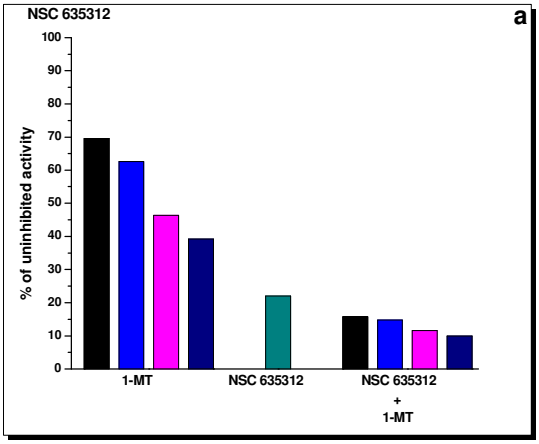
NSC 635312
a
% of uninhibited activity
100
90
80
70
60
50
40
30
20
10
0
1-MT
NSC 635312
NSC 635312
+
1-MT

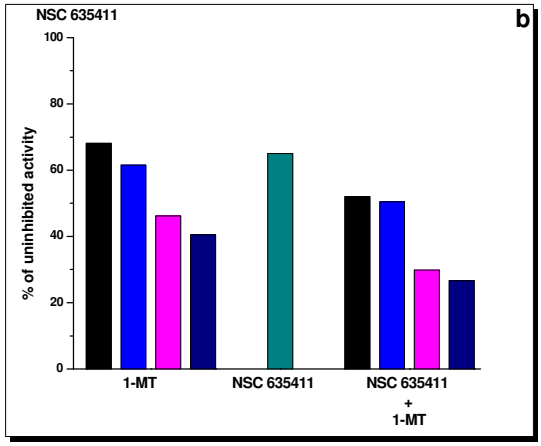
NSC 635411
b
% of uninhibited activity
100
80
60
40
20
0
1-MT
NSC 635411
NSC 635411
+
1-MT

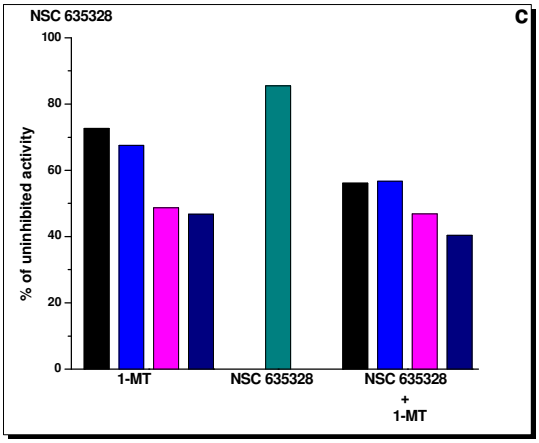
NSC 635328
c
% of uninhibited activity
100
80
60
40
20
0
1-MT
NSC 635328
NSC 635328
+
1-MT

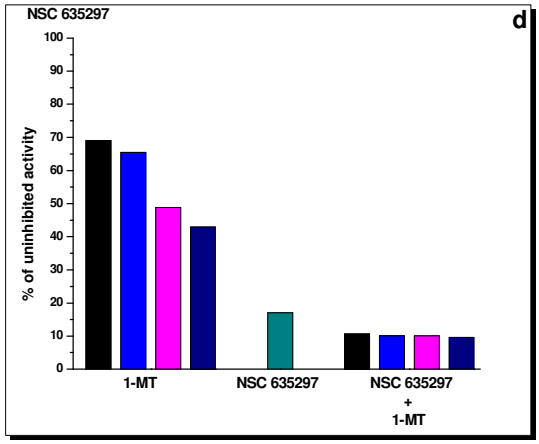
NSC 635297
d
% of uninhibited activity
100
90
80
70
60
50
40
30
20
10
0
1-MT
NSC 635297
NSC 635297
+
1-MT

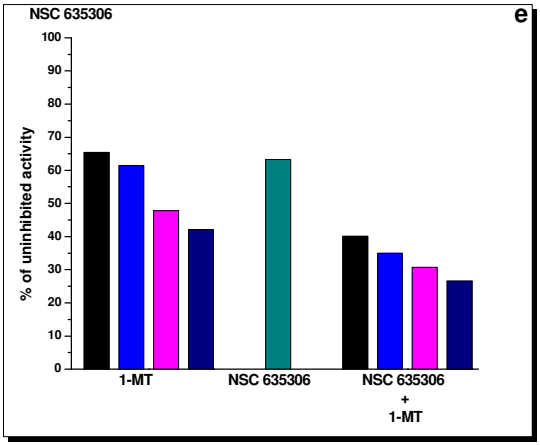
NSC 635306
e
% of uninhibited activity
100
90
80
70
60
50
40
30
20
10
0
1-MT
NSC 635306
NSC 635306
+
1-MT

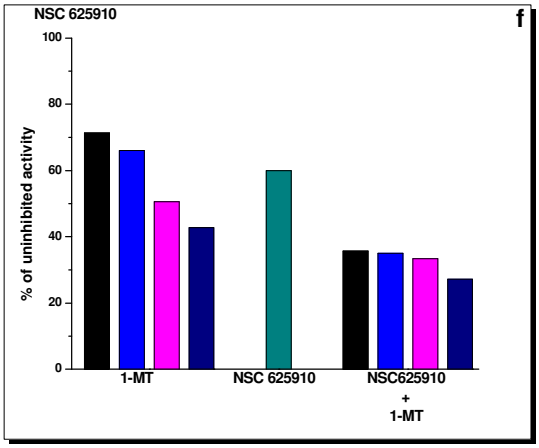
NSC 625910
f
% of uninhibited activity
100
80
60
40
20
0
1-MT
NSC 625910
NSC625910
+
1-MT

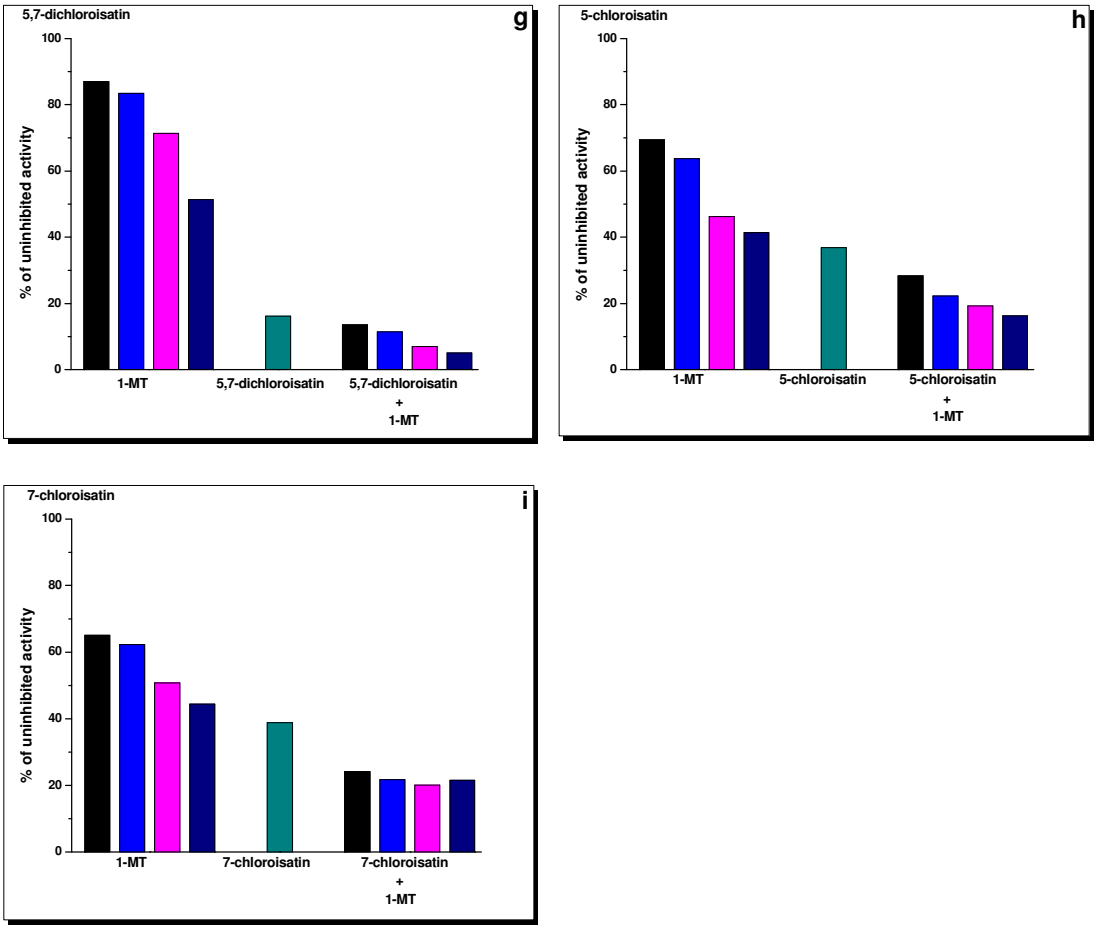

Figure 4.12: Combination of 1-MT with the isatin derivatives; **a)** NSC 635312, **b)** NSC 635411, **c)** NSC 635328, **d)** NSC 635297, **e)** NSC 635306, **f)** NSC 625910, **g)** 5,7-dichloroisatin, **h)** 5-chloroisatin and **i)** 7-chloroisatin. The black, blue, pink and navy blue columns represent 50 μM, 100 μM, 200 μM and 400 μM of 1-MT without and with 100 μM NCI inhibitors. In dark cyan is the NCI inhibitor/isatin derivative at the same concentration as it is in the presence of 1-MT in the right hand columns.

4.7. Discussion

In this chapter a number of isatin derivatives have been investigated as potential inhibitors of IDO and TDO. Figure 4.13 illustrates the main outcomes. Starting with 1-methylisatin it has been demonstrated that methylation of the nitrogen atom of isatin reduces the effectiveness of the produced inhibitor, something which suggests hydrogen bonding between the nitrogen atom and the active sites of both enzymes. Inhibition of TDO by 1-methylisatin also suggests that the molecule does not have the same orientation as 1-methyltryptophan, which is ineffective as a TDO inhibitor, presumably due to a clash with the active site histidine. This finding may explain why isatin derivatives and 1-MT act in combination for inhibition of IDO.

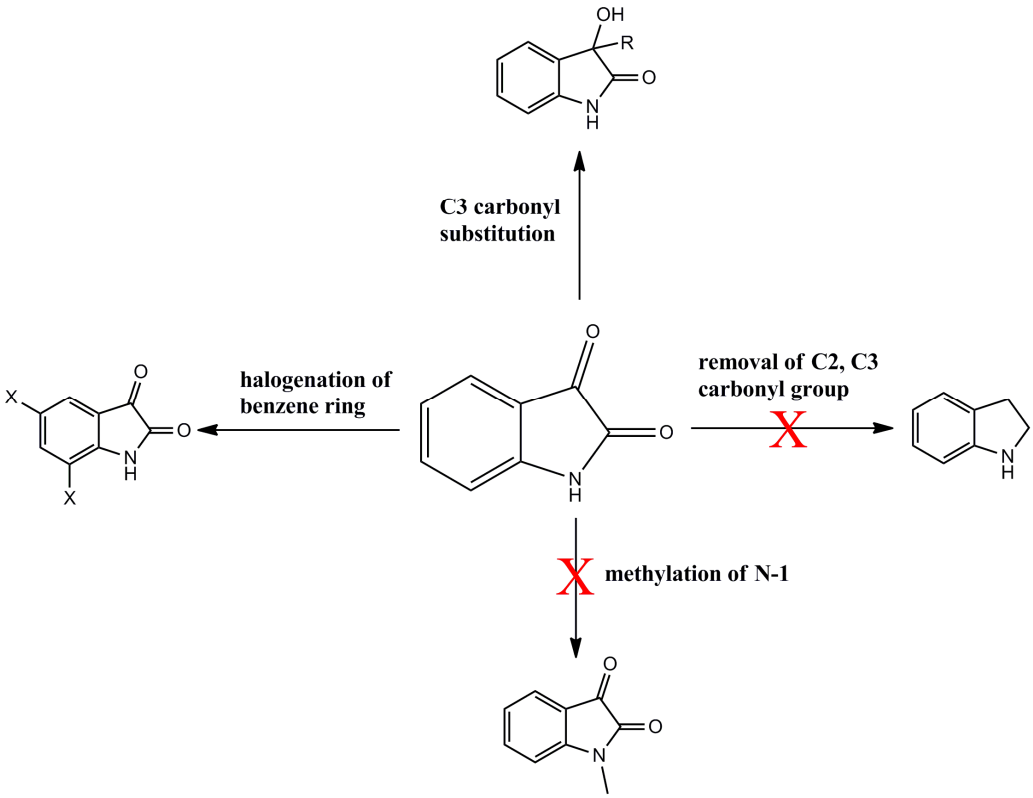

Figure 4.13: Isatin modifications for optimization of TDO and IDO inhibition.

The importance of halogenation of the 6-membered ring is also clear, showing an increase of the inhibition potency by 12-fold and 6-fold for TDO and IDO respectively. Increase of the inhibition potency of halogen-containing isatins might be related with the electronegativity of the halogen or it could be a steric effect. Whereas neither TDO nor IDO crystal structure with a halogenated isatin is currently available, both assumptions are equally possible.

The breakdown/removal of the pyrrolidine ring has a dramatic effect on the inhibition of both enzymes. 5,7-dichloroisatin inhibits TDO and IDO in the nanomolar and lower micromolar regions respectively, but without the presence of the pyrrolidine ring the molecule becomes an ineffective inhibitor, indicating that halogenation is favourable only when the indole moiety is intact. It has also been shown that the C2 carbonyl group is desirable for inhibition. The comparison between 2-oxindole and indole clearly shows that the carbonyl group at the C2 position increases notably the inhibition effectiveness of the molecule. In addition, replacement of a pyrrolidine ring (5-membered) with a piperidine ring (6-membered) affects the relative orientation of the C2 carbonyl group, which in turn affects the efficiency of the inhibitor. Further to this, examination of the C3 carbonyl group showed that its removal has a negative result, similar to C2 carbonyl group removal. However, it can be replaced by two other functional groups, of which one should be a hydroxyl group, in order to retain its inhibitory properties. By comparing the outcomes of this work for both TDO and IDO, it can be said that these inhibitors are more effective for TDO than for IDO. In order to optimize IDO inhibition, combination of the IDO-specific 1-MT with the most potent dichlorinated inhibitors was tested. The results revealed an additive effect between the two kinds of inhibitors. In most of the cases, combination of 1-MT with the dichlorinated derivatives of isatin resulted in an increase in IDO inhibition by around 50% more than the inhibition effect offered by isatins alone. This study aimed to identify, understand and develop a new class of IDO and TDO inhibitors. Through this examination, the potential for use of isatin and its derivatives as lead molecules has been shown.

4.8 References

(1) Opitz C.A., Litzenburger U.M., Sahm F., Ott M., Tritschler I., Trump S., Schumacher T., Jestaedt L., Schrenk D., Weller M., Jugold M., Guillemin G.J., Miller C.L., Lutz C., Radlwimmer B., Lehmann I., Deimling A.V., Wick W. and Platten M., *An endogenous tumour-promoting ligand of the human aryl hydrocarbon receptor*, ***Nature***, 2011, 478, 197-203

(2) Pandeya S.N., Smitha S., Jyoti M. and Sridhar S.K., *Biological activities of isatin and its derivatives*, ***Acta Pharm.***, 2005, 55, 27–46

(3) Vine, K. L, Matesic L., Locke J.M., Ranson M. and Skropeta D., *Cytotoxic and Anticancer Activities of Isatin and Its Derivatives: A Comprehensive Review from 2000-2008*, ***Anti-Cancer Agents in Medicinal Chemistry,*** 2009, 9, 397-414

(4) Gillam E.M.J., Notley L.M., Cai H., De Voss J.J. and Guengerich F.P., *Oxidation of indole by cytochrome P450 enzymes*, ***Biochemistry***, 2000, 39, 13817-13824

Chapter 5

Biochemical Characterization of Human Indoleamine 2,3-Dioxygenase-2

5.1 Introduction

Indoleamine 2,3-dioxygenase-2 (IDO2) is a third enzyme, along with tryptophan 2,3-dioxygenase (TDO) and indoleamine 2,3-dioxygenase (IDO), that catalyses the incorporation of molecular oxygen into L-tryptophan in the first step of the kynurenine pathway [(1)]. Human IDO2 (hIDO2) was discovered in 2007, and its encoding gene is adjacent to the human IDO (hIDO) gene on chromosome 8 [(2)], suggesting that it may have arisen as the product of gene duplication. Nevertheless, the distinct characteristics of hIDO2 raise the possibility of the protein having an immunomodulatory role unrelated to that of IDO. Studies in mice showed that both IDO and IDO2 are expressed in particular tissues (e.g. epididymis), supporting the idea of IDO2 implication in an unidentified signalling pathway [(3)].

In 2009, Löb *et al.* first suggested a possible role for IDO2 in cancer, demonstrating the presence of hIDO2 mRNA in gastric, colon and renal tumours [(4)]. Following this, Sørensen *et al.* came to verify the importance of IDO2 in tumour escape and survival [(5)] by showing that in peripheral blood samples obtained from both healthy donors and cancer patients there was observed a spontaneous cytotoxic T-cell reactivity against IDO2. These T-cells were shown to be cytotoxic effector cells that recognize and kill tumour cells [(5)]. The proposed involvement of IDO2 in cancer, in combination with the established immunomodulatory role of IDO, led to these enzymes being potential drug target molecules, and thus the identification and development of specific inhibitors for both enzymes is desirable. Studies on 1-methylated tryptophan derivates have shown that 1-Me-D-Trp has superior *in vivo* antitumour activity compared with 1-Me-L-Trp [(6)]. For this reason, 1-Me-D-Trp is currently the subject of clinical trials as an inhibitor of IDO enzymes (http://clinicaltrials.gov/show/NCT00739609). Considering the specificity of 1-Me-L-Trp for IDO [(4)], 1-Me-D-Trp antitumour activity could be related to IDO2

function. However, the efficacy of 1-Me-D-Trp as an inhibitor of hIDO2 is yet to be evaluated. It has been variously reported that 1-Me-L-Trp is a more effective inhibitor of vertebrate IDO2 [7, 8] than 1-Me-D-Trp, and *vice versa* [9]. In this chapter the characterisation of human IDO2 (hIDO2) with respect to substrate specificity (the various potential substrates that were tested are shown in Appendix B), electrochemical properties and inhibition selectivity is described. These data are compared with the corresponding data for IDO and potential similarities evaluated. This work in combination with previous findings suggests a physiological function for hIDO2 that is distinct from that of IDO.

5.2 Determination of the optimum pH and buffer conditions

Prior to the biochemical characterization of hIDO2 it was necessary to define the optimum pH for function of the enzyme. For this reason the activity of IDO2 was measured in 100 mM potassium phosphate buffer at pH values between pH 5.8 and 8.0 (at intervals of 0.2 pH units). The findings clearly showed that optimal enzymatic activity occurs around pH 7.5 (figure 5.1). This finding is in good agreement with previously reported data for mouse IDO2 (mIDO2) where the optimal pH for activity was also found to be 7.5 [8]. This is perhaps unsurprising, because the human and mouse enzymes have sequences that are 74% identical [13]. Examination of several buffers at pH 7.5 indicated 100 mM potassium phosphate buffer as the most suitable for this study.

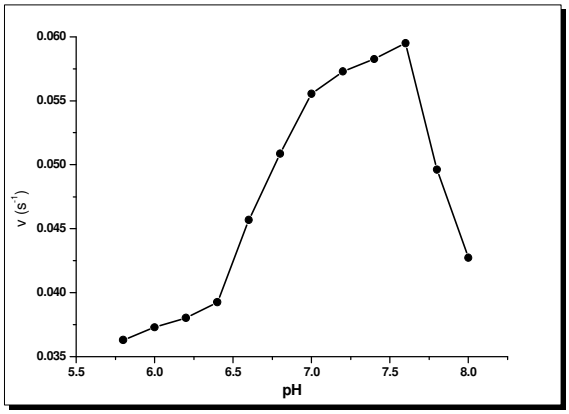

Figure 5.1: Examination of hIDO2 optimum activity using 100 mM potassium phosphate buffer pH 5.8 - 8.0

5.3 Kinetic activity

The kinetic parameters (k_{cat}/K_m, K_m and k_{cat}) obtained for hIDO2 activity with L-Trp, D-Trp and a number of tryptophan analogues are shown in table 5.1.The structures of the characterised substrates and their turnover plots are also shown in figures 5.2 and 5.3 respectively. These molecules were chosen, from the 54 potential substrates that were screened, as the most effective substrates for IDO2.

Name	k_{cat} / K_m ($M^{-1}s^{-1}$)	K_m (μM)	k_{cat} (s^{-1})
5-MeO-D,L-Trp	**256**	**559 ± 23**	**0.143 ± 0.015**
5-Me-D,L-Trp	**210**	**1664 ± 151**	**0.35 ± 0.01**
6-Me-D,L-Trp	**37**	**2783 ± 174**	**0.102 ± 0.010**
5-F-D,L-Trp	**28**	**1708 ± 85**	**0.048 ± 0.002**
1-Me-L-Trp	**16**	**679 ± 24**	**0.011 ± 0.005**
L-Trp	**15**	**6821 ± 63**	**0.100 ± 0.005**
1-Me-D-Trp	**6.4**	**776 ± 42**	**0.0050 ± 0.0002**
D-Trp	**2.8**	**3798 ± 267**	**0.0105 ± 0.0007**

Table 5.1: Kinetic characteristics for hIDO2 with L-Trp and other tryptophan analogues. The molecules were put in order starting with the best substrate for IDO2, based on k_{cat}/K_m values. Substrates such as 5-OH-L-Trp and melatonin revealed negligible activity and for that reason are not included in the table.

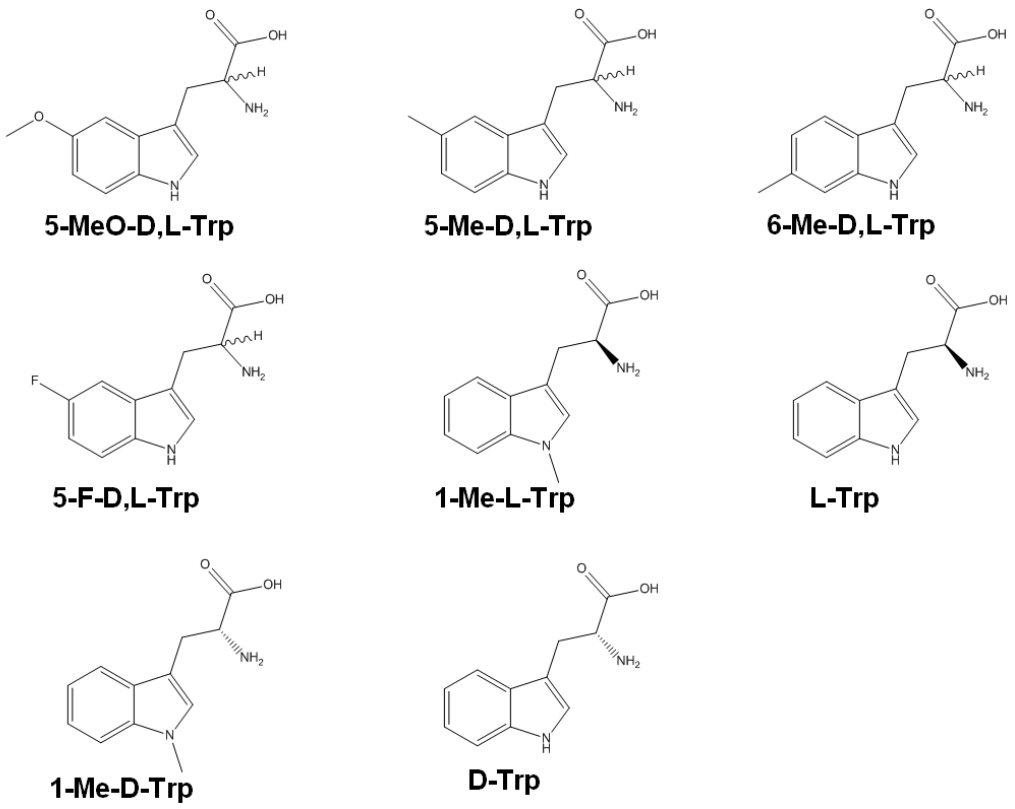

Figure 5.2: The structures of tryptophan derivatives that were used in this work

From table 5.1 it can be seen that hIDO2 shows greatest catalytic efficiency with 5-methoxy-D,L-tryptophan, largely due to its low K_m value (559 ± 23 μM)**.** Interestingly however, replacement of the 5-methoxy group by a methyl group has a negative influence in the binding of the molecule, decreasing its affinity 3-fold. On the other hand, this modification positively affects the turnover rate, increasing k_{cat} from 0.143 ± 0.015 s^{-1} for 5-methoxy-D,L-tryptophan to 0.35 ± 0.01 s^{-1} for 5-methyl-D,L-tryptophan. Furthermore, moving the methyl group from the 5- to the 6-position has the effect of decreasing both the affinity of the enzyme for the molecule and its turnover rate, resulting in a decrease in k_{cat}/K_m from 210 $M^{-1}s^{-1}$ for 5-methyltryptophan to 37 $M^{-1}s^{-1}$ for 6-methyltryptophan (Table 5.1). Regarding 5-fluorotryptophan, it is shown that this molecule is a better substrate for IDO2 than the presumed natural substrate of the enzyme. 1-Me-L-Trp and L-Trp displayed similar overall efficiencies as substrates but clearly dissimilar kinetic parameters.

Binding of 1-Me-L-Trp is more favourable than binding of L-Trp, although L-Trp turnover occurs around 10 times faster than for 1-Me-L-Trp. In comparison with 1-Me-L-Trp, the D-enantiomer of 1-Me-Trp showed a similar binding affinity (K_m = 776 ± 42 µM) but a much lower turnover ability (k_{cat} = 0.0050 ± 0.0002 s^{-1}).

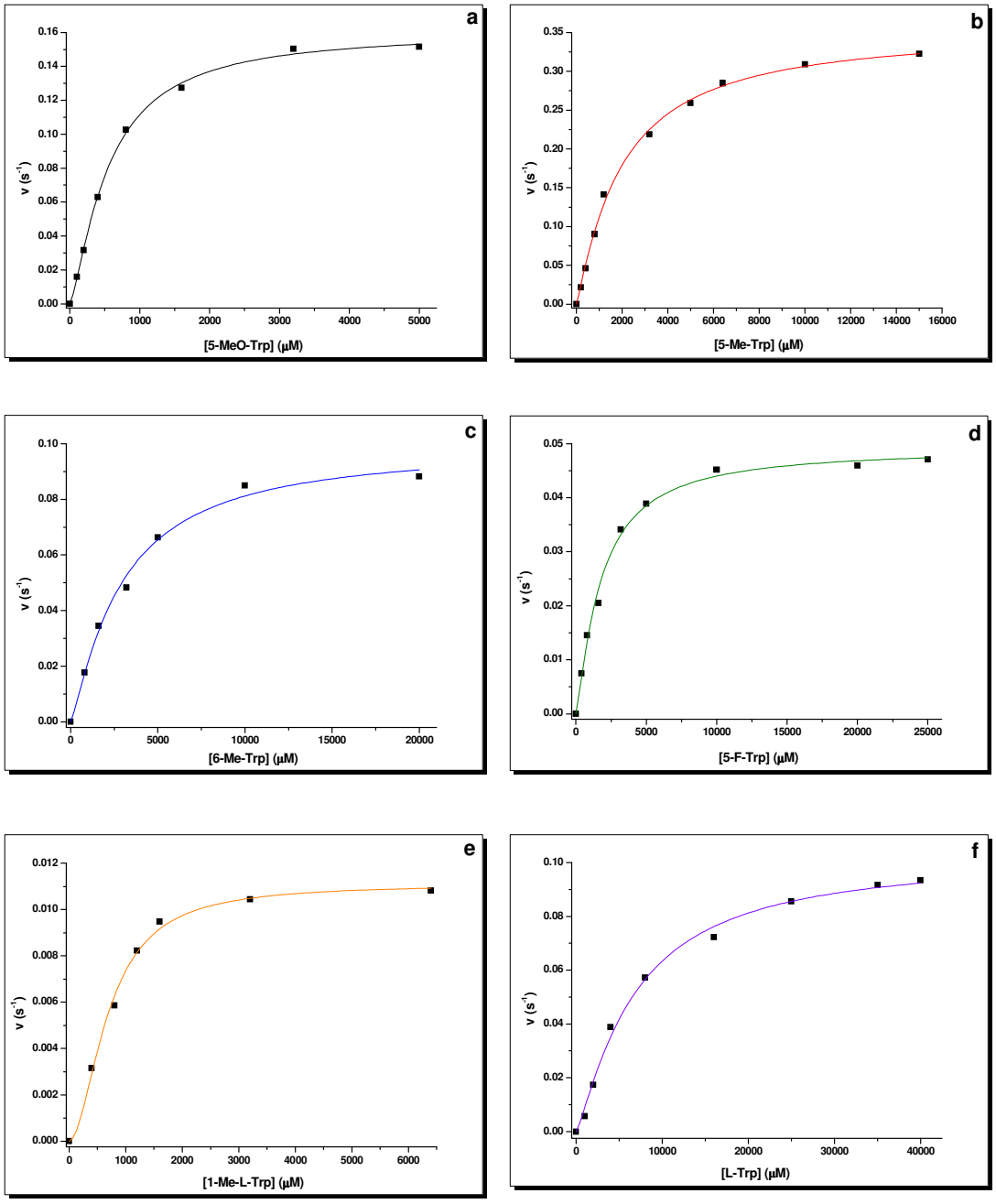

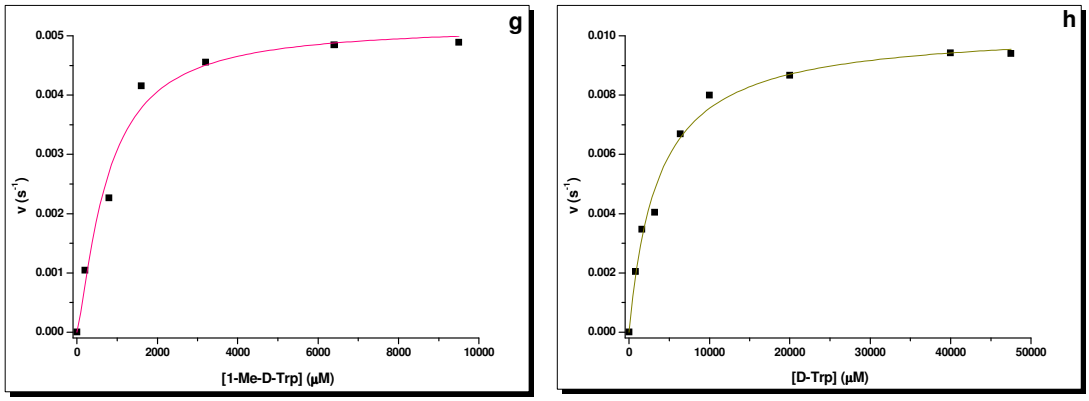

Figure 5.3: Michaelis-Menten plots for hIDO2 with a) 5-MeO-Trp, b) 5-Me-Trp, c) 6-Me-Trp, d) 5-F-Trp, e) 1-Me-L-Trp, f) L-Trp, g) 1-Me-D-Trp and h) D-Trp

5.4 Inhibition activity

Due to the discovery of IDO2 mRNAs in a variety of human cancers [4], and the strong inhibitory effect of 1-Me-D-Trp in mouse tumour models [6], it is desirable to clarify the selectivity of 1-methyltryptophan inhibition of IDO and IDO2. Consequently, the effectiveness of inhibition was investigated with D-Trp, 1-Me-L-Trp and 1-Me-D-Trp as inhibitors of recombinant human IDO2, and the findings are illustrated in figure 5.4

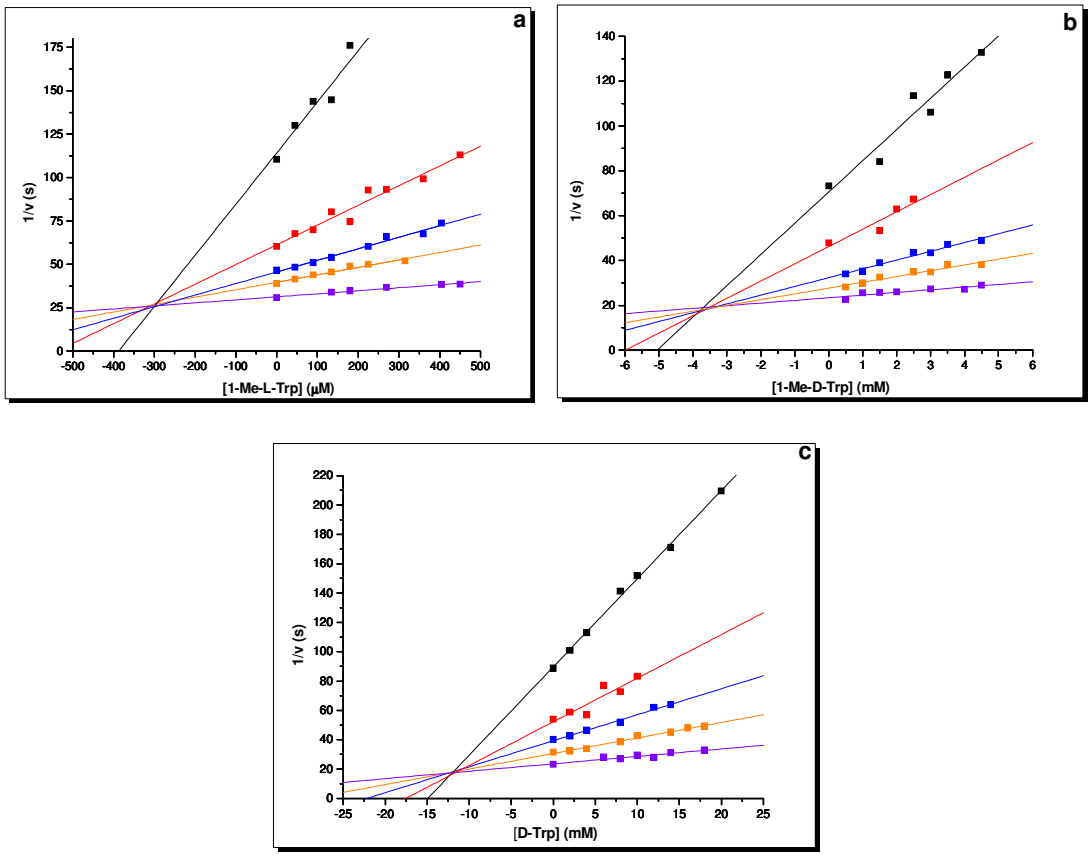

Figure 5.4: Dixon plots of hIDO2 using a) 1-Me-L-Trp, b) 1-Me-D-Trp and c) D-Trp. a) 1-Me-L-Trp. Substrate concentrations used (all mM) were: 1 (black), 2 (red), 3 (blue), 4 (orange), 6 (violet). b) 1-Me-D-Trp. Substrate concentrations (mM) were: 1 (black), 2 (red), 3 (blue), 4 (orange), 6 (violet).c) D-Trp. Substrate concentrations used (all mM) were: 1 (black), 2 (red), 3 (blue), 5 (orange), 7 (violet)

The fairly high affinities (low K_m) of both 1-Me-L-Trp and 1-Me-D-Trp for the enzyme, (K_m= 679 ± 24 μM and 776 ± 42 μM respectively) in combination with their poor turnover rates, enable inhibition of IDO2 by both molecules. In contrast with these methylated derivatives, D-Trp showed weak binding affinity and is unlikely to represent an effective inhibitor of the enzyme. These findings are summarised in table 5.2. For comparison, data for hIDO are also given.

	L-Trp	**D-Trp**	**1-Me-L-Trp**	**1-Me-D-Trp**
	K_{si} (μM)	**K_i (μM)**	**K_i (μM)**	**K_i (μM)**
hIDO	**50**	**543 ± 35**	**18.0 ± 3.4**	**ni**
hIDO2	**ni**	**12460 ± 562**	**306 ± 17**	**3419 ± 259**

Table 5.2: Inhibition data of hIDO and hIDO2 using D-Trp, 1-Me-L-Trp and 1-Me-D-Trp as inhibitors.

These results clearly show that, of these molecules, 1-Me-L-Trp is the best inhibitor of human IDO2. In comparison with the D-enantiomer, 1-Me-L-Trp is ~10-fold more potent as an inhibitor. Considering that 1-Me-D-Trp is not found to inhibit IDO, the weak inhibition ability of the molecule on IDO2 should be mentioned. In line with the turnover data, D-Trp is an implausible inhibitor of IDO2 with an inhibition constant of 12460 ± 562 μM. In comparison with IDO, it is clear that IDO2 demonstrates differing behaviour against L-Trp and its analogues. Indeed, in the case of IDO, L-Trp substrate inhibition is observed. This phenomenon is not observed for hIDO2 and this is in agreement with previous observations on other species [(7)].

5.5 Redox Potentiometry

In addition to kinetic and inhibition studies, the electrochemical behaviour of IDO2 was examined in the presence of L-Trp, D-Trp and their N-methylated analogues. Using the above substrates the reduction potentials of substrate-free and substrate-saturated IDO2 were measured, and the results are shown in table 5.3. For comparison, data for hIDO are also given.

Substrate	E_m hIDO (mV *vs.* SHE)	E_m hIDO2 (mV *vs.* SHE)
Free	**- 54 ± 8**	**-49 ± 1**
L-Trp	**-16 ± 6**	**-9 ± 1**
D-Trp	**-57 ± 12**	**-6 ± 3**
1-Me-L-Trp	**-48 ± 8**	**-27 ± 3**
1-Me-D-Trp	**-55 ± 4**	**-46 ± 6**

Table 5.3: Reduction potentials of hIDO and hIDO2 as free enzyme or saturated with D-Trp, 1-Me-L-Trp and 1-Me-D-Trp.

While the mid point potential of substrate free IDO2 is E_m = -49 ± 1 mV, saturation of the enzyme with L-Trp caused a positive shift in the potential of 40 mV (fig. 5.5). Although this shift is smaller than that observed human TDO (chapter 3), it reflects the changes that occur in the heme environment during binding of L-Trp. This shift indicates stabilization of the reduced form in the presence of the ligand and may be roughly correlated with the ligand affinity. Interestingly, a similar shift in midpoint potential was observed in the presence of D-Trp. Further to this, the reduction potential obtained in the presence of 1-Me-L-Trp was positively shifted by 22 mV relative to the substrate-free enzyme, around half the magnitude of the shift that occurred with L-Trp and D-Trp. In contrast with 1-Me-L-Trp, binding of 1-Me-D-Trp results in no change in the midpoint potential. The redox behaviour of hIDO2 shows distinct dissimilarities with that of hIDO. In the absence of any ligand or in the presence of L-Trp both enzymes display similar midpoint potentials, but only for IDO2 does binding of D-Trp induce a similar shift in potential. In the case of 1-Me-L-Trp and 1-Me-D-Trp, IDO2 again shows interesting behaviour. While in the

presence of 1-Me-D-Trp both IDO and IDO2 possess similar midpoint potentials, in the presence of 1-Me-L-Trp the two enzymes differ in their response. IDO is not significantly affected by 1-Me-L-Trp binding, retaining its midpoint potential at that of the free enzyme (E_m = -48 mV), whilst IDO2 reveals a small but noticeable modulation in potential, from -49 mV to -27 mV.

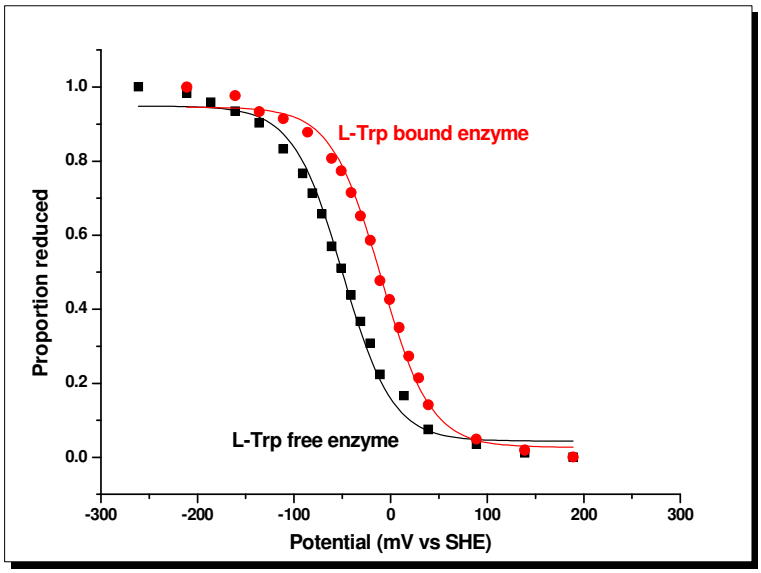

Figure 5.5: Reduction potentials of hIDO2 as the free enzyme and in the presence of L-Trp.

5.6 Comparison of IDO with IDO2

The study of IDO2 substrate and inhibition specificity in combination with its electrochemical characteristics shows that the enzyme is very inefficient as an L-Trp dioxygenase, the physiological function of IDO. Firstly, the two enzymes have different pH-activity profiles, with an optimum pH of 6.5 for IDO, and 7.5 for IDO2. Regarding the kinetic parameters (K_m, k_{cat}) and substrate specificity of the two enzymes, important dissimilarities were observed. Data for IDO and IDO2 are summarised and presented below (Table 5.4).

	hIDO		**hIDO2**	
Substrate	**k_{cat} (s^{-1})**	**K_m (μM)**	**k_{cat} (s^{-1})**	**K_m (μM)**
L-Trp	**2. 97 ± 0. 20**	**20. 90 ± 3. 95**	**0.100 ± 0.005**	**6821 ± 63**
D-Trp	**2. 7 ± 0. 3**	**296 ± 19**	**0.0105 ± 0.0007**	**3798 ± 267**
1- Me-L-Trp	**0.062 ± 0.001**	**70 ± 1**	**0.011 ± 0.005**	**679 ± 24**
1-Me-D-Trp	**0. 095 ± 0. 007**	**660 ± 43**	**0.0050 ± 0.0002**	**776 ± 42**
5-F-D,L-Trp	**0.76 ± 0. 01 [14]**	**6.0 ± 0.8**	**0.048 ± 0.002**	**1708 ± 85**
5-Me-D,L-Trp	**3.78 ± 0. 16 [14]**	**98 ± 14**	**0.35 ± 0.01**	**1664 ± 151**
5-HO-L-Trp	**0.0250 ± 0.0004 [14]**	**17.0 ± 1.1**	**No activity**	-

Table 5.4: Kinetic characteristics for hIDO and hIDO2 using L-Trp and other tryptophan analogues as substrates. Data for hIDO with 5-F-D,L-Trp, 5-Me-D,L-Trp and 5-HO-L-Trp were taken from *ref. 14*. Assays of IDO and IDO2 were carried out in 100 mM KP_i pH 6.5 and 7.5 respectively.

Molecules such as 5-MeO-D,L-Trp and 6-Me-D,L-Trp are shown to be substrates for IDO2, something which has not been reported so far for IDO. In this chapter the potency of 5-HO-L-Trp and melatonin as substrates for IDO2 is also determined. While neither showed any activity for IDO2, 5-HO-L-Trp is a published substrate of IDO with good affinity for the enzyme (K_m = 17.0 ± 1.1 μM) but poor turnover rate (k_{cat} = 0.0250 ± 0.0004 s^{-1}) [14]. Interestingly, 5-Me-D,L-Trp was found to be, relatively speaking, a very good substrate for IDO2 and a very poor substrate for

IDO. Like 5-Me-D,L-Trp, 5-F-D,L-Trp demonstrated two different behaviours for IDO and IDO2. In the case of IDO, 5-F-D,L-Trp is an important substrate with activity similar to that found for L-Trp (Table 5.4). In addition, 5-F-D,L-Trp showed high affinity for the enzyme (K_m = 6 ± 0.8 μM), higher even than the L-Trp K_m value (20. 9 ± 3. 95 μM). For IDO2 though the findings differ, with the 5-fluoro substrate showing lower activity than 5-Me-D,L-Trp. Examination of L-Trp turnover revealed surprising kinetic parameters for IDO2. According to the various enzymatic efficiencies presented in figure 5.6, L-Trp is the fourth most active substrate for IDO2 after 5-Me-D,L-Trp, 5-F-D,L-Trp and 1-Me-L-Trp, with a level of activity which seems unlikely to be biologically relevant. Amongst the several molecules that have been characterised as substrates for IDO2, the L-Trp data revealed the worst binding affinity (K_m = 6821 ± 63 μM).

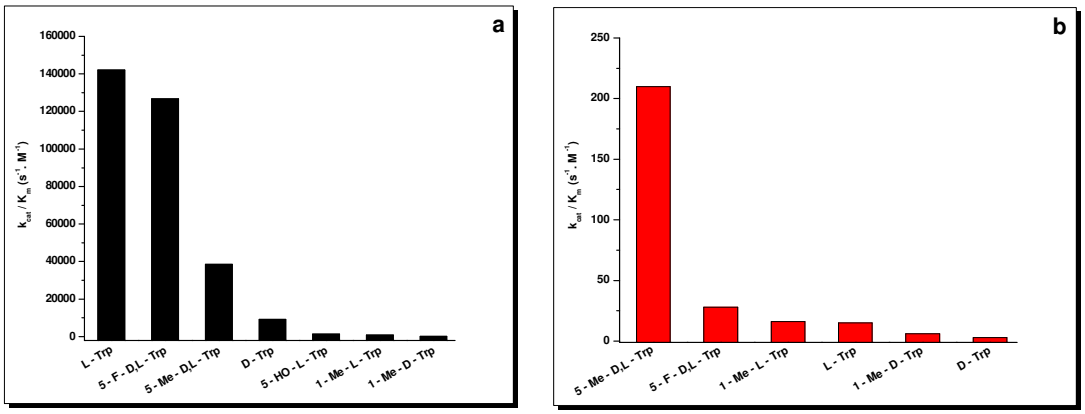

Figure 5.6: a) IDO and b) IDO2 catalytic response against L-Trp and other tryptophan analogues.

Both 1-Me-L-Trp and 1-Me-D-Trp seem to fulfil the characteristics of a good inhibitor for IDO2 (high affinity and low turnover rates) in contrast with IDO where 1-Me-L-Trp excels. Considering all the data, it appears that 1-Me-L-Trp is the best inhibitor of both IDO and IDO2 enzymes.

5.7 Discussion

The aim of this study was to examine the biochemical behaviour of recombinant human IDO2 and from there to extract useful conclusions about its function and catalytic preferences. In addition to this, the specificity of inhibition of IDO and IDO2 by the two isomers of 1-MT was investigated, in the light of recent publications on the antitumour activity of 1-Me-D-Trp. From all of this work it can be seen that hIDO differs significantly from hIDO2. The pH profile, substrate and inhibition specificity and the redox behaviour show distinct differences between the two enzymes. Although these findings cannot exclude the chance of IDO2 being an evolutionary ancestor of IDO, expression of both enzymes in particular tissues [(3)] in combination with the verified importance of IDO2 in tumour escape and survival [(5)] suggest that the enzyme is likely to be involved in an identified biological pathway. With respect to the two isomers of 1-MT, *in vitro* studies of the enzyme identified 1-Me-L-Trp as the more likely inhibitor for IDO2, leaving question marks over the origins of the antitumour activity of 1-Me-D-Trp. While the inhibition constant for IDO2 with 1-Me-D-Trp (K_i = 3419 ± 259 μM) suggests that the molecule cannot inhibit the enzyme effectively, the enzyme's affinity for the same molecule (K_m= 776 ± 42 μM) comes in conflict with the above result. Although this chapter provides important information about the behaviour of hIDO2 *in vitro*, its biological significance is yet to be determined.

5.8 References

(1) Batabyal D. and Yeh S.R., *Human Tryptophan Dioxygenase: A comparison with Indoleamine 2,3-Dioxygenase*, ***J. Am. Chem. Soc.***, 2007, 129,15690-15701

(2) Ball H.J., Perez A.S., Weiser S., Austin C.J.D., Astelbauer F., Miu J., McQuillan J.A., Stocker R., Jermiin L.S. and Hunt N.H., *Characterization of an indoleamine 2,3-dioxygenase-like protein found in humans and mice*, ***Gene***, 2007, 396, 203–213

(3) Ball H.J., Yuasa H.J., Austin C.J.D., Weiser S. and Hunt N.H., *Indoleamine 2,3-dioxygenase-2; a new enzyme in the kynurenine pathway*, ***The International Journal of Biochemistry & Cell Biology***, 2009, 41, 467–471

(4) Löb S., Königsrainer A., Zieker D., Brücher B.L.D.M., Rammensee H.G., Opelz G. and Terness P., *IDO1 and IDO2 are expressed in human tumors: levo- but not dextro-1-methyl tryptophan inhibits tryptophan catabolism*, ***Cancer Immunol Immunother***, 2009, 58, 153–157

(5) Sørensen R.B., Køllgaard T., Andersen R.S, Huibert van den Berg J., Svane I.M., Straten P.T. and Andersen M.H., *Spontaneous Cytotoxic T-Cell Reactivity against Indoleamine 2,3-Dioxygenase-2*, ***Cancer Res***, 2011, 71, 2038-2044

(6) Hou D.Y., Muller A.J., Sharma M.D., DuHadaway J., Banerjee T., Johnson M., Mellor A.L., Prendergast G.C., and Munn D.H., *Inhibition of Indoleamine 2,3-Dioxygenase in Dendritic Cells by Stereoisomers of 1-Methyl-Tryptophan Correlates with Antitumor Responses*, ***Cancer Res.***, 2007, 67, 792-801

(7) Yuasa H.J., Ball H.J., Austin C.J.D., and Hunt N.H., *1-L-methyltryptophan is a more effective inhibitor of vertebrate IDO2 enzymes than 1-D-methyltryptophan*, ***Comparative Biochemistry and Physiology***, Part B, 2010, 157, 10–15

(8) Austin C.J.D., Mailu B. M., Maghzal G. J., Sanchez-Perez A., Rahlfs S., Zocher K., Yuasa H. J., Arthur J. W., Becker K., Stocker R., Hunt N. H. and Ball H. J., *Biochemical characteristics and inhibitor selectivity of mouse indoleamine 2,3-dioxygenase-2*, ***Amino Acids***, 2010, 39,565–578

(9) Metz R., DuHadaway J.B., Kamasani U., Laury-Kleintop L., Muller A.J. and Prendergast G.C., *Novel Tryptophan Catabolic Enzyme IDO2 Is the Preferred Biochemical Target of the Antitumor Indoleamine 2,3-Dioxygenase Inhibitory Compound D-1-Methyl-Tryptophan*, ***Cancer Res***, 2007, 67, 7082-7087

(10) Chauhan N., Thackray S.J., Rafice S.A., Eaton G., Lee M., Efimov I., Basran J., Jenkins P.R., Mowat C.G., Chapman S.K., and Raven E.L., *Reassessment of the Reaction Mechanism in the Heme Dioxygenases*, ***J. Am. Chem. Soc.***, 2009, 131, 4186 – 4187

(11) Takikawa O., Kuroiwa T., Yamazaki F., and Kido R., *Mechanism of interferon-gamma action. Characterization of indoleamine 2,3-dioxygenase in cultured human cells induced by interferon-gamma and evaluation of the enzyme-mediated tryptophan degradation in its anticellular activity*, ***J. Biol. Chem.***,1988, 263, 2041-8

(12) Ost T. W. B., Clark J. P., Anderson J. L. R., Yellowlees L. J., Daff S. and Chapman S. K., *Oxygen Activation and Electron Transfer in Flavocytochrome P450 BM3*, ***J. Am. Chem. Soc.***, 2003, 125, 15010-15020

(13) Chang M.Y. *et al.*, IDO2 (indoleamine 2,3-dioxygenase 2) (2009)
Atlas Genet Cytogenet Oncol Haematol, URL:
http://atlasgeneticsoncology.org/Genes/IDO2ID44387ch8p11.html

(14) Basran J., Rafice S.A., Chauhan N., Efimov I., Cheesman M.R., Ghamsari L. and Raven E.L., *A Kinetic, Spectroscopic, and Redox Study of Human Tryptophan 2,3-Dioxygenase*, ***Biochemistry***, 2008, 47, 4752–4760

Chapter 6

Conclusions

6.1 Previously published inhibitors

The study of various known inhibitors of TDO and IDO has led to clarification of their specificity against either enzyme. The only specific inhibitor of IDO, 1-MT, will be discussed in the following section, while pyridyls revealed no specificity for TDO. The inhibition potency of these molecules is a subject of argument between this work and the previously published results [(1)]. According to Madge and co-workers, *in vitro* examination of 2-, 3- and 4-pyridyl compounds (40-60% purity) provided inhibition constants between 30-100 nM. The screening results presented here, though, show fairly weak inhibition with inhibition constants in the region of >100 μM. Considering the low purity of their samples, this disagreement is possibly related to the high percentage of contamination which could easily affect assay accuracy. Synthesis and purification of the pyridyl inhibitors used here was undertaken by Dr. Sarah J. Thackray and after NMR examination, they were characterized as ≥90% pure.

Examination of ebselen, a published inhibitor of IDO, yielded information which may be useful for the future optimization of TDO purification and crystallisation. Because of the unsatisfactory level of heme occupancy in preparations of human TDO, trials to crystallise the protein led to either formation of microcrystals or amorphous non-diffracting material. A standard procedure that is often followed for optimization of the purification process is substitution of a protein's cysteine residues in order to prevent dimerisation/oligomerisation *via* disulfide bond formation. Studies with ebselen showed that in the case of TDO, cysteine substitution could optimise the purification process. The construction of a model of hTDO, based on the structure of *X. campestris* TDO (by Dr. Sarah J. Thackray) showed that Cys4 is likely to be located on the surface of the protein and therefore its substitution will be a priority.

6.2 The specificity of 1-methyltryptophan for IDO and IDO2

With regard to 1-MT, it can be said that the molecule shows a clear selectivity for IDOs. The L-isoform of 1-MT is the only valid inhibitor for IDO while IDO2 findings do not provide a clear answer. Despite the fact that both 1-Me-L-Trp and 1-Me-D-Trp revealed similar K_m values for IDO2 (679 ± 24 μM and 776 ± 42 μM for 1-Me-L-Trp and 1-Me-D-Trp respectively) the inhibition outcomes (1-Me-L-Trp K_i= 306 ± 17 μM and 1-Me-D-Trp K_i= 3419 ± 259 μM) show a clear preference of the enzyme for the L-isomer over the D-isomer. Important to report is that the data presented herein explains only the *in vitro* behaviour of recombinant IDO and IDO2. The higher anticancer potency of 1-Me-D-Trp, *in vivo*, is still to be explained.

6.3 National Cancer Institute (NCI) inhibitors

Having examined a significant number of TDO and IDO potential inhibitors (~ 3000), a series of inhibitors for both enzymes was subsequently identified and characterised. For the NCI compounds, seven molecules with robust inhibition activity against both enzymes were discovered (Table 3.6). In addition to their inhibition action against TDO and IDO, these molecules were also found be active in tumour cell assays (as mentioned in Chapter 3). All seven revealed synergism with 1-MT for inhibition of IDO. Because of their sizes and structural variety, the inhibitors NSC 26326, NSC 36398, NSC 111041 and NSC 261726 will be studied further (*structures fig. 3.13*). The previous encouraging published result for NSC 26326 [(2)-(5)] (low toxicity to normal tissue, selectivity against cancer cells and a synergistic effect with radiation therapy) in combination with the strong inhibition activity that the molecule has on TDO and IDO give confidence that the further study of β-lapachone can produce a new class of promising inhibitors. Additionally, it is important to note the good inhibition potency of the flavone-like inhibitor, NSC 36398, on TDO in contrast with IDO. Having as an ultimate goal the development of a specific inhibitor for TDO, the study of this family will continue. Whilst NSC 111041 and NSC 261726 are not well studied inhibitors, further examination of these molecules is necessary.

6.4 Isatin derivatives

The effort that has been made towards the development of a new class of TDO and IDO inhibitors has resulted in the identification of a new class of inhibitors with inhibition constants in the low micromolar range. Starting with isatin itself, and after making various structural various modifications, a number of promising inhibitors with tryptophan-like structure were detected (fig. 6.1-structure 6).

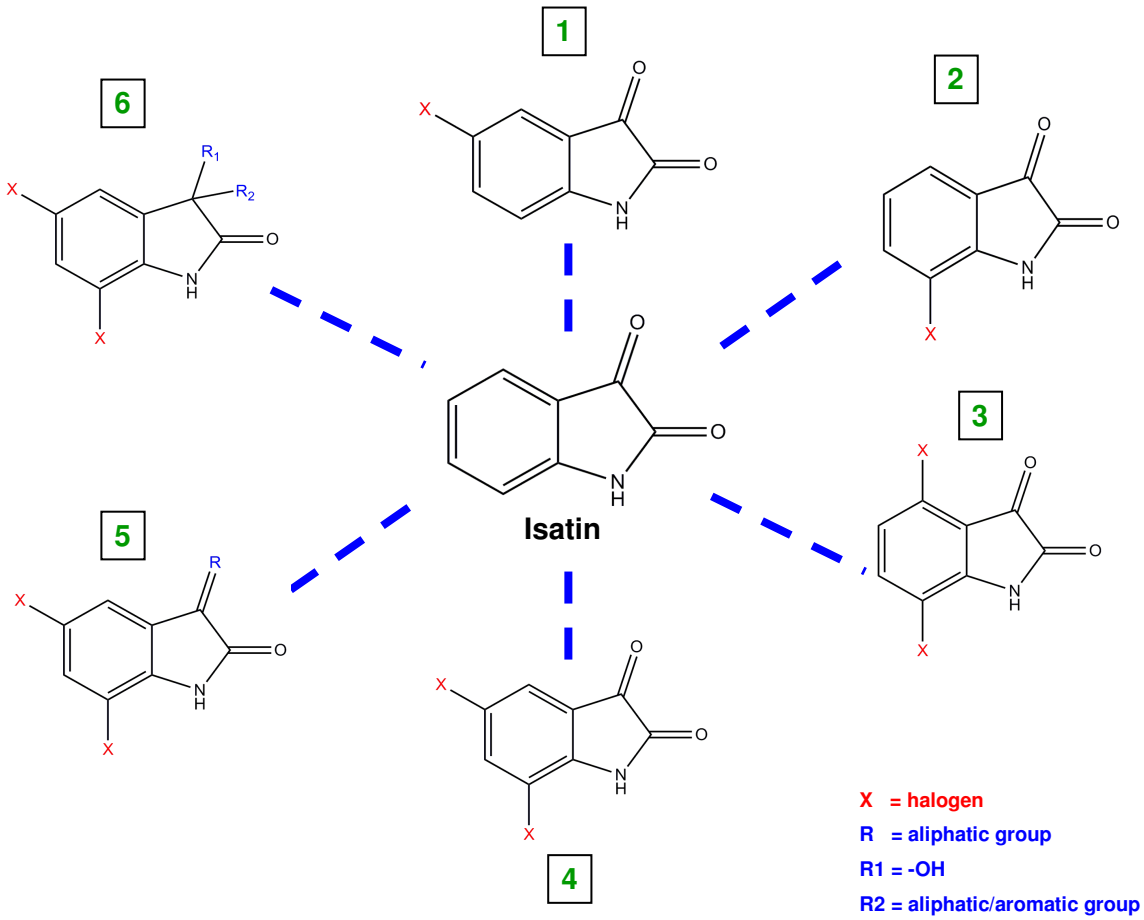

Figure 6.1: Illustration of the trials that have been made towards the identification and characterization of the potent inhibitors with general structure 6. These molecules revealed the highest inhibition activities for both TDO and IDO and development of new inhibitors will be based on this structure.

Trials involving modification of the core moiety of isatin had the result of decreasing the inhibition potency of these molecules (fig. 6.2). None of the molecules shown in figure 6.2 showed inhibition of either TDO or IDO. However, while molecules with the general structure 6 in figure 6.1 provided satisfactory inhibition activities, trials to optimize their inhibition properties will continue. A series of modifications at the C3 atom of the indole ring will help gain further understanding of the effect that the C3-modifications have on inhibition of TDO and IDO.

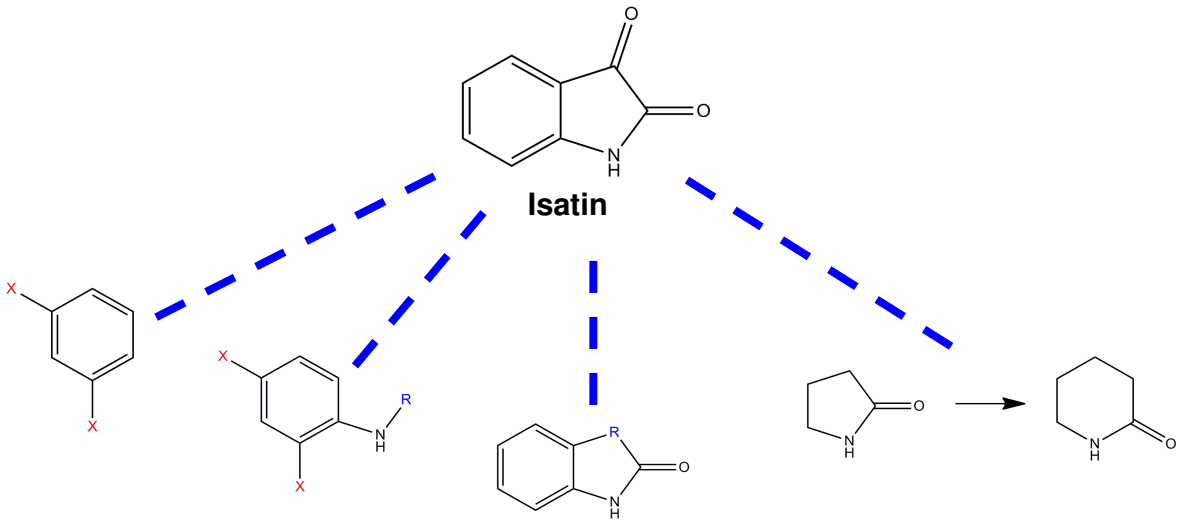

Figure 6.2: Modifications of isatin that result in the loss or decrease of its inhibition potency.

6.5 Characterization of IDO2

In vitro examination of hIDO2 was undertaken in order to clarify the enzyme's biological role. Clearly IDO2 demonstrated noticeable dissimilarities in comparison with IDO. Because of its weak *in vitro* ability to produce L-kynurenine, it can be said that IDO2 is unlikely to have an active role in the kynurenine pathway. Assuming that the enzyme is biologically redundant, its efficiency with 5-MeO-Trp and 5-Me-Trp raises questions. Although this study offered important information regarding IDO2 *in vitro* behaviour, *in vivo* study of the enzyme is needed to securely determine to what degree IDO1 and IDO2 are similar in their preference for substrates and reaction pathways to generate product.

6.6 Future work

The inhibition outcomes of the current thesis provide a number of inhibitors with good inhibition potencies (in either nanomolar or low micromolar range) for both hTDO and hIDO. Utilizing the previous published crystal structures of xcTDO [6] and hIDO [7], it will pursue their co-crystallization with particular inhibitors such as NSC 26326 (97 ± 14 nM IDO and 30-70 nM TDO), NSC 36398 (>100 μM IDO and 16.3 ± 3.8 μM TDO) and NSC 111041 (4.3 ± 0.9 μM IDO and 1.1 ± 0.3 μM TDO) (*for structures see fig 3.13*). Preliminary crystallographic results of xcTDO with NSC 26326 indicate that binding of inhibitor(s) into the active site pocket of the enzyme is likely to occur only in the ferrous active form. In addition, mutagenesis of active site residue(s) that are involved in the induced fit motion of xcTDO might help as well. In our trial to obtain the crystal structure of hTDO, mutation of Cys4 residue will be attempted in line with co-crystallisation of the mutant with NSC 26326.

The most promising inhibitors, identified herein, will be used as templates for the development of new inhibitors of hTDO and hIDO. NSC 36398 is the only inhibitor that revealed selectivity for hTDO and thus study of this molecule will continue. Following the development of the daughter inhibitors, their inhibition activity will be evaluated both *in vitro* and *in vivo*. Combinations of 1-MT (hIDO only) with the newly developed inhibitors will be examined and their toxicity in a cell based assay will be assessed. Regarding the isatin derivatives, a number of new modifications (replacement of C2 carbonyl oxygen with fluorine and substitutions of C5 and C3 atoms) will be tried and their activity in a cell based assay will be evaluated as well.

Examination of 1-Me-L-Trp and 1-Me-D-Trp inhibition activity against hIDO and hIDO2 provides information in regards with the *in vitro* behaviour of these inhibitors. Although these results come in agreement with the cell-based findings of 1-Me-L-Trp, they can not explain the high anticancer potency of 1-Me-D-Trp [8]. Using affinity proteomics it will be attempted to identify new *in vivo* targets of 1-Me-D-Trp [9]. Identification of new *in vivo* targets of 1-Me-D-Trp will provide insight into the molecule's anticancer potency and will help us to understand better

the way that 1-MT functions. Last but not least is hIDO2. All the results presented in this work support the idea that hIDO2 function *in vivo* is still to be clarified. The enzyme shows a clear role in cancer biology and obvious differences from hIDO. High-throughput screening (HTS), for the identification of small molecules that act either as substrates or inhibitors, can provide useful information regarding the actual role of this protein. Crystallisation of hIDO2 will be also attempted.

6.7 References

(1) Madge D.J., Hazelwood R., Iyer R., Jones H.T. and Salter M., *Novel Tryptophan Dioxygenase Inhibitors and combined Tryptophan Dioxygenase/5-HT Reuptake Inhibitors*, ***Bioorganic & Medicinal Chemistry Letters***, 1996, 6, 857-860

(2) Bey E. A., Bentle M. S., Reinicke K. E., Dong Y., Yang C.-R., Girard L., Minna J. D., Bornmann W. G., Gao J., and Boothman D. A, *An NQO1- and PARP-1-mediated cell death pathway induced in non-small-cell lung cancer cells by β-lapachone*, ***PNAS***, 2003, 104, 11832-37

(3) Li Y., Sun X., Mont J.T.L., Pardee A.B. and Li C.J., *Selective killing of cancer cells by β-lapachone: Direct checkpoint activation as a strategy against cancer*, ***PNAS***, 2003, 100, 2674-78

(4) Li L.S., Bey E.A., Dong Y., Meng J., Patra B., Yan J., Xie X.J., Brekken R.A., Barnett C.C., Bornmann W.G., Gao J. and Boothman D.A., *Modulating Endogenous NQO1 Levels Identifies Key Regulatory Mechanisms of Action of b-Lapachone for Pancreatic Cancer Therapy*, ***Clin Cancer Res***, 2011,17, 275-285

(5) Dong Y., Bey E.A., Li L.S., Kabbani W., Yan J., Xie X.J., Hsieh J.T., Gao J., and Boothman D.A., *Prostate Cancer Radiosensitization through Poly(ADP-Ribose) Polymerase-1 Hyperactivation*, ***Cancer Res***, 2010, 70, 8088-8096

(6) Forouhar F., Anderson J.L., Mowat C.G., Vorobiev S.M., Hussain A., Abashidze M., Bruckmann C., Thackray S.J., Seetharaman J., Tucker T., Xiao R., Ma L.C., Zhao L., Acton T.B., Montelione G.T., Chapman S.K., Tong L., *Molecular insights into substrate recognition and catalysis by tryptophan 2,3-dioxygenase*, ***Proc. Natl. Acad. Sci.***, 2007, 104, 473-478

(7) Sugimoto H., Oda S.I, Otsuki T., Hino T., Yoshida T., and Shiro Y., *Crystal structure of human indoleamine 2,3-dioxygenase: Catalytic mechanism of O2 incorporation by a heme-containing dioxygenase*, ***Proc. Natl. Acad. Sci.***, 2006,103, 2611-2616

(8) Hou D.Y., Muller A.J., Sharma M.D., DuHadaway J., Banerjee T., Johnson M., Mellor A.L., Prendergast G.C., and Munn D.H., *Inhibition of Indoleamine 2,3-Dioxygenase in Dendritic Cells by Stereoisomers of 1-Methyl-Tryptophan Correlates with Antitumor Responses*, ***Cancer Res.***, 2007, 67, 792-801

(9) Bantscheff M., Hopf C, Savitski M. M., Dittmann A., Grandi P., Michon A-M., Schlegl J., Abraham Y., Becher I., Bergamini G., Boesche M., Delling M., Dümpelfeld B., Eberhard D., Huthmacher C., Mathieson T, Poeckel D., Reader V., Strunk V., Sweetman G., Kruse U., Neubauer G., Ramsden N.G. and Drewes G., *Chemoproteomics profiling of HDAC inhibitors reveals selective targeting of HDAC complexes*, ***Nature Biotechnology***, 2011, 3, 255-265

Appendix A

The list of TDO and IDO potential inhibitors

Number	Name	MW (g/mol)	Supplier
0	L-tryptophan	204.3	Sigma/Aldrich
1	D-tryptophan	204.23	Sigma/Aldrich
2	indole	117.15	Sigma/Aldrich
3	5-methyl-D/L-tryptophan	218.26	Sigma/Aldrich
4	3-(2-hydroxyethyl) indole	161.21	Sigma/Aldrich
5	Nα-me-L-tryptophan	216.26	Sigma/Aldrich
6	5-hydroxyindole	133.15	Sigma/Aldrich
7	6-methyl-D/L-tryptophan	218.25	Sigma/Aldrich
8	L-kynurenine	208.2	Sigma/Aldrich
9	3-hydroxykynurenine	224.2	Sigma/Aldrich
10	benzofuran-2-yl-me-ketone	160.17	Sigma/Aldrich
11	indole-3-carboxaldehyde	145.15	Sigma/Aldrich
12	L-tryptophanol	190.25	Sigma/Aldrich
13	indole-3-acetic acid	175	Sigma/Aldrich
14	1-methyl-D-tryptophan	218.26	Sigma/Aldrich
15	Boc-D-3-benzothiethylalanine	321.4	Sigma/Aldrich
16	3-D/L-indoleacetic acid	175	Sigma/Aldrich
17	melatonin	232.28	Sigma/Aldrich
18	indole 3-acetamide	174.2	Sigma/Aldrich
19	5-fluoro-D/L-Tryptophan	222.22	Sigma/Aldrich
20	L-alanine	89.09	Sigma/Aldrich
21	benzofuran-3-acetonitrile	157.17	Sigma/Aldrich
22	3-indoleacrylic acid	187.2	Sigma/Aldrich
23	4-(1H-imidazol-1-yl) aniline	161.21	Sigma/Aldrich
24	4-(imidazol-1-yl) phenol	162.19	Sigma/Aldrich
25	L-histidine	155.2	Sigma/Aldrich
26	L-homoserine	105.09	Sigma/Aldrich
27	Fmoc-β-(3-benzothienyl)-L-alanine	443.52	Sigma/Aldrich
28	2-pyridyl	219	In house
29	R963453	305.338	Sigma/Aldrich

30	S065081	224.223	Sigma/Aldrich
31	3-(2-(2-pyridyl)ethyl) indole	222.291	Sigma/Aldrich
32	s293520	211.228	Sigma/Aldrich
33	3-pyridyl	219	In house
34	4-pyridyl	219	In house
35	(1H-indol-3-methylene)-pyridin-3-yl-amine	221.263	Sigma/Aldrich
36	1H -1,2,3-triazol	69.07	Sigma/Aldrich
37	2,2-dithiodipyridyl	220	Sigma/Aldrich
38	$C_{10}H_{11}O_3N$	193.2	St Andrews
39	$C_{10}H_{17}O_3N$	199.25	St Andrews
40	$C_{14}H_{13}O_3N$	243.26	St Andrews
41	$C_9H_{12}O_4NP$	229.17	St Andrews
42	$C_{12}H_{13}O_3N$	219.24	St Andrews
43	$C_{11}H_{11}O_3N$	205.21	St Andrews
44	$C_{10}H_{10}O_5N$	260.65	St Andrews
45	$C_{10}H_{10}O_3NCl_3$	298.55	St Andrews
46	A2425/0102738	227.257	Ambinter
47	A0345/0015908	263.275	Ambinter
48	PHAR061831 - 28SPH1-397-776	256.261	Ambinter
49	STOCK1S-37397	354.388	InterBioScreen
50	STOCK5S-29375	234.295	InterBioScreen
51	STOCK1S-38338	260.359	InterBioScreen
52	STOCK2S-19248	305	InterBioScreen
53	T3018147	279.255	Tim Tec
54	T3175372	274.28	TimTec
55	ST5026463	271.316	Tim Tec
56	ST009518	221.263	TimTec
57	1-methyl-L-tryptophan	218	Sigma/Aldrich
58	7-chloro-L-tryptophan	238	St Andrews
59	norharman	168.19	Sigma/Aldrich
60	JFD00036	209	Maybridge
61	r433950	207.237	Sigma/Aldrich
62	r493171	235.291	Sigma/Aldrich
63	r351687	406.229	Sigma/Aldrich
64	s293520	211.228	Sigma/Aldrich
65	11B-126	190.22	Key organics

66	10w-0241	301.08	Key organics
67	t0516-4089	319.3	Enamine
68	T3227834	270.288	Tim Tec
69	ST042376	266.222	Tim Tec
70	T3012398	240.328	Tim Tec
71	ST245307	257.289	Tim Tec
72	anthraquinone 2-sulfonate	288	Sigma/Aldrich
73	2-hydroxy-1,4-napthaquinone	174	Sigma/Aldrich
74	5- hydroxy-1,4-nathaquinone	174	Sigma/Aldrich
75	1,2-napthaquinone	158	Sigma/Aldrich
76	5,8-dihydroxy-1,4-napthaquinone	190	Sigma/Aldrich
77	anthroquinone- 2,6- disulfonic	412	Sigma/Aldrich
78	1,4-napthoquinone	158	Sigma/Aldrich
79	2-methyl-1,4-benzoquinone	122	Sigma/Aldrich
80	1,4-benzoquinone	108	Sigma/Aldrich
81	2,3-dichloro-5,6-dicyano-para-benzoquinone	227	Sigma/Aldrich
82	tetrachloro-ortho-benzoquinone	238	Sigma/Aldrich
83	1,2-napthaquinone-4-sulfonic acid	172	Sigma/Aldrich
84	anthraquinone	184	Sigma/Aldrich
85	vitamin K1	451	Sigma/Aldrich
86	2,3-dichloro-5,8-dihydroxy-1,4-naphthoquinone	259.05	Sigma/Aldrich
87	L-serine -7- amido-4-methyl-coumarin hydrochloride	298.7	Sigma/Aldrich
88	indigo	262.26	Sigma/Aldrich
89	isatin	147.13	Sigma/Aldrich
90	benzophenone	182.21	Sigma/Aldrich
91	2-indanone	132.16	Sigma/Aldrich
92	6-methyl-indan-1-one	146.18	Sigma/Aldrich
93	unknown	226	Sigma/Aldrich
94	NSC1460	205.22	NCI
95	NSC14159	160.19	NCI
96	NSC22128	221.263	NCI
97	NSC106090	212.27	NCI
98	NSC175825	385.241	NCI
99	NSC103253	338	NCI

100	mitomycin C	334.33	Tocris Biosc.
101	carbazole	167.206	Sigma/Aldrich
102	riboflavin	376.36	Sigma/Aldrich
103	SPB08034	235.305	RyanScientific
104	KM04716	286.379	RyanScientific
105	KMO08843	246.226	RyanScientific
106	S760269	235.242	Sigma/Aldrich
107	S42065	205.215	Sigma/Aldrich
108	CA 199	306	Leicester Uni.
109	trans-4-hydroxy-L-proline	131.13	Sigma/Aldrich
110	N-(2-oxo-2,3-dihydro-1h-indol-3-yl)-acetamide	190.203	Sigma-Adrich
111	3-hydroxy-3-(2-(hydroxymino)-propyl-2-indolinone	220.23	Sigma-Adrich
112	(3Z)-1H-indole-2,3-dione-3-(N-methylthiosemicarbazone)	234.81	Sigma-Adrich
113	b-nicotinamide adenine dinucleotide phosphate (b-NADP)	765.4	Sigma/Aldrich
114	flavin adenine dinucleotide (FAD)	829.5	Sigma/Aldrich
115	flavin mononucleotide sodium salt (FMN)	478.3	Sigma/Aldrich
116	b-nicotinamide mononucleotide (b-NMN)	334.2	Sigma/Aldrich
117	adenosine	267.2	Sigma/Aldrich
118	adenosine 5'-triphosphate disodium salt	551.1	Sigma/Aldrich
119	guanine	151.13	Sigma/Aldrich
120	unknown	222	Sigma/Aldrich
121	biotin	244.31	Sigma/Aldrich
122	thiamine	337.27	Sigma/Aldrich
123	pyridoxine hydrochloride	205.64	Biochemical
124	lumiflavin	256.3	Sigma/Aldrich
125	5,7-dichloroisatin	216.02	Sigma/Aldrich
126	chlophacinon	374.82	Sigma/Aldrich
127	1-cyclohexyluracil	194.2	Sigma/Aldrich
128	allethin	302.41	Sigma/Aldrich
129	dihydro-4,4-dimethyl-2,3-furandione	128.13	Sigma/Aldrich

130	(–)-2,3-*O*-isopropylidene-D-erythronolactone	158.15	Sigma/Aldrich
131	(2S)-7-benzyl-2-[(trityloxy)methyl]-1-oxa-7-azaspiro[4.4]nonane-6,9-dione	517.63	Sigma/Aldrich
132	1-methylisatin	161.16	Sigma/Aldrich
133	(S)-(-)-2-hydroxy-N-methylsuccinimide	129.12	Sigma/Aldrich
134	uracil	112.1	Sigma/Aldrich
135	thymine	126.11	Sigma/Aldrich
136	adenine	135.13	Sigma/Aldrich
137	5-bromo-3-(2-(4-bromo-phenyl)-2-oxo-ethyl)-3-hydroxy-1,3-dihydro-indol-2-one	425.079	Sigma/Aldrich
138	7,8-dihydro-1,3-dioxolo(4,5-G)-quinazolin-6(5H)-one	192.176	Sigma/Aldrich
139	(3AR,4S,6AS)-5-benzyl-4-hydroxydihydro-3AH-spiro[[1,3]dioxolo[4,5-C]pyrrole-2,1'-cyclohexan]-6(6AH)-one	303.361	Sigma/Aldrich
140	2-(3,4-dihydroxy-phenyl)-3,5,7-trihydroxy-chromen-4-one	302.243	Sigma/Aldrich
141	2-benzoyl-cyclopentanone	188.288	Sigma/Aldrich
142	1,3-indandion	146.15	Sigma/Aldrich
143	2-acetyl-1,3-indanedione	188.18	Sigma/Aldrich
144	citalopram	324	Sigma/Aldrich
145	6,8-dichloro-3-methylchromone	229.06	Sigma/Aldrich
146	5,7-dichloro-1-indanone	201.05	Sigma/Aldrich
147	5,7-dichloro-8-quinolinol	214.05	Sigma/Aldrich
148	5-chloroisatin	181.58	Sigma/Aldrich
149	7-chloroisatin	181.58	Sigma/Aldrich
150	N-(2,3-dichlorophenyl)-1-methyl-2-oxo-3-indolinecarboxamide	335.19	Sigma/Aldrich
151	quercetin hydrate	302.24	Sigma/Aldrich
152	myricetin	318.24	Sigma/Aldrich
153	quercetin 3-b-D-glucoside	464.38	Sigma/Aldrich
154	3-(4-hydroxy-phenylimino)-1,3-dihydro-indol-2-one	238.248	Sigma/Aldrich

155	isatin, azine with 3,5-dichlorosalicylaldehyde	334.164	Sigma/Aldrich
156	3-hydroxy-3-(2-oxo-2-phenyl-ethyl)-1,3-dihydro-indol-2-one	267.287	Sigma/Aldrich
157	flavone	222.24	Sigma/Aldrich
158	ebselen	274.2	Cayman
159	NSC 635312	412	NCI
160	NSC 635326	381	NCI
161	NSC 635435	392	NCI
162	NSC 167410	448	NCI
163	NSC 100445	306	NCI
164	NSC 123115	376.4	NCI
165	NSC 275428	361.8	NCI
166	2-amino-benzoic acid (2-oxo-1,2-dihydro-indol-3-ylidene)-hydrazide	280.288	Sigma/Aldrich
167	alpha-(3-hydroxy-2-oxo-3-indolinyl)-2-methylpyridine	240.264	Sigma/Aldrich
168	3-((4-oxo-thiazolidin-2-ylidene)-hydrazono)-1,3-dihydro-indol-2-one	260.276	Sigma/Aldrich
169	3-hydroxy-3-(6-methyl-2-pyridylmethyl)-2-indolinone	254.291	Sigma/Aldrich
170	3-(benzothiazol-2-YL-hydrazono)-1,3-dihydro-indol-2-one	294.337	Sigma/Aldrich
171	3-(4-hydroxy-6-methyl-2-pyrimidinylhydrazono)-2-indolinone	269.265	Sigma/Aldrich
172	isonicotinic acid(1-methyl-2-oxo-1,2-dihydro-indol-3-ylidene)-hydrazine	280.288	Sigma/Aldrich
173	1,4-dihydroxynaphthalene	160.17	Sigma/Aldrich
174	1,4-dihydroxynaohthalin-2,3-dicarbonsaeuredintril	210.19	Sigma/Aldrich
175	1,4-dihydroxy-2-naphthoic acid	204.19	Sigma/Aldrich
176	5-chloroindole	151.59	Sigma/Aldrich
177	5-chloro-2-oxindole	167.59	Sigma/Aldrich
178	2-oxindole	133.15	Sigma/Aldrich
179	indoline	119.17	Sigma/Aldrich
180	3,4-dihydro-2(1H)-quinolinone	147.18	Sigma/Aldrich
181	2-hydroxybenzimidazole	134.14	Sigma/Aldrich

182	N-(2,4-dichloroohenyl)acetamide	204.057	Sigma/Aldrich
183	6-chlorobenzoxazol-2(3H)-one	169.57	Sigma/Aldrich
184	4,5-dichlorophthalimide	216.02	Sigma/Aldrich
185	N-acetylphthalimide	189.17	Sigma/Aldrich
186	CH47471	153.61	TimTec
187	2,4-dichloroaniline	162.02	Sigma/Aldrich
188	2,4-dichloro-*N*-methylaniline	176.04	Sigma/Aldrich
189	3-hydroxyanthranilic acid	153.14	Sigma/Aldrich
190	kynurenic acid	189.17	Sigma/Aldrich
191	4-(N-(2,4-dichlorophenyl)carbamoyl)morpholine	275.136	Sigma/Aldrich
192	2,5-dichloroformanilide	190.03	Sigma/Aldrich
193	6,8-dichlorocinchophen	318.162	Sigma/Aldrich
194	6,8-dichloro-2-hydroxy-4-quinolinecarboxylic acid	258.062	Sigma/Aldrich
195	6,8-dinitro-1,2-dihydro-quinolin-2-ol	237.173	Sigma/Aldrich
196	salicylic acid	138.12	Sigma/Aldrich
197	2-amino-3-chlorobenzoic acid	171.58	Sigma/Aldrich
198	2-amino-3-methylbenzoic acid	151.16	Sigma/Aldrich
199	anthranilic acid	137.14	Fluka
200	ST4146353	220.23	TimTec
201	pn20	230.05	St. Andrews
202	pn14	288.13	St. Andrews
203	pn21	303.14	St. Andrews
204	7-bromoisatin	226.03	Sigma/Aldrich
205	7-fluoroisatin	165.12	Sigma/Aldrich
206	5-iodoisatin	273.03	Sigma/Aldrich
207	5-bromoisatin	226.03	Sigma/Aldrich

Appendix B

The list of IDO2 potential substrates

Number	Name	MW	Supplier
1	L-tryptophan	204.3	Sigma/Aldrich
2	D-tryptophan	204.3	Sigma/Aldrich
3	indole	117.15	Sigma/Aldrich
4	5-methyltryptophan	218.26	Sigma/Aldrich
5	3-(2-hydroxyethyl) indole	161.21	Sigma/Aldrich
6	5-hydroxyindole	133.15	Sigma/Aldrich
7	6-methyltryptophan	218.25	Sigma/Aldrich
8	L-kynurenine	208.2	Sigma/Aldrich
9	3-hydroxykynurenine	224.2	Sigma/Aldrich
10	benzofuran-2-yl-me-ketone	160.17	Sigma/Aldrich
11	indole-3-carboxaldehyde	145.15	Sigma/Aldrich
12	L-tryptophanol	190.25	Sigma/Aldrich
13	indole-3-acetic acid	175	Sigma/Aldrich
14	1-methyl-D-tryptophan	218.26	Sigma/Aldrich
15	1-methyl-L-tryptophan	218.26	Sigma/Aldrich
16	melatonin	232.28	Sigma/Aldrich
17	indole 3-acetamide	174.2	Sigma/Aldrich
18	5-fluorotryptophan	222.22	Sigma/Aldrich
19	L-alanine	89.09	Sigma/Aldrich
20	benzofuran-3-acetonitrile	157.17	Sigma/Aldrich
21	3-indoleacrylic acid	187.2	Sigma/Aldrich
22	4-(1H-imidazol-1-yl) aniline	161.21	Sigma/Aldrich
23	L-histidine	155.2	Sigma/Aldrich
24	2-pyridyl	219	in house
25	C10H11O3N	193.2	st andrews
26	C14H13O3N	243.26	st andrews
27	7-chlorotryptophan	238	St Andrews

28	norharman	168.19	Sigma/Aldrich
29	10w-0241	301.08	key organics
30	isatin	147.13	Sigma/Aldrich
31	2-indanone	132.16	Sigma/Aldrich
32	6-methyl-indan-1-one	146.18	Sigma/Aldrich
33	NSC1460	205.22	NCI
34	NSC106090	212.27	NCI
35	carbazole	167.206	Sigma/Aldrich
36	SPB08034	235.305	RyanScientific
37	6,8-dichloro-3-methylchromone	229.06	Sigma/Aldrich
38	5,7-dichloro-1-indanone	201.05	Sigma/Aldrich
39	5-chloroindole	151.59	Sigma/Aldrich
40	2-oxindole	133.15	Sigma/Aldrich
41	indoline	119.17	Sigma/Aldrich
42	3,4-dihydro-2(1H)-quinolinone	147.18	Sigma/Aldrich
43	2-hydroxybenzimidazole	134.14	Sigma/Aldrich
44	N-(2,4-dichlorophenyl)acetamide	204.057	Sigma/Aldrich
45	6-chlorobenzoxazol-2(3H)-one	169.57	Sigma/Aldrich
46	3-hydroxyanthranilic acid	153.14	Sigma/Aldrich
47	kynurenic acid	189.17	Sigma/Aldrich
48	2,5-dichloroformanilide	190.03	Sigma/Aldrich
49	2-amino-3-methylbenzoic acid	151.16	Sigma/Aldrich
50	ST4146353	220.23	Tim Tec
51	indene	116.16	Sigma/Aldrich
52	s-tryptophan	207.2	in house
53	indole-3-glyoxylic acid	189.167	Sigma/Aldrich
54	trans-indole-3-acrylic acid	187.194	Sigma/Aldrich

Appendix C

The amino acid sequences of TDO and IDO enzymes

Xanthomonas Campestris TDO (Length: 298aa, Mass: 34,617 Da - His tag)

```
         10         20         30         40         50         60
MPVDKNLRDL EPGIHTDLEG RLTYGGYLRL DQLLSAQQPL SEPAHHDEML FIIQHQTSEL

         70         80         90        100        110        120
WLKLLAHELR AAIVHLQRDE VWQCRKVLAR SKQVLRQLTE QWSVLETLTP SEYMGFRDVL

        130        140        150        160        170        180
GPSSGFQSLQ YRYIEFLLGN KNPQMLQVFA YDPAGQARLR EVLEAPSLYE EFLRYLARFG

        190        200        210        220        230        240
HAIPQQYQAR DWTAAHVADD TLRPVFERIY ENTDRYWREY SLCEDLVDVE TQFQLWRFRH

        250        260        270        280        290
MRTVMRVIGF KRGTGGSSGV GFLQQALALT FFPELFDVRT SVGVDNRPPQ GSADAGKRLE

HHHHHH
```

Human TDO (Length: 406aa, Mass: 47,872 Da - His tag)

```
         10         20         30         40         50         60
MSGCPFLGNN FGYTFKKLPV EGSEEDKSQT GVNRASKGGL IYGNYLHLEK VLNAQELQSE

         70         80         90        100        110        120
TKGNKIHDEH LFIITHQAYE LWFKQILWEL DSVREIFQNG HVRDERNMLK VVSRMHRVSV

        130        140        150        160        170        180
ILKLLVQQFS ILETMTALDF NDFREYLSPA SGFQSLQFRL LENKIGVLQN MRVPYNRRHY

        190        200        210        220        230        240
RDNFKGEENE LLLKSEQEKT LLELVEAWLE RTPGLEPHGF NFWGKLEKNI TRGLEEEFIR

        250        260        270        280        290        300
IQAKEESEEK EEQVAEFQKQ KEVLLSLFDE KRHEHLLSKG ERRLSYRALQ GALMIYFYRE

        310        320        330        340        350        360
EPRFQVPFQL LTSLMDIDSL MTKWRYNHVC MVHRMLGSKA GTGGSSGYHY LRSTVSDRYK

        370        380        390        400
VFVDLFNLST YLIPRHWIPK MNPTIHKFLY TAEYCDSSYF SSDESDLEHHHHHHHH
```

Human IDO (Length: 403aa, Mass: 45,326 Da - His tag)

```
                          10         20         30         40
MRGSHHHHHHGSACELGTAHAMENSWT ISKEYHIDEE VGFALPNPQE NLPDFYNDWM

        50         60         70         80         90        100
FIAKHLPDLI ESGQLRERVE KLNMLSIDHL TDHKSQRLAR LVLGCITMAY VWGKGHGDVR

       110        120        130        140        150        160
KVLPRNIAVP YCQLSKKLEL PPILVYADCV LANWKKKDPN KPLTYENMDV LFSFRDGDCS

       170        180        190        200        210        220
KGFFLVSLLV EIAAASAIKV IPTVFKAMQM QERDTLLKAL LEIASCLEKA LQVFHQIHDH

       230        240        250        260        270        280
VNPKAFFSVL RIYLSGWKGN PQLSDGLVYE GFWEDPKEFA GGSAGQSSVF QCFDVLLGIQ

       290        300        310        320        330        340
QTAGGGHAAQ FLQDMRRYMP PAHRNFLCSL ESNPSVREFV LSKGDAGLRE AYDACVKALV

       350        360        370        380        390        400
SLRSYHLQIV TKYILIPASQ QPKENKTSED PSKLEAKGTG GTDLMNFLKT VRSTTEKSLL


KEG
```

Human IDO2 (Length: 407aa, Mass: 45,424 Da - His tag)

```
                                        10         20         30
MSYYHHHHHHLESTSLYKKAGSAAAPFTMEPHRPNVKT AVPLSLESYH ISEEYGFLLP

        40         50         60         70         80         90
DSLKELPDHY RPWMEIANKL PQLIDAHQLQ AHVDKMPLLS CQFLKGHREQ RLAHLVLSFL

       100        110        120        130        140        150
TMGYVWQEGE AQPAEVLPRN LALPFVEVSR NLGLPPILVH SDLVLTNWTK KDPDGFLEIG

       160        170        180        190        200        210
NLETIISFPG GESLHGFILV TALVEKEAVP GIKALVQATN AILQPNQEAL LQALQRLRLS

       220        230        240        250        260        270
IQDITKTLGQ MHDYVDPDIF YAGIRIFLSG WKDNPAMPAG LMYEGVSQEP LKYSGGSAAQ

       280        290        300        310        320        330
STVLHAFDEF LGIRHSKESG DFLYRMRDYM PPSHKAFIED IHSAPSLRDY ILSSGQDHLL

       340        350        360        370        380        390
TAYNQCVQAL AELRSYHITM VTKYLITAAA KAKHGKPNHL PGPPQALKDR GTGGTAVMSF

       400
LKSVRDKTLE SILHPRG
```

Appendix D

Derivation of kinetic equations

(i) Michaelis-Menten equation

The Michaelis-Menten equation explains the kinetic behaviour of enzymes using the model shown in figure D1. According to that, the substrate (S) binds to the enzyme (E), reversibly, producing an intermediate enzyme-substrate (ES) complex which in turn produces the product (P). The reaction rates for formation of ES complex, E+ S and E+ P are given by k_1, k_2 and k_{cat} respectively. In order to be valid, the Michaelis-Menten model enquires two main assumptions. Firstly, the whole system must be in steady-state meaning that the complex ES remains constant regardless of ongoing processes to modify it and secondly the concentration of the enzyme is negligible compared to that of substrate.

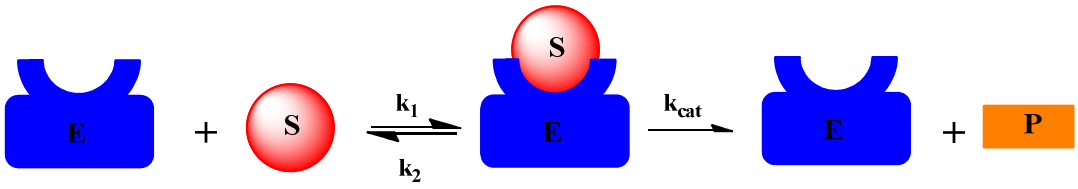

Figure D1: Illustration of Michaelis-Menten model. The enzyme (**E**), substrate (**S**) and product (**P**) are shown in blue, red and orange colours respectively while the rate constants are shown with **k** on the top of each arrow.

The Michaelis constant (K_m), which is equilibrium constant, is equal to:

$$K_m = \frac{k_{cat} + k_2}{k_1} \quad (1)$$

Considering that we are talking for an isolated system, the total enzyme concentration [E_{tot}] is equal to the concentration of free enzyme [E] plus the concentration of the substrate bound enzyme [ES]:

$$[E_{tot}] = [E] + [ES] \quad (2)$$

The rate of production of [ES] over time is given by the following equation:

$$\frac{d[ES]}{dt} = k_1[E][S] - k_2[ES] - k_{cat}[ES] \quad (3)$$

While the rate of production [P] over time by the equation:

$$v = \frac{d[P]}{dt} = k_{cat}[ES] \quad (4)$$

Because the system is in steady state the equation **(3)** is equal to zero. Rearrangement of that equation in combination with equation **(2)** gives:

$$\frac{[ES]}{[E_{tot}] - [ES]} = \frac{k_1 [S]}{k_2 + k_{cat}} \qquad (5)$$

Combination of equation **(5)** with equation **(1)** gives:

$$[ES] = \frac{[E_{tot}][S]}{K_m + [S]} \qquad (6)$$

Finally, combination of **(6)** with **(4)** gives the Michaelis-Menten equation:

$$v = \frac{k_{cat} [E_{tot}][S]}{K_m + [S]} \qquad (7)$$

Graphical demonstration of Michaelis-Menten equation is shown in figure D2.

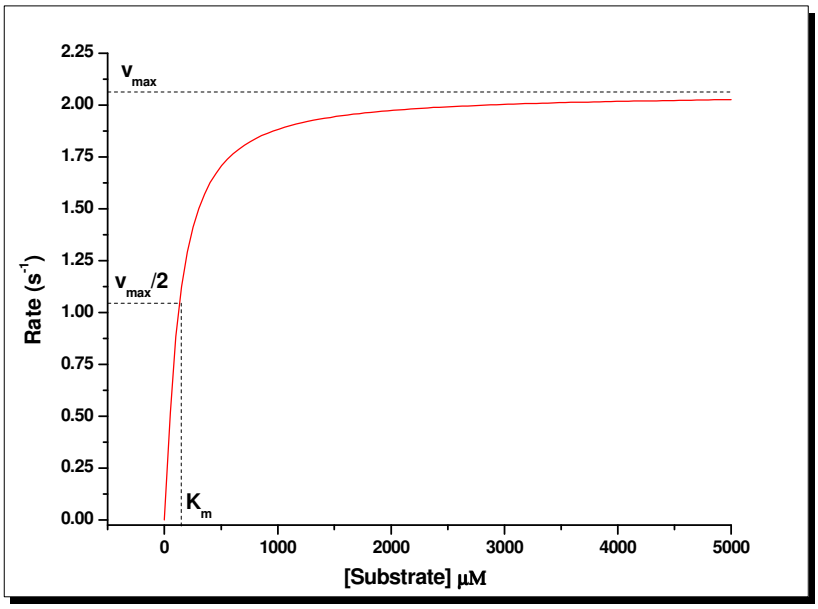

Figure D2: The Michaelis-Menten curve as it is derived from equation **(7)**

When the concentration of substrate is much higher that the Michaelis constant ($S>>K_m$), then the equation **(7)** can be modified into:

$$\mathbf{v_{max} = k_{cat}\,[E_{tot}]} \qquad \textbf{(8)}$$

On the other hand, when the concentration of substrate is negligible compared to Michaelis constant ($S<<K_m$), then the equation **(7)** can be modified into:

$$\mathbf{v = \frac{k_{cat}\,[E_{tot}][S]}{K_m}} \qquad \textbf{(9)}$$

(ii) Lineweaver-Burk equation

The Lineweaver-Burk equation is the reciprocal illustration of Michaelis-Menten equation (both sides), providing a linear analysis of enzymes kinetics. Combination of equations **(7)** with **(8)** gives:

$$v = \frac{v_{max}[S]}{K_m + [S]} \qquad (10)$$

The double reciprocal rearrangement of equation **(10)** provides the Lineweaver-Burk equation, plot of which is shown in figure D3:

$$\frac{1}{v} = \frac{K_m}{v_{max}[S]} + \frac{1}{v_{max}} \qquad (11)$$

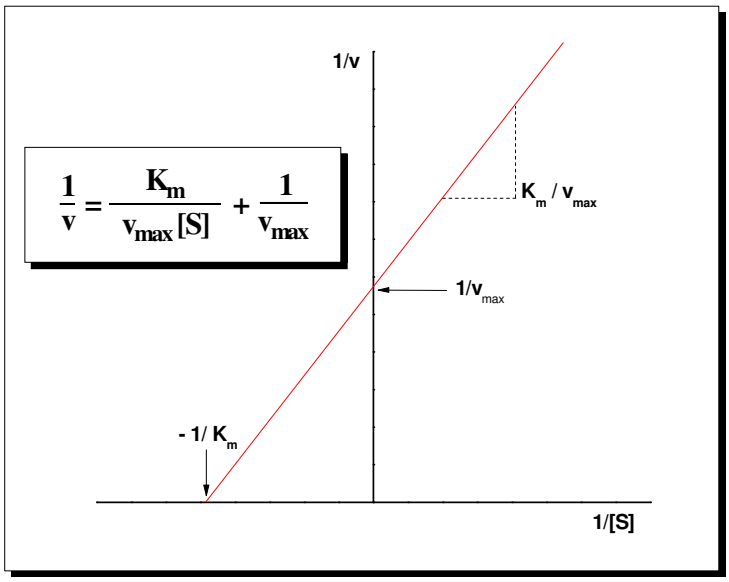

Figure D3: The Lineweaver-Burk plot

Appendix E

Types of enzyme inhibition

Macromolecular inhibition studies indicated two major classes of enzyme inhibitors, the non-specific inhibitors and the specific ones. While the non-specific inhibitors affect all the enzymes in the same way, the specific inhibitors act on particular enzymes attracting in that way all the interest of the drug development industry. This class of inhibitors can be further classified into irreversible and reversible. This section is dedicated to reversible inhibitors so whatever presents below refers to them. According to the position of binding, the reversible inhibitors can be grouped into competitive, uncompetitive and non-competitive. The models of their action are illustrated in the following figure (fig. E1).

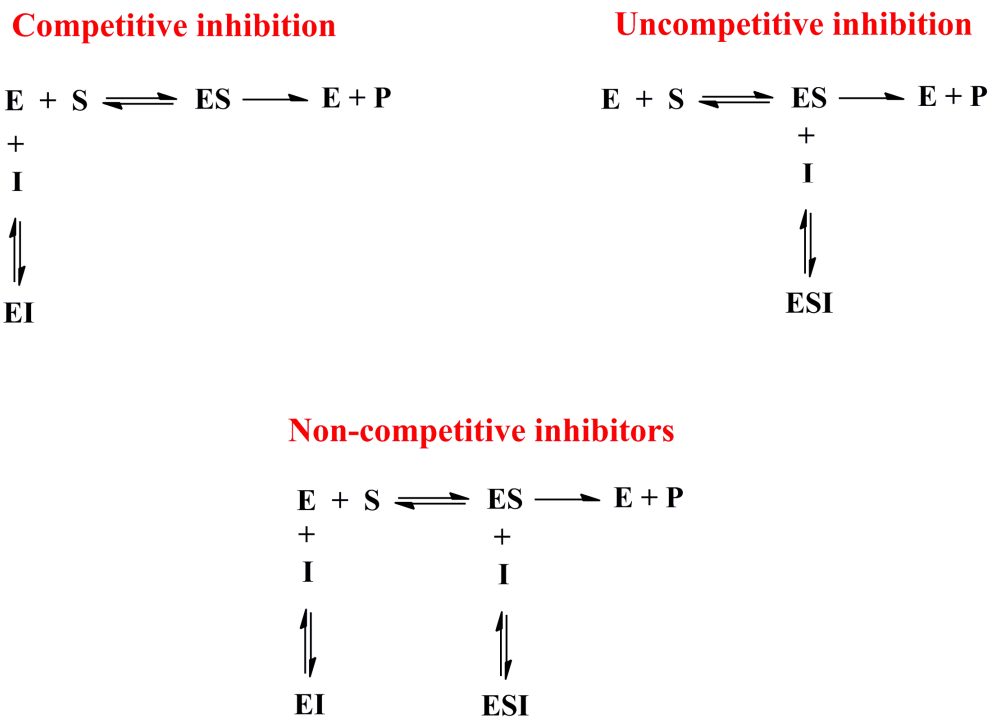

Figure E1: Competitive, uncompetitive and non-competitive type of enzyme inhibition

i) Competitive type of inhibition

The competitive inhibitors act by "competing" with substrate for binding in the active site of the enzyme. These molecules bind exclusively in the active site and the inhibition effect, they cause, can be reversed by increasing the substrate concentration. Classification of a potential inhibitor as competitive including its inhibition constant can be easily determined using the plots of figure E2.

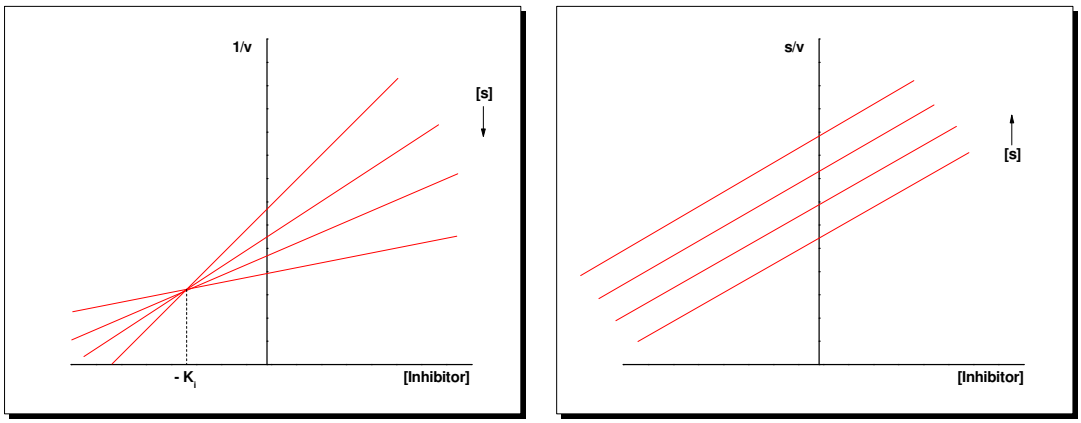

Figure E2: Determination of inhibition constant of a competitive inhibitor. The reaction rate is illustrated as v while the substrate and the inhibition constant of the complex EI are given as s and K_i respectively

Uncompetitive type of inhibition

While a competitive inhibitor binds exclusively in the active site of a given enzyme, the uncompetitive one demands binding of substrate. As the model of figure E1 shows, an uncompetitive inhibitor forms a complex with the enzyme while the substrate is already bound. This is a rare type of inhibition and it can be characterized using the graphs of figure E3.

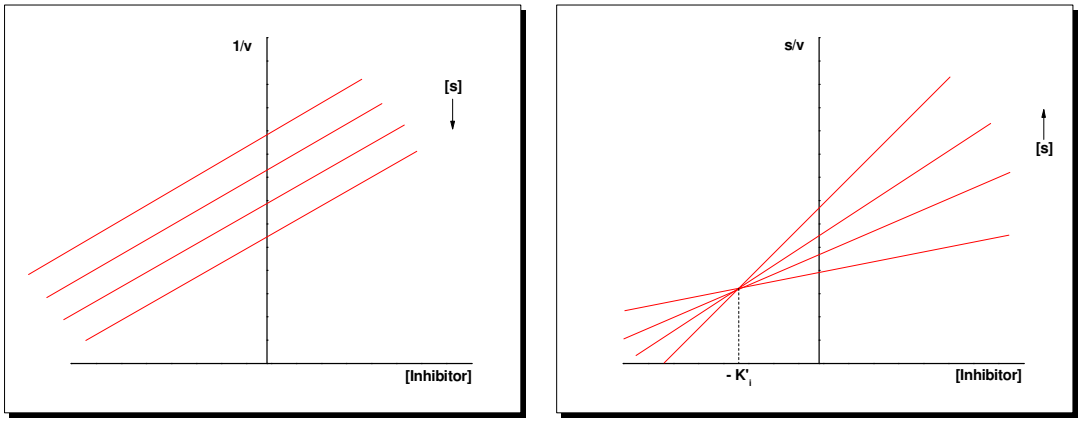

Figure E3: Determination of inhibition constant and the type of inhibition of an uncompetitive inhibitor. The reaction rate, substrate and inhibition constant of the complex ESI are presented as v, s and K´$_i$ respectively

Non-competitive type of inhibition

The inhibition graphs of the last and most interesting type of enzyme inhibition are illustrated in figure E4. While the inhibitor is not affected by binding of substrate, K_i (EI complex) and K´$_I$ (ESI complex) are equal.

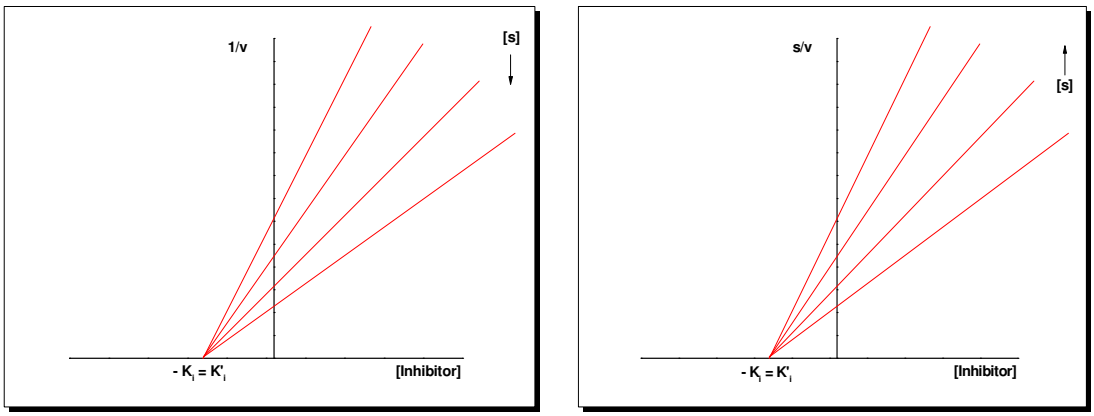

Figure E4: Determination of inhibition constant and the type of inhibition of a non-competitive inhibitor. The reaction rate, substrate and inhibition constants of the complexes EI and ESI are presented as v, s, K_i and K´$_i$ respectively

Appendix F

hTDO and hIDO2 gel filtration results

(a) hTDO

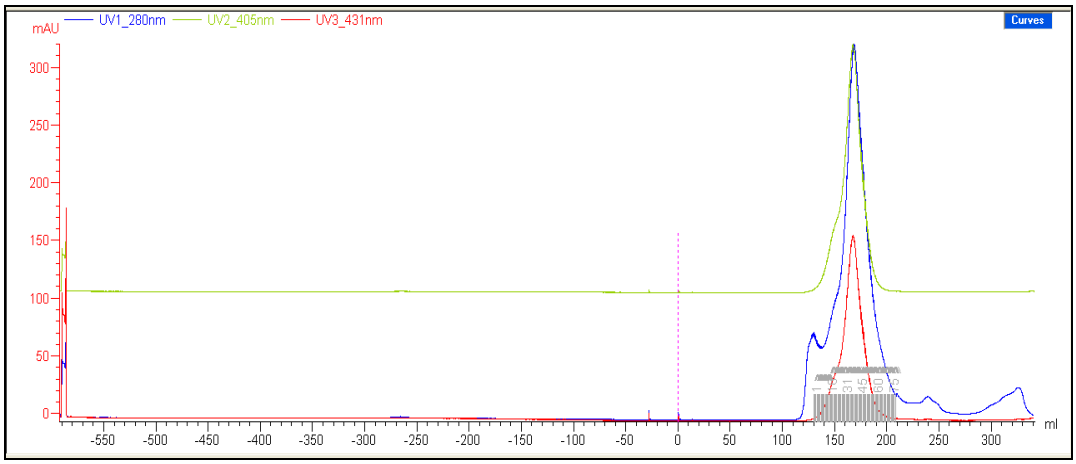

(b) hIDO2

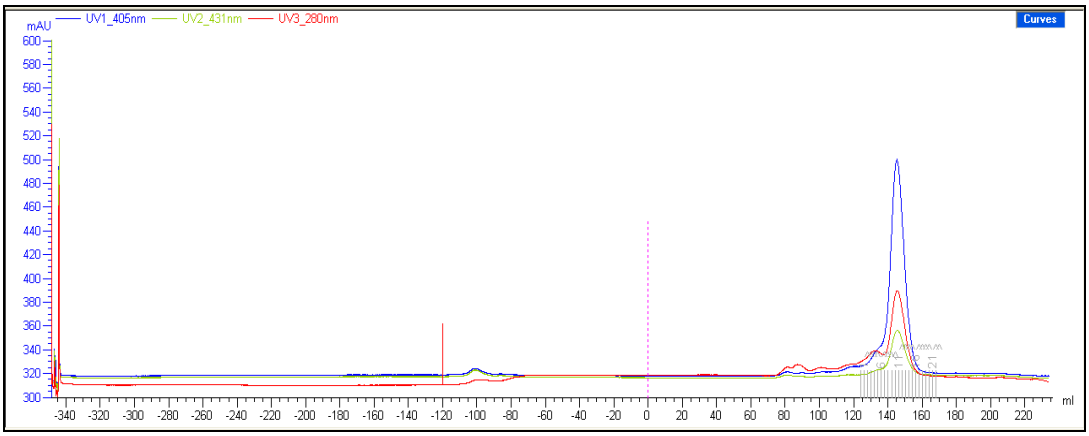

Figure F1: Illustration of (a) hTDO and (b) hIDO2 gel filtrations. hTDO is eluted in 20mM TrisHCl buffer pH 8.0, 1mM TCEP using Superdex-200 (hTDO fraction = ~150-200 ml); hIDO2 is eluted in the same buffer using Superdex-75 (hIDO2 fraction = ~140-160 ml).